Optimisation of Substrate and Growth Conditions of Retinal Pigment Epithelial Cells Destined for Transplantation

A thesis submitted to University College London for the degree of Doctor of Philosophy (PhD)

2015

Ahmad Ahmado

Department of Ocular Biology and Therapeutics (ORBIT)
UCL Institute of Ophthalmology
University College London
11-43 Bath Street
London EC1V 9EL

Declaration

I, Ahmad Ahmado, confirm that the work presented in this thesis is my own. Where information has been derived from other sources, I confirm that this has been indicated in the thesis

Abstract

Retinal Pigment Epithelium (RPE) transplantation efforts have been ongoing for three decades . To this day no feasible cure exists for diseases such as age-related macular degeneration (AMD). The key to treatment of AMD is to replenish the RPE. Establishing cells that accurately represent their native tissue is a considerable challenge. RPE cells undergo de-differentiation in culture losing important characteristics after repeated passage. Furthermore, RPE cells are anchorage-dependant and require a substrate for survival. Attempts at replenishing the RPE using suspensions have been met with scepticism due to the high degree of apoptosis.

ARPE-19, a human RPE line, retains several phenotypic characteristics of primary RPE although current passages have lost some established features. A variety of polymers with diverse chemistries, specialised coatings, and optimised media were tested to optimally grow ARPE-19 cells. Using information gathered from these experiments, optimal conditions were selected for Human Embryonic Stem Cell (HESC)-derived RPE cells. Cell/substrate composites were transplanted in pigs to validate their efficacy.

Differentiation of ARPE-19 cells was enhanced by utilising a superior substrate, polyester filter, together with an optimal growth medium containing pyruvate. HESC-derived RPE grown in optimal conditions developed differentiation characteristics identical to native RPE. This was assessed by morphology, immunohistochemical profile, trans-epithelial resistance, electron-microscopy, and growth factor secretion. A higher porosity version of this filter supported growth and differentiation of HESC-RPE and this was chosen as the basis for a transplantation project due to its good permeability. Transplanted HESC-RPE/polyester composites survived surgical delivery in a pig model and were eventually chosen for a phase I clinical trial.

Conclusion: This thesis investigated optimal conditions for the human RPE line ARPE-19. Optimal growth conditions were then applied to HESC-RPE cells which achieved a high level of differentiation. Composites were transplanted in pigs and led to their selection for use in clinical trials.

Table of Contents

List of Tables

List of Figures

List of Abbreviations

ºC	Degrees Celsius
4-CIN	α-cyano-4-hydroxycinnamic acid
AB	AlamarBlue® (Resazurin)
AMD	Age-related Macular Degeneration
ARPE-19	Spontaneously arising human retinal pigment epithelium (RPE) cell line derived in 1986 by Amy Aotaki-Keen from the normal eyes of a 19-year-old male who died from head trauma in a motor vehicle accident (American Type Culture Collection, Manassas, VA, USA)
BEST	Bestrophin
bFGF	basic Fibroblast Growth Factor (or FGF2, FGF-β)
BM	Basement Membrane
BME	Basement Membrane Extract
BrM	Bruch's Membrane
CB	Cacodylate Buffer
CRALBP	Cellular Retinaldehyde Binding Protein
CS-1	Fibronectin Connecting Segment-1 peptide
D407	Spontaneously arising, transformed human retinal pigment epithelium (RPE) cell line derived in 1995 from the globe of the eye of a 12-year-old white male child. At the time of writing this thesis this line is no longer available.
DAPI	4',6-diamidino-2-phenylindole
DFH	DMEM:F12 High glucose (glucose corrected to 4.5 g/L)
DHP	DMEM High glucose with Pyruvate
DH	DMEM High glucose
DLP	DMEM Low glucose with Pyruvate
DMEM	Dulbecco's Modified Eagle's Medium
DMEM/F12	A growth medium consisting of a 1:1 mixture of DMEM and F12 growth media
DPBS	Dulbecco's Phosphate-Buffered Saline
DMSO	Dimethyl sulfoxide
dsHESC	dissociated re-seeded Human Embryonic Stem Cell
ECM	Extra-Cellular Matrix

EDTA	Ethylenediaminetetraacetic acid
EHS	Abbreviation for a murine sarcoma cell line named Engelbreth-Holm-Swarm sarcoma.
EM	Electron Microscopy
EPC-1	Early population doubling level cDNA-1 (original name of PEDF)
ePTFE	expanded-PTFE
ESC	Embryonic Stem Cell
F12	Ham's F12 Nutrient Mixture
FCS	Foetal Calf Serum (Foetal Bovine Serum)
FESEM	Field Emission Scanning Electron Microscope
FGF	Fibroblast Growth Factor
FITC	Fluorescein isothiocyanate
FN	Fibronectin
FN-C/HI-III	The official abbreviations for a group of peptide sequences residing within the carboxy terminal heparin-binding 33kd fragment of the fibronectin-A chain
fhRPE	foetal human Retinal Pigment Epithelium
g	gram
GFR	Growth Factor Reduced
GFR-BME	Growth Factor Reduced BME
GFR-MG	Growth Factor Reduced-Matrigel®
GRGD	Glycine-Arginine-Glycine-Aspartate
GRGDS	Glycine-Arginine-Glycine-Aspartate-Serine
h	hour
HBSS	Hank's Balanced Salt Solution
HES(C)	Human Embryonic Stem (Cell)
HESC-RPE	HESC-derived Retinal Pigment Epithelium
HPPEF	High Porosity Polyester Filter
ICC	Immuno-Cyto Chemistry
IGF	Insulin-like Growth Factor
IHC	Immuno-Histo Chemistry
IPE	Iris Pigmented Epithelium
IPS(C)	Induced Pluripotent Stem (Cell)
ISCI	International Stem Cell Initiative
IKVAV	Isoleucine-Lysine-Valine-Alanine-Valine

IOL	Intra-Ocular Lens
IU	International Unit
JEOL	Brand of software for recording of electron microscopy images
KSR	Knock-Out Serum Replacement
KRT8	Keratin 8 (Cytokeratin 8)
L	Litre
LAP	Latency Associated Peptide
M	Molar
m	metre
MCT	Mono-Carboxylate Transporter
MEF	Mouse Embryonic Fibroblast
MERTK	C-Mer Proto Oncogene Tyrosine Kinase
MG	Matrigel®
MIDAS	Metal Ion-Dependant Adhesion Site
MITF	Microphthalmia-associated Transcription Factor
Na,K	Na^+,K^+-ATPase (or simply Na,K-ATPase)
NRT	No reverse transcriptase
OCT	Optical Coherence Tomography
OTX	Orthodenticle homeobox
Pax6	Paired box gene 6
PBS	Phosphate Buffered Saline
PDMS	Polydimethylsiloxane (commonly referred to as silicone)
PE	Polyester = polyethylene terephthalate in this thesis
PET	polyethylene terephthalate
PEDF	Pigment Epithelium-Derived Factor (serpin F1)
PFA	Paraformaldehyde
PLGA	Poly-Lacto-Glycolic Acid (Poly-D,L-Lactide-co-Glycolide)
Pmel17	Pre-melanosome 17 (GP100)
PO	Propylene Oxide
POS	Photoreceptor Outer Segments
PRF-HBSS	Phenol red-free HBSS
PS	Penicillin-Streptomycin mixture
PTFE	Polytetrafluoroethylene (commonly known as Teflon®)
PU	Polyurethane
RGD	Arginine-Glycine-Aspartate

RGDS	Arginine-Glycine-Aspartate-Serine
RP	Retinitis Pigmentosa
RPE	Retinal Pigment Epithelium
RT	Room Temperature
rpm	Revolution Per Minute
SEM	Scanning Electron Microscopy
SOX2	Sex-determining region Y-box 2
SSEA	Stage-specific embryonic antigen
TCPS	Tissue Culture Polystyrene
TGF-β	Transforming Growth Factor-β
TER	Trans-Epithelial Resistance
TEM	Transmission Electron Microscopy
TRA-1-xx	Keratan sulphate antigen e.g. TRA-1-60, TRA-1-85
TRITC	Tetramethylrhodamine
UV	Ultra-Violet
VEGF	Vascular Endothelial Growth Factor
w/v	weight/volume
YIGSR	Tyrosine-Isoleucine-Glycine-Serine-Arginine
ZO-1	Zonula Occludens-1

Dedication

I am thankful that I have had the time and support to complete this thesis. First and foremost, I dedicate my work to my mother and father, for their relentless support through numerous means, and to my wife and children for their persistent love, faith and understanding.

The last of my experiments were completed by early 2011 and most of this thesis was written during the rebellion in my country of origin, Syria. This uprising, along with the people's dedication to achieve freedom, has been a great source of motivation.

Abraham Lincoln was quoted during his second annual message to Congress in 1862 "Without slavery the rebellion could never have existed; without slavery it could not continue". Ironically, as the Syrian uprising approached its seventh month, I was saddened by the departure of one of the most resilient and determined American entrepreneurs in our time, Steve Jobs. Through watching a documentary commemorating Job's perseverant life, I was astounded to learn about his half-Syrian roots. Unfortunately Homs, the city of Job's father, is today in ruins. It remains a besieged de-electrified war arena with swathes of demolished neighbourhoods. An impotent ghost city with little potential for life let alone any knowledge or talent.

As depressing as the news may be, the resoluteness and will-power of both the Syrian people, as well as everyone who came to their aid have been a beacon which beckoned me to soldier on and complete my work.

I dedicate this thesis to all innocents affected by the Syrian conflict and to the memory of all innocent life lost in the conflict. To all health, charity, and aid workers, many of whom were systematically targeted in their line of duties, as well as all journalists who risked their lives exposing this ugly conflict to the world. I dedicate my work to them all irrespective of religion or race. Their memory of courage and persistence lives on as an inspiration. They will all but be forgotten.

Acknowledgements

I would like to sincerely thank all the members of our laboratory, without whom this work would not have been possible. My supervisors Professor Peter Coffey and Professor Lyndon da Cruz have been the masterminds and driving force behind the project. They have successfully guided the directions and aims of the work in our laboratory all along and ensured our laboratory was always at the forefront of scientific discovery. In particular they have been a constant source of motivation and positive feedback which enabled me to keep going. Anthony Vugler, a strong member of the team, and now principal investigator in his own right was a de facto mentor and has been a constant source of motivation as well as pearls of knowledge. Amanda Carr has been my second mentor and an inspiration as she excels in all the practical tissue culture and molecular skills I can think of. I am sincerely grateful for her assistance with a crucial ELISA experiment as well as the western blots, and qPCR's which helped promote and publish part of this thesis. Jean Lawrence, who is now retired, was a major contributor to the project and histology protocols anchor, provided constant valuable input into my work and helped refine my immunochemistry and histology techniques. Li Li Chen has been a crucial member of the lab and in particular has been the mainstay of our lab's embryonic stem cell production line. Ma'ayan Semo and Carlos Gias have guided me with data analysis throughout and have been my statistical mentors. Yasmyn Rybak-Rajewski, PA to Peter Coffey and another linchpin in our team, withstood the never-ending administrative and organisational tasks associated with the London Project and ensured our team's energy was channelled in the most efficient way. I cannot thank her enough for that. I would like to thank Iwan Roberts for his help with a pilot experiment as well as the rest of our lab members Matthew Smart, Amelia Lane and Michael Powner for their supportive comments and intriguing discussions, I wish them all the best in their post-doc years. I am grateful to the London Project to Cure Blindness who have supported me and the project team as a whole, and I am glad to have been able to finally present this work as well as help forward the project to its current level where it has been approved for a human phase I clinical trial at Moorfields Eye Hospital. As part of this approval, I passed the baton to Shazeen Hasan and Sakina Gooljar who took over all of my stem cell work under the direction of Pfizer pharmaceuticals. They committed to preparing the cells in a Good Medical Practice-compliant lab until the baton was passed yet again to their successors at the Roslin

Institute, University of Edinburgh. I wish them both the best and thank them for their efforts at our GMP facility which isn't work for the faint-hearted.

All the electron microscopy has been done with technical assistance of Robin Howes (who has now retired) as well as Peter Munro. Acquisition and optimisation of all confocal microscopy could not have been done properly without the generous help of Peter. He is a true asset to the Institute and is well known for his thorough assistance. Karen Cheetham from UCLB has been a true friend to the project especially during its initial stage. She contributed hugely to the early direction of the project's substrate selection as well as its current patent and device manufacturing affairs, and helped introduce our team to other experts within UCL. Glenn Jeffery has helped me interpret results in one my main chapters and examined me for my upgrade. Glenn as an office neighbour has, on many occasions, provided indispensable developmental perspective for RPE, as well as numerous bouts of happiness with his bright sense of humour. John Greenwood supervised the early stages of my project before it became "The London Project" and provided expert guidance on RPE and ECM biology during my early PLGA and peptide experiments, and I truly thank him for that.

It is an enormous privilege to have been at UCL and work at one of the best centres for ocular and neuroscience, the UCL Institute of Ophthalmology, and I would like to express my genuine appreciation to all the staff at UCL and especially our Institute for making things work and happen for students and researchers every day.

As always, my eternal thanks and gratitude go to my mother and father who have never ceased to encourage me, even in the most difficult times. I feel they raised me in the best possible way that motivated me to learn with passion. I truly owe them for my thirst for knowledge and this very thesis. They have always, with their kind words, made me feel my best.

Again, my utmost appreciation goes to my other half, as well my two kids who are unaware of the much better dad they are missing. My family have, with their unfaltering love, innocent understanding and kindness, endured the most. They have tolerated my lack of time and apparent inattention as well as my plentiful mood swings. I really couldn't have done it without them. This thesis is a direct result of their time and effort too. Thank you all!

Foreword

In this thesis I have adopted a stepwise approach to the subject of optimising a cell-substrate composite destined for sub-retinal transplantation in the eye. In brief, my thesis argues the various aspects of selection of a substrate, followed by the importance of optimising growth medium and finally selection of an optimal cell source.

Following an introduction and methods in chapters 1 and 2 respectively, I present my work in a series of experimental chapters 3 – 8.

In Chapters 3, 4, and 5, I present studies relating to various substrates, and selection of a superior substrate for transplantation. The studies highlight the importance of the substrate not only to survival, but the maturation of our cell of choice the retinal pigment epithelium (RPE).

In Chapter 6, I present work signifying the importance of growth media and its considerable impact on the phenotype of the ARPE-19 cell line, given an optimal substrate is used.

Chapter 7 and 8, I present my work on the Shef-1 human embryonic stem cells, and the correspondingly derived RPE cells. Chapter 7 includes experiments done on standard commercially available culture-grade surfaces. Chapter 8 presents similar work done an alternative highly porous version of the optimal substrate.

In Chapter 9 I show some practical applications of this research in animal models.

I conclude with my discussion and thoughts for future directions in Chapter 10, and my bibliography in Chapter 11.

1

Introduction

1 Introduction:

1.1 Project Aims, the importance of the Retinal Pigment Epithelium in Age-Related Macular Degeneration and retinal disease

Age-related Macular Degeneration (AMD) is the most common cause of untreatable visual handicap in the industrialised world (Klaver et al. 1998). AMD is a multifactorial disease which comprises several problems. First and foremost retinal pigment epithelium (RPE) cells become dysfunctional due to accumulation of lipofuscin granules (Feeney-Burns and Eldred 1983), loss of melanosomes and melanin (Boulton, Roanowska, & Wess 2004;Bonilha 2008), reduction in cell density, loss of organelles with concomitant increase in drusen deposits (Hageman et al. 2001). Secondly, the RPE basement membrane known as Bruch's membrane (BrM) becomes progressively hydrophobic, crosslinked, and calcified (Booij et al. 2010), and RPE cell attachment to BrM is subsequently weakened while these cells are unable to restore or repair these extra-cellular matrix (ECM) changes (Tezel, Del Priore, & Kaplan 2004). In addition, the complement system (Anderson et al. 2010), cytokines and excessive production of growth factors such as vascular endothelial growth factor (VEGF) (Ohno-Matsui et al. 2001) and lack of protective factors such as pigment epithelium-derived factor (PEDF) (Bhutto et al. 2006;Bhutto et al. 2008) have been implicated in the development of AMD pathology. The importance of the RPE in retinal homeostasis has been known for many decades. This is best illustrated by the number of retinal diseases arising from defects in the RPE cells. Autosomal dominant and recessive retinitis pigmentosa (RP), Best's disease, Sorsby's Fundal Dystrophy have all been demonstrated to be due defects in the RPE (Marmorstein et al. 1998;Gal et al. 2000). Sadly, experiments utilising RPE transplantation aimed at AMD or RP have been ongoing for nearly three decades (Gouras, Flood, & Kjeldbye 1984;Gouras et al. 1989). Despite all these efforts, to this day no feasible cure exists for either condition.

The key to treatment of these diseases is to replenish the layer of cells situated directly underneath the retina, the RPE. This step must be accomplished before the inevitable and irreversible stage of photoreceptor loss (da Cruz et al. 2007). Replacement of these dysfunctional cells can occur either by injection of cell suspensions or by the surgical

placement of a membranous patch populated by a monolayer of pre-grown RPE underneath the retina i.e. a cell-substrate composite. Whichever method is used, the cells must resemble the cells they are replacing as closely as possible. In other words, the cells must have differentiated to a point resembling their native counterpart. If the patch placement method is to be used, additional requirements such as polymer flexibility, thickness, porosity and chemistry are to be considered. Thus the aims of my project were to investigate these components: i) the cells and to what degree they are, or can be differentiated; ii) the polymer and whether it is suitable for transplantation; iii) the characterisation of the combination of the cells plus polymer; iv) testing necessary coatings that may help achieve these aims.

1.2 Functions of the RPE

The RPE performs a multitude of functions essential to vision and photoreceptor survival: 1) The daily shedding of rod & cone outer-segments by the photoreceptors requires active phagocytosis (Young and Bok 1969;Steinberg 1974;Feeney-Burns & Eldred 1983;Long et al. 1986) and subsequent lysosomal digestion by the RPE (Bosch, Horwitz, & Bok 1993). 2) The constant photo-bleaching of rhodopsin (visual pigment) requires the rhodopsin isomerase which enzymatically replenishes 11-cis-retinal and renews the visual pigment cycle. This enzyme is harboured mainly by the RPE (Bridges et al. 1984). 3) It is imperative that the RPE, which is adjacent to the blood-rich choroid, shields the retina and photoreceptors from various blood-borne insults. This is achieved through RPE tight junctions which, together with the retinal capillary tight junctions, form the blood-retina barrier (Cunha-Vaz 1976). 4) Fluid, electrolyte and small molecule transport is an active process in the RPE. It has been shown that hydraulic conductance of the Bruch's-Choroid complex is more than doubled in the presence of RPE cells (Ahir et al. 2002). In particular, the apical and basolateral membranes of RPE cells are rich in ion transport proteins that maintain ionic flux in favour of creating osmolar gradient across the RPE which facilitates water transport towards the choroid and away from the retina (Miller, Steinberg, & Oakley 1978). 5) The RPE functions as a dark shielding layer which absorbs light. This is a fundamental requirement for vision since this provides directional information to the eye apparatus as well as absorbing stray stumuli and improving optical quality. Thus, the existence of pigmented cells adjacent to photoreceptors has been preserved in many phylae including the most basic organisms' eyes (Vopalensky and Kozmik 2009). In humans, the presence of abundant

melanin granules in the RPE is a topic of many discussions. Apart from minimising internal reflection of light within the retina, and protection from UV light (STEIN 1955;Hu, Simon, & Sarna 2008), melanosomes have a role in eye development (Jeffery 1998). They have also been implicated in the poorly understood photo-transduction capability of RPE cells (Brown and Crawford 1967a;Brown and Crawford 1967b;Linsenmeier and Steinberg 1983;Steinberg, Linsenmeier, & Griff 1983;Hao and Fong 1999). 6) Synthesis of growth factors and immuno-modulatory factors by the RPE is essential for the proper functioning of their environment. The RPE is a potent source of growth factors such as PEDF (Tombran-Tink et al. 2005), platelet-derived growth factor (Campochiaro et al. 1989), insulin-like growth factor (IGF) (Ocrant, Fay, & Parmelee 1991), basic fibroblast growth factor (bFGF)(Ishigooka, otaki-Keen, & Hjelmeland 1992;Shima et al. 1995), transforming growth factor-β (TGF-β), thrombospondin (Tanihara et al. 1993;Zamiri et al. 2005), placental growth factor (Hollborn et al. 2006), as well as VEGF (Adamis et al. 1993;Sone et al. 1996a). Not surprisingly, the interplay of these growth factors with their environment i.e photoreceptors and inter-photoreceptor matrix form part of an essential outer retina autocrine-paracrine system (Waldbillig et al. 1991). 7) Lastly, the RPE are involved in the secretion of extra-cellular matrix (ECM) proteins that form the basement membrane layer of BrM (Aisenbrey et al. 2006). These ECM proteins in turn serve a multitude of functions, such as controlling proliferation, differentiation and most importantly maintaining attachment of RPE cells to BrM (Booij et al. 2010).

1.3 Substrate Importance in Survival and Differentiation of RPE Cells

It is well known that certain cell types are entirely dependent on the presence of a substrate. Such cells are described as being anchorage-dependent, and thus can undergo apoptosis when deprived of interaction with a substrate. Such substrate related apoptosis is known as *anoikis* and RPE cells are believed to be similarly dependent on substrate for their survival (Tezel and Del Priore 1997).

Bruch's membrane is a pentalaminar structure serving as the native substrate for the RPE. BrM is divided into the RPE basement membrane, the inner collagenous layer, the elastin layer, the outer collagenous layer and the basement membrane of the choriocapillaris. The basement membranes of both the RPE and choroid are similar and

are rich in collagen IV, collagen V, laminin, and proteoglycans, but they differ in fibronectin which is a more prominent feature of the RPE BM, and collagen VI which is abundant in the choroid BM but not present in that of the RPE (Booij et al. 2010). Collagen VI also may be involved in anchoring of the choriocapillaris to the choroid (Marshall et al. 1994). Both inner and outer collagenous layers are rich in collagens I, III, V and glycosaminoglycans. The elastin layer also contains collagen VI and fibronectin (Booij et al. 2010).

Ageing of BrM occurs on several fronts. BrM undergoes calcification (Spraul et al. 1999;Booij et al. 2010), cross-linking (Ramrattan et al. 1994) and accumulation of hydrophobic debris with age (Sheraidah et al. 1993;Guymer, Luthert, & Bird 1999;Huang et al. 2007). Thus it seems aged macular BrM is hostile to attachment and growth of cells that it is simply unsuitable for repopulation by seeded cells, regardless of source of cells and the division of BrM being resurfaced (Tezel & Del Priore 1997;Tezel, Del Priore, & Kaplan 2004;Del Priore, Tezel, & Kaplan 2006;Sugino et al. 2011a;Sugino et al. 2011b). Furthermore, previous studies have demonstrated that young BrM is more efficient than old BrM in supporting cell attachment (Tezel, Kaplan, & Del Priore 1999;Gullapalli et al. 2005). It has also been shown that hydraulic conductance of BrM declines substantially with age, halving almost every decade (Starita et al. 1996). This rapid decline is due to remodelling up to the age of 40, after which lipid retention contributes to further decline (Starita, Hussain, & Marshall 1995;Starita et al. 1996).

Native BrM thickness is normally 2μm, but this more than doubles due to age (Ramrattan et al. 1994), with a concurrent decline in chorio-capillaris density. In AMD, there is particular reduction in choriocapillaris density, while the thickness of both BrM and choroid is no different from normal aged maculae, indicating age as the main determinant of BrM thickness, whereas disease affects thickness of the choriocapillaris (Ramrattan et al. 1994). This principle also applies to the elastin layer integrity (elastic lamina) in geographic AMD which does not affect elastin thickness or abundance compared to normals. However elastin integrity is significantly lower in all other forms of AMD compared to age-matched normals, as is thickness in advanced and late AMD. Surprisingly even in normal adults, macular elastin was thinner and more permeable than peripheral elastin in all individuals, confirming the macular region to be particularly susceptible irrespective of age (Chong et al. 2005).

Extra-cellular matrix provides vital cues for differentiation, polarisation and correct orientation of epithelial cells (Mak et al. 2006;Moyano et al. 2010). Turowski et al, found that ARPE-19 phenotype and gene expression is modulated by lens capsule basement membrane (Turowski et al. 2004). Others have found growth factor secretion to be increased with polarisation in culture (Sonoda et al. 2010), while some have stated that the phenotype of their embryonic stem cells could be modulated by seeding onto various substrate (Gong et al. 2008). Thus substrate will have a profound effect on overall health, as well as the functional profile of the overlying cells.

The wide use of plastic culture-ware for cell culture is made possible by ionizing the plastic surface to make it more hydrophilic by either enabling the surface to be predominantly positive or negatively charged. The interaction of cells with ECM in vivo follows similar patterns where ECM molecules carry specifically charged binding sites, such as collagen I carrying binding sites abundant in positively charged amino acids (Meyer, Notari, & Becerra 2002). The nature of these ECM molecule charged regions is such that these are binding sites for multiple ligands and share affinity to ligands with some integrins. The advantage of this setup is that it enables in vivo cell adhesion to be open to regulation by various factors such as heparin and PEDF (Meyer, Notari, & Becerra 2002). Thus, in vitro cell adhesion could be subject to these effectors depending on the abundance of ECM-mimicking charged sites such as an optimally ionised surface or even short active peptide sequences. Furthermore, substrate has been implicated in effective differentiation of epithelial cells. In particular, cells have been shown to polarize in the presence of laminin and to subsequently lose polarity and tight junction formation when their attachment to laminin was disrupted (Zinkl et al. 1996;Yu et al. 2005). Peter A. Campochiaro and collaborators have provided a wealth of evidence that RPE differentiation in response to optimal matrix appears to be dependent on laminin (Campochiaro and Hackett 1993). Growth of cells on laminin also induces significant VEGF and particularly dramatic increases in PEDF secretion as a sign of differentiation (Ohno-Matsui et al. 2001). However laminins are central ECM molecules and are the most abundant glycoproteins comprising any BM. In addition to providing a mechanical scaffold for their overlying cells, they interact and regulate the orientation of other components of the ECM and can bind cations and growth factors. Thus they can control a considerable array of cellular functions through direct interaction as well as indirect regulatory or surrogate means (Aumailley and Smyth 1998).

1.4 Integrins are important for RPE survival

Adhesion of RPE cells to BrM components is mediated by receptors called integrins. Integrins are vital to adhesion of cells in multicellular organisms and are evolutionarily highly preserved and exist in all metazoans including sea sponges and corals. In humans they function alongside cadherins, selectins, immunoglobulin superfamily receptors, and syndecans in mediating adhesion to the ECM and also play roles in cell-cell interaction, growth factor modulation as well as regulation and maintenance of the ECM itself.

Numerous studies have characterised the specificity of individual integrin dimers for certain ECM molecules. It is known that α1β1, α2β1, and α9β1 are receptors for laminin and collagen whereas α6β1, α6β4 and α7β1 are receptors for laminin alone (Belkin and Stepp 2000), and α10β1, α11β1 are for collagen alone (van der Flier and Sonnenberg 2001). The major receptors for the fibronectin arginine-glycine-aspartate (RGD) sequences are α4β1, α5β1 (Mostafavi-Pour et al. 2003), α8β1 (which also binds vitronectin and tenascin) (Schnapp et al. 1995), α9β1 (Liao et al. 2002), and the αv-class integrins αvβ1, αvβ3, αvβ5 (Jin et al. 2011;Schiller et al. 2013), αvβ6 and αvβ8 (Busk, Pytela, & Sheppard 1992;van der Flier & Sonnenberg 2001). α3β1 also binds fibronectin via its RGD site, but also is a receptor for laminin and collagen, through non-RGD sequences (Elices, Urry, & Hemler 1991). Additionally, α3β1 (along with α2β1) also serves cell-cell interactions (van der Flier & Sonnenberg 2001). It is also known that the major receptors for (the RGD sequence in) vitronectin are αvβ1, αvβ3 and αvβ5 (Plow et al. 2000). Thus integrin interaction with specific peptide sequences residing within ECM molecules has been broadly investigated.

Furthermore, αv-class integrins serve additional vital functions, in particular αvβ3, which serves to activate TGFβ1 by cleavage of the latency associated peptide (LAP) from TGFβ1-LAP. Activated TGFβ1 in turn regulates further expression of ECM molecules (Moyano et al. 2010). In addition to being a receptor for vitronectin αvβ5 is a receptor for (RGD sequence in) outer segments (Anderson, Johnson, & Hageman 1995) and equally for apoptotic cell debris (Finnemann and Rodriguez-Boulan 1999). Other major integrins mediate functions critical to survival of the organism and this is illustrated by the lethality of certain integrin knockouts such as β1 (Hynes 2002). Integrins also associate with other receptors that carry out primarily non-adhesive

functions while aiding adhesive functions. In relevance to AMD, a membrane bound complement regulatory protein CD46 (also known as Membrane Cofactor Protein) which works alongside Factor H in the cleavage of C3b from host cells and protects cells from autologous complement attack, associates with β1 integrin. Immunohistochemistry and confocal studies have shown the β1 integrin unit to be polarised to the basal surface of RPE along with CD46 in both primary cultured and ARPE19 cell types, and thus may yet serve in adhesive functions together with integrin proteins (McLaughlin et al. 2003).

Several RPE studies have demonstrated the presence of specific integrin subunits in RPE cells (β1,β5, α 1-6 and αv) as well as integrin heterodimers e.g, α2β1, α5β1, αvβ3, αvβ5, and α6β1 (Anderson, Johnson, & Hageman 1995;Finnemann et al. 1997;Zarbin 2003;Hoffmann et al. 2005;Aisenbrey et al. 2006). Of these α3, α5, α6 and β1 are on the basal side of RPE (Aisenbrey et al. 2006) as is β3 (Finnemann & Rodriguez-Boulan 1999) whereas αv and β5 localise apically (Finnemann et al. 1997).
αvβ5 integrin is one of few integrin receptors that localize to the apical surface of the retinal pigment epithelium (Anderson, Johnson, & Hageman 1995;Finnemann et al. 1997;Li et al. 2009), and it is this receptor that mediates retinal adhesion and binding of photoreceptor outer segments (POS) as well as apoptotic cells (Finnemann & Rodriguez-Boulan 1999;Nandrot et al. 2006). Interestingly αvβ3 is the integrin analogue in macrophages which equally recognises POS as well as debris particles arising from apoptotic cells. Furthermore, it is known that both apoptotic cells and POS actually compete for binding to both these integrin receptors, indicating that both particles harbour a common surface signal recognizable by both RPE cells and macrophages via αvβ5 and αvβ3 respectively. As proof of this concept, binding of both POS and apoptotic cells was inhibited equally in both RPE and macrophage by RGD-containing peptide solution in vitro (Finnemann & Rodriguez-Boulan 1999). Both POS ingestion and apoptotic cell clearance that have been initiated by the aforementioned integrins depend on a tyrosine kinase, MerTK, which is regarded as the essential "phagocytosis receptor" (Nandrot et al. 2006;Carr et al. 2009a) since it is known that lack of MerTK results in binding of these particles to the cell surface without their ingestion (Strick and Vollrath 2010). MerTK, a transmembrane receptor, receives signals from these two integrins (via focal adhesion kinase) and allows the cytoskeletal re-arrangement needed for phagocytosis. In RPE cells this process is critical to retinal function and happens once a day in response to circadian photoreceptor shedding (Strick & Vollrath 2010).

Another apically located integrin is α5β1 which is essential for adhesion to fibronectin (as is the case with endothelial cells), serum-induced proliferation, as well as bFGF and PDGF-BB dependant migration (Li et al. 2009). However in RPE cells, it appears that this α5β1 expression closely correlates with proliferative capacity of RPE cells and declines in post mitotic cells (Proulx, Guerin, & Salesse 2003;Li et al. 2009).

More recent reports have compared integrin expression in human embryonic RPE and foetal RPE, and found that both cell types express integrin subunits α1-6 and αv as well as β1-β4 and β6. However, although there were differences in integrin subunit expression (a relative abundance of α2 and β3 subunits and a relative scarcity of αv and α6 in foetal RPE), this did not correlate well with attachment rates to BrM explants, so there remains some uncertainty regarding the role of individual integrins when it comes to attachment to complex composited substrates such as BrM (Sugino et al. 2011b). Thus RPE attachment mechanisms via integrin receptors are thoroughly under investigation but as mentioned above this can occur through small sequences of RGD-containing peptides occurring within ECM molecules.

1.5 Considerations for methods of cell therapy delivery

Delivery of cells for cell therapy can be achieved using cell suspensions, cells attached to biodegradable substrates, and cells attached to non-biodegradable substrates. The type of tissue being transplanted can range from core tissue replacements such as transplanting diseased heart tissue with contractile myocytes (Zimmermann and Eschenhagen 2003), to cellular linings or coatings on artificial substrates. After a brief review of the literature concerning the latter type of cell transplantation one can easily distinguish several categories of substrates with cellular coatings. Such substrates utilising cellular coatings can be grouped as: 1) Temporary vehicle: here the substrate acts merely as a means to deliver the cells into the target tissue and is not needed once the transplant process is complete, rendering the substrate a functionally inert component e.g. soft tissue replacement using adipose-derived stem cells attached to a carrier substance (Santiago et al. 2006), 2) Coated mechanical implant: where the mechanical strength of the substrate is of prime interest and the cells solely provide a biocompatible interface to increase long-term host tolerance. Examples of such are endothelial coatings on the inner surface of artificial vascular prostheses (Jun and West

2004;Kannan et al. 2005;Jun and West 2005), and cellular coatings on titanium implant surfaces (Frosch et al. 2006). Thus, the mechanical properties of the artificial substrate maintain physical strength and integrity while the cells act solely as a tissue interface. 3) A cell transplant supported by a substrate: where the cells are of primary interest as they carry out most (if not all) of the intended function(s) of this composite, while requiring the continuous presence of the substrate to be able to carry out this function. This is probably the most complex type of cell-substrate composite and such is the case for RPE transplantation. RPE cells are required to interact heavily with the retina following transplantation. It is anticipated that a successful substrate material in this case will provide a mould that firstly, fits into the desired location to keep the cells in an anatomically optimal position, while secondly, supporting the overlying cell profile as a monolayer. Thus, whatever the artificial scaffold material is, it must be able to support the target-cell adhesion, migration and proliferation requirements. Failure of any of the above will likely translate into failure of re-population of the substrate surface. An additional unique requirement for the RPE is that the material must be permeable enough for water and small molecule exchange. Lack of permeability will result in RPE dysfunction due to decreased transport capacity and this is a potential pitfall when working with the RPE.

1.6 Natural and Artificial Substrates for RPE

Many artificial and natural substrates have been considered as scaffolds for RPE cell therapy. Amorphous soluble natural substrates such as alginate (Eurell et al. 2003), gelatine (amorphous denatured collagen I) (Del Priore, Tezel, & Kaplan 2004;Falk et al. 2012) or collagen gels (Yeung et al. 2004) have seen limited success as beaded or encapsulating carriers. Some of these amorphous substrates have even been superseded as encapsulating material by artificial plastics in clinical trials (Falk et al. 2012). On the other hand, native ECM matrix-derived substrates such as engineered collagen I foils (Thumann et al. 2006;Thumann et al. 2009;Ulbrich et al. 2011), and native acellular basement membranes such as anterior lens capsule (Turowski et al. 2004;Lee, Fishman, & Bent 2007), and amniotic membrane (Ohno-Matsui et al. 2005;Ohno-Matsui et al. 2006) have shown a much superior performance as RPE growth substrates in addition to their better physical strength. These natural substrates have a high tensile strength due to presence of collagen which allows considerable reduction in thickness typically to 10 microns and less (Thumann et al. 2009). Unfortunately, surgical handling of these

natural membranes has proven tricky (Binder et al. 2007). Recently, in the natural membrane category, arthropod-derived materials such as *Bombyx mori*- (moth silkworm) silk fibroin have been investigated as an RPE substrate. Silk fibroin's supreme strength have enabled Shadforth and colleagues to manufacture membranes as thin as 3μm (compare aforementioned collagen foils which are around 10μm) while maintaining an acceptable rigidity suitable for forceps handling. This, together with silk's documented biocompatibility as a suture material makes silk a viable option for future studies, although it must be emphasised this material was not comparable to plastic unless coated with vitronectin (Shadforth et al. 2012). In such circumstances, a logical next step would be to consider an artificial plastic substrate whose thickness could be manufactured to be as thin as desirable, while harbouring a special coating. This will be one of the topics of investigation in this thesis.

1.7 Attachment of RPE cells is key to their survival both in situ as well as after transplantation

Numerous attempts at replacing diseased RPE with a subretinal injection of healthy cell-suspensions of RPE have been tried with promising, but short-lived, results. This time-limited success could not be explained by immunologic rejection mechanisms alone (Algvere et al. 1997;Crafoord et al. 1999;Crafoord et al. 2000). Thus, apoptosis has been suggested as an alternate factor of limited success, and indeed this is confirmed in similar studies (Tezel, Kaplan, & Del Priore 1999). Apoptosis is a usually physiological, programmed, and energy consuming type of cell death. Cells become rounded then undergo cytoplasmic shrinkage while specialized peptidases called caspases are activated rendering the cell irreversibly committed to death (Sedlak and Snyder 2006). Such cells express specific 'find me' signals that attract phagocytes, followed by 'eat me' signals which allow recruited phagocytes to remove these apoptotic cells in a programmed fashion. This programmed cell removal can occur even if apoptosis is not completed thereby avoiding an inflammatory reaction (Chao, Majeti, & Weissman 2012). It is this silent disappearance of transplanted cells that probably accounts for the non-immunologic mechanisms of cell removal. It follows that since this process is programmed, specific signalling pathways must be involved. Indeed, a significant number of apoptotic cells are seen after subretinal injections of RPE suspensions in a study by Tomita et al (Tomita et al. 2005), and it has now becoming widely accepted that RPE cells must be attached to a suitable substrate to avoid

apoptosis (Tezel & Del Priore 1997;Tezel, Kaplan, & Del Priore 1999;Tezel, Del Priore, & Kaplan 2004;Del Priore, Tezel, & Kaplan 2006;Sugino et al. 2011a;Sugino et al. 2011b). This specific type of apoptosis triggered in response to lack of ECM binding is also known as *anoikis* and such cells are described as *anchorage dependent*. Thus, RPE cells are now widely accepted as anchorage dependant and will undergo anoikis unless bound to a suitable surface. While this dependence may seem as a nuisance to some suspension-based transplantation efforts, we must appreciate the ability to readily undergo apoptosis in the absence of ECM cues is actually a desirable anti-tumourigenic characteristic (Alfano, Iaccarino, & Stoppelli 2006).

1.8 Transplant logistics, suspension or patch?

It has now become widely accepted that the more viable approach to AMD treatment is to transplant RPE cells that have been pre-grown on a substrate into the sub-retinal space. This substrate (usually a polymer) not only controls the size and placement of the transplant, but also avoids problems normally associated with cell-suspension injections such as cell death, apoptosis, migration and reflux (Tomita et al. 2005). Histological evidence from suspension studies also indicates digestive stress on the host RPE when injecting a surplus of cells, as host cells seem to ingest surplus cells with subsequent accumulation of vacuoles and lipofuscin granules. In addition, RPE cell density remains static despite donor cell incorporation indicating concomitant host cell loss (Engelhardt et al. 2012). Even previous proponents of the subretinal RPE-suspension technique, now acknowledge that a scaffold is best for RPE transplantation efforts (Binder 2011).

With regards to the patch transplantation method, at present there are two schools of thought regarding the choice of the substrate. The first is to use a non-degradable permanent membrane which acts as a permanent scaffold for the cells at the cost of introducing a foreign body into the eye. The second is to use a bio-degradable membrane, where the membrane is degraded over a period of time dependent on the substance nature, ranging from weeks up to a few years (Tomita et al. 2005;Thomson et al. 2011). Each method has its advantages and the superiority of each method is a matter of current debate. While the latter method eventually avoids the presence of a permanent foreign body in the eye, only a single layer of cells is left behind, held together only by its intercellular junctions, basement membrane, and the surrounding host tissues. This donor monolayer is susceptible to chemical exposure to the products

of bio-degradation as well as immune disruption from either side once the original scaffold has been degraded. On the other hand, the wide success of artificial intra-ocular lenses (IOL) now used extensively in cataract surgery is suggestive of a potential safety of a much smaller and substantially thinner plastic sheet when placed permanently in the eye. Thus the wide use and tolerance of IOLs could be regarded as a proof of concept and is in support of the permanent (non-biodegradable) substrate school of cell transplantation.

1.9 Sources of RPE cells for transplantation

Establishing cultured cells that faithfully model their native tissue is a considerable challenge. Hence one the dilemmas of RPE transplantation has been the choice of a suitable cell type that can perform in vivo as efficiently as, if not better than, the cells they are replacing. Several transplantation studies utilising autologous RPE have been conducted where cells are harvested from the same patient undergoing the procedure, yet none have yielded a dramatic result (da Cruz et al. 2007). The problem with autologous cells is they are aged to the same extent as the cells they are replacing. Another potential problem is they would carry identical genetic susceptibilities that might have contributed to the disease scenario in the first place. Despite these criticisms of the autologous approach, this method has been attractive since the risk of immune rejection is absent. Nevertheless, the advent of powerful and well-tolerated immunosuppressants in recent years (Peters et al. 2014) combined with the limited results of the autologous method (Binder 2011) has called for an alternative approach: human cells that have been grown in a tissue culture laboratory.

1.9.1 RPE Primary Culture

Primary cultures are known to best retain native tissue characteristics. However preparing primary cultures from eyes repeatedly may create problems of consistency with experimental results in addition to being a laborious endeavour. Furthermore, RPE cells undergo de-differentiation in culture losing favourable characteristics (Opas 1989;McKay and Burke 1994;Hu and Bok 2001;Alge et al. 2003). This phenomenon appears to be a product of cell-substrate (Opas and Dziak 1988;Opas 1994) as well as growth media (Hu & Bok 2001;Luo et al. 2006). This is particularly true after repeated

passage since cell spreading and proliferation are known to be inversely related to differentiation (Opas 1989;Krugluger et al. 2007;Steindl-Kuscher et al. 2009).

1.9.2 RPE Cell Lines: ARPE-19, D407:

The ARPE-19 cell line is a spontaneously arising human RPE cell line derived in 1986 from the normal eyes of a 19-year-old male who died from head trauma in a motor vehicle accident (American Type Culture Collection, Manassas, VA, USA). It has become an alternative, although not superior, to primary culture (Maminishkis et al. 2006). Dunn et al. extensively characterised this cell line in 1996 (Dunn et al. 1996) and demonstrated several phenotypic characteristics similar to primary RPE such as pigmentation, CRALBP and cobblestone morphology. However, available passages for this cell line are now limited to those above p20 and it has become difficult to replicate some differentiation characteristics, e.g. pigmentation, initially reported by these authors, especially when using DMEM/F12, the standard recommended growth medium for ARPE-19. One suggested reason for this may be that higher passages of this cell line have become sensitive to culture conditions and unless specialised media are employed, the RPE phenotype is sub-optimal, and lacks pigmentation (Luo et al. 2006). Furthermore, this cell line has suffered from a low trans-epithelial resistance (TER) and lacks some major RPE differentiation and polarity markers (Luo et al. 2006;Carr et al. 2009a). Indeed ARPE-19 has been described as 'amelanotic' and lacking tyrosinase in recent literature (Biesemeier et al. 2010), such that many have resorted to incubation of ARPE-19 with non-human melanin-granules to produce melanosome-rich cultures (Wang, Dillon, & Gaillard 2006;Song et al. 2008;Burke and Zareba 2009). Additionally, western blot analysis of ARPE-19 cells shows they do not produce RPE65 protein (Vugler et al. 2008) under standard culture conditions. RPE65 is necessary for retinoid recycling, and mutations in RPE65 in humans can produce serious cases of childhood-onset blindness.

D407 is also a spontaneously arising human RPE line but, in contrast to ARPE-19, is transformed and has become anueploid at the current passages. It was derived in 1995 from the globe of the eye of a 12-year-old white male child. It exhibits a multitude of RPE characteristics such as cobblestone morphology, RPE-specific cytokeratins and CRALBP as well as possessing good phagocytic activity (Davis et al. 1995). However, at the time of writing this thesis it has become no longer available.

1.9.3 Iris Pigment Epithelium (IPE):

Iris Pigment Epithelium has been considered as an attractive alternative to RPE cells, and has been extensively studied due to its similar phenotype to RPE (Thumann et al. 1998), shared embryonic origin (Martinez-Morales, Rodrigo, & Bovolenta 2004), it's ability to be harvested during simple anterior ocular surgery, as well as it's autologous nature and virtual lack of immune rejection (Abe et al. 2000). However in vitro studies suggest IPE machinery is not as optimised as RPE machinery for certain secreted RPE proteins such as PEDF, which is minimal in IPE (Ohno-Matsui et al. 2006). In addition, generation of per-patient autologous RPE cultures is necessary which, apart from introducing patient identification and labelling issues, can induce uncharacterised changes in the transplanted cell properties. This has led to occasional host retinal inflammation in humans (Abe et al. 2007).

1.9.4 Human Embryonic Stem Cells (HESC):

Primary RPE cultures prepared from young donors are known to be more active than cultures prepared from older people (Pfeffer 1991). In addition several studies have found RPE primary cultures derived from aborted foetuses to be highly efficient and resemble native tissue in many respects (Maminishkis et al. 2006;Sonoda et al. 2009;Sonoda et al. 2010). Thus embryonic stem cells have become very promising since they not only provide a youthful source of cells, but they are expected to provide more consistency than primary culture as a vast amount of cells can be generated from similar if not identical batches.

The first human embryonic stem cells (HESC) were isolated by Thomson and colleagues in 1998 (Thomson et al. 1998). By the time the international stem cell initiative (ISCI) was established in 2004 over a 100 HESC lines had been derived worldwide (Andrews et al. 2005), and by 2010 a single group from Sweden alone had derived 30 HESC lines (Strom et al. 2010) which was one of 30 articles written by members of ISCI each describing their own experience of derivation (Andrews et al. 2010). This explosion in HESC derivation was accompanied by parallel efforts attempting the conversion of HESC into differentiated tissues. Only 4 years after the

first HESC were isolated by Thomson et al, Kawasaki and colleagues published the first account of in vitro differentiation of primate ESC into pigmented polygonal RPE-like cells in 2002. This was achieved using a primate ESC/stromal cell (PA6) co-culture system (Kawasaki et al. 2002). These RPE-like cells were also positive for paired box gene 6 (Pax6), a marker for all cells deriving from the optic cup, which was a significant finding since during development all ocular pigmented epithelia are positive for Pax6 (Graw 2010) though the Pax6 is eventually absent in RPE at the late optic cup stage (Martinez-Morales, Rodrigo, & Bovolenta 2004). Another study by Kawasaki's colleague Haruta et al followed (Haruta et al. 2004) which demonstrated expression of RPE65, MERTK and CRALBP genes, and suggested further differentiation of these HESC towards the RPE fate. Then a ground-breaking study by Klimanskaya et al (Klimanskaya et al. 2004) showed that HESC are capable of differentiating into RPE-like cells when deprived of FGF even in the absence of feeder layers. This made absolute sense since FGF is a strong repressor of RPE specification in vivo (Martinez-Morales, Rodrigo, & Bovolenta 2004). Klimanskaya also reported the transcriptome of these HESC-RPE was more reminiscent of primary RPE transcriptome than two of the most popular human RPE lines at the time: ARPE-19 and D407 (Klimanskaya et al. 2004).

In 2007 our laboratory reported similar findings to the Klimanskaya group (Vugler et al. 2007) and this led to various improvements on HESC-RPE generation and culture methods that we reported in 2008 (Vugler et al. 2008). In contrast to previous studies, we used only basic HESC medium with neither bFGF nor FCS and our HESC-RPE differentiated fully in 5 weeks despite the lack of exogenously added factors. Indeed our HESC-RPE developed a high degree of differentiation and polarisation with this simplified protocol. We reported by immunocytochemistry (ICC), good expression of CRALBP, bestrophin, and cytoplasmic PEDF as well as both ICC and western blots of RPE65 whereas previous reports, such as the one by Gong et al could not achieve this (Gong et al. 2008). Expression of Pax6, microphthalmia-associated transcription factor (MITF) and orthodenticle homeobox1/2 (OTX1/2) persisted throughout our 2008 study, and this is a welcome finding since these factors are implicated in inititation of RPE specification and pigmentation (Martinez-Morales, Rodrigo, & Bovolenta 2004) although our team never encountered the eventual loss of Pax6 expression in vitro, as is expected of fully developed native RPE. However, our 2008 study demonstrated that upon transplantation into the RCS rat, HESC-RPE distributed under the retina in

laminar sheets or rosettes, were able to phagocytose outer segments and eventually down regulated Pax6. Thus, our team's in vivo transplanted HESC-RPE, unlike their in vitro counterparts, managed to downregulate Pax6 as is expected of mature RPE phenotype. This was a very welcome finding in our 2008 study since Pax6 expression is lost in RPE by the late optic cup phase (Martinez-Morales, Rodrigo, & Bovolenta 2004).

Despite these numerous successes in deriving HESC and differentiating them into HESC-RPE there have been reservations about transplanting these cells in humans, since embryonic stem cells carry the risk of developing into teratomas. Nevertheless preclinical studies on NIH-III immune deficient mice performed by our laboratory as well as other laboratories (Schwartz et al. 2012) provide relative assurance against the risk of subsequent teratomas. Secondly it is not clear how these HESC-RPE cells should be delivered into the eye. I have already mentioned that previous proponents of the cell suspension-injection technique are moving away from this approach for many reasons (section 1.8). Nevertheless Steven D. Schwartz and colleagues performed the first non-placebo controlled trial of HESC-RPE cell-suspension injections as part of a multicentre phase I/II clinical trial (Pan et al. 2013). These suspensions were injected into the subretinal space of AMD and Stargardt's disease human patients and reported findings with photographic as well as tomographic indicators of presumed HESC-RPE attachment. These included an increase in pigmentation in the area of the injection as well as presumed migration towards the central macula, with a corresponding increased hyper-reflectivity immediately above BrM on OCT suggesting the increased pigmentation is consistent with donor RPE. Apart from these presumptions, there was no definitive proof of transplant survival or seeding efficiency. These imaged findings were combined with a modest improvement in vision but this result was not controlled with a placebo arm (Schwartz et al. 2012;Schwartz et al. 2015). As of the time of writing this thesis, there have been no attempts to transplant a cell-substrate composite in humans other than our own planned Pfizer sponsored Phase I trial at Moorfields Eye Hospital which is due to commence during summer of 2015.

1.9.5 Induced Pluripotent Stem cells

In the recent years it has become possible to utilise adult somatic cells to produce stem cells. This is achieved by activation of several embryonic transcription factors in an

adult cell which produces pluripotent cells that are morphologically identical to HESC and share similar transcriptome profiles and epigenetic characteristics as these cells. These induced pluripotent stem (IPS) cells are capable of differentiating into a multitude of tissue types including RPE. Therefore IPS-derived RPE have become an extremely valuable prospect in treatment of AMD (Carr et al. 2009b). The obvious advantage of these cells over HESC is that they can be derived on a per-patient basis to produce autologous cultures of the desired tissue type thus negating the need for powerful immunosuppressants. Alternatively, several HLA-typed cell banks of the desired target tissue can be generated. This latter method may still require some immunosuppression but will allow patients to be transplanted with the most efficient and well characterised cells available (de Rham and Villard 2014). However, IPS cells became available at the time when the majority of the experiments in this thesis had been completed.

1.9.6 Non-ocular cells

Several studies from our lab (Lawrence et al. 2000;Keegan et al. 2003;Lawrence et al. 2004) have demonstrated the ability of non-RPE cells in rescuing photoreceptor degeneration in an RPE disease setting by using cultured Schwann cells in RCS dystrophic rats and rhodopsin knockout (rho -/-) mice. Studies utilising the dystrophic RCS rat demonstrated visual functional rescue for at least 6 months, while the study on on rho -/- mice showed rescue for upto 5 weeks. The mechanism of such non RPE cell-induced photoreceptor rescue is believed to be related to neuro-protective growth factor secretion, since many studies have demonstrated the importance of CNTF, BDNF, GDNF, and bFGF in neural regeneration in the central nervous system (Meyer et al. 1992;Sendtner et al. 1992;Neuberger and De Vries 1993;Hammarberg et al. 1996). Furthermore, the more recent Lawrence study demonstrated a significantly superior photoreceptor rescue by a Schwann cell line when over-expressing GDNF and BDNF, than the non-engineered version of this cell line. A bonus finding was that GDNF over-expressing Schwann cells resulted in longer preservation of vision in the RCS rat than their BDNF counterparts (Lawrence et al. 2004). Thus it has become clear that the photoreceptor preservation by Schwann cells is dependent on their growth factor secretion. Sadly, this is a single documented useful function of Schwann cells and they are not expected to perform other RPE functions such as melanin and visual pigment synthesis and certainly not diurnal phagocytosis of POS.

2

Materials and Methods

2 Materials and Methods

2.1 Cell Culture

Unless otherwise stated, reagents were purchased from Invitrogen (Paisley, UK) and culture plastics from Fisher Scientific (Loughborough, UK). ARPE-19 cells were a kind gift from Naheed Kanuga and John Greenwood (University College London, UK). ARPE-19 cultures were typically maintained in Dulbecco's Modified Eagle's Medium (D-MEM) with 4.5g/L glucose (high glucose), L-glutamine and sodium pyruvate (Gibco, Invitrogen). All ARPE-19 growth media in this thesis were supplemented with 1% heat-inactivated Foetal Calf Serum (FCS). Penicillin-Streptomycin (PS) liquid containing 10,000 units/mL of penicillin and 10mg/mL of streptomycin in 0.85% saline (Gibco, Invitrogen) was added to all culture medium types at a final concentration of 1% to give 100U/mL penicillin and 100µg/mL streptomycin. All additives were filter sterilised using a 0.22µm Millex-GP PES filter unit (Millipore, Carrigtwohill, Co. Cork, Ireland) before mixing with base growth media to maintain sterility. A 90% media exchange was performed twice a week. All cultures were maintained in a humidified incubator at 37ºC with an atmosphere of 5% CO_2 and 95% air. I have reported this method previously which is known to promote differentiation and pigmentation of this cell line (Ahmado et al. 2011). For some experiments cells were maintained in DMEM/F12 (1:1 mixture of Dulbecco's Modified Eagle's Medium and Ham's F12) or other versions of DMEM media. Cell cultures were split when required as follows: cultures were dissociated using freshly prepared 0.25% Trypsin from Porcine Pancreas (Sigma-Aldrich) solution in Dulbecco's Phosphate Buffered Saline without Calcium and Magnesium (DPBS, Sigma-Aldrich) at 37ºC for 10-20 minutes. The reaction was quenched with fresh medium followed by centrifugation in a Heraeus Labofuge 400R (Thermo Scientific, Basingstoke) centrifuge at 1200rpm (280 x g) for 5 minutes, followed by re-suspension in fresh culture medium. The cell passages used in this thesis ranged between p22 – p33. Confluent cultures of ARPE-19 were trypsinised as mentioned above. The resultant cell-suspensions were diluted to the desired cell density. Cell density was measured using a Neubauer® Haemocytometer with Trypan Blue 1:1 dilution. Trypan Blue staining confirmed cell viability to be greater than 93% in every case and typically 95% or more. Cells were either seeded onto Corning Transwell® Polyester filters with a pore size of 0.4µm (Corning, Lowell, Massachusetts), or where the testing of a substrate was required, the commercial polyester was cut out using a

micro-surgical blade and the new substrate mounted onto the remaining Transwell plastic. This was performed by sanding the insert base until all remaining polyester was removed, then mounting the new material using household cyanoacrylate adhesive (Loctite, Henkel Corporation, Avon, Ohio) since this method has been reported previously (Turowski et al. 2004) and since cyanoacrylates have been used extensively in ocular surgery (Refojo et al. 1968;Refojo 1971). Alternatively a biological research grade vinyl-based silicone sealant was used (Kwik-Sil™, World Precision Instruments, Stevenage, Hertfordshire). The mounting procedure was followed by thorough rinsing in sterile DPBS followed by sterilisation with a UV-lamp in a laminar flow hood for 30 – 60 minutes each side. In one series Transwell® Polyester filters with a pore size of 3µm were used to allow population of both sides of the insert membrane. Final cell seeding densities were calculated per unit area and ranged between of 80,000 – 180,000 cell/cm². Higher densities were used for reducing time-to-confluence. Medium in both apical and basal chambers was changed twice a week. In some cases the amount of medium used had to be adjusted in proportion to the time of post-confluence of the culture to avoid senescence. In some cultures this was up to 0.6mL/cm². For example, a 6.5mm inserts with a growth area of 0.3cm² were fed with 180µl when cells became heavily pigmented otherwise senescence could be observed in the insert as localised loss of pigmentation corresponding to cell death.

2.2 Human Embryonic Stem Cell (HESC) Culture

Shef1 HES cells were a kind gift from the Centre for Stem Cell Biology (CSCB) under direction from Professor Peter Andrews and Professor Harry Moore. Shef1 HESC were maintained in pre-prepared flasks T25 that were coated with gelatine 0.1% and subsequently seeded with mitomycin-C inactivated mouse embryonic fibroblasts (MEF; from E14-16 MF-1 mice embryos) at a density of 0.9 - 1 x 10^4/cm² as a feeder layer as described by Draper et al (Draper et al. 2002). Growth medium for maintenance of HESC cells (HESC medium) was prepared as follows: High glucose (4.8 g/L) KnockOut™ Dulbecco's Modified Eagle's Medium (DMEM, Invitrogen) with 20% KnockOut™ serum replacement (KSR; Invitrogen), 1% non-essential amino acid solution (Invitrogen), 1 mM L-glutamine (Invitrogen), 4 ng/mL human basic fibroblast growth factor (bFGF; Invitrogen) and 0.1 mM β-mercaptoethanol (Sigma). For some experiments KSR was reduced to 7%, and FCS was substituted for the remaining added to a final concentration of 5% instead of the remaining KSR (indicated in text as Lanza

et al modification). Media were changed every 2 days and HESC were split regularly (1:4) in order to maintain sufficient undifferentiated HESC colonies. This pluripotency was assessed by staining for the embryonic markers stage-specific embryonic antigens-3 and 4 (SSEA3/4) and keratan sulphate antigens TRA-1-60 and TRA-181.

2.2.1 Induction and expansion of differentiated HESC-RPE colonies

When HESC became confluent (usually 10 days after passage), bFGF was withdrawn from growth medim due to its ability to suppress of RPE phenotype (Martinez-Morales, Rodrigo, & Bovolenta 2004;Moshiri, Close, & Reh 2004). The media changing regime was altered from once every 2 days to once every day using the basic HESC medium detailed above (minus bFGF). Approximately 7-14 days after bFGF withdrawal, pigmented foci started to appear in the culture, and it is these pigmented foci that will give rise to RPE-like cells known as HESC-RPE. Cultures were maintained for a minimum of 5 weeks to enable pigmented foci to achieve a manageable size suited for manual dissection. These pigmented foci were excised manually from the flasks using a micro-surgical blade and a glass Pasteur pipette. Every effort was made to only excise pigmented material to avoid contamination with presumed non-RPE cells. This was only practical when utilising foci of 1mm or greater in diameter. Further purification and amplification of this HESC-RPE was achieved by placing typically 5-10 or more of these pigmented foci in 3.5 cm culture dishes that were coated with either growth factor reduced (GFR-) Matrigel® (BD Biosciences), or its pathogen-tested equivalent Pathclear®, Cultrex® Reduced Growth Factor Basement Membrane Extract (GFR-BME; Trevigen Inc., MD, USA), diluted to a final concentration of 0.35mg/mL. These foci were allowed to grow on Matrigel-coated dishes for a further 5 weeks in HESC medium without bFGF, and media was changed every 2–3 days. This second step yielded pigmented and occasionally non-pigmented expanding foci or sheets of cells. Using a soft plastic Pasteur pipette only pigmented sheets were excised for further studies. These pigmented sheets were presumed to be a pure population of HESC-RPE cells which were further characterised as part of this thesis. Previous experiments in our laboratory have shown this dissection method to be more efficient at generating sheets of HESC-RPE than an embryoid body/re-plating approach (Vugler et al. 2008). HESC-RPE foci or sheets were then either used whole for attachment or transplantation studies, replated whole onto culture-ware or dissociated for re-seeding. Thus our method differs from other published protocols (Klimanskaya et al. 2004;Lund et al.

2006) as follows: 1. For most experiments a higher standardised concentration of KSR is used (20% as opposed to 8-15% variable by Lanza group). 2. We do not use Plasmanate, human leukemia inhibitory factor or bFGF during the production of RPE cells from super-confluent HESC cultures. 3. To date we have not expanded the RPE cells to form cell lines but this can be achieved using a medium containing 5% FCS (Klimanskaya et al. 2004;Lund et al. 2006).

2.2.2 Dissociation of HESC-RPE to generate cell suspensions

For most experiments HESC-RPE foci were dissociated and re-seeded using a novel method which I devised (see section 7.4 for more details). Briefly, in a process very similar to dissociation of other cell lines, HESC foci/sheets were incubated at 37ºC with 1:10 dilution of 2.5% Trypsin from porcine pancreas using a proprietary non-enzymatic dissociation buffer as a diluent (Sigma-Aldrich) for 20-30 minutes (final trypsin concentration 0.25%) and subsequently washed and eventually resuspended in HESC medium ready for seeding.

2.2.3 Assembly of custom plastic filters onto culture inserts

Original filters were excised from 6.5mm Transwell Polyester inserts and discarded. 13mm polyester filter discs with a pore size of 0.4µm (Sterlitech, Kent, WA, USA) were attached to the inserts in place of the original filters using a biological grade vinyl-based silicone elastomer (Kwik-Sil, World Precision Instruments Inc. Sarasota, Florida). The inserts were rinsed once in PBS, air-dried, and irradiated with a UV lamp in a laminar-flow hood for 30 minutes each side for sterilisation. Sterilised inserts were then stored in a sterile laminar flow hood.

2.2.4 Coating and Seeding of the prepared culture inserts

Sterilised inserts were coated with 1:30 diluted Growth Factor Reduced Matrigel (GFR-MG) for 30 minutes at 37ºC. Matrigel was aspirated immediately before cell seeding. Cell density of the HESC-RPE suspension was measured using a Neubauer® Haemocytometer with Trypan Blue 1:1 dilution. Lack of staining was used to confirm cell viability which was greater than 93% in every case. Cells were seeded at densities between 50,000 - 450,000 cell/cm², however cultures required a minimum seeding density of 200,000 cell/cm² to maintain pigmented polygonal phenotype. Phenotypic instability was observed at seeding densities below 100,000. Typically HESC-RPE were seeded between 350,000 – 410,000 cell/cm² for experiments aimed at achieving optimal

RPE phenotype (the rationale is obtained from the result of one of the outlined HESC experiments). Seeded cells were allowed to attach for at least 24 hours and typically 48 hours before the first media change. Media were changed 3 times a week thereafter.

2.3 Extra-Cellular Matrix Coatings and Other Non-ECM Coatings

2.3.1 ECM Coatings

All ECM coatings were implemented as per manufacturer's instructions unless stated otherwise. Thawing of ECM samples was done at 4ºC overnight or on ice for at least 2 hours to avoid gelling (clotting) of temperature sensitive ECM. Pipette tips and tubes were chilled in a refrigerator prior to use. Media used for dilution of ECM samples were used directly from the refrigerator. This was to minimise loss of ECM through gelling of solution against warm surfaces. Coatings were usually incubated at 4ºC overnight or at 37ºC for 30 – 120 minutes depending on protocol. Any rinsing thereafter was performed with warm solutions only. As an additional step, a murine collagen IV from Murine Engelbreth-Holm-Swarm (EHS) tumor (R&D Systems Inc., Minneapolis, MN, USA) was required to dry for 2 hours before use as instructed. For some experiments, ECM coatings were visualised with scanning electron microscopy (SEM) to confirm success and extent of coating (not shown). GFR-MG is received from manufacturer at a concentration between 9-12mg/mL. This was diluted 1:30 and used at 100-200µL/cm². This corresponds to a final working concentration of 35-70µg/cm². Since the pathogen-tested Pathclear® version of matrigel (Cultrex™) is received at a higher concentration (12-18mg/mL) it was necessary to dilute it 1:40 to achieve the same working concentration.

For peptide coatings please refer to the separate heading within this methods chapter. All other non-ECM coatings were applied infrequently and will be described in individual methods within experimental chapters.

2.4 AlamarBlue® Cell Viability Assay

AlamarBlue® was purchased from Invitrogen (Paisley, UK). Experimental cell cultures mounted in 6.5mm inserts (Costar) or 96-well plates were synchronised by serum-

starvation for at least 24 hours after seeding onto experimental membranes. At the given experimental time points, cells were washed with phenol red-free Hank's balanced salt solution (PRF-HBSS), followed by incubation of apical chamber with 200µL of 1:10 alamarBlue:PRF-HBSS solution for 45 minutes at 37ºC. During dye incubation the basal chamber was left empty. This doubled as a water-tightness test for glued experimental membranes. Leaking membranes were discounted from the assay. Supernatants were collected after the incubation period and samples were pipetted into a 96-well plate for reading by a fluorescence reading machine (FLUOstar OPTIMA fluorescence plate reader, BMG Labtech GmbH, Offenburg, Germany). Following the alamarBlue assay cultures were fed and returned to the incubator, or fixed and stained for ICC.

.

2.5 Poly(D,L-Lactide)-co-Glycolic Acid (PLGA)

PLGA membranes were a kind gift from Erin B. Lavik and Robert Langer (Department of Chemical Engineering, MIT, Cambridge, Massachusetts). PLGA material was originally purchased by our collaborators as Resomer® 503H (Boehringer-Ingelheim, Ingelheim, Germany), and asymmetric PLGA membranes were synthesized in a process described previously by these authors (Lavik et al. 2001;Lavik et al. 2002). This asymmetric profile allows cell attachment to the smooth upper surface while also allowing cells to communicate with the basal environment through the polymer's highly-porous lower side. PLGA asymmetric membrane was mounted onto 6.5mm Corning Transwell® inserts (Corning, Lowell, Massachusetts). The original polyester filters were removed from the inserts, and PLGA membrane mounted using household cyanoacrylate adhesive (Loctite, Henkel Corporation, Avon, Ohio). These composite inserts were sterilized by exposure of each side to a UV lamp in a laminar flow hood for 30-60 minutes. Passage 28 ARPE-19 cells were seeded onto the glossy surface of membranes at a density of 150,000 cell/mL. This would correspond to a final seeding density of 90,000 cell/cm².

In another series, asymmetric PLGA membrane was mounted onto empty inserts (as above). The inserts as well as tissue culture polystyrene dishes (for control) were coated with laminin-1 at a standard working concentration of 2µg/cm² (Sigma-Aldrich, derived from the murine Engelbreth-Holm-Swarm tumour). Both dishes and inserts were then seeded with p30 ARPE19 at the higher density of 180,000 cell/cm² to reduce time to

confluence. Cultures were maintained with DMEM x1 + 4.5g/L glucose +L-glutamine +pyruvate with 20mM Hepes Buffer to control pH and hence prevent degradation of the polymer. This was important since polymer degradation into lactic and glycolic acids, visibly reduced pH as was apparent from the colour of phenol red within the growth medium. The buffer would therefore help prolong the lifespan of the polymer and ultimately the integrity of the cellular component.

2.6 Trans-epithelial Resistance and Impedance

Trans-epithelial resistance (TER) measurements were taken at 1.5 – 2 weekly intervals or in proportion to the duration of culture post-seeding. This was to assess confluence and junctional maturation. Measurements were taken using an EVOM® with an STX2 electrode (World Precision Instruments Inc. Sarasota, FL, USA). All measurements were performed at ambient temperature within 5 minutes of removal from the incubator. Only one tray of inserts/cultures was removed from the incubator at one time, and measurements were performed as quickly as possible following removal, within 5 minutes. This was to avoid temperature-related changes in TER (Gonzalez-Mariscal, Chavez de, & Cereijido 1984). At least 2 and up to 5 measurements were taken per culture, and the final raw TER value was the average. Blank readings were obtained from all inserts after necessary matrix coatings were applied without cells i.e measurements taken after coatings but before cell seeding. Blank inserts were incubated in media at least 2 hours prior to measurement to ensure complete wetting, then an average blank reading was measured per culture. For future TER readings from cellular inserts, the blank value was subtracted from raw TER readings and the outcome was multiplied by the insert growth area (cm^2) to give the final TER value (Ohm x cm^2). For some experiments involving HESC TER, readings were taken using an EVOM® with a modified (shortened) STX2 electrode (World Precision Instruments Inc. Sarasota, Florida) in order to eliminate possible contact with cells. The STX2 was modified by sanding the short arm by 0.5mm as per manufacturer's guidelines, and this was performed by our institution's workshop using professional precision tools. This protocol provided the most consistent results for the STX2 electrode in my experience of TER with the EVOM.

Some TER experiments utilising peptide coatings were confirmed and corroborated successfully with impedance sensing (impedance data not shown). This was tested using

an Electric Cell-substrate Impedance Sensing system (ECIS Model 1600R; Applied Biophysics Inc., Troy, New York). ECIS multi-chamber slides were treated as usual, and were coated with identical batches of the test substrate/coating as the non-ECIS slides. The only difference is ECIS chambers have a unique square design and a 0.9 cm² growth area for the cells.

2.7 Immunocytochemistry

Most of our methods and antibodies have been described in detail previously (Vugler et al. 2008). Samples were fixed in either ice-cold 100% methanol for 5 minutes, or 2 – 4% paraformaldehyde (PFA) for 30 minutes. Following gradual rinsing (for methanol), or complete (for PFA) rinsing with PBS, samples were blocked in either PBS plus 0.5% bovine serum albumin (BSA) for at least 1 hour (methanol fixed samples) or 5% donkey serum (PFA-fixed samples; Jackson ImmunoResearch, West Grove, PA, USA) with 0.15 – 0.3% Triton in phosphate buffered saline.. This was followed by overnight incubation at room temperature (slides in a humidified chamber) or at 4°C (cells in dishes). The primary antibody solution was made up in PBS using an identical solution to the blocking solution (0.5% BSA or 5% donkey-serum) and included one or a combination of several of the following antibodies: **Mouse monoclonals:** Na^+,K^+-ATPase (Na,K-ATPase; 1:100, Abcam); Cytokeratin 8 (1:2000, Chemicon); Pax6 (1:1000, DSHB); PMEL17 (1:100 Dako); Cellular Retinaldehyde Binding Protein (CRALBP, 1:1000, Affinity BioReagents); RPE65 (1:500, Chemicon); Bestrophin (1:200, Chemicon); Pigment Epithelium Derived Factor (PEDF, 1:1000, Chemicon); Human Nuclear Antigen (HNA, 1:1000, Chemicon); TRA-1-85 (1:10, Peter Andrews laboratory, University of Sheffield); βIII tubulin (1:1000, Chemicon); Claudin-5 (1:25 – 1:50, Zymed); **Rabbit polyclonals:** Claudin-1 (1:200, Zymed, Invitrogen); Claudin-2 (1:50, Zymed); Claudin-3 (1:100, Zymed); Occludin (1:500, Zymed); ZO1 (1:50, Zymed); Mitf (1:1000, Chemicon); Pax6 (1:300, Covance); OTX1/2 (1:1000, Chemicon); Laminin (1:50, Dako); Collagen IV (1:100, Morwell Diagnostic Biosciences); Ki67 (1:2000, Vector labs); MerTK (1:50 – 1:250, Abcam); MCT3 (1:100, Alpha diagnostics) .**Other polyclonals:** goat anti-claudin-3 (1:100, Santa Cruz); goat anti-OTX2 (1:500, Santa Cruz); goat anti-Sox2 (1:500, Santa Cruz); goat anti-MCT1 (1:100, Serotec).

Antibodies were visualised by incubation in fluorescent secondary antibodies (Jackson ImmunoResearch). Phalloidin staining for F-Actin (Actin) was done with either Oregon Green® 488 phalloidin (1:500, Molecular Probes, Invitrogen; kind gift from Dr. Patric Turowski) or Phalloidin–Tetramethylrhodamine B isothiocyanate (Phalloidin-TRITC; 1:50, Sigma-Aldrich; courtesy of John Greenwood) at the secondary antibody stage. Cell nuclei were counterstained with 4'6-diamindino-2-phenylindole dihydrochloride (DAPI, 1:5000, Sigma-Aldrich, Dorset, UK), and samples mounted in Vectashield® (Vector Labs, Peterborough, UK).

Secondary antibody staining was as follows: After rinsing 3 times in PBS, samples were incubated either at room temperature for 2h or overnight at 4ºC in appropriate combinations of fluorescent secondary antibodies (all raised in goat, diluted 1:100-1:200 in PBS with 5% BSA or 2% donkey serum and conjugated to either fluorescein isothiocyanate (FITC), tetramethylrhodamine (TRITC) or cyanine 5.18 (Cy5). The secondary antibodies were from Jackson ImmunoResearch and are specifically designed for multiple labelling, being pre-adsorbed to various species, including rat and human. After washing, cell nuclei were counterstained with DAPI (4'6-diamindino-2-phenylindole dihydrochloride, Sigma-Aldrich), washed in PBS and mounted with Vectashield (Vector Labs).

2.8 Phase Microscopy

Phase microscopy was conducted with a Leica DM IL inverted contrasting microscope which is designed for work with liquid-containing live cell cultures. A suitable 10X, 20X or 40X phase optic (marked PH) was selected. Phase images were captured with a specifically designed Leica DC200 colour digital camera. Subsequently, manual digital subtraction for some phase images was performed with the Subtract Background process found in ImageJ version 1.42q software (Abramoff, Magelhaes, & Ram 2004) using a rolling-ball radius of 25 pixels.

2.9 Cell Counting

For some experiments quantification of seeded ARPE-19 cells was performed by cell counting. At the given time point, for each culture well three phase contrast micrographs were randomly chosen and captured using a 10x objective and this was in turn performed in triplicate (n = 3). One experiment was run in quadruplicate (n = 4) but

a very large number of cells became adherent so counting of 10x fields was not feasible. In this case five randomly chosen micrographs were captured using a 40x objective instead. Microscopic fields were captured by randomly moving the platform horizontally and vertically just before attempting microscopic examination. This was repeated until several acceptable non-overlapping frames were captured. Average cell counts were calculated per well and was considered representative of the individual well. Since several wells existed per group, comparisons of cell counts were made by statistical methods (section 2.19).

2.10 Electron Microscopy

All of the chemicals and consumables used to prepare specimens for electron microscopy were obtained form Agar Scientific, Stansted, UK) and unless otherwise stated, all steps were carried out at room temperature with a rotator used during alcohol dehydration. Cell monolayers grown on filters were fixed in a mixture of 3% (v/v) glutaraldehyde and 1% (w/v) PFA in 0.08M sodium cacodylate buffer (CB), pH 7.4 for 2 hours at room temperature or 12 hours at 4ºC. Following two brief rinses in CB, specimens were osmicated for 2 hrs in 1% (w/v) aqueous osmium tetroxide, dehydrated by 10 minute incubations in 50%, 70%, 90% and 3 x 100% ethanol. At this point specimens destined for examination by SEM were either critical point dried using carbon dioxide as the transmission medium or air dried following two 5 minute passages through hexamethyldisilazane. Once dried, specimens were mounted on conductive carbon and sputter coated with gold-palladium using an Emitech K 550 sputter coater (Emitech, Ashford, UK) prior to imaging in a JEOL 6100SEM operating at 15kV. Digital images were recorded using JEOL Semafore software.

Following the last change of absolute alcohol, specimens for transmission electron microscopy (TEM) were passed through two 15 minute incubations of propylene oxide (PO) and placed in a 50:50 mixture of PO:araldite and left to infiltrate overnight. This solution was changed for 100% araldite and infiltration continued for a further 4 -16 hours, prior to embedment in fresh araldite and overnight curing in a 60ºC oven. Semi-thin sections (0.75µm) for light microscopy and ultra-thin sections (50 – 70nm) for electron microscopy were cut with diamond knives (Diatome/Leica , Milton Keynes, UK). Semi-thin sections were stained with 1% toluidine blue/borax mixture at 60ºC and ultra-thin sections with Reynold's lead citrate. Stained ultra-thin sections were

examined in a JEOL 1010 TEM operating at 80kV and images recorded using a Gatan Orius B digital camera and Digital Micrograph software.

2.11 Peptide Assays

All peptides were purchased from Sigma-Aldrich. All peptides were reconstituted in double-distilled water, and filter sterilised using a 0.22μm Millex-GP PES filter unit (Millipore) to maintain sterility. Sonication was necessary for some peptides that did not spontaneously dissolve. Peptide solutions requiring sonication were placed in an ice-immersed vessel and sonication was performed in a Soniprep 150 sonicator (MSE, London) for up to 30 minutes. Sonicated solutions were sterile filtered as above. Experimental surfaces were incubated with high concentration peptide solutions (25 – 250 μg/cm²) for at least 12 hours at 4ºC. This concentration range exceeds the binding capacity of even the most avid plastic surfaces designed for immunoassay (Stevens and Kelso 1995). This was done in order to saturate the surface of the substrate and to favour maximum cell adhesion (Neff, Caldwell, & Tresco 1998). Peptide-incubated surfaces were then washed thoroughly with PBS (3 rinses), and blocked for 1 hour with 1% FCS at 37ºC prior to seeding with cells in order to minimise non-specific adhesion.

2.12 ELISA for VEGF and PEDF

Secreted vascular endothelial growth factor (VEGF-A) was measured using an enzyme-linked immunosorbent assay (Elisa) as follows. Unless specified, at 10 weeks post-seeding, media were collected 4 days after the last media change from apical and basal chambers of 6.5mm and 24mm Transwell® inserts. Samples were either kept on-ice or at 4ºC and processed the same day or otherwise stored at -80^{o}C. Elisas were conducted on conditioned experimental media (n = 3 per treatment group) using the RayBio® Human VEGF ELISA Kit (RayBiotech, Inc., Norcross, GA) according to manufacturer's guidelines. Each individual sample was further run in duplicate. Plates were read with a FLUOstar OPTIMA fluorescence plate reader (BMG Labtech GmbH, Offenburg, Germany) and the concentration of VEGF extrapolated from a VEGF standard curve for each sample. Secreted VEGF was measured in pg/cm²/24 hours. Total VEGF was calculated for each insert as the sum of apical and basal values. PEDF was measured as for VEGF (above) using the Millipore-Chemicon Chemikine™ PEDF

Elisa kit (Millipore). Total PEDF measurements were enabled by an additional 8M urea extraction step as indicated by the manufacturer.

2.13 Quantitative real-time PCR

Cells were twice washed in PBS and RNA extracted using TRIzol reagent (Invitrogen) according to the manufacturers protocol. Three micrograms of RNA were digested with RQ1 DNase (Promega, Southampton, UK) to remove genomic DNA. First strand cDNA was synthesised using Superscript III Reverse transcriptase and an oligo-(dT)20 primer (Invitrogen) in a total volume of 20µl for 1 hour at 50^{o}C. For each sample a control reaction containing no reverse transcriptase was prepared (NRT). Following cDNA synthesis all reactions were treated with RNase H (Invitrogen).

Quantitative PCR was performed on a 7900HT Fast Real-Time PCR System (Applied Biosystems, Warrington, Cheshire, UK). Triplicate PCR reactions were prepared for each cDNA sample (n=3 per treatment group) using 0.2µM intron-spanning gene specific primer (Eurofins MWG Operon) and Power SYBR Green PCR Master Mix (Applied Biosystems) in a total reaction volume of 25µl. Non-template controls (NTC) and NRT controls were also prepared for each primer set. The PCR cycle parameters consisted of an initial denature step of 95^{o}C for 10 minutes followed by 40 cycles of 95^{o}C for 15sec and 60^{o}C for 30 sec. Results were collected and analysed in SDS 2.2.2 (Applied Biosystems). Data was exported to DART-PCR (Version 1.0)(Peirson, Butler, & Foster 2003) to calculate Ro values, which were then normalised to the geometric mean of the reference genes, Gapdh, β-tubulin (Tubb) and β-2-microglobulin (B2M). Primer specificity was tested by electrophoresis, sequencing and melt curve analysis. Amplification was not observed in the NTC and NRT controls.

2.14 Western Blots

ARPE-19 cells were cultured for 3 months as above and harvested from 24mm inserts. Western blotting was performed in triplicate. ARPE-19 cells were placed on ice, washed with ice-cold PBS and harvested by scraping in cell lysis buffer (10mM HEPES, 1% Triton, 150mM KCl, 1mM PMSF, 10ng/mL Leu, 1mM DTT, 50ng/mL Aprotonin, 10mM NaF, 100µM Sodium Vanidate). Samples were incubated at 4^{o}C on a tube roller for 30min and then centrifuged at 13,000rpm for 30mins to pellet cell debris.

Supernatants were collected and the protein content determined for each sample using Biorad Protein assay reagent (Bio-Rad, Hertfordshire). Samples were diluted (1:1) in Laemmli sample buffer and denatured at 100^{o}C for 5min. Equal amounts of protein were separated on a 10% SDS-PAGE gel alongside a protein marker (Bio-Rad). Separated proteins were transferred to Hybond-P membrane (GE Healthcare Life Sciences, Buckinghamshire) by electrophoresis in 1xTRIS/Glycine buffer (AGTC Bioproducts, Yorkshire) containing 20% methanol.

Membranes were blocked in 10% milk in 0.05% Tween-20/PBS for 2 hours at room temperature prior to incubation with the following primary antibodies overnight at 4^{o}C: **Mouse monoclonals:** CRALBP (1:2000, Affinity BioReagents, CO, USA), Cytokeratin8 (1:2000, Millipore, Watford), RPE65 (1:2000, Millipore) and PEDF (1:500, Millipore). **Rabbit monoclonals:** MerTK (1:500, Abcam, Cambridge), and Tyrosinase (1:2000, Abcam). Membranes were washed in 0.05% tween-20/PBS and incubated with HRP conjugated secondary antibodies (Dako, Cambridge) in blocking solution for 45mins at room temperature. After 2 washes in 0.05% Tween-20/PBS membranes were incubated in LumiLight western blotting solution (Roche, Hertfordshire), and proteins detected by exposure to autoradiographic film. Blots were stripped by immersing in 8M Guanidium-HCl and re-probed with primary GAPDH antibody (1:1000, Goat Polyclonal, Everest) as a loading control. Protein levels were quantified by densitometry of western blot film using ImageJ software (Abramoff, Magelhaes, & Ram 2004) and protein expression normalised to GAPDH.

2.15 Phagocytosis Assay - Human Photoreceptor Outer Segments

Surplus retina was collected from a patient undergoing retinal translocation surgery at Moorfields Eye Hospital. Requirements of the Central Office for Research Ethics Committees (COREC, UK) and the UK Human Tissue Authority (HTA) were fully adhered to. Thus, the study adhered to the tenets of the Declaration of Helsinki. ARPE-19 was seeded onto GFR-MG-coated cellulose filters (Millicell®, Sigma-Aldrich) and maintained in high glucose DMEM with pyruvate for 10 weeks prior to co-culture. The retinal explant was incubated with cell cultures for up to 48 hours using a method described previously (Carr et al. 2009a). The ARPE-19 cells, substrate plus neural retina composites were fixed for TEM at 24 and 48 hours after co-culture.

2.16 Cellular Regularity Index

For one experiment, in order to analyse the morphology of HESC-RPE cells, a cellular regularity index was calculated. This was done by implementing a method to quantify cellular regularity using triangulation between the centre of adjacent cells reported previously (Dryden, Taylor, & Faghihi 1999). The method uses a scaleless statistical algorithm based on the coefficient of variation between the squared sizes of triangles generated from Delaunay triangulations of sampled regions of RPE which our laboratory has used previously (Vugler et al. 2008). RPE morphology from monolayers of dsHESC-RPE were analysed from 3 separate regions of HESC-RPE within each experimental group. The regularity algorithm was implemented in MatLab (Mathworks Inc., Mass, USA).

2.17 Pyruvate Transport Inhibition

A well established reversible pyruvate transport-inhibitor alpha-cyano-4-hydroxycinnamate (Halestrap and Denton 1975) (4-CIN; Sigma-Aldrich) was dissolved in pure dimethyl sulfoxide (DMSO; Sigma-Aldrich), and diluted into high glucose DMEM with 1mM pyruvate. 4-CIN was adjusted to final concentrations of 50μM and 500μM. DMSO concentration was adjusted in all experimental media including control media to 0.1%. ARPE-19 cells in this category were cultured as above for 3 months.

2.18 Karyology

A private karyotyping service (TDL Genetics, London) was utilised. A total of 17 ARPE-19 cells (p26) were karyotyped. Briefly, cells were treated with Colcemid (Sigma-Aldrich) and dividing cells were removed by trypsinisation. Following three cycles of fixation, centrifugation and re-suspension, cells were dried on a slide. Slides were aged in a drying oven, then trypsinised, rinsed and stained with 3:1 Leishman/Giemsa (Merck KGaA, Darmstadt, Germany). Slides were examined for metaphases using high power objectives.

2.19 Statistics

Stastical analysis was conducted with the SPSS and Sigmastat software. One-way analysis of variance followed by a Tukey's HSD multiple comparison test was used to compare more than two groups. Repeated measures (two way) ANOVA was used for data with multiple time points. A 2-tailed value of $p < 0.05$ was considered significant. All data was checked for normality, and homogeneity of variance. The latter was tested with Levene's F test for means or medians. A non-parametric Levene's F test was conducted for groups that did not satisfy the original Levene's test. Sphericity and homogeneity of covariance matrices was satisfied for experiments involving repeated measures ANOVA, or greater than one-way ANOVA. For one experiment the Student-Newman-Keuls analysis was used. Unless stated, all experiments were conducted at least in duplicate or repeated at least twice on different occasions.

3

Poly Lactic-co-Glycolic Acid (PLGA) as a Substrate for ARPE-19 Cells

3 Poly Lactic-co-Glycolic Acid (PLGA) as a Substrate for ARPE-19 Cells

3.1 Introduction

The availability of Poly Lacto-Glycolic Acid as a medical grade bio-degradable substance, its approval by the FDA, and its extensive history of clinical use which is now approaching its third decade (Yang et al. 2001;Porjazoska et al. 2004;Tomita et al. 2005) attracted our interest in PLGA. Also known as Poly [D,L-Lactide-co-Glycolide] or PDLLGA, PLGA is a mixture (co-polymer) of two α-hydroxy-ester polymers which are approved for human use (Lu et al. 2009). These two components are: (1) poly D,L-Lactide, a polymer of lactate dimers where each dimer consists of one D- (dextro) and one L- (laevo) version of lactic acid (D,L-Lactide or mesolactide). (2) poly-glycolic acid (poly-glycolide), a polymer of a naturally occurring acid. These two polymers are then combined during a manufacturing process in the desired proportion e.g. 50:50, 70:30 etc. to produce PLGA.

PLGA degrades mainly through bulk erosion (as opposed to surface erosion) in an aqueous environment by hydrolysis of its chemical bonds (Lu, Garcia, & Mikos 1999;Lu et al. 2000). This means that water can penetrate the polymer and degrade the whole structure rather than just attack the surface. There is also evidence that enzymes may indirectly play a role in degradation by rapid removal of degradation products and modulation of the environment pH, and water content (Cai et al. 2003). Most studies are in agreement that the rate of hydrolysis is dependent on the ratio of the hydrophilic glycolide to the hydrophobic lactide polymers from which the co-polymer mixture is made. For example, a 50:50 ratio of poly-lactide to poly-glycolide degrades quicker than a mixture of 75:25 both in vitro and in vivo settings i.e. the higher content of hydrophilic glycolic acid units within the polymer promotes faster degradation (Lu, Garcia, & Mikos 1999;Yang et al. 2001;Thomson et al. 2011). This process is also proportional to temperature, and water content of the solution, and inversely proportional to pH (Yoshioka et al. 2008) and molecular weight i.e alkalinity and high molecular weight slow down the bio-degradation (Thomson et al. 1996;Lu, Garcia, & Mikos 1999;Cai et al. 2003). Since PLGA degradation yields the acidic monomers lactate and glycolate, this further accelerates degradation, a phenomenon known as

autocatalysis. This results in an "S-curve" rapid degradation in the polymer (Cai et al. 2003).

3.2 Results

3.2.1 Degradation of PLGA

Degradation of PLGA can be monitored in solution, and was seen as a reduction of the size of the membrane to complete disappearance. Proportionately to this degradation, acidification of the ambient solution due to release of lactic acid and glycolic acid monomers occurred with a resultant drop in pH. After incubation at 37ºC with an atmosphere of 5% CO_2 and 95% air for 1 week PLGA degraded rapidly in Hank's balanced salt solution (HBSS), but less so in growth medium (DMEM/F12 with 1% FCS). Equal sized PLGA fragments were compared in equal volumes of solution. PLGA membrane was reduced to a thin string of white sediment in HBSS, whereas the membrane appeared largely intact in growth medium (Figure 3.1, arrows). Additionally, the phenol red indicator was bright yellow (pH must be below 6.8) in HBSS but orange in growth medium (pH is approximately 7.5; Figure 3.1) further indicating PLGA degradation had occurred to a larger extent in HBSS. This difference in degradation was attributed to the well known bicarbonate buffering capacity of growth medium, in addition to the natural buffering provided by anionic proteins in the FCS component of growth medium (e.g albumin).

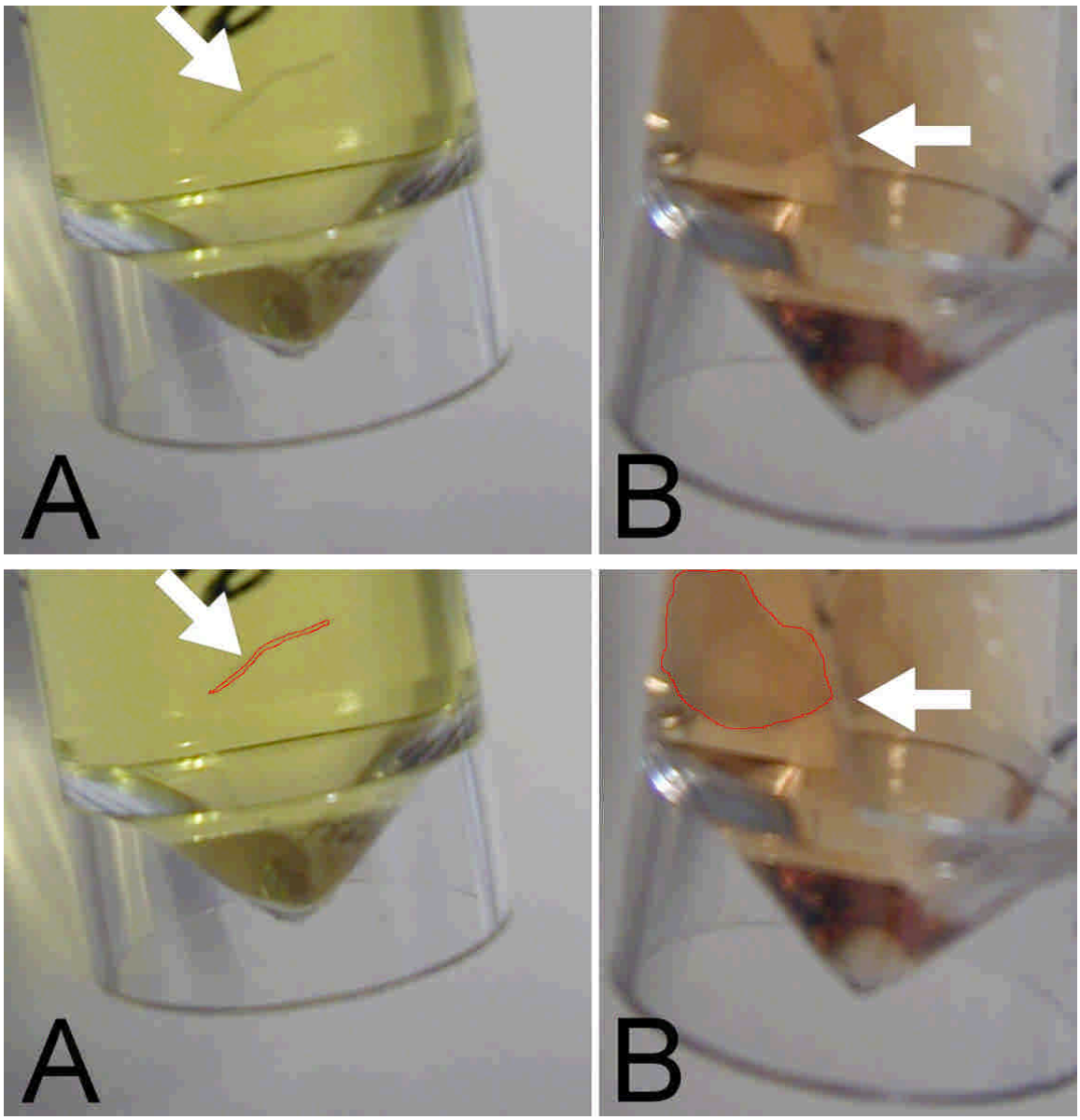

Figure 3.1 Degradation of plain PLGA membrane in equal solution. A) Degradation of PLGA in HBSS is more rapid and resulted in a thin linear sediment (white arrow) along the wall of the universal tube. B) Degradation in growth medium is more subtle and integrity of the membrane (white arrow) is preserved. The membranes are also circumscribed in red to aid visualisation (lower panels).

3.2.2 Scanning Electron Microscopy to confirm structure

SEM on a dry, unused membrane confirmed the asymmetric profile of the PLGA membranes (Figure 3.2). A low voltage Field Emmission Scanning Electron Microscope (FESEM) was used since traditional SEM visibly affected the integrity of the membrane by causing real-time deformation and disintegration due to its higher voltage (not shown). The FESEM confirmed the presence of a smooth surface which was designed for cell attachment while the rest of the polymer appeared to have a porous structure. This highly-porous lower side forms a larger surface area which is intended to allow

diffusion of nutrients across the polymer thus allowing communication between the cells' basal side and the surrounding basal environment (Figure 3.2).

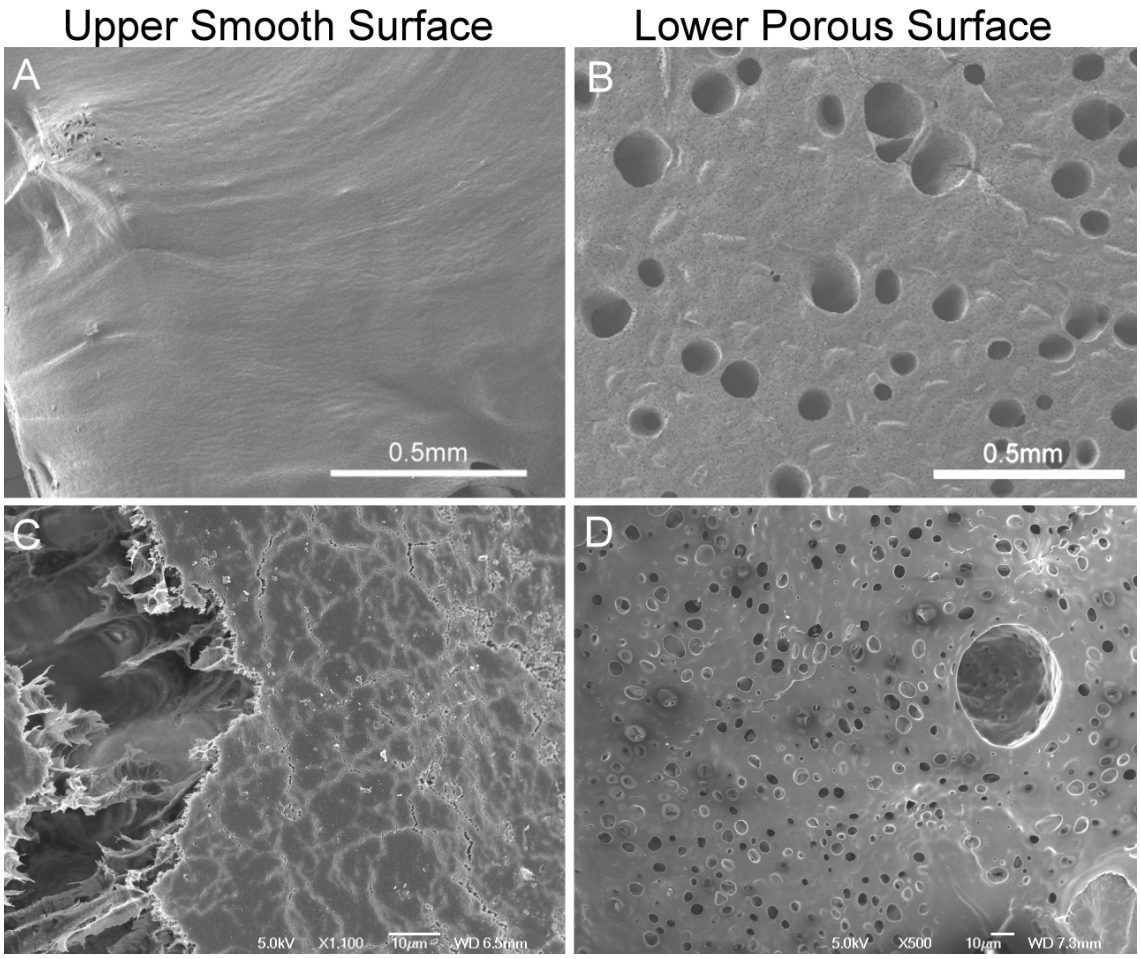

Figure 3.2. Low Voltage Field Emission Scanning Electron Microscope (FESEM) views of upper (A, C) and lower (B, D) surfaces of Resomer® 503H PLGA asymmetric membrane. (A and B) Low magnification. (C and D) High magnification. The magnification of C (x1,100) is twice that of D (x500) to emphasise smooth surface details which are usually more difficult to discern. (Courtesy of Peter Munro and the Ear Institute who granted permission for use of their FESEM)

3.2.3 Uncoated PLGA as a substrate for ARPE-19 cells

3.2.3.1 Immunocytochemistry

ARPE-19 cells adhered to, and proliferated on PLGA as confirmed by ICC. Na,K-ATPase is an essential trans-membrane ion transporter that moves three sodium ions out and two potassium ions into the cell per pump cycle (Rajasekaran et al. 2003). It has been described extensively as an epithelial marker expressed apically in native RPE cells (Rizzolo 1990;Okami et al. 1990;Hu & Bok 2001). Cultures were positive for

Na,K-ATPase from week 1, and by week 3 basolateral staining was evident. While the in situ RPE normally expresses Na,K-ATPase apically, cultured RPE cell lines are known to express this protein basolaterally unless the media is optimized (Hu & Bok 2001). There was some weak ZO-1 junctional staining at 1 week, but at 3 weeks cultures were strongly immune-positive for ZO-1. Occludin was also detected although the signal was weaker than for ZO-1 (not shown). However, it was observed during the course of the experiment that the PLGA membrane became considerably swollen to at least twice its size, and this was confirmed later when the membrane was fixed and mounted. During mounting of the membrane, it was found to be disintegrating to the point of being very soft with an almost gel-like consistency (not shown). A similar observation has been reported previously for PLGA, especially where the co-polymer ratio was 50:50 (Lu, Garcia, & Mikos 1999;Cai et al. 2003).

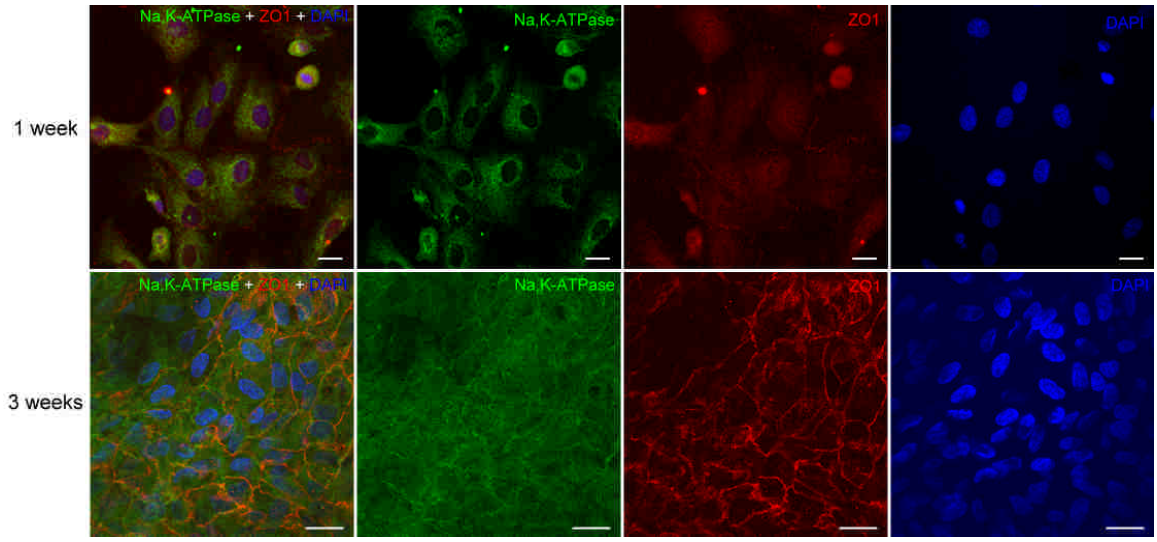

Figure 3.3. Distribution of RPE markers in ARPE-19 cells grown on PLGA for 1 or 3 weeks. Junctional ZO-1 expression is faint at 1 week, compared to 3 weeks. Na,K-ATPase expression is cytoplasmic after 1 week whereas it lateralises after 3 weeks. DAPI staining shows healthy nuclei and confirms viability at the time of fixation. Bars = 20µm.

3.2.4 Coated PLGA as a substrate for ARPE-19 cells

The aim of coating the PLGA membrane with laminin was twofold: Firstly, a coating on the membrane would, in theory, impede access of water molecules to the body of the polymer structure and therefore delay the hydrolytic degradation process. This was felt necessary since in the first experiment, it was observed that the polymer degraded considerably and lost most of its consistency (above). Second, the ARPE-19 cell line is

reported to respond favourably to a laminin coating with improved differentiation characteristics (Dunn et al. 1996). ARPE-19 cells proliferated and showed good morphology and ICC profile when compared to growth on uncoated tissue-culture polystyrene (TCPS). This profile is not significantly different from that on uncoated PLGA at the same time point (3 weeks; compare Figure 3.3 and Figure 3.4).

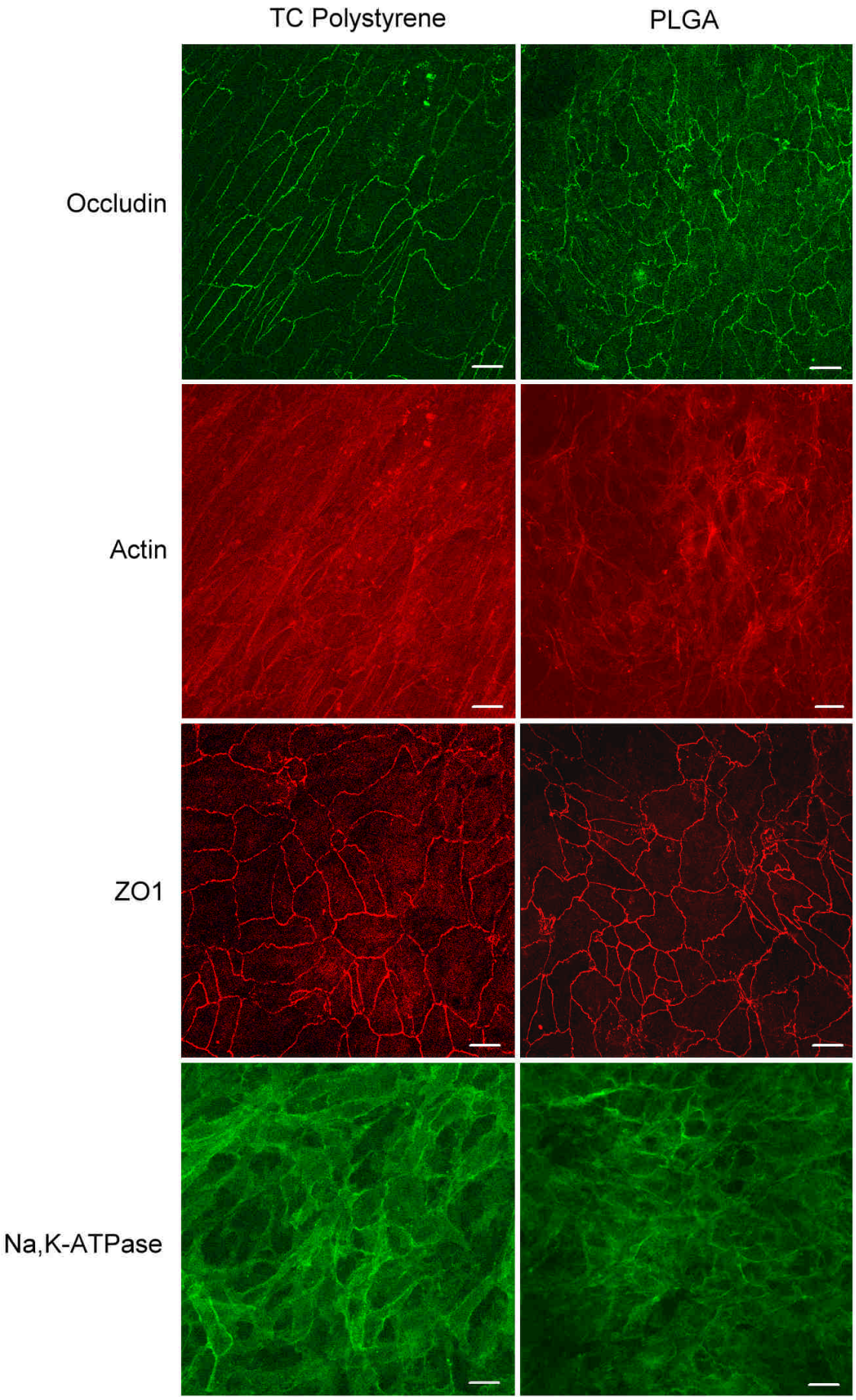
TC Polystyrene
PLGA
Occludin
Actin
ZO1
Na,K-ATPase

Figure 3.4. Distribution of RPE markers is similar in RPE cells grown on laminin-coated PLGA versus tissue culture polystyrene at 3 weeks. However it is apparent that RPE morphology is consistently elongated in the TCPS group compared to the more rounded cells in the PLGA group, the latter being a better sign of differentiation. Na,K-ATPase appears basolateral in any condition.

3.3 Conclusion

PLGA is a suitable substrate for culturing of RPE cells per se in vitro. However there are several concerns from a transplantation perspective. Its degradation yields acidic monomers that acidify growth media. This visible pH change is un-welcome as it may exceed the buffering capacity of a limited potential space such as the subretinal compartment. Furthermore, the initial swelling (doubling of size; not shown) followed by the rapid loss of size that a PLGA membrane undergoes may result in untoward structural shift that will not only affect the placement of the overlying RPE cells but also the viability of these cells as the RPE are anchorage-dependent cells by nature. Furthermore, PLGA membranes are brittle and need to be stored at -20ºC to avoid physical ageing (Yoshioka et al. 2011). Membrane original thickness varied obviously from part to part within the same sample which necessitated choosing the thinner areas for insert preparation using the naked eye. From side-by-side comparison to other membranes of known thickness, it appears the thickness of our PLGA membrane is at least, if not more than, 100 microns. Additional problems included swelling of the membrane in excess of double its original size (not shown) but such swelling (>3 fold) has been reported previously (Lu et al. 2000). Finally, its consistency becomes semi-solid as it degrades thus losing all physical strength.

An ideal substrate should be chemically and immunologically inert, and biodegradable membranes were initially widely investigated due to the hypothesis that biodegradation will remove the foreign substance, a potential source for macrophage and immune cell attraction. However, recent as well as past studies (Gullapalli et al. 2004;Gullapalli et al. 2005;Sugino et al. 2011a) indicate that newly seeded RPE cells may not provide enough ECM synthesis for their own existence, and aged macular BrM –the in vivo substrate of the RPE– has long been known as a hostile lipid rich environment that does not support new RPE cell attachment (Tezel, Del Priore, & Kaplan 2004). Thus the direction of many studies has now steered toward a non-biodegradable substrate, which has the

added benefit of strong physical support for the newly placed RPE layer as well as a physical barrier against the immune system and neovascular in-growth.

4

The Assessment of ARPE-19 Affinity to Polyurethane Substrates Commonly Used as Endothelial Cell Supports for Vascular Grafts

4 The Assessment of ARPE-19 Affinity to Polyurethane Substrates Commonly Used as Endothelial Cell Supports for Vascular Grafts

4.1 Introduction

Artificial vascular grafts consisting of synthetic materials are commonly implanted in humans during surgical procedures. Polyurethane-based vascular grafts have been investigated and coated with endothelial cells following surface modification to a more hydrophilic state to create an endothelialised artificial vascular graft (Krijgsman et al. 2002;Kannan et al. 2004). Due to the porous nature of polyurethane and its superior tensile strength, we investigated the suitability of this material for RPE transplantation as a non-degradable option. All polyurethane-based polymers were a kind gift from Prof. A. M. Seifalian, Academic Division of Surgical and Interventional Sciences, The Royal Free Hospital, University College London. They included a hydrophilic solid (H solid), a special polyurethane designated P9 in solid and porous forms, an equal mixture of H and P9 (P9/H mix) and electrosprayed P9.

4.2 Results

4.2.1 Examination of Surface Profile and Porosity using SEM

Polyurethane membranes were processed and examined under SEM at low (x10 – x250) and high (x1000 – x10,000) magnification to assess porosity and surface continuity, as well as response to UV and ethanol sterilisation methods. Both P9 and Hydrophilic polyurethane types were unaffected by either UV or ethanol sterilisation (not shown) as their surfaces appeared identical to non-sterilised membranes as in Figure 4.1. This figure shows the profile of both upper (smooth) and lower (rough) surfaces for each membrane at the relevant magnification.

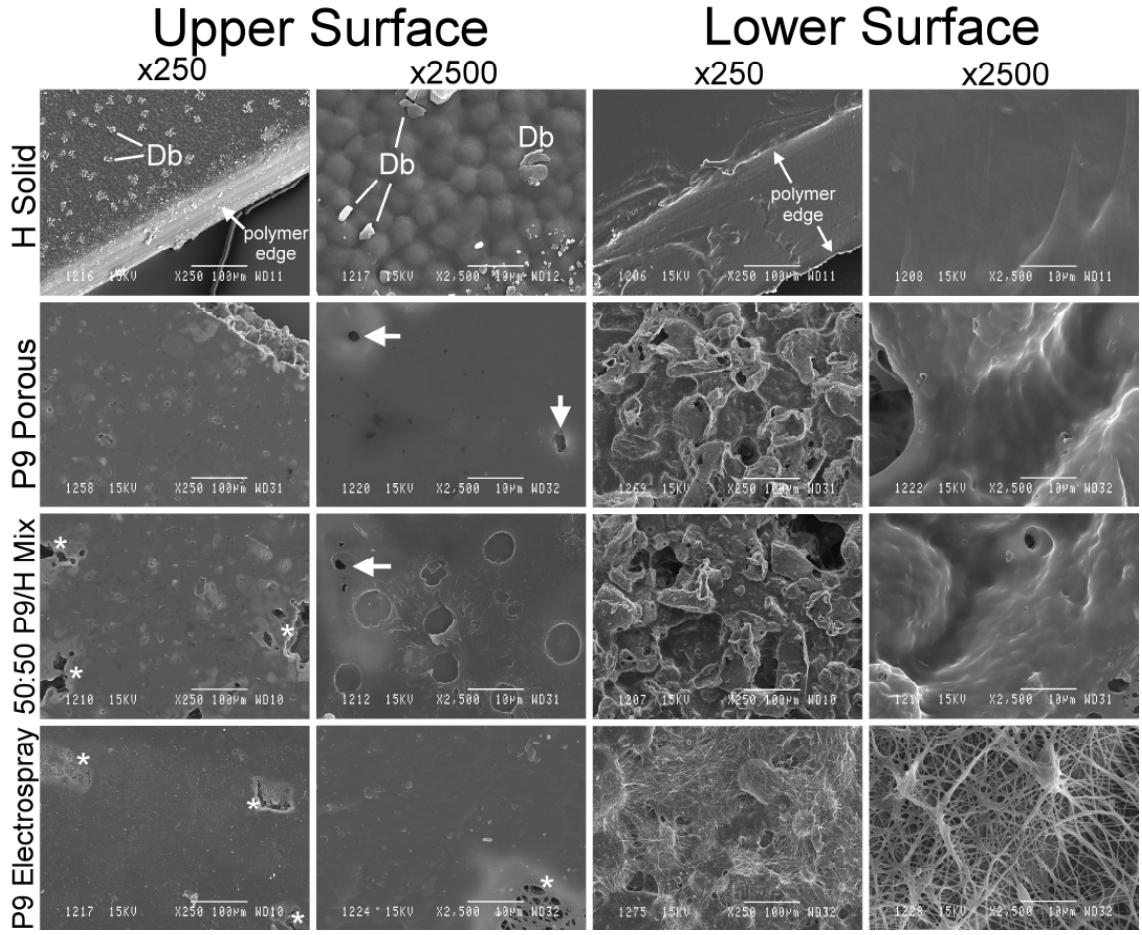

Figure 4.1 SEM of experimental polyurethane membranes used in this chapter (P9 solid SEM unavailable). H Solid: due to the intensely hydrophilic nature of this membrane it attracted a certain amount of non-specific debris (Db). An oblique view at this polymer confirms it is a truly solid membrane (x250). A high magnification view of the upper surface shows a unique 'bumpy' design feature (x2500). P9 porous and P9 mix: The manufacturing process has intentionally been varied to produce small pores (arrows) in both versions as well as some larger ones in the latter, to the point of creating large defects (asterisks). P9 Electrospray: This membrane also harbours some defects (asterisks) on its upper surface, revealing the inside body of the membrane. Lower magnification bars = 100µm, higher magnification bars = 10µm.

4.2.2 The evaluation of polyurethane membrane suitability by Alamar Blue cell viability assay

Since polyurethane is a non-transparent polymer, it was not possible to assess live adhesion or proliferation using light microscopy. Therefore a cell proliferation assay, AlamarBlue® (AB) was used to assess cell density. AB is a proprietary (Invitrogen, Paisley, UK) resazurin dye which crosses the cellular membrane and enters viable cells where it is reduced to a red fluorescent dye (resorufin) within these cells. Diffusion of this fluorescent dye from the cells occurs readily allowing measurements of viability by quantification of fluorescence on the supernatant medium. The resulting fluorescence

from these cells will be a function of cell density and increases proportionally to viable cell numbers. Thus cell growth and density are rapidly evaluated and quantitatively measured by a fluorescence reader.

ARPE-19 cells were seeded simultaneously on all membrane types, and these cultures were synchronised in serum free medium for at least 24 hours. In the first experiment (n = 3, N = 72), inserts were treated serially with AB at given time points: 0 hours (first measurement after a period of synchronisation), 24 hours, 7 days, and 4 weeks i.e. each culture was subjected to the AB assay 4 times. A one-way ANOVA was conducted to investigate effects of polymer, and time on total cell density. Polymer was a significant factor: Polyester (control membrane) produced significantly higher average fluorescence compared to all polyurethane membranes i.e. supported higher average cell density ($F(5,12) = 304.07$, $p < 0.001$, $\eta_p^2 = 0.992$; Figure 4.2A) thus average cell growth on the control membrane (polyester) is superior to all polyurethane membranes. A 2-way (repeated measures) ANOVA confirmed the same significance level between polymers (($F(5,12) = 304.07$, $p < 0.001$, $\eta_p^2 = 0.992$), confirming polyester as a far superior substrate at every time point (Figure 4.2B and C). It is worth noting that initial attachment of RPE cells to polyurethane was quite poor (0 hours) as indicated by the minimal initial fluorescence. Among the polyurethane membranes, all P9 polymer groups were superior to H solid (P9 Electrospray and P9 solid versions $p <= 0.005$, P9 Porous $p < 0.05$), and so was P9/H mixed porous ($p < 0.01$). A significant interaction existed between polymer and time ($p < 0.001$) but this interaction appeared only to affect relationships between polyurethanes and did not impact on the superiority of polyester i.e. interaction changed the order of superiority between the polyurethane membranes. However polyester remains significantly the best (Figure 4.2C). The effect of time on increased fluorescence is very significant ($F(3,36) = 132.86$, $p < 0.001$, $\eta_p^2 = 0.917$) indicating cell density changed significantly in relation to time which is a universally accepted effect of cell growth in culture. This also suggests that polurethanes do not impede cell growth, and that their poor performance is down to the initial poor cell attachment and not inhibition of growth.

A

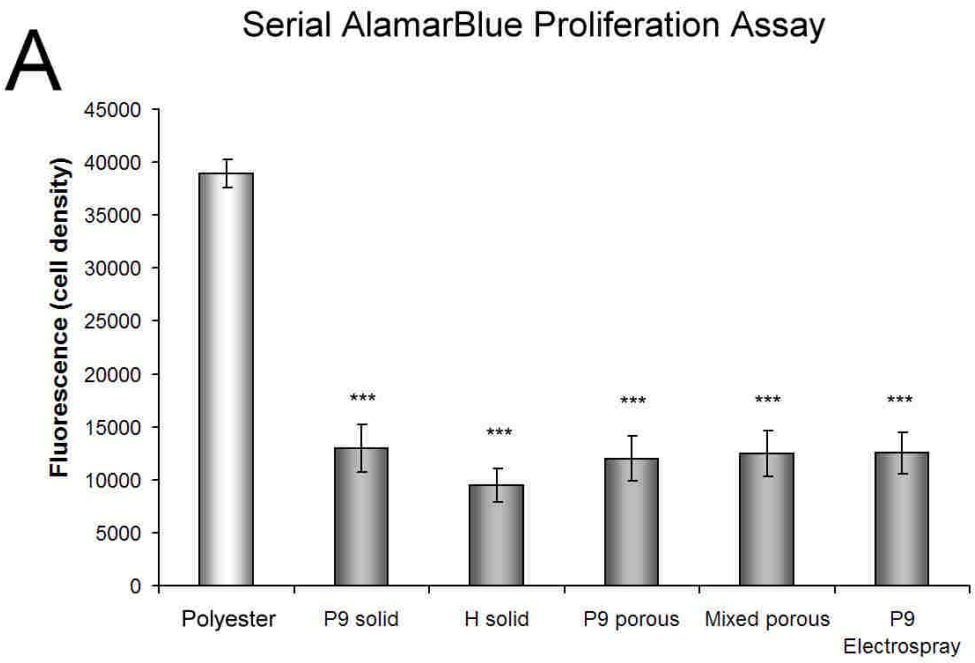
Serial AlamarBlue Proliferation Assay
Fluorescence (cell density)
45000
40000
35000
30000
25000
20000
15000
10000
5000
0
***
***
***
***
***
Polyester
P9 solid
H solid
P9 porous
Mixed porous
P9 Electrospray

B

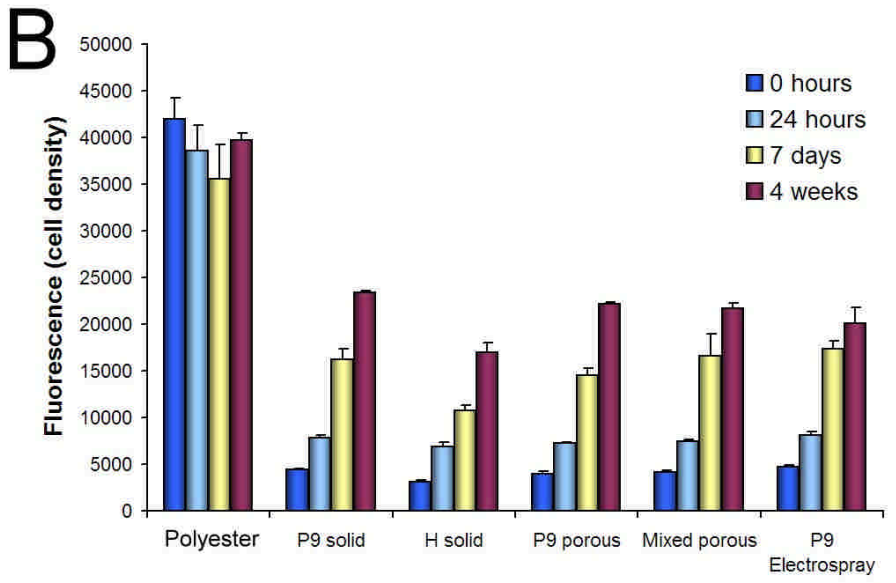
Fluorescence (cell density)
50000
45000
40000
35000
30000
25000
20000
15000
10000
5000
0
0 hours
24 hours
7 days
4 weeks
Polyester
P9 solid
H solid
P9 porous
Mixed porous
P9 Electrospray

C

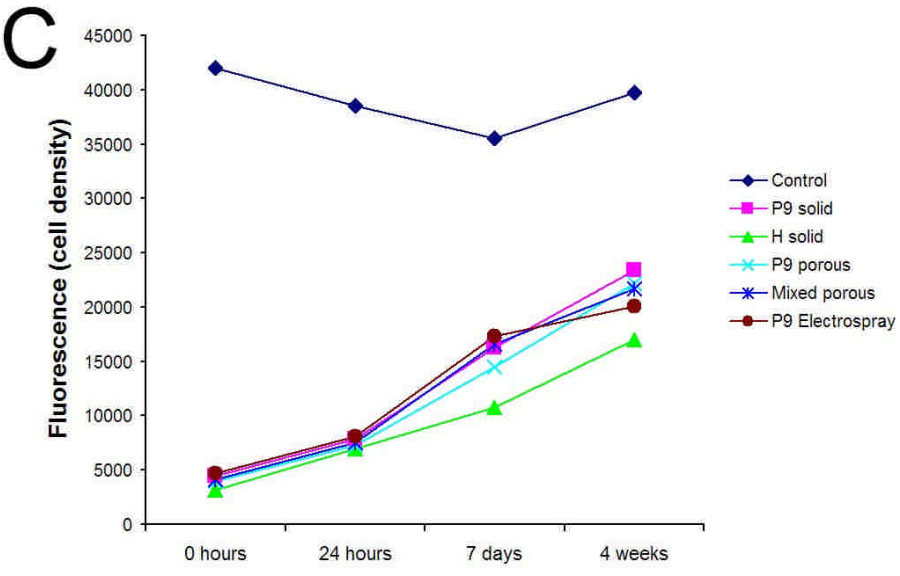
Fluorescence (cell density)
45000
40000
35000
30000
25000
20000
15000
10000
5000
0
Control
P9 solid
H solid
P9 porous
Mixed porous
P9 Electrospray
0 hours
24 hours
7 days
4 weeks

Figure 4.2 AlamarBlue proliferation/adhesion assay. ARPE-19 cells were seeded simultaneously on various membrane types, and these cultures were synchronised in serum free medium for at least 24 hours. (A) Average fluorescence i.e the average of all time points for each polymer. Polyester (control) is superior to all polyurethane membranes (* = p < 0.001). There was no significant difference between the polyurethanes in terms of average fluorescence. (B) The same data as in (A) but individual time points are displayed. Results are consistent with polyester being superior at every time point. It is worth noting that initial attachment of RPE cells to polyurethane was quite poor (0 hours) as indicated by low fluorescence. A repeated measures ANOVA reveals control membrane to be superior, p < 0.001. Among the polyurethane membranes, All P9 polymer groups were superior to H solid (P9 Electrospray and P9 solid versions p <=0.005, P9 Porous p < 0.05), and so was mixed porous (p < 0.01). C) Plot showing the relationship between time and polymer types. The effect of time on increased fluorescence is very significant and correlates with expected cell growth in proportion to culture duration, p < 0.001. Although there is significant interaction between time and polymer type (p < 0.001), this interaction seems only to have changed the order of superiority between the polyurethane membranes. However polyester remains significantly the best (n = 3, N = 72, data are means ± SEM).**

Given the progressive decline in cell density between 0 hours and 7 days, it is conceivable that AB could have had a negative impact on cell growth in the serial experiment (Figure 4.2).Therefore, a similar but smaller experiment was repeated with an identical number of culture inserts per polymer, but this time instead of re-treating the same 3 membranes with alamarBlue® at different time points (serial method), a separate insert was subjected (sacrificed) to the assay at each given time point in case there was either a toxic effect of AB or an interaction of AB with the polymer creating a presumed negative artefact (parallel method; Figure 4.3). This meant that at each time point there was only one test chamber per polymer (n = 1, N = 15), however this method precluded exposure of cells to any presumed toxic effect of repeated alamarBlue interaction with the test polymer. Surprisingly, all groups failed to show a visible growth beyond initial seeding and synchronisation period (72 hours). There are two main possibilites that could have given rise to this anomaly in this particular series. The first possibility is that the cells grew to their maximum potential during the attachment and early synchronisation period, and this theory is supported by the high level of fluorescence in polyester (control group) which almost exceeds the highest reading of the previous (serial) experiment and therefore understandably fails to increase further. It follows that each polymer had similarly reached it's given 'saturation' point. However the continued growth of cells far beyond this saturation point in the first experiment

goes against this idea. The second possibility is that, due to sampling of different cultures at different time points a growth effect was masked by the variations in cell densities between cultures *within* each group, combined with the smaller sample size than the first study (This presumed artefact will likely have been eliminated by the larger sample and averaging procedure in the first study). Nevertheless, it was reassuring to see that the overall result did not change in that control polyester was superior in this second experiment, consistent with the first experiment.

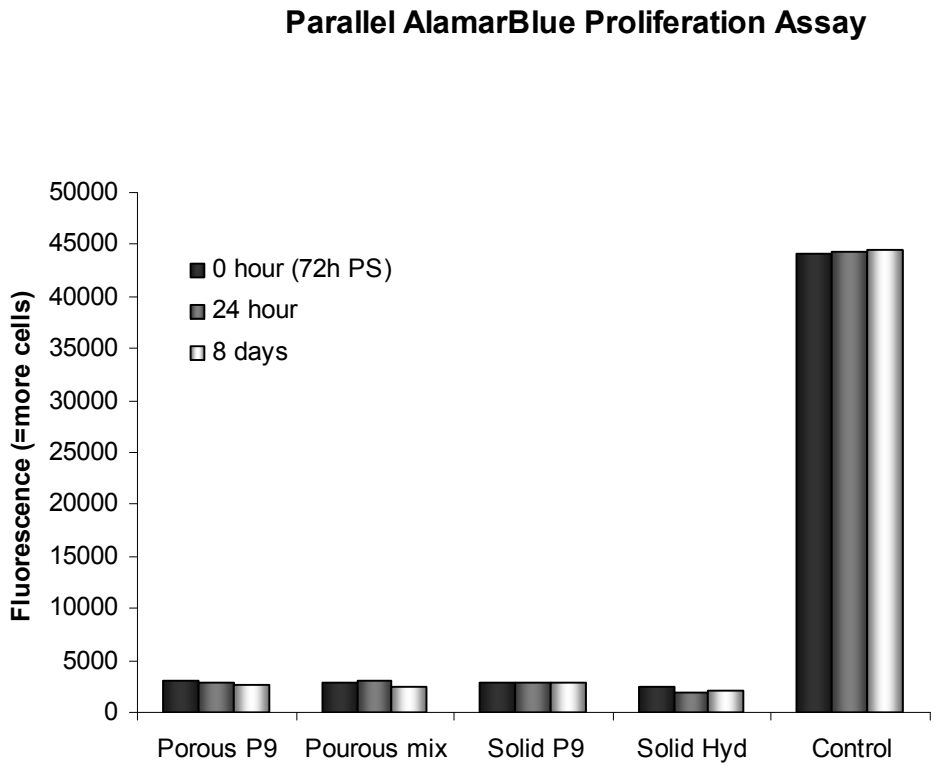

Figure 4.3. Alamarblue assay repeated with separate inserts for each time point so that inserts are not re-used after treatment with the dye. A separate insert was subjected (sacrificed) to the assay at each given time point to eliminate presumed toxicity due to either repeated AB exposure, or a presumed interaction of AB with the polymer. This meant that at each time point there was only one test chamber per polymer. This experiment confirms the superiority of polyester over all other polyurethanes (n = 1, N = 15).

4.2.3 The Evaluation of polyurethane membrane suitability using Immuno-cytochemistry (ICC)

ICC was attempted however cell sheets were visibly detaching from polyurethane samples. Thus, due to the poor adhesion of the cells to polyurethane, combined with the

frequent washing associated with this method, all samples of polyurethane were eventually rendered acellular. Hence ICC was not possible on any of the tested polyurethane membranes.

4.2.4 The evaluation of membrane suitability by scanning electron microscopy

Preparation for electron microscopy appeared to preserve ARPE-19 cells grown on polyurethane membranes although they were loosely attached and there were frequent large areas of acellular membrane or areas of cellular sheet detachment observed by SEM (Figure 4.4).

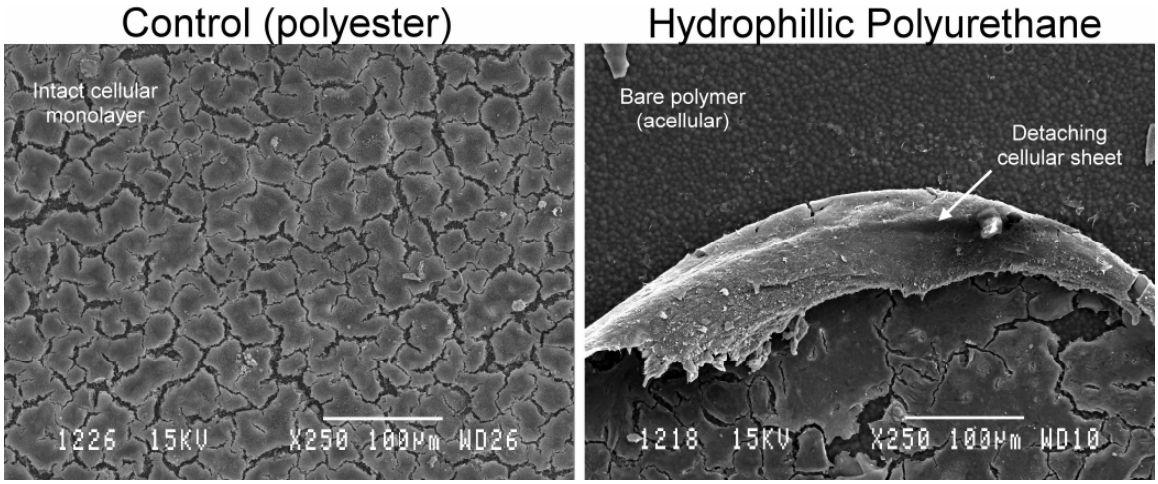

Figure 4.4 SEM of fixed ARPE-19 cells. Left panel: Cells are seeded onto uncoated control (polyester) membrane which shows a confluent monolayer of polygonal cells that are separated at more or less regular intervals by a fracture artefact due the dehydration process of SEM (which tended to shrink cellular matter and not the polymer). Right panel: A continuous sheet of ARPE-19 cells appears to be folding over itself and detaching from hydrophilic solid polyurethane (right). Frequently, large areas of bare polymer were observed indicating its poor affinity for cellular matter.

4.3 Conclusion

AlamarBlue® is a minimally toxic, efficient fluorometric assay for assessing attachment and proliferation of ARPE-19 cells on non-transparent surfaces.
Even the most hydrophilic of the polyurethane membranes did not support sufficient attachment and subsequent growth of the human ARPE-19 cells in comparison to polyester filter. This effect is a combination of poor initial cell-substrate adhesion followed by propensity of cell sheets to detach from the membrane at a later stage as seen during sample fixation (not shown) and SEM (Figure 4.4). This data is in support

of polyester filters as a superior membrane for the growth of ARPE-19 cells. Our results are consistent with a previous study measuring endothelial cell attachment to segmented polyurethane (Kaibara et al. 1996). This study also demonstrates AB as a useful tool for measuring cell density on surfaces that prohibit cell counting due to their completely opaque nature.

5

The Assessment of ARPE-19 Affinity to Peptide-Adsorbed Surfaces

5 The Assessment of ARPE-19 Affinity to Peptide-Adsorbed Surfaces

5.1 Introduction

Integrins are the most important receptors mediating cell adhesion to the ECM, and are present in all metazoan organisms. In vertebrates they also mediate certain cell-cell interactions (Hynes 2002;Gullapalli, Sugino, & Zarbin 2008). They are a family of transmembrane heterodimeric glycoproteins. These dimers are composed of one α chain and one β chain. There are eighteen α, and eight β subunits which assemble into 24 distinct integrin dimers in mammals (Hynes 2002). The RPE—like other anchorage-dependent cells—recognizes and attaches to its surroundings primarily through these membrane-based proteins. Thus, integrins play a vital role in adhesion, survival as well as phagocytic functions of the RPE and possibly its interaction with the complement system (McLaughlin et al. 2003).

Integrins function by recognising specific short active peptide sequences offered to them by their surroundings, whether through neighbouring cell receptors, soluble proteins or -most commonly- immobilised peptide sequences found within the ECM (Carlisle et al. 2000;Hynes 2002). Collagen type IV, laminin, and fibronectin are the main components of the RPE basement membrane and ECM (Booij et al. 2010). With aging, these components have all been found to be reduced in the RPE basement membrane (Pauleikhoff et al. 2000).Since integrins are known to recognise these components found in ECM through their interaction with short active peptide sequences within extracellular molecules I sought to test the response of RPE cells to such short peptides deriving from these molecules.

The Arg-Gly-Asp (RGD) sequence is well known as an active component of most extracellular proteins such as fibronectin, laminin and collagen and promotes adhesion by acting as a recognition site for integrins on the cell surface (Pierschbacher and Ruoslahti 1984;Carlisle et al. 2000). In addition, RGD-containing tetrapeptides such as RGDS have been shown to be an important factor affecting RPE attachment in vitro (Imoto et al. 2003). The active sequences Tyr-Ile-Gly-Ser-Arg (YIGSR) (Grant et al. 1989;Carlisle et al. 2000) and Ile-Lys-Val-Ala-Val (IKVAV) are derived from β1 and α1 laminin subunits respectively (i.e. β and α subunits of laminin-1). Laminin is an

extracellular basement membrane protein essential for adhesion, growth and migration of a variety of cell types such as epithelial, Schwann cells, myoblasts, and tumour cells (Tashiro et al. 1989). Additionally, laminin is a major component of the native RPE basement membrane, and is known to promote multiple in vivo characteristics as well as modulate cytokine secretion in RPE in vitro (Uetama et al. 2003). Thus laminin supports a variety of cellular functions in addition to its primary role as ECM molecule for attachment. Nonetheless, it has been reported that laminin is a superior attachment matrix for RPE that exceeds the attachment capacity of fibronectin and collagen (Zhou, Dziak, & Opas 1993;Mousa, Lorelli, & Campochiaro 1999;Aisenbrey et al. 2006) Laminin also has roles in promoting differentiation of RPE (Campochiaro & Hackett 1993;Ohno-Matsui et al. 2001), reduction of inflammatory markers in RPE (Uetama et al. 2003) and providing signals for epithelial cell polarisation and orientation (Yu et al. 2005) as well as regulation of spreading, migration and proliferation (Mak et al. 2006). The documentation of these numerous potent functions of laminin is no surprise since past studies have long relied on purified laminin as a valid culture model for RPE due to its ability to reproduce in vivo developmental behaviour and support progressive increase of TER in culture (Ban and Rizzolo 1997). In short, laminin is critical for maintenance of cell phenotype and survival (Colognato and Yurchenco 2000) thus it is an attractive molecule to mimick with short peptides.

In this chapter, I will test the effects of RGD peptide and its variants, as well as laminin-derived peptide fragments YIGSR and IKVAV. I will discuss the effect of these surface-immobilised peptides on several aspects of growth of ARPE-19 cells.

5.2 Results

Cell adhesion assays were performed using the peptides outlined in Table 5-1 in order to elucidate a cell-friendly peptide that could be used as a coating to modify other experimental surfaces.

Name	Full Sequence	Product code
RGD	RGD	A8052
GRGD	GRGD	G3892
RGDS	RGDS	A9041
GRGDS	GRGDS	G4391
YIGSR	CDPGYIGSR	C0668
IKVAV	CSRARKQAASIKVAVSADR	C6171
ALL	Equal mixture of all above	All of above

Table 5-1 Commercial peptides tested in this chapter. All peptides were purchased from Sigma-Aldrich.

5.2.1 The effect of peptide-adsorbed glass on cell behaviour

It is known that glass has the capacity to adsorb peptides and proteins (Massia and Hubbell 1991). A repeated measures experiment was conducted to compare the effect of different peptide-adsorbed glass multi-chamber slides on cell attachment over the course of 4 days (n = 3, N = 96). The peptide concentration tested was 25μg/cm². Cells were counted per 10x phase microscopy field as a means to assess cell attachment. Although time was a significant factor that increased the cell density of the peptide-adsorbed surfaces ($F(3,48) = 14.83$, $p < 0.001$, $\eta_p^2 = 0.481$), there was no significant effect of peptide type on cell behaviour as a repeated measure ($p = 0.59$; Figure 5.1), and interaction between time and peptide type was also non-significant. In addition, analysing the 1 hour initial attachment time point was non-significant between peptides ($p = 0.85$), as were other time points. However, the following trend was observed: all of the peptide groups had greater attachment than control group at the earliest time point. This trend was reversed during later time points. This observation is consistent with good attachment, but a weaker spreading profile compared to control surface. Thus there is no significant effect of peptide type on peptide-adsorbed glass cell counts within this time frame. However as would be expected, time increased the cell counts

significantly, which is evidence of active proliferation of cells. As a result most groups show an increasing sigmoid trend.

Phase contrast microscopy demonstrated cobblestone morphology of the cells. However poor spreading, manifested by lack of cell coverage across the well (in particular, lack of cell spreading towards the centre of the well and in some areas only solitary cells), was observed in the laminin-peptide containing groups IKVAV and ALL (Figure 5.2, column C). These cultures were maintained for a further week (total 5 weeks) after which they were fixed and immunostained. All cultures showed good junctional maturation (ZO-1; Figure 5.2 column A). Monocarboxylate transporters (MCTs) are the major lactate, pyruvate and proton transporters in the RPE. MCTs polarise to the cell membrane. Whereas MCT1 is present in many tissues, MCT3 is only detected in RPE and the choroid plexus epithelium (Daniele et al. 2008). Polarisation (lateral staining of MCT1; Figure 5.2 column B) was best in the following RGD-based peptides: RGD, GRGD and RGDS, but not so in GRGDS and the laminin-derived fragments YIGSR and IKVAV. There was virtually no MCT3 detected by immunostaining (not shown). Although very faint cytoplasmic MCT3 is evident in the IKVAV and ALL groups, this is not relevant as this is a cell membrane marker (not shown). Lack of MCT3 is likely due to the relatively de-differentiated state of the ARPE-19 cell line.

Seeding efficiency was assessed by dividing the observed attached-cell density by the seeding density (cells per cm^2). Since dimensions of the 10x field measured with a graticule is 1.350mm x 1.085mm, dividing the average cell counts at 1 hour by the resultant area of 0.014648cm2 (1.4648mm2) would yield the observed attached-cell density. This figure is subsequently divided by the actual seeding density. Seeding efficiency ranged between 2.4% and 4.8% which means more than 95% cells were lost through the seeding process in all groups.

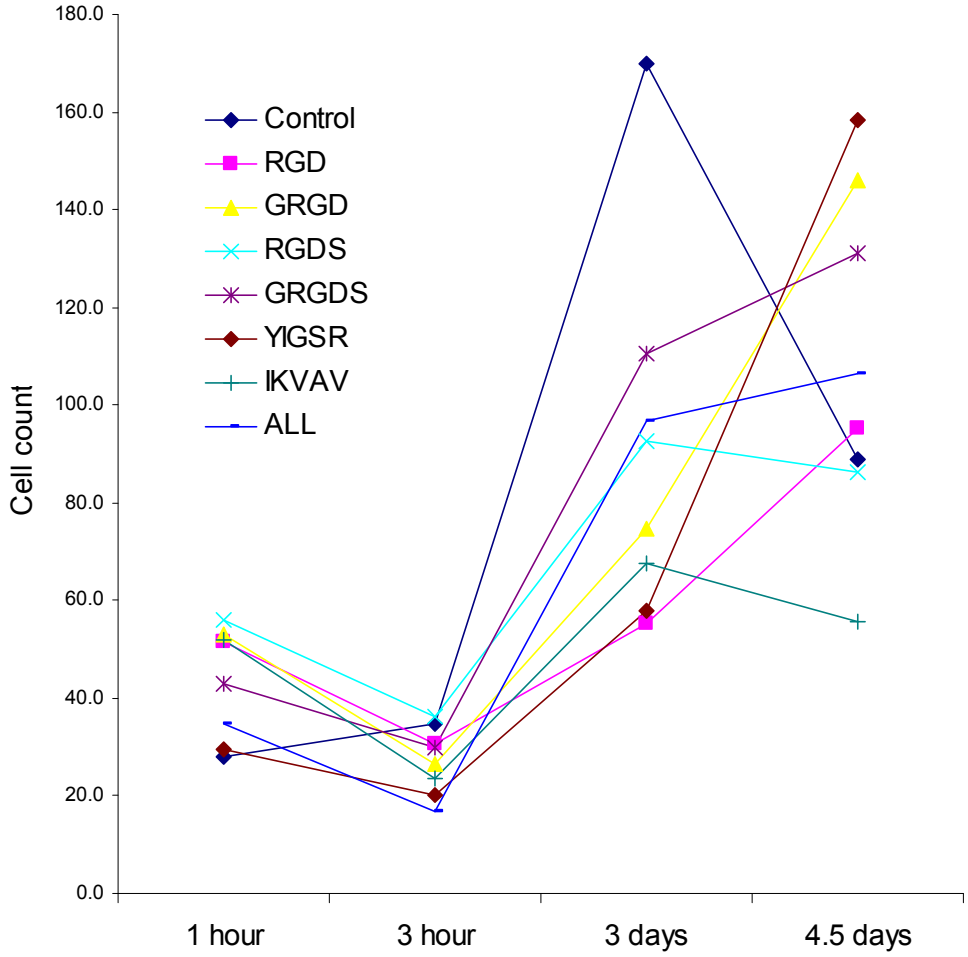

Figure 5.1 Cell counts of attached p33 ARPE-19 cells on peptide-adsorbed glass surfaces per 10x microscopic fields at the given time points. Cells counts were assessed between 1 hour and 4.5 days (n = 3). No significant effect of peptide type on cell counts could be detected within this time frame ($p = 0.59$). However time was a factor that increased the cell counts significantly, which is evidence of active proliferation of cells ($p < 0.001$). As a result most groups show an increasing sigmoid trend.

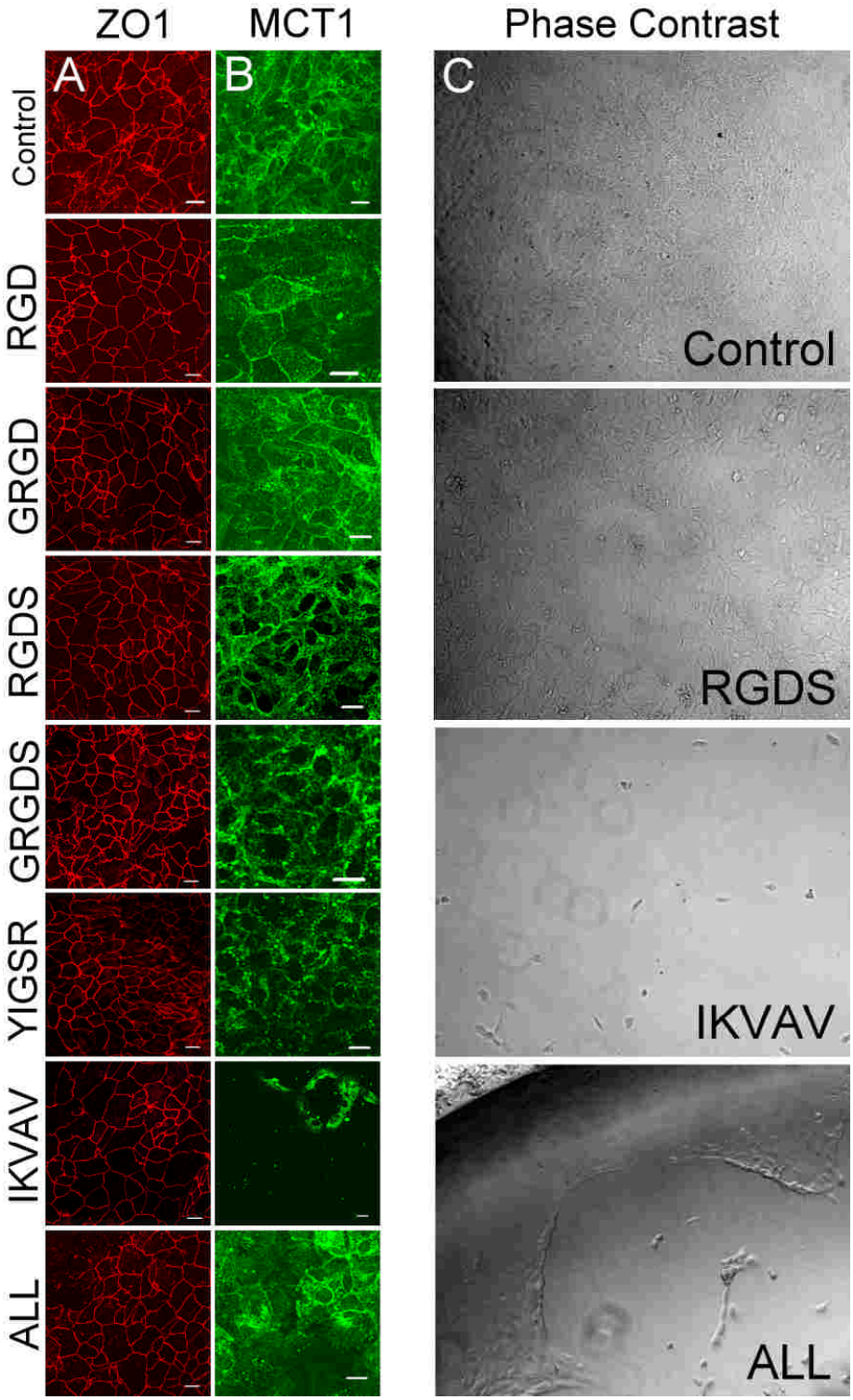

Figure 5.2 The effect of peptide-adsorbed glass on p33 ARPE-19 behaviour. (A, B) Immunostaining of cells at 5 weeks. ZO-1 staining reveals favourable morphology in most RGD-containing groups especially the ALL mixture. Polarisation (lateral staining of MCT1 was best in the following RGD-based peptides: RGD, GRGD and RGDS, but not so in GRGDS and the laminin-derived fragments YIGSR and IKVAV. All bars = 20µm. (C) Phase contrast images of live cultures of proliferating cells at 4 weeks demonstrate cobblestone morphology of the cells in control, RGD-based groups and YIGSR (Control and RGDS shown; upper panels). Poor spreading capability, manifested by lack of cell coverage across the well especially towards the centre of the well is seen in only in the groups containing IKVAV (IKVAV and ALL; lower panels).

5.2.2 The effect of peptide-adsorbed polyester filter on cell behaviour

So far, I have tested peptide adsorption on culture-grade glass. Polyesters are polymers with a functional ester group, and can occur naturally such as cutin (cuticle of plants). Synthetic polyesters are numerous and can be thermoplastic, thermoset, or cured by hardeners to produce resin. The term "polyester" however commonly refers to a specific polymer called polyethylene terephthalate (commonly abbreviated as PET), and this is the polyester that I refer to throughout this thesis.

It is difficult to microscopically observe non-pigmented cells on Transwell® polyester filters due to the interference of pores with transmitted light (the dark contrast of pores within the filter makes cellular structures almost invisible due to their comparatively subtle contrast). However one very useful characteristic of polyester filters is their application in measurement of trans-epithelial resistance (TER). I conducted a repeated measures experiment with 3 time points to compare TER among peptide-coated filters ($n = 3$; $N = 72$) seeded simultaneously with the above experiment. The peptide concentration tested was 25μg/cm². Time was a highly significant factor that increased TER ($F(2,30) = 39.55$, $p < 0.001$, $\eta_p^2 = 0.725$) and this confirms our general knowledge of epithelial cell behaviour, particularly RPE cell junction maturation in culture. However, there was no significant effect of peptide type on the TER of ARPE-19 cells whether as a repeated measure ($p = 0.712$) or whether average TER over the same period was compared ($p = 0.675$). There was also no significant interaction between time and peptide type ($p = 0.857$). Nevertheless the following trend was observed: IKVAV peptide maintained the highest TER compared to the control group and all other peptides (Figure 5.3).

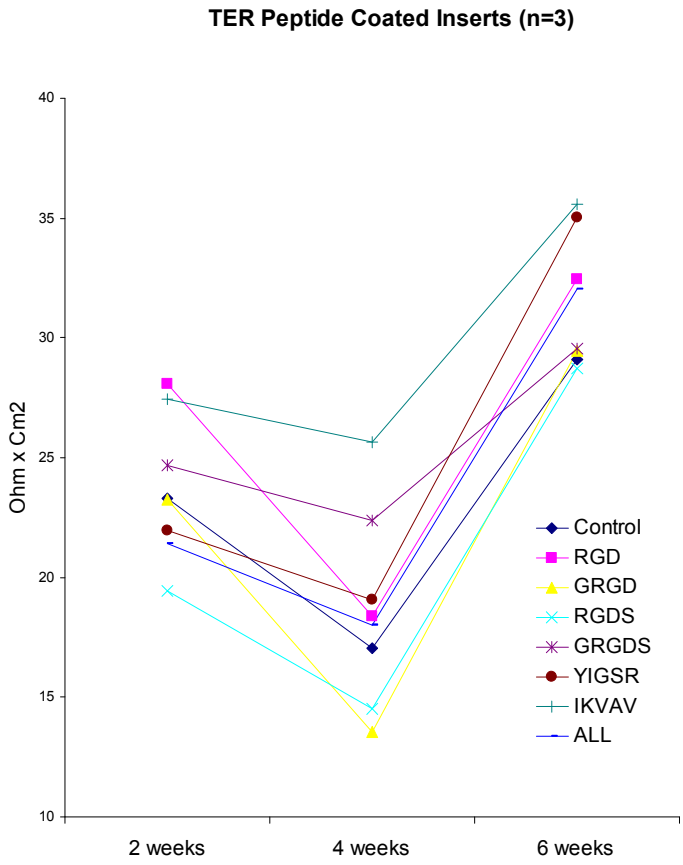

Figure 5.3 Transepithelial resistance (TER) of p33 ARPE-19 cells grown on various peptide-adsorbed polyester filter surfaces at 2, 4 and 6 weeks. Time was a highly significant factor that increased TER ($p < 0.001$) and this confirms our general knowledge of RPE cell junction maturation in culture. No significant effect of peptide type on the TER whether as a repeated measure ($p = 0.712$) or whether average TER over the same period was compared ($p = 0.675$). There was also no significant interaction between time and peptide type ($p = 0.857$). Nevertheless the following trend was observed: IKVAV peptide maintained the highest TER compared to the control group and all other peptides ($n = 3$, $N = 72$).

At 7 weeks, cells of this experiment were fixed and stained for ICC markers (Figure 5.4). Compared to the previous experiment on glass (Figure 5.2), cells on polyester had generally improved morphology (see RGD-based groups and ALL) and polarity (as evidenced by improved MCT1 lateral staining) at 7 weeks. This effect is likely due to the cells being able to communicate with their basal environment as a result of growing on a porous surface (filter). Unfortunately, MCT3 was still negative (not shown). Na,K-ATPase showed only cytoplasmic staining whereas it is polarised in native RPE (Figure 5.4). The possibility of culture time as a reason for the better morphology of cells grown on polyester was also considered, and this will be dealt with in the next section.

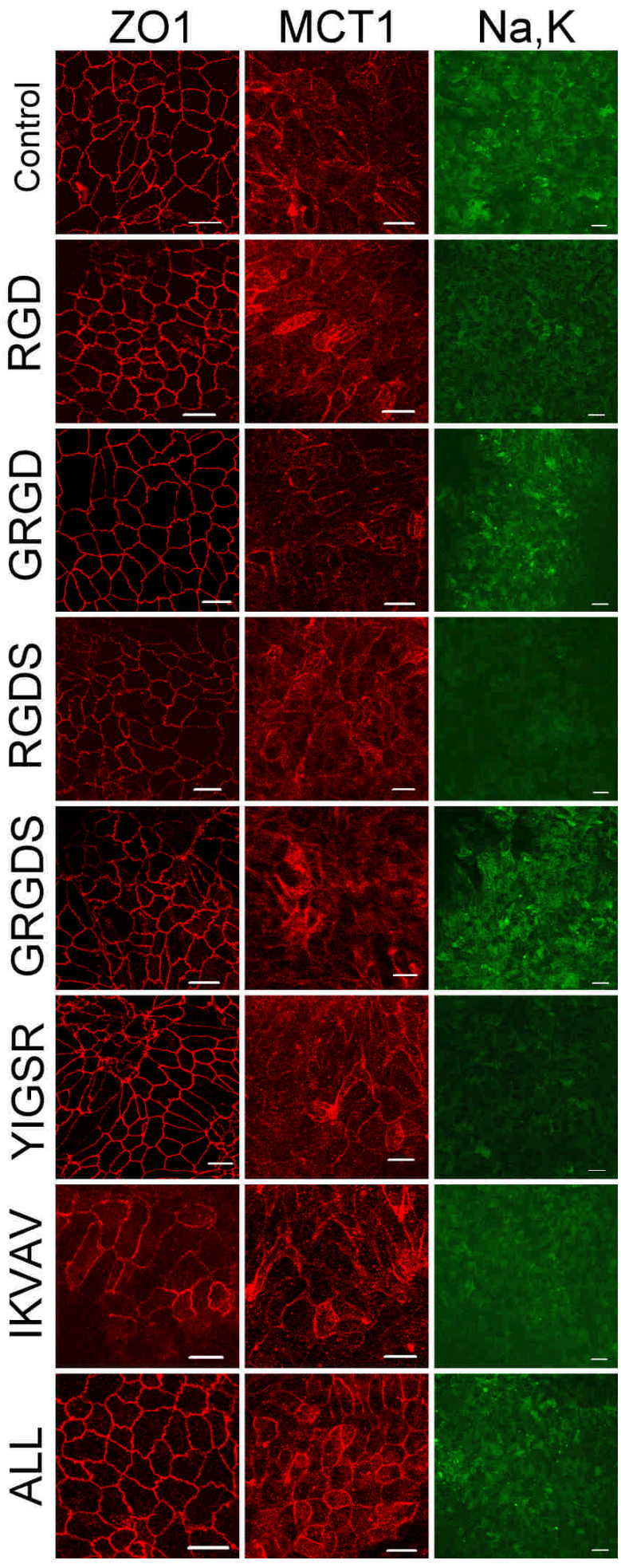
ZO1
MCT1
Na,K
Control
RGD
GRGD
RGDS
GRGDS
YIGSR
IKVAV
ALL

Figure 5.4 Immunostaining of p33 ARPE-19 cells grown on peptide-adsorbed polyester filter inserts at 7 weeks. Compared to the previous experiment on glass (Figure 5.2), cells on polyester have a generally improved morphology (see RGD-based groups and ALL) and polarity (as evidenced by improved MCT1 lateral staining). This effect is likely due to the cells being able to communicate with their basal environment as a result of growing on a porous surface (filter). Unfortunately, MCT3 was still negative (not shown). Na,K-ATPase showed only cytoplasmic staining whereas it is polarised in native RPE. Na,K = Na,K-ATPase. All bars = 20μm.

5.2.3 The effect of a ten-fold peptide concentration on the profile of cells grown on peptide-adsorbed surfaces

5.2.3.1 Glass

The assumption so far has been that during initial incubation of surfaces with peptides, all of the peptide in solution is available to become adsorbed to the test surface. However, what if somehow a small fraction of peptide was eventually available for adsorption due to one or more factors e.g. a unique electrostatic profile present on the test surfaces? Thus the possibility of poor performance of these peptides due to low concentration was considered. Therefore I conducted an experiment this time using 250μg/cm² i.e. a ten-fold concentration of peptide used so far. Since I have already shown successful attachment and reasonable proliferation of cells with the lower concentration of these peptides, I conducted this experiment with the objective of observing the histochemical profile of these cells. It is conceivable that a ten-fold peptide concentration could improve expression of certain markers such as MCT3 (which has so far been negative), improve pigmentation, distribution of Na,K-ATPase or even morphology of the cells, if the original concentration of peptide was sub-optimal. Additionally this ten-fold concentration may also unmask potential toxicity to the cells and will help determine the safest choice of peptide.

ARPE-19 cells were seeded and maintained in culture on these surfaces for up to 4 months (Figure 5.5). Both micro- and macroscopic pigmentation was observed on all surfaces except IKVAV. The ALL group which is an equal mixture of all the test peptides meant that IKVAV was diluted by one in six, and surprisingly this dilution allowed pigmentation to occur in the ALL group (Figure 5.5F and G). Both YIGSR and IKVAV produced polarisation that was poor as shown by weak lateral staining for MCT1 and Na,K-ATPase. All RGD peptides demonstrated ICC evidence of good differentiation, and polarisation especially the GRGD peptide which was best for polarisation of MCT1 and Na,K-ATPase. RGD and GRGDS also demonstrated evidence of polarisation but to a lesser degree than GRGD, and also showed a weak positivity for CRALBP staining. RGDS was the weakest of the RGD peptides in terms of its ICC profile. The lack of regular polygonal morphology on the positive control laminin (Figure 5.5Lam), indicates a problem with the glass surface per se, as we will confirm from the next experiment.

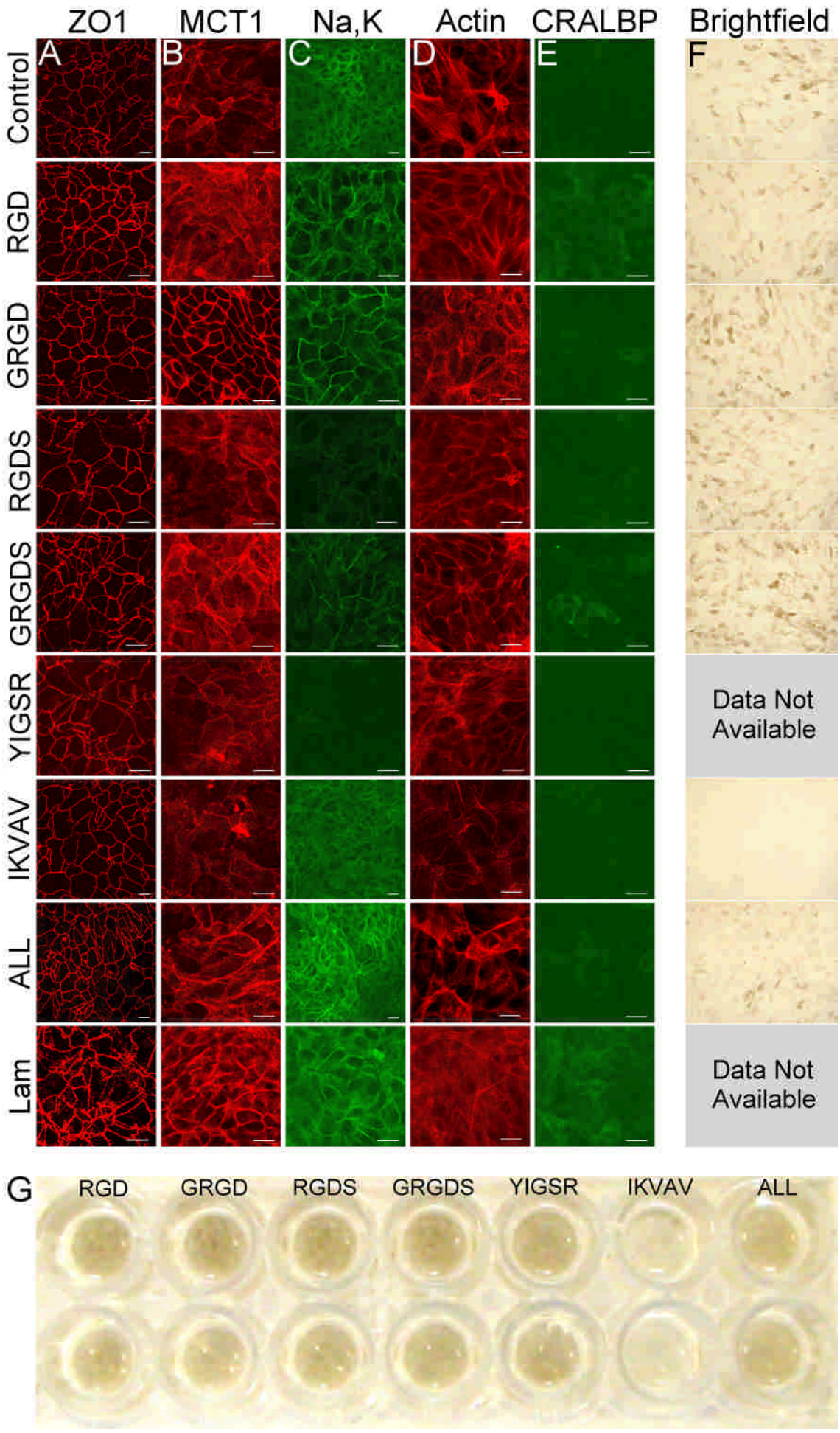
ZO1
MCT1
Na,K
Actin
CRALBP
Brightfield
A
B
C
D
E
F
Control
RGD
GRGD
RGDS
GRGDS
YIGSR
IKVAV
ALL
Lam
Data Not Available
Data Not Available
G
RGD
GRGD
RGDS
GRGDS
YIGSR
IKVAV
ALL

Figure 5.5 Columns A – E). ICC of p32 ARPE-19 cells grown on various peptide-adsorbed glass surfaces at 7-8 weeks. F). Bright-field microscopy of cells from the same experiment at 4 months. Note the lack of pigmentation in the IKVAV group (F, G). The ALL group (equal mixture of all test peptides) contains IKVAV 1:6, and surprisingly this dilution permits pigmentation to occur in the ALL group. Similar pigmentation is seen in all other peptides both microscopically and macroscopically (F, G). YIGSR and IKVAV both produce polarisation that was poor as shown by weak lateral staining for MCT1 and Na,K-ATPase (B, C). RGD-based peptides demonstrate ICC evidence of good differentiation, and polarisation especially GRGD (best for polarisation of MCT1 and Na,K-ATPase; B, C). RGD and GRGDS also demonstrate polarisation but to a lesser degree than GRGD, and also show a weak positivity for CRALBP staining (E). RGDS is the weakest of RGD peptides in terms of ICC profile. Lack of regular polygonal morphology on the positive control laminin (Lam), indicates a problem with glass substrate per se. Cells grown on the IKVAV peptide deposited a characteristic extra-cellular matrix which could be seen both with brightfield (column F) and contrasted against background staining in confocal microscopy (not shown). All bars = 20µm.

5.2.3.2 Polyester filters

ICC staining shows remarkably good junctional staining of ZO-1 and improved morphology (Figure 5.6) over the previous experiment on glass (Figure 5.5). In particular, the RGD-based peptides together with laminin (positive control) demonstrated superior polarity of MCT1 and a more rounded and polygonal morphology (ZO-1) compared to non-RGD peptides. RGD itself demonstrated polarisation of MCT1 to the apical membrane, similar to positive control, laminin (z-sections not shown). Remarkable lateral staining of Na,K-ATPase was obvious in all groups except IKVAV where it is intensely cytoplasmic in parts.

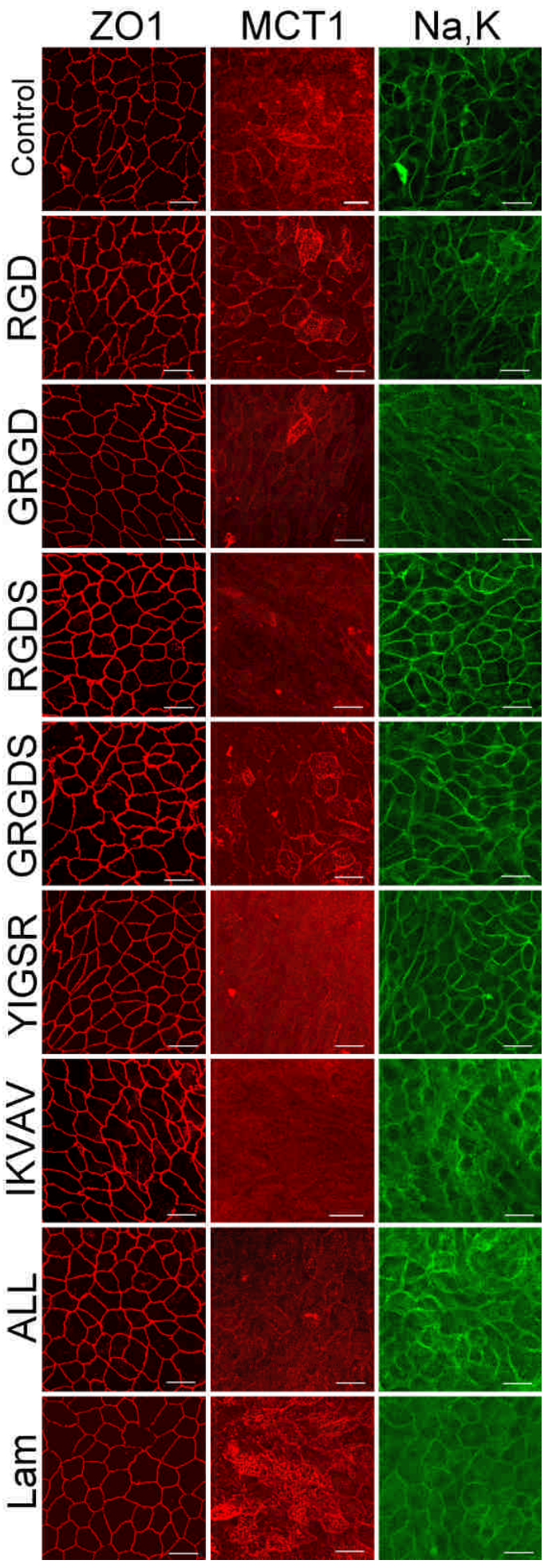
ZO1
MCT1
Na,K
Control
RGD
GRGD
RGDS
GRGDS
YIGSR
IKVAV
ALL
Lam

Figure 5.6 ICC of p32 ARPE-19 cells grown on various peptide adsorbed-polyester filters at 7-8 weeks. ICC staining shows remarkably good junctional staining of ZO-1 and improved morphology over the previous experiment on glass (Figure 5.5). Specifically, RGD-based peptides together with laminin (positive control) demonstrate superior polarity of MCT1 and more rounded polygonal morphology (ZO-1) compared to non-RGD peptides. RGD itself demonstrated apical polarisation of MCT1, similar to positive control, laminin (z-sections not shown). Remarkable lateral staining of Na,K-ATPase was obvious in all the groups except IKVAV where it is cytoplasmic. In summary morphology and Na,K-ATPase polarisation is remarkable except for IKVAV. MCT1 expression is generally better in RGD peptides particularly the RGD sequence itself. All bars = 20µm.

5.2.4 The effect of peptide-adsorbed polyolefin on cell behaviour

Permanox® is a proprietary plastic resin (Nunc, Thermo Scientific) belonging to the popular poly-olefin family which includes extensively used plastics such as polyethylene (plastic bags) and polypropylene (household plastic boxes, cryo-tubes). Furthermore, polypropylene sutures have been used in humans for over half a century and are regarded as biologically inert (Usher et al. 1962), and other polyolefin-based materials are now approved for implantation in humans (Kurtz et al. 2009;Meir et al. 2013).

Permanox ® has many good characteristics and meets the growth requirements of many anchorage dependent cells. It has very low auto-fluorescence, is resistant to many organic solvents, acid and alkali solutions, withstands temperatures from -25 ºC up to 180ºC, and has exceptional oxygen/gas permeability which makes it particularly attractive as a cell culture vessel.

Due to the vast number of cells adherent in the IKVAV and ALL groups cell counting of 10x or 20x fields was not feasible. Thus cell counts were recorded from 40x microscopic fields in this series. All of the tested peptides allowed comparable cell adhesion to the control surface. A one-way ANOVA revealed a significant difference between the cell counts of peptide groups tested ($F(7,24) = 9.30$, $p < 0.001$, $\eta_p^2 = 0.731$). IKVAV appeared to significantly promote cell adhesion ($p < 0.001$) at 90 minutes post seeding as shown in Figure 5.7. An equal mixture of all the peptides tested (ALL) appeared to promote adhesion significantly ($p < 0.01$), suggesting that neither a dilution of IKVAV, nor the presence of other peptides was detrimental to its cell-adhesiveness in

this situation. Strikingly, the large number of cells attached to IKVAV and ALL columns was immediately apparent to the naked eye as a loss of surface gloss during media exchange (not shown). However, only this time point was tested as cells on this plastic rapidly became confluent making cell counting technically difficult especially in the superior groups IKVAV and ALL. Additionally, cells grown on this plastic became heavily multilayered. This was confirmed by ICC and confocal microscopy (not shown).

Seeding efficiency was assessed by dividing the observed attached-cell density by the actual seeding density (cells per cm^2) as carried out in section 5.2.1. The average observed cell counts were divided by the area of a 40x field, which in turn was divided by the actual seeding density. Seeding efficiency ranged between 4.1% for RGD and 66.74% for IKVAV. This suggests a generally higher seeding efficiency for peptide adsorbed-Permanox compared to glass, whose seeding efficiencies were 2.4 – 4.8% among all groups.

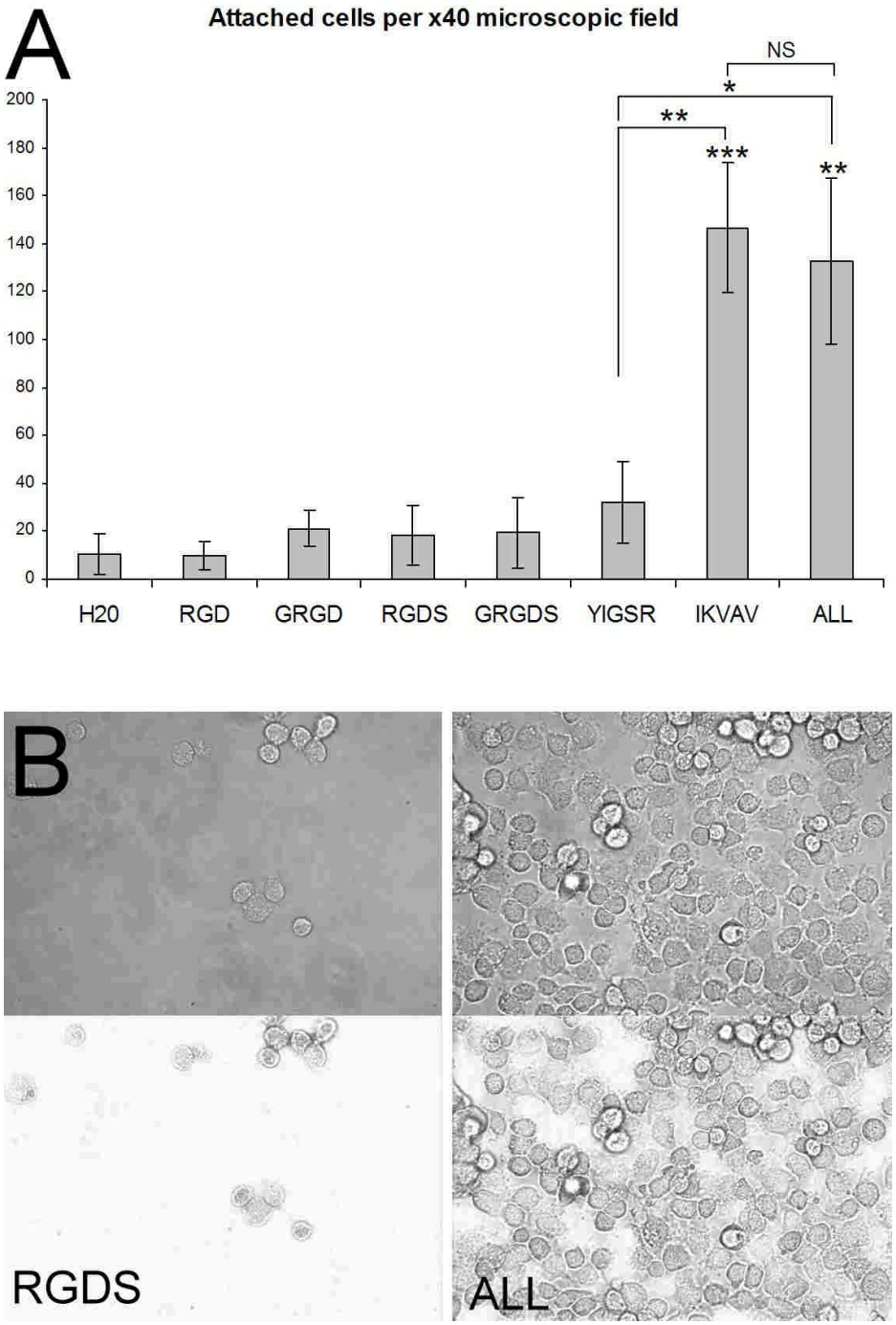

Figure 5.7 A) The average number of cells visible per x40 microscopic field, compared among various peptide-adsorbed permanox® slides. IKVAV appears to significantly promote cell adhesion ($p < 0.001$) at 90 minutes post seeding. ALL appears to promote adhesion significantly ($p < 0.01$), suggesting that neither dilution of IKVAV, nor presence of other peptides is detrimental to cell-adhesiveness hereto. The large number of cells attached to IKVAV and ALL was immediately apparent to the naked eye as loss of surface gloss during media exchange (not shown). Only this time point was tested as cells rapidly became confluent making cell counting impossible especially in IKVAV and ALL. Unless specified, asterisks indicate the following significance levels compared with H2O: *P < 0.05, **P <0.01, ***P <0.001 (n = 4). B) Phase contrast image (top) of cells seeded on RGDS peptide (left) 1 hour post-seeding versus ALL peptides (right), and the same image with digital background subtraction to highlight the cells (bottom).

5.3 Conclusion:

Peptide-adsorption is a feasible method for testing active short peptide sequences, and some significant differences were observed between certain peptide groups. The best performing peptide for cell adhesion is IKVAV and this result is significant on permanox®, and shows a similar initial attachment trend on glass surface. It also maintains the highest trend in TER on a polyester surface for up to 6 weeks. Nevertheless this peptide lagged behind other peptides with regards to spreading on glass, including when it was diluted 1:6 as a mixture with other peptides, indicating its propensity to inhibit spreading. When spreading was complete by 4 months, IKVAV also failed to allow pigmentation which could be a secondary effect of delayed confluence. Surprisingly, pigmentation was detected in the ALL mixture at 4 months on glass surface indicating that although 1:6 dilution of IKVAV with other peptides was detrimental to spreading, it was sufficient to rescue pigmentation on glass. It is worth noting here that morphology of cells in the ALL group tended to follow that of the RGD-based groups and not IKVAV. The other laminin-derived peptide YIGSR however, was not significantly different to the other peptides on any surface.

None of the RGD-based peptide groups demonstrated significantly superior attachment to control on any surface, but they did allow spreading of the cells. RGD-based peptides generally showed good ICC profiles in all experiments, such as better polarisation of the cells when grown both on glass and polyester. As for the morphology of cells, adsorbed polyester was generally better than adsorbed glass for all peptides (compare ZO-1 morphology in Figure 5.2 and Figure 5.5 versus Figure 5.4 and Figure 5.6). Additionally, RGD-based peptides tended to have cells with a more rounded and regular polygonal shape than the laminin-derived peptides, and this effect was most apparent on polyester surface experiments. In summary, IKVAV supported the best attachment while RGD peptides supported the best morphology and polarisation which further improved on polyester. These data are in support of polyester filter as a superior substrate compared to solid glass.

6

The Importance of Media in Retinal Pigment Epithelium Transplantation

6 The Importance of Media in Retinal Pigment Epithelium Transplantation

6.1 Acknowledgement

I am grateful to Amanda Carr (ORBIT, UCL) for providing all western blot and qPCR data in this chapter.

6.2 Introduction:

As I have discussed in the previous chapter, substrate type and surface profile is of paramount importance to the cell phenotype and function. However it is also known that certain markers of polarity may not respond to substrate cues, but instead rely on other signals in the environment (Rizzolo 1991). ARPE-19 is a spontaneously arising RPE cell line that is a popular alternative to primary culture owing to its preservation of certain RPE characteristics. However the currently available higher passages of this line have become sensitive to culture conditions (Luo et al. 2006). Under standard culture conditions ARPE-19 are amelanotic and do not synthesise pigment. They have also consistently lacked key RPE proteins such as RPE65.

6.2.1 The role of media in differentiation

It is well known that media can be modulate the phenotype of RPE (Hu & Bok 2001). As the phenotype of ARPE-19 has become reliant on media type, I decided to explore the effect of alternative growth media some supplemented with pyruvate, in order to optimise differentiation without resorting to specialised additives. Pyruvate was selected because of its importance as metabolic substrate and because there is a wealth of evidence demonstrating the protective effect of pyruvate on cells in vivo and in vitro (Bui, Kalloniatis, & Vingrys 2004;Frenzel, Richter, & Eschrich 2005;Paquin et al. 2005;Hegde and Varma 2008).

6.2.2 The importance of pyruvate in survival and differentiation

The role of pyruvate as an energy source has been known for almost a century (Quastel 1925). Glycolysis, the anaerobic pathway for glucose metabolism yields two molecules

of pyruvate per molecule of glucose (Stryer et al. 1995). Since 1940, it was well documented that, given there is sufficient oxygen within the cell, pyruvate undergoes enzymatic decarboxylation to produce acetyl CoA which heralds the beginning of the citric acid cycle (Krebs 1940).

The importance of pyruvate in acid-base balance is also firmly established. It is well known that cells increase their glycolysis rate in hypoxic states, producing more pyruvate which undergoes reduction to lactate. The conversion of pyruvate to lactate is controlled by the *lactate dehydrogenase* enzyme (Stryer et al. 1995) which is tightly regulated to such an extent that the ratio of lactate to pyruvate (L/P) ratio remains relatively stable across a broad range of scenarios. This relationship between lactate and pyruvate has been known since the 1950s, and has been paramount in measuring acid-base status (HUCKABEE 1956;HUCKABEE 1958a;HUCKABEE 1958b;HUCKABEE 1958c). Under normal conditions, the blood L/P ratio ranges from approximately 4:1 to 10:1 (Luft 2001).

With the L/P ratio having held such a central position in acid-base balance, it comes as no surprise that pyruvate is becoming increasingly attractive as a buffer in clinical settings (Luft 2001). Together with arterial blood gas measurements, the L/P ratio has been an important indicator of acid-base status in acute and critical care settings. Pyruvate excels in management of acidotic diseases as well as a protectant for dysfunctional vital organs. Unlike the more popular buffer, bicarbonate, pyruvate attenuates intracellular acidosis without directly producing CO_2, therefore it is an excellent buffer for controlling intracellular pH (Zhou 2005). In vivo studies have indicated therapeutic effects of increased pyruvate on vital organs such as the heart (Taylor et al. 2005;Arya et al. 2006;Li et al. 2008;Miyamoto et al. 2009), the brain during haemorrhagic shock or cardiopulmonary resuscitation (Mongan et al. 1999;Mongan et al. 2001;Sharma and Mongan 2010), the immune system during sepsis (Das 2006a;Das 2006b), the pancreas from induced-pancreatitis (Ziolkowski et al. 2008).

There is a wealth of evidence demonstrating the protective effect of pyruvate in vitro on non-ocular as well as ocular cells in terms of oxidative stress, function, and improved energy metabolism. In addition to its role as an intracellular buffer, one other reason for such widely reported beneficial effects in vitro maybe that pyruvate, like other α-keto-

acids, non-enzymatically reacts with and eliminates hydrogen peroxide (H_2O_2) through an oxidative de-carboxylation reaction (Andrae, Singh, & Ziegler-Skylakakis 1985;Giandomenico et al. 1997). Thus toxic levels of H_2O_2 that would normally result in near-total death of cultured cells are rendered virtually harmless by pyruvate (Andrae, Singh, & Ziegler-Skylakakis 1985). Not surprisingly, numerous studies have emerged demonstrating the beneficial effects of pyruvate: It has been shown to protect cultured cells from induced oxidative stress in human fibroblasts (Babich et al. 2009), primary mouse striatal neurons (Desagher, Glowinski, & Premont 1997), in human neuroblastoma cells (Wang et al. 2007), mouse neuronal cultures (Paquin et al. 2005) as well as in neonatal rat cerebrocortical slices (Zeng et al. 2007a;Zeng et al. 2007b). Pyruvate's protective effect against zinc toxicity has also been documented and was reported to be superior to niacinamide in murine embryonic neuronal cultures (Sheline, Behrens, & Choi 2000).

In ocular cells, pyruvate has been shown to preserve glutathione levels, as well as inhibit lipid peroxidation in murine retinal explants exposed to oxidising medium (Hegde & Varma 2008). A similar glutathione preserving effect has been observed in lens cultures (Varma, Hegde, & Kovtun 2006). Frenzel and colleagues showed that glucose-deprived primary rabbit Muller cells exposed to oxidant stress were protected from cell death by pyruvate, not lactate, and that this effect was related to free radical scavenging by pyruvate. They further demonstrated that this effect was reversible by a mono-carboxylate transporter (MCT) inhibitor (Frenzel, Richter, & Eschrich 2005). Others have shown that both glucose-deprived rat retinal neurons and RPE can benefit from pyruvate and lactate as an energy source: a process described as metabolic coupling (Wood et al. 2004;Wood et al. 2005). Pyruvate, not lactate, protected against ischaemia-induced cell death of rat retina in vivo as well as zinc-induced death of rat retinal cell cultures (Yoo et al. 2004) and cadaveric human RPE cultures (Wood and Osborne 2003). Functional data are in support of the beneficial effect of Pyruvate: A functional study showed that MCT inhibition resulted in deterioration of the electroretinogram (ERG) in the rat, and that partial recovery was possible by exogenous pyruvate and lactate administration, as well as glutamine (Bui, Kalloniatis, & Vingrys 2004). Thus the importance of pyruvate both in vitro and in vivo is previously established.

6.3 Specific methods of ARPE-19 media experiments:

Post-confluent cultures of ARPE-19 were maintained in high glucose DMEM with pyruvate (DHP) for up to 2 months in T75 flasks (Nunc) to ensure a potential for pigmentation before use. Experimental cells deriving from an identical pool of cells were simultaneously seeded onto uncoated Transwell® polyester filters pore size of 0.4µm (Costar). In some experiments filters were coated with 1:30 growth factor reduced-Matrigel® (GFR-MG, BD Bioscience, Oxford, UK). Final cell seeding densities were between 1 – 1.5 x 10^5 cell/cm². Standard maintenance medium was removed and the experimental media were applied at least 24 hours after seeding. Medium in apical and basal chambers was changed twice a week. For 6.5mm inserts feeding volumes were 200µL apical, and 700µL basal. For 24mm inserts, 2mL apical, and 3mL basal. However basal volumes were adjusted to eliminate hydrostatic pressure for trans-epithelial resistance measurements (see results below). Inserts were maintained for up to 3 months. I compared four commercially available media types: High glucose DMEM with and without pyruvate (DH+P, DH respectively), low glucose DMEM with pyruvate (DL+P), and DMEM/F12, which were purchased as liquids and tested simultaneously using identical batches of all the usual additives mentioned in section 2.1. Unless otherwise indicated, the glucose concentration in DMEM/F12 (3.15 g/L) was adjusted to that of high glucose DMEM (4.5 g/L) and thus the letter H is included in its abbreviation (DFH).

6.4 Results:

6.4.1 Visible Pigmentation of ARPE-19 and Light Microscopy

Cells grown on uncoated transwell® filters in DMEM with pyruvate (irrespective of glucose concentration - which will also be referred to as DMEM/pyruvate) developed heavy pigmentation at 3 months, often visible with the naked eye, compared to those grown without pyruvate (Figure 6.1A – D, Figure 6.2A). Pigmentation was never observed in DMEM/F12 even when corrected to 1mM pyruvate (not shown) and glucose. Pigmentation was also evident in DMEM/pyruvate-maintained cells grown on matrigel®-coated polyester and cellulose filters (below), as well as coated/uncoated glass, and tissue-culture polystyrene flasks (not shown). Microscopic pigmentation was usually evident at 2 – 3 months post seeding (Figure 6.1A – D, Figure 6.2A).

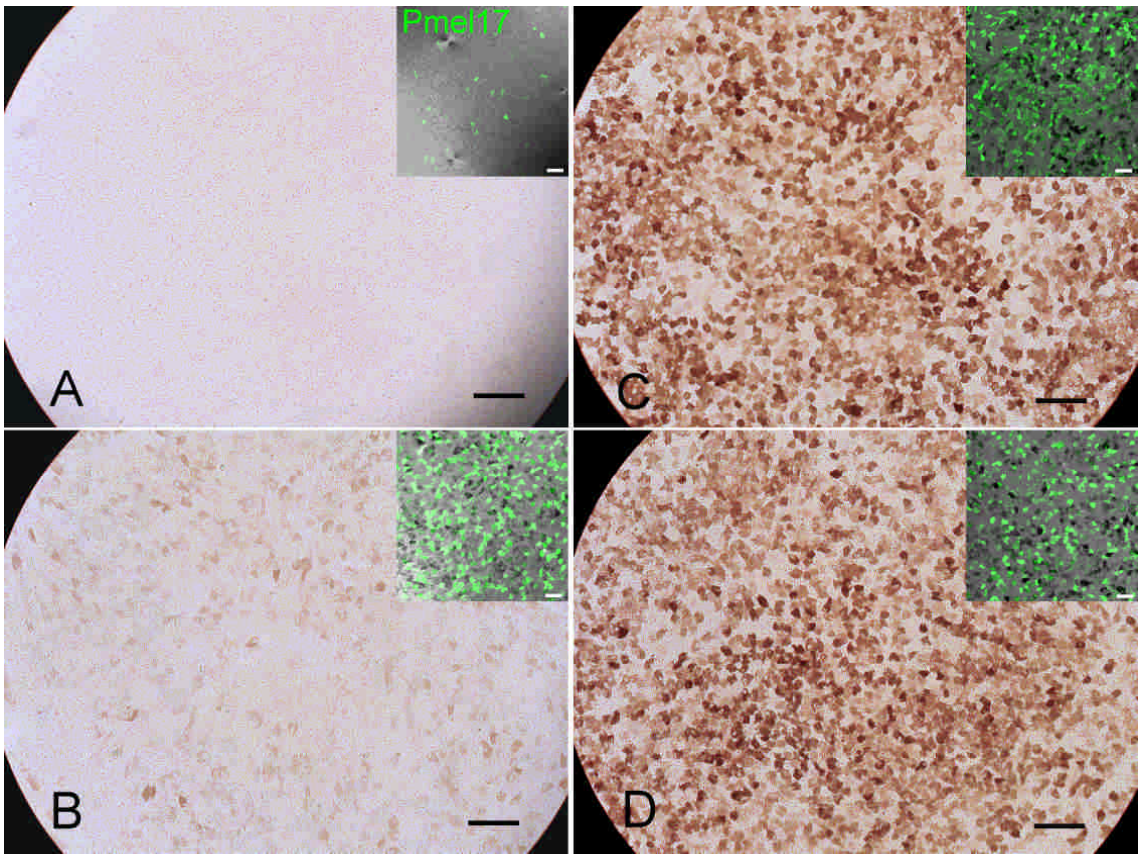

Figure 6.1. Assessment of pigmentation in cultured RPE (ARPE-19) in various media conditions with and without pyruvate at 14 weeks post-seeding. (A) No pigment is seen in DMEM/F12. B) Some pigmentation is seen in high glucose DMEM medium. (C) Heavily pigmented cells grown in DMEM/pyruvate with low glucose. (D) A similar appearance in DMEM/pyruvate with high glucose. Insets: Abundance of the immature melanosome marker pmel17 (green) in a low-magnification confocal image with Nomarski optics. Note that both pmel17 staining and Nomarski pigment correlate with the presence/absence of pigmentation in the light micrographs. Bar = 100µm, Inset bar = 50 µm.

6.4.2 Immunocytochemistry Suggests DMEM and Pyruvate are Important Factors in Differentiation

RPE differentiation markers were examined in ARPE-19 cultures under all media conditions. Cells grown in DMEM/pyruvate (DH+P, DL+P) developed several RPE differentiation markers found in native RPE cells. The expression of the immature melanosome marker Pmel17 correlated well with the development of pigmentation. There were abundant Pmel-17-positive cells in all DMEM media irrespective of pyruvate and glucose concentrations, indicating that melanogenesis had been initiated under these conditions (Figure 6.1B–D). However there were only few Pmel17-positive

cells in DFH cultured cells (Figure 6.1, insets) which is consistent with the above pigmentation results.

Actin distribution was also affected by culture medium. Cells maintained in DMEM/pyruvate displayed circumferential distribution of actin fibres which is similar to native RPE (Opas 1989;McKay & Burke 1994). Onset of this more natural distribution of actin fibres was delayed in the absence of pyruvate (DH) and DFH, and stress fibres were abundant in DFH (Figure 6.2B, see also Figure 6.3A).

Cytokeratins (or simply keratins) have been used to confirm the epithelial origin of cultured RPE cells (McKechnie et al. 1988). The RPE express keratins similar to those in simple or glandular epithelia, the most prominent being keratins 8 and 18 (McKechnie et al. 1988;Kivela and Uusitalo 1998). Cells cultured in DMEM/pyruvate lacked keratin 8 (KRT8), i.e. the expression of keratin 8 showed a negative correlation with pigmentation, since positive staining was observed only in DFH cultured cells and to some extent in DH (Figure 6.2C). This is consistent with previous studies including RPE from various sources which demonstrated that although Keratin 8 is a marker for RPE cells (alongside 18) expression of Keratin 8 is lost in confluent RPE cultures (Hunt and Davis 1990;Riley 1993;Hunt 1994;McKay & Burke 1994;McKay et al. 1997;Schraermeyer and Heimann 1999;Lopes et al. 2007;Rozanowski et al. 2008;Vugler et al. 2008). This behaviour is similar to that of keratin 18. Keratin 18 is a weak perinuclear marker in native RPE, but becomes strongly prominent in the cytoplasm appearing as a widespread cytoskeletal structure in cells of proliferating cultures (McKechnie et al. 1988). Subsequently, in resting cells, the keratin 18 positive structure reduces in size and contracts around the nucleus. This behaviour is attributed to the involvement of keratin 18 in active cell migration (Robey, Hiscott, & Grierson 1992).

Cellular retinaldehyde-binding protein (CRALBP) is widely expressed in native-RPE and is involved in retinol recycling.(Saari et al. 2001) Cells grown for 15 weeks in DMEM/pyruvate developed widespread CRALBP expression, while cultures at 8 weeks developed CRALBP to a lesser extent, although intense staining was still apparent in a subpopulation of cells (Figure 6.2D). CRALBP expression in DFH was absent (Figure 6.2D, DFH), although correction of pyruvate levels to 1mM induced a subset of weakly positive cells (not shown). Another marker of native RPE, RPE65 was detected weakly

in limited areas within DH+P-maintained cultures (Figure 6.4G), which prompted quantification of RPE65 and this is demonstrated by our western blot and Q-PCR data (Figure 6.4).

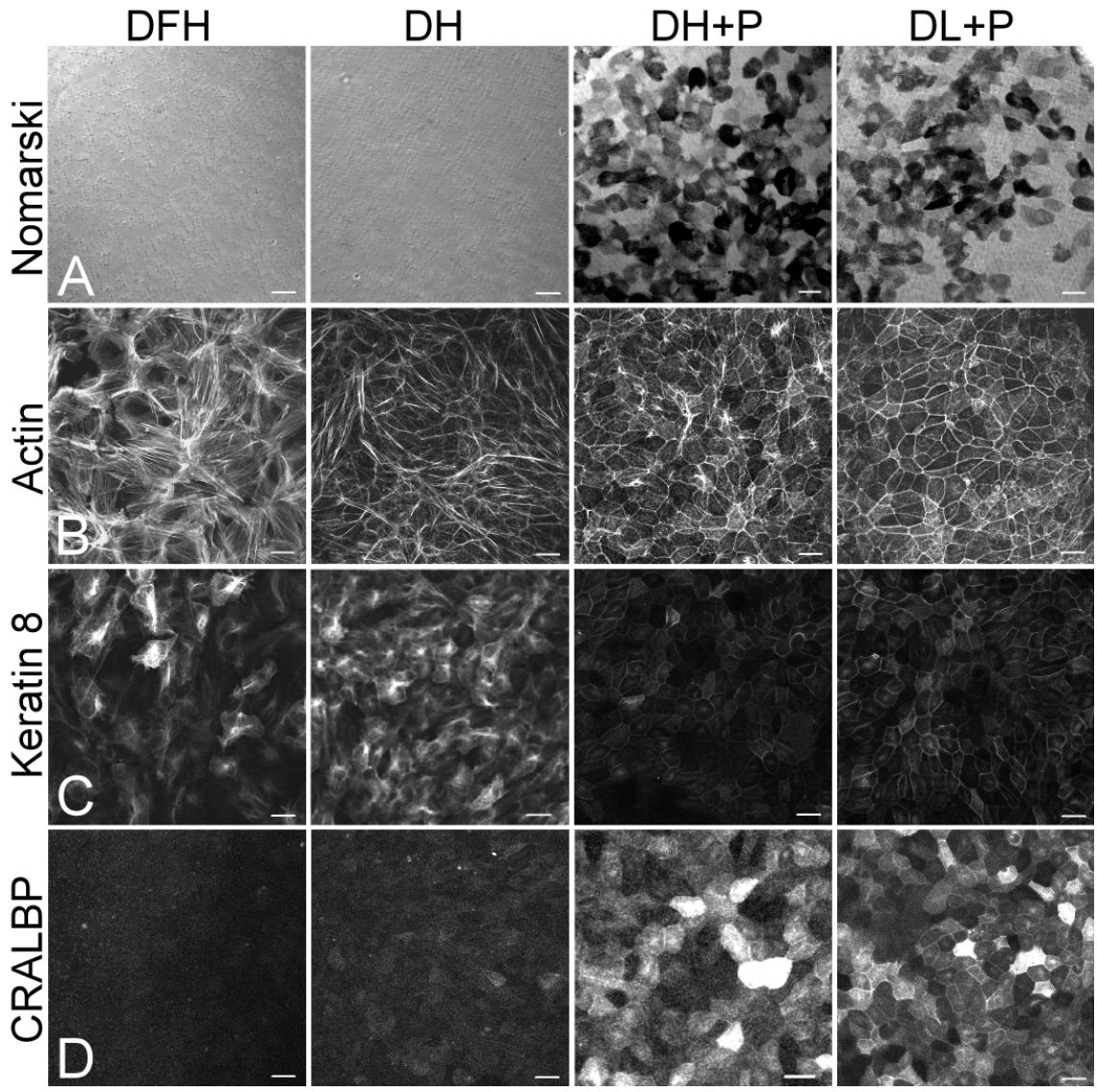

Figure 6.2. Confocal micrographs of immunostained ARPE-19 under various commercially available media conditions at 8 weeks. (A) Nomarski view of ARPE-19 cells. In DMEM-based medium pigmentation of the cells is intense in the presence of pyruvate (DH+P and DL+P). The morphology of the cells is polygonal producing a characteristic mosaic. In DMEM/F12 and DMEM without pyruvate there is no detectable pigmentation at this time point. (B) Confocal projections of actin reveal a favourable circumferential actin distribution throughout the height of the cells in DH+P and DL+P. (C) There is no Keratin 8 expression in DH+P or DL+P irrespective of glucose. Keratin 8 expression is retained in DMEM without pyruvate and DMEM/F12. (D) CRALBP expression is markedly increased in DH+P and DL+P with a subset of intensely positive cells. DFH = DMEM/F12 High glucose, DH = DMEM High glucose, DH+P = DMEM High glucose + Pyruvate, DL+P = DMEM Low glucose + Pyruvate. Bar = 20 µm.

Another feature of differentiated RPE cells is that they are normally polarised as evidenced by apical expression of Na,K-ATPase. At 15 weeks post-seeding, we analysed whether fixed and immunostained pigmented cells in DMEM/pyruvate are able to produce polarised Na,K-ATPase which is a characteristic marker in native RPE cells. Although ARPE-19 generally expressed this marker basolaterally, a subset of pigmented cells produced a subtle appearance consistent with apically localised Na,K-ATPase as seen in z-sections (Figure 6.3G, white arrows). This suggests better polarisation in pigmented cells. Single confocal frames were taken through the upper portion of the cells to analyse Actin distribution. This reveals extensive stress fibres in DFH medium while all DMEM media (DH, DH+P, DL+P) have circumferential actin staining at 15 weeks. The basal compartment of the cells demonstrated stress fibres of varying appearance in all media.

The junctional proteins ZO1 and occludin were present in all preparations (Figure 6.3, C and D) and both were invariably polarized towards the apical segment of the cellular membrane as seen in (Figure 6.3G) which indicates good junctional development.
Junctional claudins 1 and 3 were detected under all media conditions, whereas claudin-2 was detected in DMEM-based media only (not shown). SEM shows numerous apical microvilli in cells grown in presence of pyruvate.

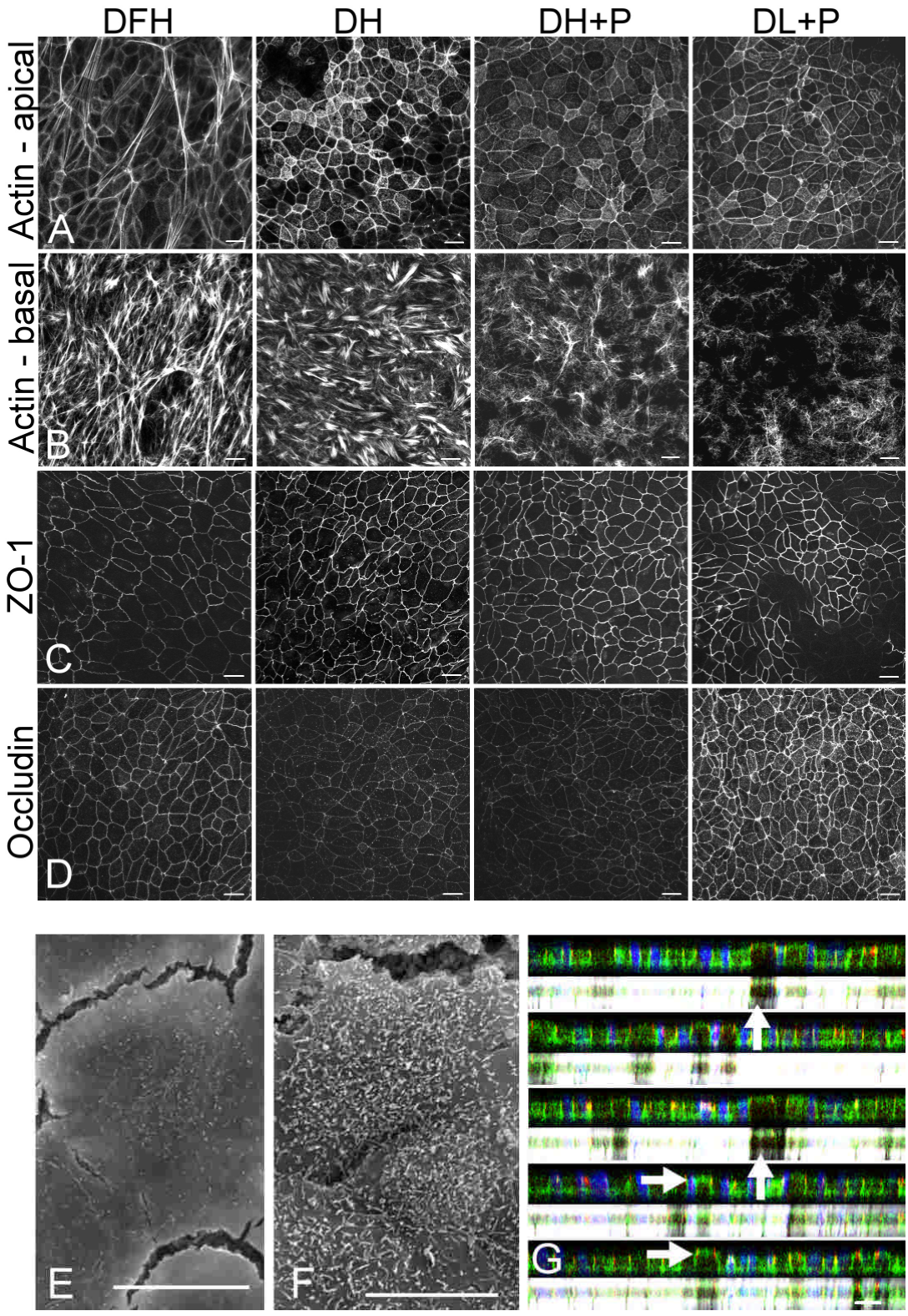

Figure 6.3. Effect of growth medium on ARPE-19 polarity at 15 weeks. (A) Single confocal frame taken through the upper portion of cells (B) Basal compartment of the cells. (C) ZO-1. (D) Occludin. (E) SEM of cells without pyruvate. (F) SEM in presence of pyruvate. (G) Z-sections with Nomarski optics to aid identification of pigmented cells (DH+P). ZO-1 (red points) in the apical region, while Na,K-ATPase (green) is basolateral except in pigmented cells (vertical arrows) which have apical expression of Na,K-ATPase (horizontal arrows). E,F Bars = 10 µm, all other bars = 20µm.

6.4.3 Quantification of Expression by Western Blots and Q-PCR Corroborates ICC Findings and Highlights the Importance of Glucose

Western blots and Q-PCR were done to quantify protein and mRNA to corroborate or complement immunocytochemistry results (Figure 6.4A). Protein expression of keratin 8 correlated negatively with pigmentation since it was only abundant in DFH, $p < 0.001$ (Figure 6.4C). DMEM/pyruvate-maintained cells expressed higher levels of RPE differentiation protein markers as follows: DMEM/pyruvate had greater CRALBP expression than either DH $p < 0.01$, or DFH $p < 0.001$ (Figure 6.4B). MerTK levels in DMEM/pyruvate were higher than DH ($p < 0.05$), but only high glucose DMEM/pyruvate, produced significantly more MerTK than DFH, $p = 0.01$ (Figure 6.4D). Surprisingly, RPE65 protein was expressed in all conditions but was greatest in DH+P. This difference was significant compared to other DMEM conditions, $p < 0.05$ (Figure 6.4E) and is corroborated by weak ICC staining (Figure 6.4G). Paradoxically, the non-pigmented cultures of DFH had significantly higher levels of tyrosinase than any other culture condition, $p < 0.01$. Therefore, DMEM-maintained cultures were associated with lower tyrosinase levels but low glucose was responsible for a further reduction among DMEM types, $p < 0.05$ (Figure 6.4F).

Messenger RNA expression generally followed a similar pattern to protein expression in most cases (Figure 6.4H–L). An obvious exception is the case of high glucose DMEM/pyruvate producing more MerTK message than its low glucose counterpart (Figure 6.4J). Table 6-1 lists the primers used for quantitative PCR.

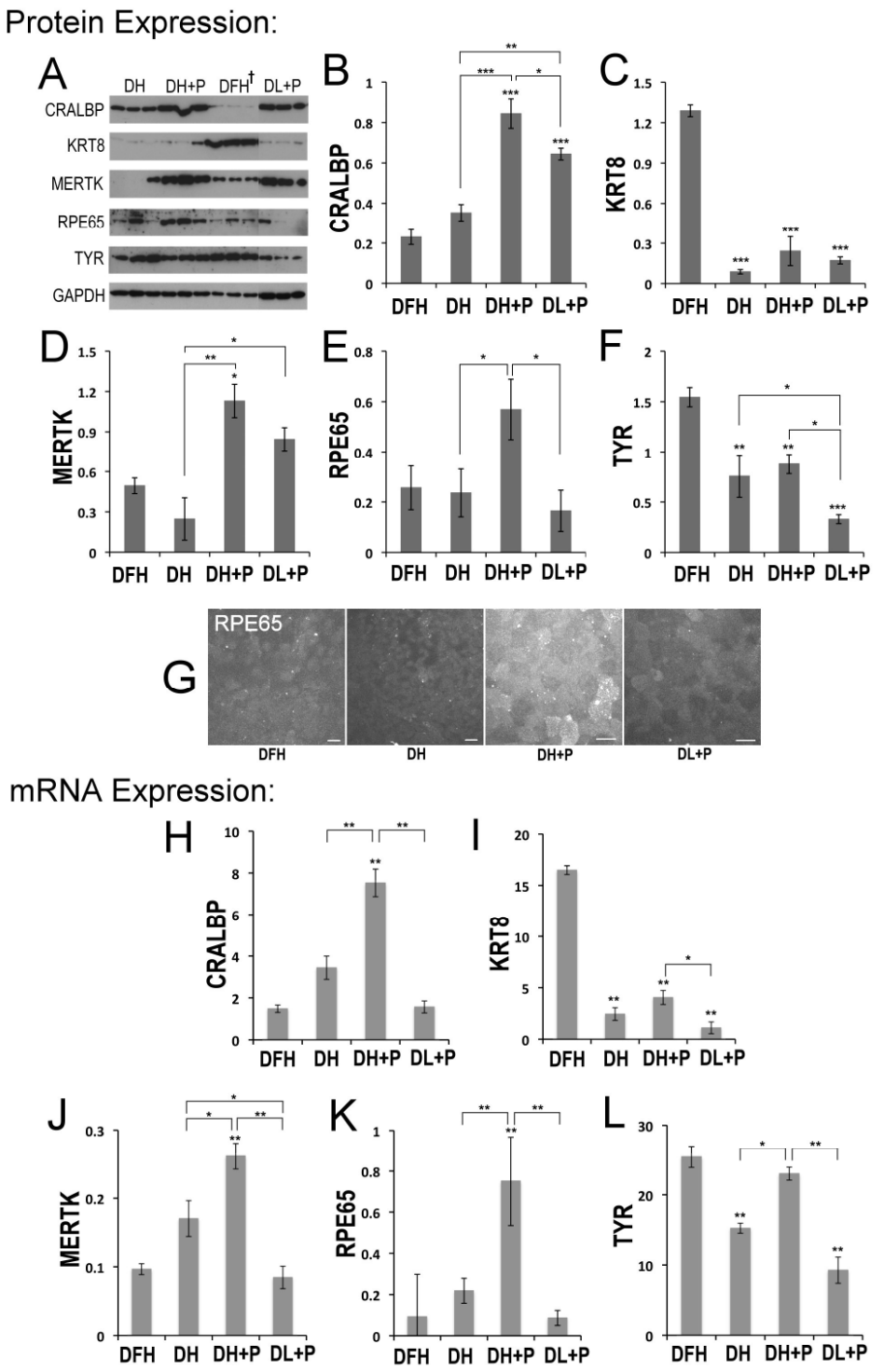

Figure 6.4. Western blot and Q-PCR in ARPE-19 cells at 15 weeks. (A–F). Proteins were probed using antibodies against CRALBP (37 kDa), Keratin 8 (KRT8 – 53 kDa), MerTK (180 kDa), RPE65 (65 kDa), Tyrosinase (TYR–70 kDa) and GAPDH (36 kDa). (A) Representative western blot image. (B–F) Relative protein expression of CRALBP, Keratin 8, MerTK, RPE65 and tyrosinase. (G) ICC of RPE65 shows a generally weak staining which is typical of this antibody. However DH+P is visibly the most intense which correlates with protein and mRNA expression. (H–I) mRNA relative expression patterns. Data = mean relative intensity ± SEM. Unless specified, asterisks indicate the following significance levels versus DFH, *p<0.05, **p<0.01, ***p<0.001 (n = 3). † Note the only occurrence of changed order of media (DFH).

Gene	Forward Primer 5'-3'	Reverse Primer 5'-3'	Accession	Size (bp)	Tm-3oC
Cralbp	GCCGAGTGGTCATGCTGTTG	AGCCTGCTGCATGGTAAGC	NM_000326	180	60
Krt8	AAGGATGCCAACGCCAAGTT	CCGCTGGTGGTCTTCGTATG	NM_002273	214	60
MerTK	ATCCTGGGGTCCAGAACCAT	TTCCGAACGTCAGGCAAACT	NM_006343	162	60
Pedf	CCCATGATGTCGGACCCTAA	CAGGGGCAGGAAGAAGATGA	NM_002615	117	60
RPE65	CAAGGCTGACACAGGCAAGA	TTGACGAGGCCCTGAAAAGA	NM_000329	118	60
Tyr	TAGCGGATGCCTCTCAAAGC	CAATGGGTGCATTGGCTTCT	NM_000372	195	60
VegfA	TCTGCTGTCTTGGGTGCATT	ATGTCCACCAGGGTCTCGAT	NM_001171623	175	60
Gapdh	CCCCACCACACTGAATCTCC	GGTACTTTATTGATGGTACATGACAAG	NM_002046	104	60
Tubb	AATCCCCACCTTTTCTTACTCC	AAAGATGGAGGAGGGTTCCC	NM_004048	119	60
B2M	TGTTGATGTATCTGAGCAGGTTG	AAGATGTTGATGTTGGATAAGAGAATC	NM_178014	100	60

Table 6-1. Primers used for quantitative PCR. Primers were designed over intron spanning regions to avoid co-amplification of any genomic DNA.

6.4.4 Transepithelial Resistance Reiterates the Benefits of DMEM and Pyruvate

Maturity of cell-cell tight junctions was assessed by TER. TER was stable in high glucose DMEM/pyruvate over the entire 6 week experimental period whereas other media showed a gradual decline (Figure 6.5A). The 6 week-average TER for DMEM/F12 was 45.4 ± 0.8 Ω.cm², for high glucose DMEM 51.8 ± 0.7 Ω.cm², and for high glucose DMEM/pyruvate was 51.3 ± 1 Ω.cm² (mean ± SEM). There was a significant difference between DMEMF12 and DMEM irrespective of pyruvate supplementation $p < 0.001$ (Figure 6.5B).

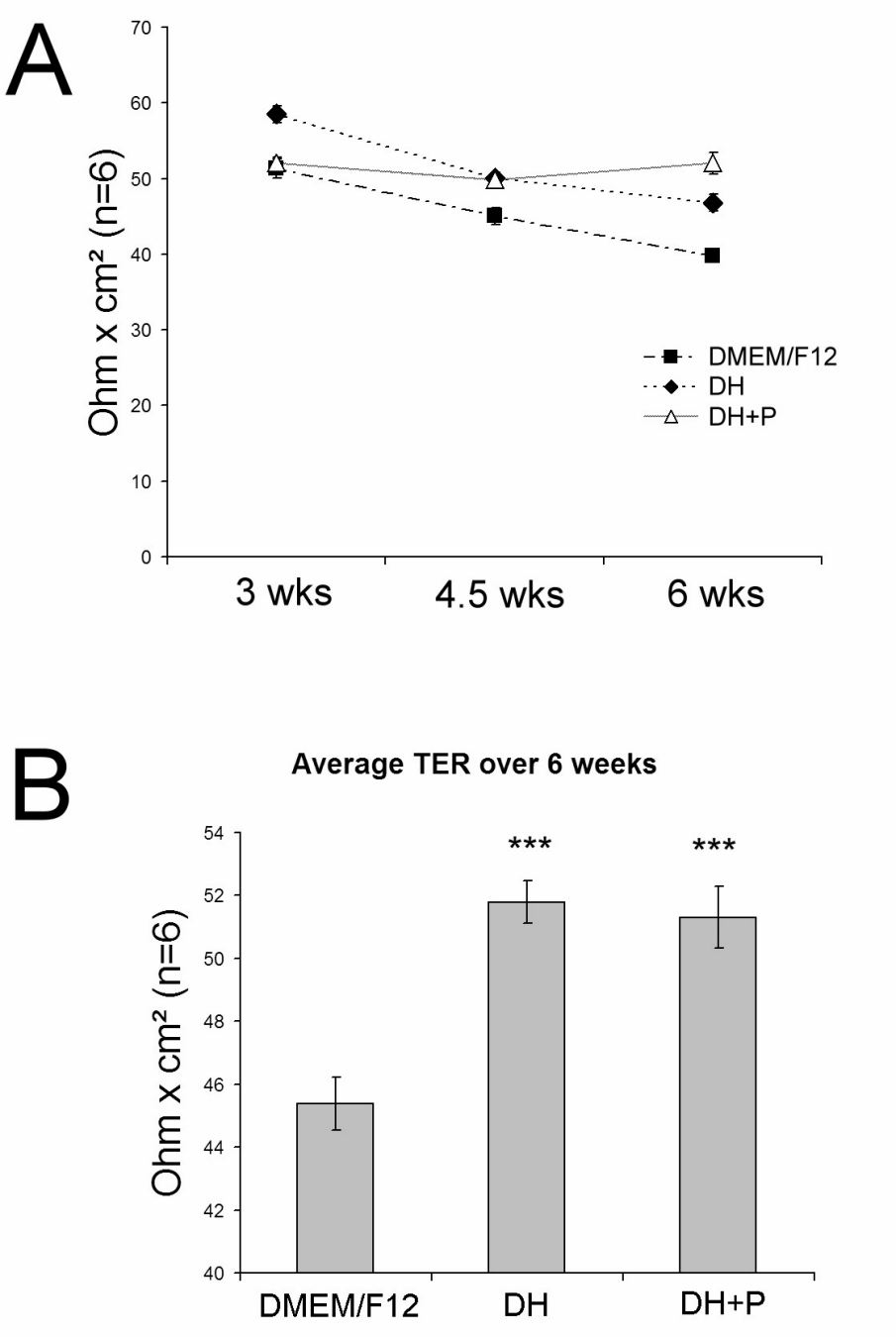

Figure 6.5. A comparison of TER of ARPE-19 cells grown on uncoated filters in various media conditions over the course of 6 weeks. (A) TER values at 3, 4.5 and 6 weeks demonstrates a relative decline in TER except in DH+P. (B) Average TER over the same time period distinguishes DH as well as DH+P as superior. Data are means ± SEM. Asterisks indicate the following significance levels versus DMEM/F12, * $p < 0.05$, *** $p < 0.001$ ($n = 6$).

6.4.5 VEGF and PEDF Expression Profiles Further Confirm Optimal Growth Conditions

Since VEGF and PEDF are major growth factors secreted by native RPE, it was hypothesised that they could change in parallel with other differentiation markers. VEGF secretion was examined by ELISA of ARPE-19 conditioned experimental media at 10 weeks. VEGF output was 2152 ± 198 pg/cm²/24h for DMEM/F12, 6136 ± 958 pg/cm²/24h for DMEM, 5997 ± 1017 pg/cm²/24h for high glucose DMEM/pyruvate, and finally 12950 ± 2030 pg/cm²/24h for low glucose DMEM/pyruvate (mean ± SEM). Total VEGF output was higher in DMEM media compared to DMEM/F12, $p < 0.05$ (Figure 6.6A). There was no difference in total VEGF output between pyruvate and non-pyruvate supplemented high glucose DMEM ($p = 0.99$). There was also no significant difference between apical and basal VEGF secretion in DMEM media, however it appears that DMEM induced a significant rise in basal VEGF when compared to DMEM/F12, $p < 0.05$ (Figure 6.6B). Low glucose DMEM/pyruvate produced significantly higher basal VEGF than its high glucose counterpart $p < 0.05$. We also examined mRNA expression of VEGF and PEDF in the same experiment at 15 weeks. Surprisingly, the effect of low glucose was to lower VEGF expression but no effect of pyruvate is seen (Figure 6.6C). Pyruvate and glucose appeared to both contribute to increased PEDF mRNA since lack of either factor caused a significant drop (Figure 6.6D). Favourable (low) VEGF/PEDF ratios are seen only in DMEM media irrespective of pyruvate and glucose (Figure 6.6E). PEDF protein was detected in western blots of high glucose DMEM/pyruvate (Figure 6.6F).

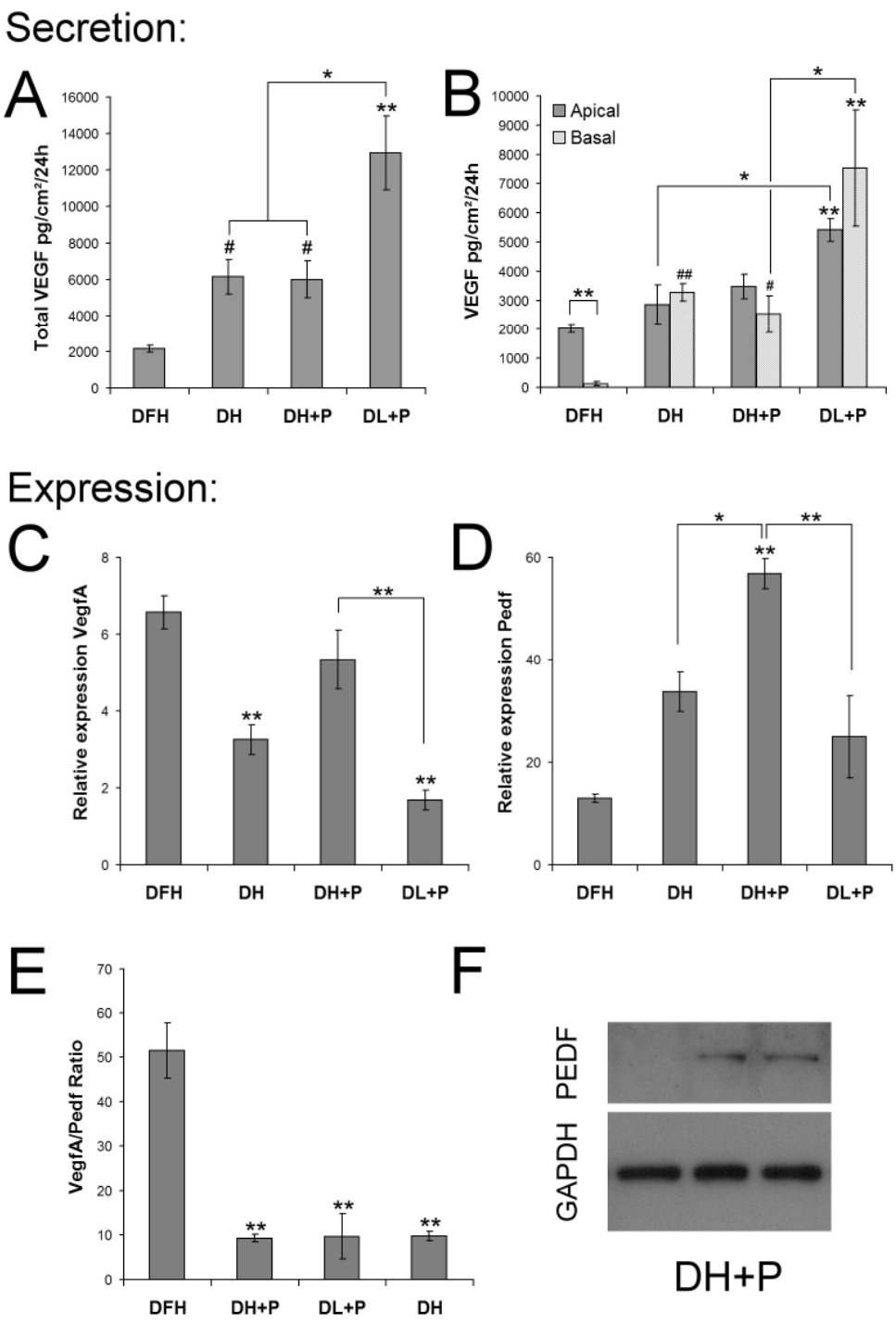

Figure 6.6. (A–B) A comparison of VEGF secretion by ARPE-19 cells grown on uncoated 24mm filters at 10 weeks. (A) Total VEGF (pg/cm²/24h) at 10 weeks. (B) The same groups with apical and basal VEGF shown separately. Basal VEGF is significantly increased in other media compared to DFH. (C–E) A comparison of VEGF and PEDF mRNA at 15 weeks. (C) The effect of low glucose was lower VEGF expression but no effect of pyruvate is seen. (D) Pyruvate and glucose contribute to increased PEDF expression. (E) Favourable (low) VEGF/PEDF ratios are seen in DMEM media. F) A triplicate western blot of PEDF expression in DH+P. All data are means ± SEM. Unless otherwise specified, asterisks indicate the following significance levels versus DFH, *p<0.05, **p<0.01. Hash symbols indicate significance versus DFH when only high glucose media are analysed (DFH, DH, DH+P), #p<0.05, ##p<0.01 (n = 3).

6.4.6 Electron Microscopy and Human Photoreceptor Outer Segment-Phagocytosis by Differentiated ARPE-19 Cells

Melanosomes of varying maturity were abundant in ARPE-19 grown in the presence of DH+P (Figure 6.7A and B), as well as DL+P (not shown) before exposure to human retina confirming the potential for pigmentation in DMEM/pyruvate. In samples incubated with retina (high glucose DMEM/pyruvate), internalised human POS could be seen within DMEM/pyruvate-maintained ARPE-19 cells in TEM sections at both 24 (Figure 6.7C) and 48 hours (Figure 6.7D–H). The same number of TEM sections was examined for both groups. Internalisation of outer segments increased with time: 4 incidences of internalised outer segments were identified in 24 hour sections compared to 35 unique incidences at 48 hours (Figure 6.7C – H).

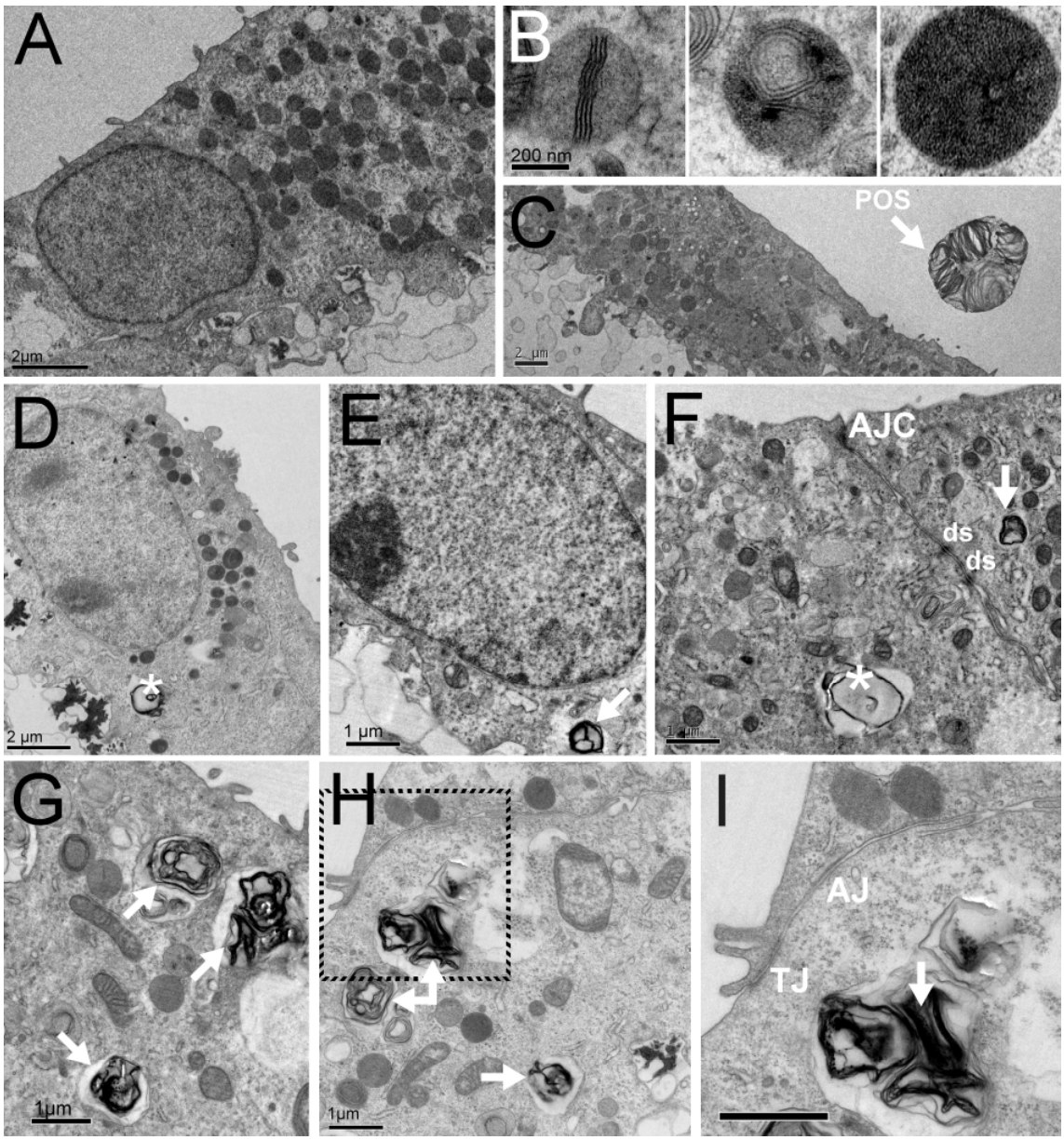

Figure 6.7. TEM of pigmented post-confluent ARPE-19 cells on matrigel-coated cellulose filters maintained with DH+P, and human POS Phagocytosis Assay at 10 weeks: (A) Control ARPE-19. (B) Various stages of melanogenesis found in these cells (increasing from left to right). (C) Cells co-cultured with human retina for 24 hours with an example of non-internalised human POS (human retina became separated from RPE cells during processing). (D–H) The presence of phagosomes in ARPE-19 cells at 48 hours post co-culture which are consistent with internalised POS. Arrows indicate internalised POS, asterisks indicate lipid-rich phagosomes which may be the result of POS digestion. (D) Note the cuboidal polarised profile of some cells. (F) Also note desmosomes (ds) at the cell-cell border and the apical junctional complex (AJC) which indicate junction development and polarity. (I) High magnification image of an ingested POS (from H). Note the features consistent with a tight-junction (TJ) and an adherens junction (AJ). A, C, D: bars = 2µm. B: = 200nm. All other bars = 1µm.

6.4.7 Karyology

Since ARPE-19 is not clonal, we sought to further characterise our cells by karyotyping, as strain variation has been suggested previously (Luo et al. 2006). A total of 17 random p26 ARPE-19 cells were karyotyped. Results of the karyotyping are outlined in Table 6-2.

Karyotype	Number of Cells	Percentage
45,XY,-15,der(19)t(15;19)(q?15;qter)	7	41%
46,XY	5	29%
46,XY,add(19)(qter)	4	24%
45,X	1	6%

Table 6-2 Various karyotypes found within a sub-confluent flask of p26 ARPE-19 maintained in DMEM High glucose medium in our lab. This is fairly consistent with karyotypic findings reported by Dunn et al (Dunn et al. 1996) who initially established and reported this cell line.

6.4.8 Inhibition of Pyruvate Transport Prevents Differentiation

A well-established pyruvate transport inhibitor alpha-cyano-4-hydroxycinnamate (4-CIN) was utilised for the pyruvate transport inhibition assay. 4-CIN was added to DH+P at either 50µM or 500µM. An almost total inhibition of pigmentation of ARPE-19 cultures was observed at the higher concentration of 4-CIN by 11 weeks post-seeding (Figure 6.8B). Abundant pigmentation could be seen in the 50µM 4-CIN (Figure 6.8A) and the control group (bright-field not shown). Upon further analysis of actin by ICC, abundant stress fibres were seen in the 500µM concentration of 4-CIN, whereas 50µM appeared to have no effect on ARPE-19 cells in this respect (Figure 6.8C). Nomarski optics confirm pigmentation extent in control, 50µM and 500µM groups respectively (Figure 6.8D; n = 3).

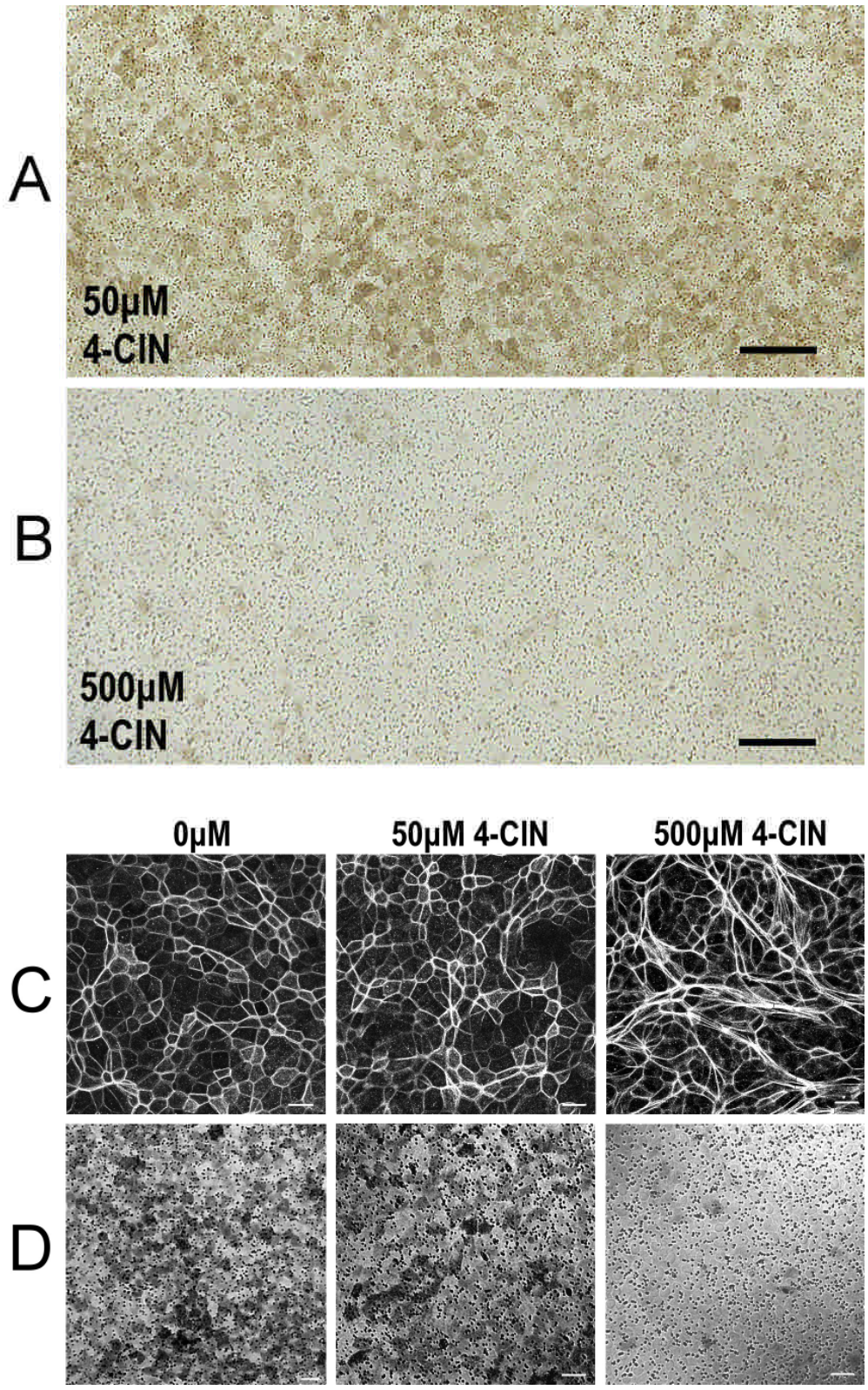

Figure 6.8. The effect of alpha-cyano-4-hydroxycinnamate (4-CIN) on the differentiation of ARPE-19 cells in high glucose DMEM/pyruvate (DH+P) medium at 11 weeks. (A) Brightfield light microscopy of cells grown in the presence of 50µM 4-CIN develop visible pigmentation, similar to controls (not shown). (B) 500µM 4-CIN visibly reduces pigmentation. A,B bars = 100µm (n = 3) (C) Actin fibres are circumferential in control and 50µM groups, but abundant stress fibres occur at the highest concentration of 4-CIN. (D) Nomarski optics confirm pigmentation levels. Bar = 20µm.

6.5 Summary of ARPE-19 Media Optimisation and Discussion

Cultured RPE may become a therapeutic option for transplantation in retinal disease. However maintaining a native-RPE phenotype in vitro has proven challenging. The human RPE cell-line ARPE-19 is used widely as an alternative to primary RPE. It is grown in DMEM/F12 medium as standard but its phenotype is dependent on culture conditions and many differentiation markers are usually absent.

Pyruvate, in combination with DMEM, induced dark pigmentation and promoted differentiation markers such as CRALBP, and MerTK. Importantly, RPE65 protein was detected by western blotting and was enhanced by pyruvate, high glucose and DMEM. ARPE-19 cells maintained in this medium could also phagocytose human POS. VEGF secretion was greater in DMEM cultures, and was affected by glucose, but not pyruvate. Another exciting result is that PEDF expression can be modulated at transcriptional level in ARPE-19 by optimising growth medium Pigmentation never occurred in DMEM/F12. I have used a well-established pyruvate transport inhibitor, 4-CIN (Halestrap & Denton 1975;Halestrap 1975) which, at 500μM, reversed the favourable effects of high glucose DMEM/pyruvate. Contrary to some groups' belief that cultured ARPE-19 are always amelanotic, my data demonstrates cultured RPE can express tyrosinase and synthesise pigment. These results favour the use of high glucose DMEM with pyruvate for future RPE differentiation and transplantation studies.

7

Human Embryonic Stem Cells as a Source for Cellular Therapy

7 Human Embryonic Stem Cells as a Source for Cellular Therapy

7.1 Acknowledgement

I am grateful to Amanda Carr for performing the VEGF and PEDF Elisa in this chapter.

7.2 Introduction

In 2002 Kawasaki and colleagues published the first report of embryonic cell-derived-RPE using primate ESC. They observed large areas of polygonal pigmented cells that resembled epithelial cells (Kawasaki et al. 2002). Another study by Kawasaki's colleague Haruta et al followed (Haruta et al. 2004) which demonstrated expression of key RPE-specific genes, promised further differentiation of these HESC towards the RPE fate. Another study by Klimanskaya et al (2004) demonstrated HESC differentiating into RPE-like cells by depriving them of FGF in the absence of feeder layers. Importantly, the transcriptome of these HESC-RPE was more representative of primary RPE cell transcriptome than the two key human RPE lines at the time: ARPE-19 and D407 (Klimanskaya et al. 2004). Our own study in 2008 confirmed HESC-RPE to be superior to adult RPE lines and we demonstrated improvements in phenotype using a simplified spontaneous differentiation protocol utilising basic HESC medium without bFGF or FCS (Vugler et al. 2008).

In this chapter I will present work that helped characterise our HESC-RPE up until the point of our 2008 study. Furthermore, having had such success with characterisation of HESC-RPE, I sought to further examine HESC-RPE as a potential source of cells for RPE transplantation through dissociation and re-seeding on an optimal surface. To date there have been few if any considerable attempts at transplanting RPE-substrate composites in humans, and this is the ultimate aim of my project.

7.3 Human Embryonic Stem Cell-derived RPE Colonies (HESC-RPE) as a source of RPE

7.3.1 Comparing effect of various matrix coatings on HESC colony behaviour on Tissue Culture Polystyrene (TCPS) vessels

Freshly harvested HESC colonies require prompt plating onto matrigel-coated dishes in order to attach and subsequently expand in size. However, matrigel is an unrefined composite ECM animal product originating from murine Engelbreth-Holm-Swarm (EHS) sarcoma cells. Thus it comprises many defined components but ultimately some undefined non-human components will exist. In order to better characterise the process of HESC colony adhesion and expansion I sought to test the better-defined laminin as well as some xeno-free ECM alternatives. Laminin-1 is the major constituent (approximately 60%) of matrigel and is widely available from murine EHS sarcoma sources (Hosokawa et al. 2002;Hayashi et al. 2004). Plasmanate® is a commercial 5% human plasma protein fraction in an isotonic electrolyte (Na, K, Cl) solution. It is made from pooled human plasma which has been heat inactivated at 60ºC for 10 hours to minimise pathogen risk and is tested for hepatitis and HIV viruses. Plasmanate is approved for use in humans hence it is a highly attractive source of human serum proteins to test as an alternative ECM coating. ECM proteins are reported to be present in human serum (Ayache et al. 2006). KnockOut™ serum replacement (KSR) is an alternative proprietary preparation (Gibco®, Invitrogen) that is used instead of FCS in HESC medium. KSR contains bovine serum albumin as a main ingredient but is a more simplified serum product than FCS (Price et al., Internat. Patent Applic. WO98/30679, 1998). Puramatrix® (BD Bioscience) is a proprietary 1% solution of standard amino acids that self assembles into a 3D hydrogel composed of a nano-scale fibrous network and provides the benefits of 3D culture in a 2D setting (this product has been discontinued by the time of writing this thesis, catalogue no. 354250). ARPE-19 cells secrete abundant amounts of collagen IV and laminin-P1 (not shown) therefore I sought to investigate whether this secreted ECM would be sufficient for HESC-RPE colony attachment.

7.3.1.1 Procedure for applying coatings

TCPS 35mm dishes were coated according to manufacturer's instructions with matrigel and laminin. The other aforementioned ECM substitutes were coated as follows: KSR and Plasmanate were used neat and incubated in dishes overnight at 4ºC. Puramatrix was used undiluted (1% solution) and applied as a thin layer onto dishes supplemented by media and incubated at 37ºC for 30 minutes. Media was changed twice within 1 hour to equilibrate the pH of the hydrogel and stored at 37ºC until use as instructed. Some additional dishes were left uncoated. ARPE-19 matrix was prepared by utilising post-confluent pigmented 75cm² TCPS flasks that had been maintained for over 8 weeks in parallel to this experiment. The cells within these flasks were removed by trypsinisation and thorough rinsing in PBS at RT to remove all cellular matter. For laminin coating in this experiment, a high concentration laminin protocol was used (approx. 10μg/cm²). Matrigel protocol was as usual and according to our protocol (this comprises 21μg/cm² of laminin as a constituent). An approximately equal number of similarly sized Shef-1 HESC-RPE colonies (6-7 per dish/flask) were removed from MEF seeded TCPS flasks and seeded onto each matrix type. All vessels were seeded in duplicate and maintained for 3 months.

7.3.1.2 Results

Attachment to matrigel and laminin-coated dishes was rapid and occurred overnight. On all other matrices, HESC-RPE colonies never became attached and were still freely floating even at 3 months. Surprisingly, Laminin induced multiple 'bleb' (in literature also known as 'dome') formation (Figure 7.1). Disappointingly, ARPE-19 matrix—which I have characterised elsewhere to contain abundant collagen IV and laminin-P1 (not shown)—was not successful in attaching HESC-RPE colonies Table 7-1.

	Laminin-1	GFR-MG	Plasmanate	KSR	Puramatrix	ARPE-19 ECM	Un-coated
Attachment	Yes	Yes	No	No	No	No	No
Spreading	+++*	+++	--	--	--	--	--
Bleb formation	8-9**	None	--	--	--	--	--

Table 7-1: Results of experiment comparing the effect of various coatings on attachment and spreading of primary HESC-RPE colonies on TCPS dishes at 3 months (n = 2). Laminin coating induced multiple bleb formation. *despite using high concentration laminin initial colony spreading was apparently slower for laminin than that observed for matrigel. However final HESC sheet size was similar. **There appeared to be a ninth bleb which had burst and as a result was flat but had a distinct border.

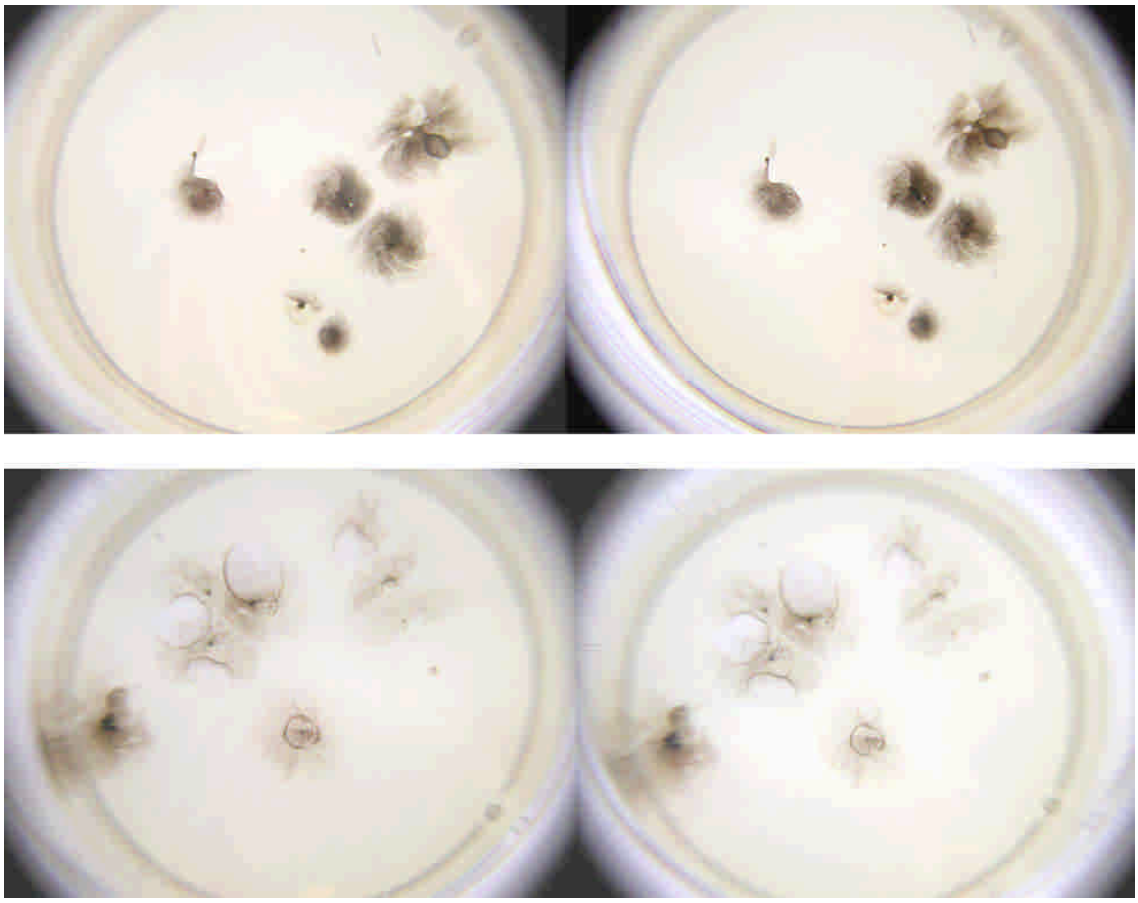

Figure 7.1: Stereo pairs of, Top: Differentiated Shef-1 HESC-RPE sheets arising from seeded colonies onto Matrigel coated TCPS at 3 months. Bottom: HESC sheets arising from seeded colonies onto Laminin-coated TCPS at 3 months. The spreading sheets of HESC-RPE here contain 8-9 blebs at 10,11,12,1 and 2 o'clock, the central bleb seems to have burst and flattened but has a distinct border. In the picture the blebs appear lighter coloured, in comparison to Matrigel induced sheets.

After observing such functional differences between laminin and matrigel supported HESC-RPE colonies, it was considered that the Na,K-ATPase pump might be more active in the laminin group thus giving rise to raised detachment blebs (domes). Therefore I sought to stain these dishes for Na,K-ATPase to observe for any differences in its expression between the laminin and matrigel groups. The results of ICC on these dishes are in Figure 7.2. There was no obvious difference in the extent of expression and localisation of Na,K-ATPase between laminin and MG groups. Laminin seemed to induce a tighter packing of the cells as evidenced by the DAPI nuclear staining. Both groups expressed OTX2 indicating preservation of RPE specification (Figure 7.2).

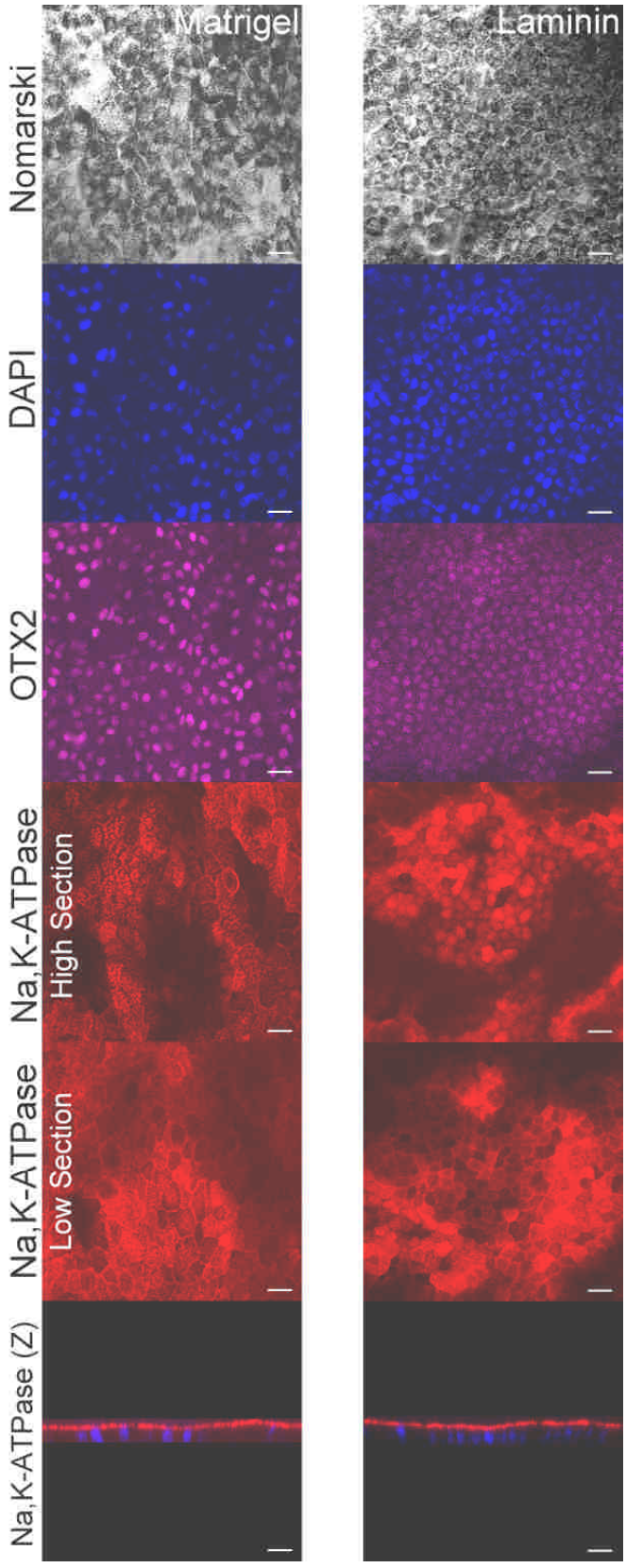

Figure 7.2 Confocal micrographs of Na,K-ATPase and OTX2 expression in expanding HESC-RPE sheets. Na,K-ATPase is equally expressed in laminin versus matrigel-coated polystyrene dishes. Note the characteristic apical distribution of Na,K-ATPase which appears to an identical degree in both conditions. These data suggest the bleb formation is probably not the result of an over expression of this ion transporter.

7.3.1.3 Discussion:

In this experiment, HESC-RPE grown on laminin coated dishes behaved similarly to those grown on matrigel, except for some apparent lag in spreading which resulted in smaller colonies, tighter packing of cells and the appearance of detachment blebs (which have also been described in literature as domes). I wondered whether development of blebs reflected a more active pump mechanism in the laminin group, or whether their attachment to their matrix was weaker. It is well established that in situ RPE as well as optimally differentiated in vitro RPE harbour apically oriented Na,K-ATPase (Hu & Bok 2001;Ahmado et al. 2011). It was reassuring to see that HESC express this marker apically in both laminin and matrigel groups. The observation that Na,K-ATPase expression appeared very similar in intensity in ICC among laminin and matrigel groups strongly suggests that detachment blebs are not related to over-expression of this apically-located ion transporter and that an alternative causation must be considered, such as cell-matrix interactions. In any case, since the apparent lag in growth remained uncharacterised, it was decided to continue further studies using matrigel or an equivalent.

In the next section I will show that HESC colonies can be enzymatically dissociated to produce cell suspensions, but it should be mentioned here that I have tested the adhesion of dissociated HES-RPE cells and indeed they follow the behaviour of their parent colonies i.e. HESC suspensions will readily attach and populate a surface coated with either laminin or matrigel whereas they will not attach to uncoated or incompatible surfaces leading to the abundant formation of spheres of cells (not shown).

7.4 Dissociation of Human Embryonic Stem Cell derived-RPE: a proof of concept and a powerful tool for investigation of HESC-RPE behaviour

7.4.1 Principle and rationale of dissociation

Cell dissociation underlies the principle of in vitro cell culture since the latter cannot happen without an initial dissociation step. There was initial worry with the concept of dissociation since it has been shown that the method of dissociation of RPE cells significantly affects their ultrastructure and final phenotype (Opas & Dziak 1988). This is strongly related to the prevalence of certain phenotypes within the culture e.g.

epitheloid versus fusiform, and the type of adhesion molecule that predominates within the dominant phenotype (McKay & Burke 1994). For example, within primary adult RPE cultures, the more favourable epitheloid phenotype enjoys stronger cell-cell adhesions than its equally common fusiform counterpart and hence favourable cells are more difficult to dissociate (McKay & Burke 1994). On the other hand, a complete dissociation of a pigmented HESC-RPE colony can be assessed by visual means and can be confirmed by microscopy of the remaining vessel. This is a welcome advantage of pigmented RPE culture dissociation and guarantees against enzymatic selection. Besides, Bruce Pfeffer (Pfeffer 1991) argues that homogeneity of phenotype and preponderance of epitheloid cells over fusiform types is a characteristic of young donor primary cultures. Since embryonic stem cells are more youthful than fhRPE (Kannan, Sreekumar, & Hinton 2011;Zhu et al. 2011) it is expected that the RPE cultures yielded would be predominantly if not wholly epitheloid. Furthermore, HESC-RPE colonies can be regarded as pigmented subclonal cell populations derived from a clonal process (Amit et al. 2000) and are thus far more homogenous than a layer of cadaver RPE that is yet to be removed from an eye cup. Therefore, it was decided that dissociation would not be a cause of a phenotypic selection bias due to visual confirmation of dissociation.

7.4.2 Dissociation of HESC-RPE using an EDTA-based solution

HESC-RPE cultures reach a high level of differentiation (Vugler et al. 2008) and form strong cell-cell adhesions as shown by their resistance to common standard cell dissociation protocols (Table 7-2).

HESC-RPE Dissociation Method	Outcome
Collagenase	No cell dissociation
Papain	No cell dissociation
Dispase	No cell dissociation
Trypsin 0.25%	Minimal cell dissociation
Trypsin 0.25% in a non-enzymatic cell dissociation buffer with EDTA (Sigma)	Complete cell dissociation

Table 7-2: The outcome of various enzymatic dissociation methods when used to dissociate HESC-RPE colonies and sheets from their dishes.

Therefore, the initial challenge with HESC-RPE was to find any feasible method that could dissociate their adherent sheets into cell suspensions. It is widely accepted that

EDTA is a potent divalent ion chelator. It is commonly used for non-enzymatic dissociation of weakly attached cultured cells. It also known that RPE cells harbour many adhesive integrin molecules that maintain both cell-matrix as well as cell-cell adhesion which I have already discussed in earlier sections. These integrins contain multiple Metal Ion-Dependent Adhesion Sites or MIDAS (Hynes 2002) which if targeted by EDTA can be deprived of their ions. Thus it may be possible to loosen HESC attachment to their matrix.

7.4.2.1 Results and discussion

I investigated various enzymatic dissociation methods for dissociating the HESC-RPE including trypsinisation (Table 7-2). The full protocol is given in Table 7-3. Despite using PBS without Ca^{++} and Mg^{++}, none of the enzymatic methods listed therein were successful except for trypsin as a 0.25% solution in non-enzymatic dissociation buffer (Sigma-Aldrich) as a solvent. The latter buffer is a proprietary buffer with an optimised concentration of EDTA. Subsequently, several of my colleagues in our laboratory reported successful dissociation using the non-proprietary and commercially combined Trypsin-EDTA (our current departmental protocol). Thus, these observations provide a proof-of-concept that divalent ions play a pivotal role in HESC-RPE cell-cell and cell-matrix adhesion which is likely brought about by Mg^{++} or Ca^{++}-dependant adhesion molecules such as integrin MIDAS (Hynes 2002) and cadherins (Alattia, Kurokawa, & Ikura 1999). The full protocol for dissociation and resuspension of pigmented HESC colonies is described in Table 7-3.

Protocol for dissociation of pigmented colonies of HESC:

1. Pigmented cell colonies are harvested from flasks by cutting around them with a sterile microblade. Separation is facilitated by pushing them with a pippete tip while aspirating simultaneously to tease them away.
2. The desired amount of pigmented colonies are collected along with their growth media in a 1.5mL eppendorf tube. (As a rough guide: 8 pigmented clusters suspended in 1mL should produce around 400,000 - 800,000 cells/mL by the end of this method)
3. Centrifuge at 1200 - 3600 rpm for 3-5 minutes
4. Care is taken while aspirating as much of the media away with a Gilson pipette, since the cells will not be firmly adherent to the bottom of the tube.
5. 0.9mL of Sigma Cell Dissociation Solution Non-enzymatic in PBS 1x (C5914) is added
6. 0.1mL of filtered sterile Trypsin 10x is also added. The final solution is now Trypsin 1x
7. Cells are placed in an incubator at 37°C for 5-15 minutes
8. After removal from the incubator the cells are triturated with a Gilson pipette at least 4-6 times. If not completely dissociated, the cells are returned to the incubator for another 5 minutes. This step is repeated until the pigmented clumps disappear as they are suspended in solution bearing in mind that trypsinisation total time must not exceed 20 minutes.
9. Centrifugation at 1200 - 3600 rpm for 5 minutes. A round pigmented pellet will have formed at the bottom of the tube.
10. Carefully aspirate of as much of the cell dissociation solution without disturbing the pellet.
11. 0.5mL of HESC media is now added followed by trituration with a Gilson pipette. The pellet disappears as all the cells are suspended once again.
12. A further 0.5-1mL of HESC media is added. Cell concentration can now be measured with a haemocytometer at this stage.
13. The cell solution is now ready for seeding onto matrigel-coated cultureware.

Table 7-3 A protocol was devised for dissociation and resuspension of pigmented HESC. The given yield is an approximate guide and will depend on the size of the HESC-RPE colonies used.

7.4.3 Low seeding density of HESC on Matrigel coated plastic promotes neuronal characteristics combined with a noticeable decline in cell population

7.4.3.1 Introduction

A pilot experiment was conducted whereby dissociated reseeded HESC-RPE (dsHESC-RPE) were seeded onto uncoated wells in a TCPS multidish. Since none of the wells showed any adherent HESC-RPE even 1 week after seeding, that experiment was aborted and ever since, matrigel has been used as a substrate for adhesion of dsHESC-RPE to the culture dishes.

I sought to characterise the behaviour of dsHESC by live observation of these cells seeded in a matrigel-coated multidish under different media conditions.

7.4.3.2 Methods

A TCPS 24 well multidish was coated with 1:30 diluted growth factor reduced matrigel overnight at 4ºC. Matrigel was aspirated immediately before cell seeding. Prior to seeding, HESC-RPE were maintained in basic HESC-medium: high glucose (4.8g/L) KnockOut Dulbecco's Modified Eagle's Medium (DMEM, Invitrogen) with 20% KSR, 1% non-essential amino acid solution, 1mM L-glutamine (Invitrogen), and 0.1mM β-mercaptoethanol (Sigma) without bFGF.

Seven pigmented HESC-RPE colonies were harvested from MEF seeded TCPS flasks and dissociated using the aforementioned dissociation technique given in Table 7-3. The cell suspension was divided equally and seeded into all 24 wells at a cell density approaching 20,000 cell/cm². Growth Media conditions tested were pure HESC media, 1:1 HESC:RPE medium and pure RPE growth medium (x1 DMEM high glucose with L-glutamine with pyruvate and 1% FCS). A subsequent group of HESC-RPE colonies were dissociated and seeded at 50,000 cell/cm² onto polyester filters for TER. Media were changed 3 times a week. Immunocytochemistry was performed as described previously (section 2.7) however it was done within the multiwell dish.

7.4.3.3 Results

7.4.3.3.1 Phase Contrast

The wells were observed weekly with a phase contrast microscope and changes to the dsHESC-RPE appearance and behaviour such as spreading and neurite outgrowth were noted.

Week 1: dsHESC-RPE demonstrated RPE-like spreading and division, in some areas this reached confluence. Some solitary cells showed early neurite-like outgrowth only in the HESC medium. Many of the cells lost their pigmentation (Figure 7.3).

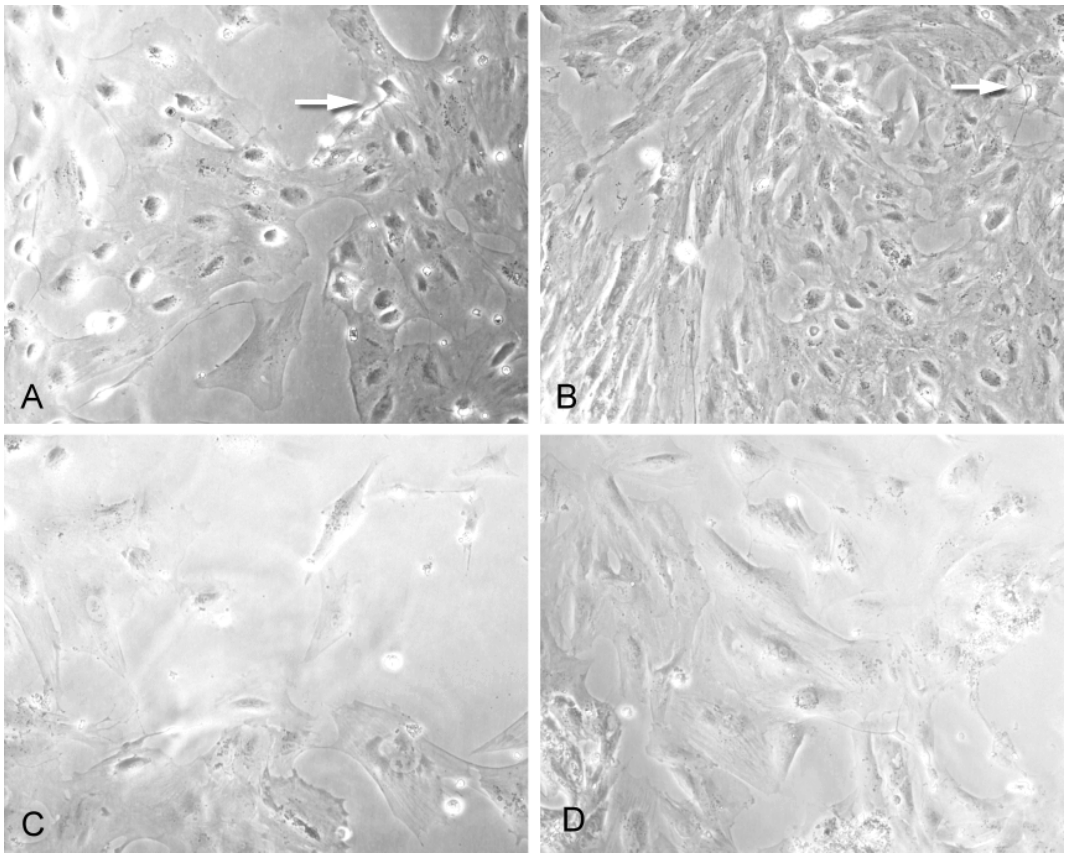

Figure 7.3 Low density seeded dsHESC-RPE demonstrate RPE-like spreading at one week post seeding. Some cells in pure HESC-medium are producing neurite-like structures (arrows). (A,B) cells are near confluence. (C,D) Some areas are less confluent. Note that most cells are de-pigmented.

Week 2: Confluent areas failed to expand to cover the entire well surface area. Some neuron-like cells are evident in HESC medium (Figure 7.4B). Increased neurite outgrowth and some 'networking' between solitary cells is evident in HESC medium > 1:1 HESC:RPE medium >= RPE medium (Figure 7.4A–D).

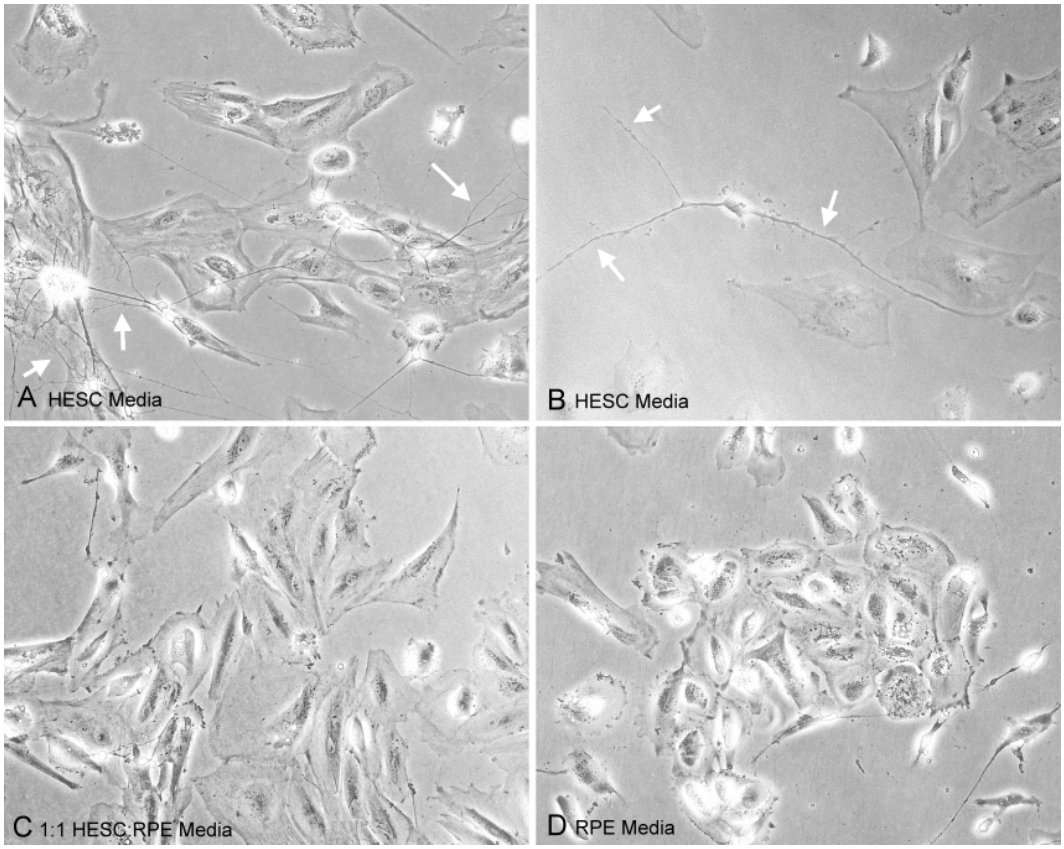

Figure 7.4. dsHESC at 2 weeks post-seeding. (A,B) dsHESC grown in HESC media develop neurite-like processes (arrows). C and D: notably less developed 'neurites' when media is mixed with RPE media indicating that HESC media promotes this phenomenon while RPE media suppresses it to some extent. Irrespective of group, confluent areas of cells fail to expand by this stage, leaving large areas devoid of cells within the well.

Week 3: There was no increase in spreading and proliferation in the less densely populated wells, while the more densely populated ones showed a marked increase in neurite outgrowth and more networking between elongated cells reminiscent of neurons. This 'neuronal' profile was most noticeable in HESC medium followed by the 1:1 HESC-RPE medium and least apparent in the RPE Medium. Cell death started to occur in the RPE medium.

Week 4: Cell death was apparent in the RPE media wells even in high density areas. The high cell density areas growing in HESC media looked the healthiest. There was no evidence of further proliferation or spreading in any of the wells, nor was there any evidence of microscopic or macroscopic pigmentation (Figure 7.5).

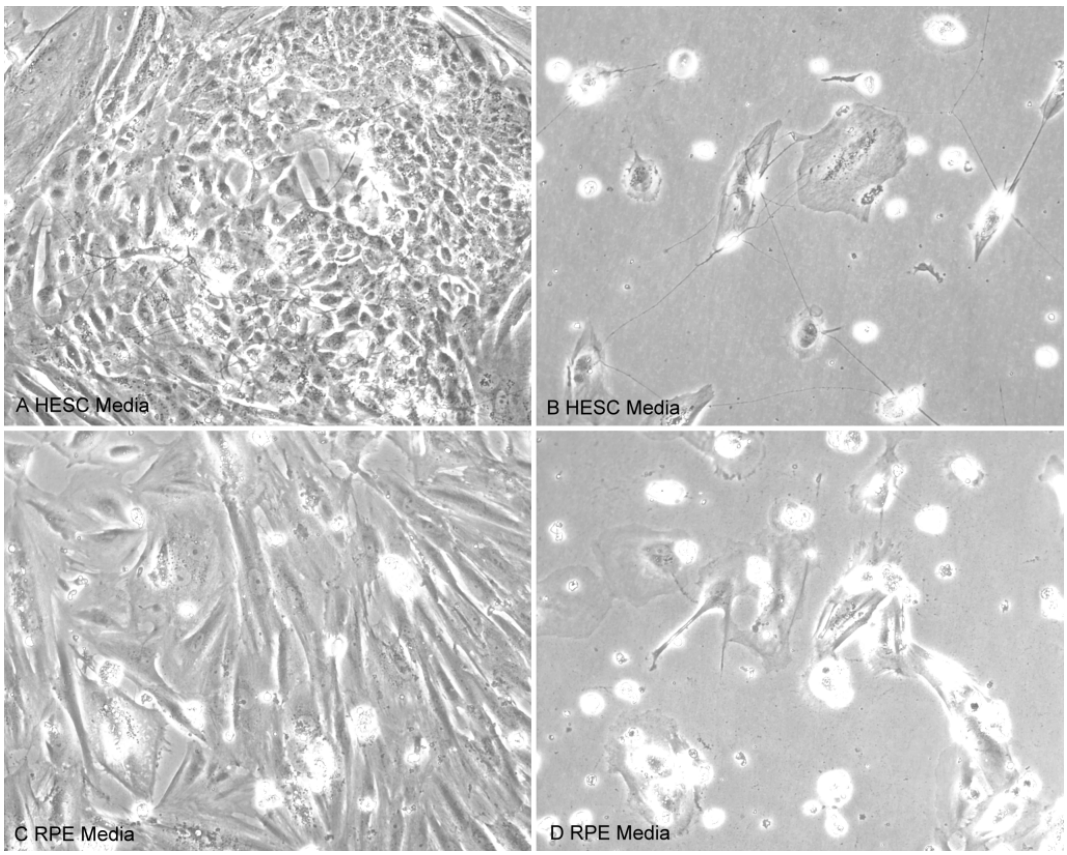

Figure 7.5. dsHESC at 4 weeks post-seeding (A) Cells appeared healthy in areas of highest cell density in the HESC Medium. (B–D) Low cell density areas are associated with high cell death in both HESC and RPE Media, while high density areas are also associated with cell death in the RPE medium.

7.4.3.3.2 Immunocytochemistry

The above experiment was fixed and stained for neuronal markers NF200 and βIII-tubulin, a lens marker alpha A-crystallin, and an epithelial marker Keratin-8. Some solitary cells stained positive for neuronal markers NF200 and βIII-tubulin. There were groups of RPE-like cells which stained positive for Keratin-8. There were no αA-crystallin positive cells.

7.4.3.3.3 Transepithelial Resistance

Due to the poor coverage of the culture growth surface at the above seeding density of 20,000 cell/cm², a subsequent group of inserts were seeded at a slightly higher density approaching 50,000 cells/cm² (n = 3). Even so, 2 month TER of HESC-RPE appeared to be slightly negative while ARPE-19 cells seeded at an identical density on matrigel maintained a TER of around 16 ± 0.7 Ω·cm². This suggests not only lack of complete coverage of the growth surface by HESC-RPE, but also loss of the matrigel coating (not

shown). This negative reading is conceivable since reference (blank) readings are always taken after matrix coatings are applied.

7.4.3.3.4 Conclusion

A significant number of dsHESC-RPE cells developed neurite-like processes and networked together irrespective of medium type. The appearance of a significant number of βIII-tubulin and some NF200 positive cells across the cultures, combined with the lack of differentiated RPE characteristics was worrying. Many cells adopted a neuron-like appearance, and there was no pigmentation in the rest of the cells. There was a failure to cover the surface area of the culture vessel. Negative TER is consistent with failure of confluence and loss of ECM coating. Therefore a low seeding density of dsHESC-RPE of 50,000 cell/ cm^2 is not recommended for differentiation or transplantation studies.

.

7.4.4 Primary HESC-RPE seeded at high density on Matrigel coated plastic. High density promotes RPE-like characteristics – Part I

7.4.4.1 Introduction and Methods

To further examine the properties of dsHESC-RPE, HESC-RPE colonies were harvested from MEF seeded tissue culture flasks (primary colonies) in preparation for dissociation. Polyester filters (6.5mm) with a pore size of 0.4µm were coated with 1:30 growth factor reduced matrigel for 30 minutes at 37ºC. Matrigel was aspirated immediately before cell seeding. Prior to seeding, HESC-RPE were maintained in basic HESC-medium (-bFGF) as above. Seven pigmented HESC-RPE colonies were harvested and dissociated as per the above dissociation technique. The cell suspension was seeded onto 2 inserts at a density of 273,000 cell/cm² and 70,000 cell/cm² respectively. Growth media were changed 3 times a week. The experiment was terminated at 3 weeks. Immunocytochemistry was performed as described above.

7.4.4.2 Results

7.4.4.2.1 Brightfield Microscopy

Examination under Brightfield revealed the higher prevalence and denser pigmentation of the higher density seeded HESC versus the lower density HESC (Figure 7.6A – B).

7.4.4.2.2 Immunocytochemistry

There was a negligible presence of βIII-tubulin across the culture in both high density (273,000 cell/cm²) and lower density (70,000 cell/cm²) cultures. Occasional raised cellular mounds contained βIII-tubulin positive cells (not shown). Junctional staining in the high density culture was excellent, with sharp ZO-1 borders and a polygonal morphology. Junctional staining in the lower density was acceptable (Figure 7.6C – D).

7.4.4.2.3 Conclusion

I have already stated that a seeding density of 50,000 cell/cm² or less is not suitable for HESC-RPE differentiation. The slightly higher density of 70,000 was minimally pigmented but seemed to achieve confluence at 3 weeks and junctional markers were expressed. The higher density in this experiment gave much more RPE-like cells with polygonal cells with a considerable degree of pigmentation. There was a lack of βIII-

tubulin positive cells and cell division had ceased as evidenced by lack of nuclear Ki67. These results are in favour of implementing a high seeding density for HESC-RPE differentiation and transplantation studies.

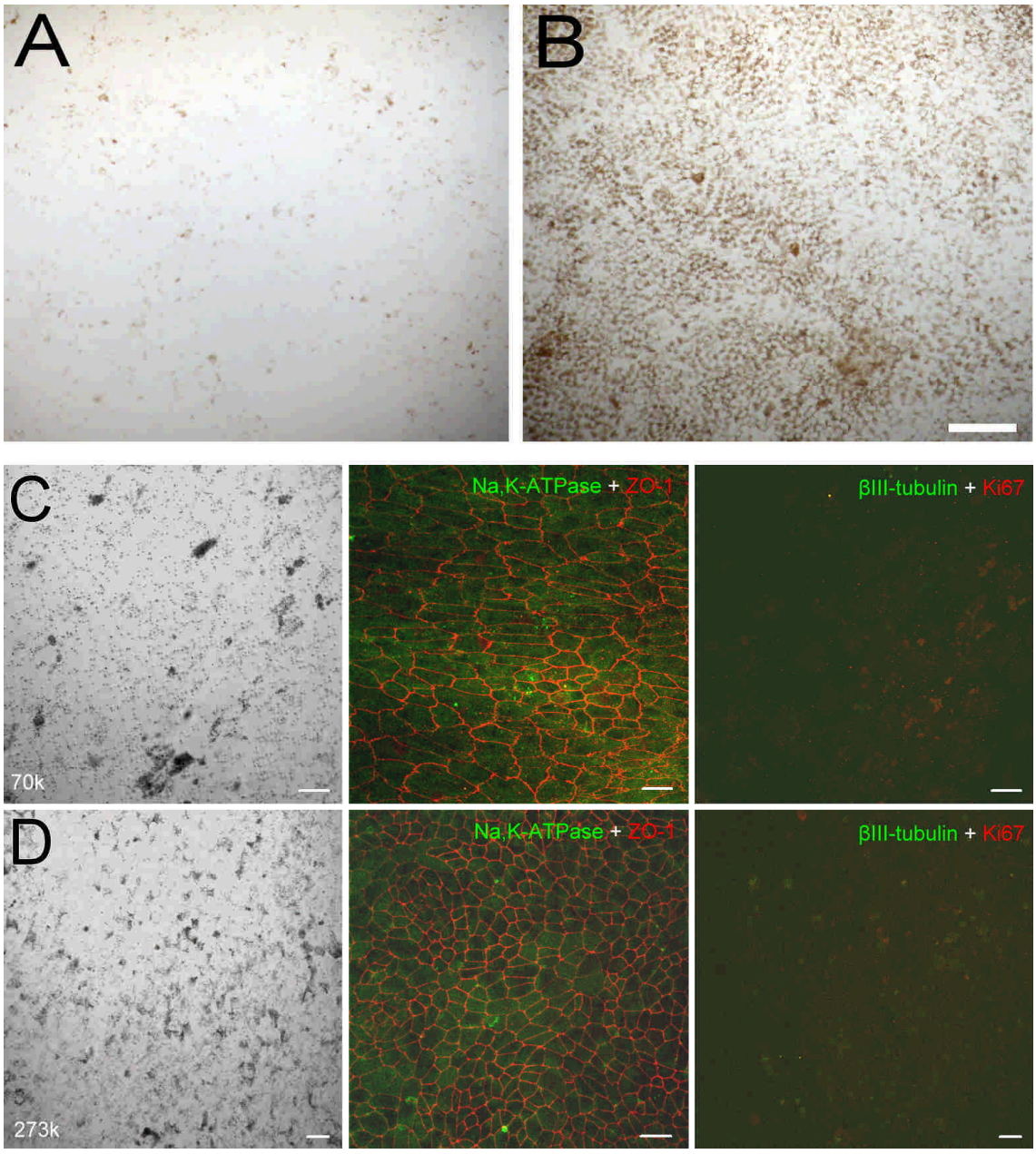

Figure 7.6 Microscopy results of seeding dsHESC at a lower (70kcell/cm²) versus a higher (270kcell/cm²) density at 3 weeks. (A - B) brightfield microscopy 20X micrographs demonstrate overall pigmentation differences between low (A) versus high density (B) dsHESC seeding. Bar = 100µm. (C) low and (D) high density dsHESC-RPE. (C – D) Confocal micrographs demonstrating pigment distribution with Nomarski optics (far left), ICC for Na,K-ATPase/ZO-1 (middle frames) and lack of βIII-tubulin/Ki67 (far right) which indicates favourable RPE-like maturation. Bars = 20µm.

7.4.5 Primary HESC-RPE seeded at high density on Matrigel coated plastic. High density promotes RPE-like characteristics – Part II

7.4.5.1 Methods

In the previous experiment, HESC-RPE colonies were harvested from MEF seeded tissue culture flasks (primary colonies—which could be regarded as passage zero). In this experiment 4 inserts were coated with 1:30 GFR matrigel for 30 mins at 37 ºC. HESC colonies that had been seeded onto matrigel coated 3.5cm TCPS dishes and grown for 7 weeks produced pigmented sheets from which HESC cells were harvested. These pigmented cells (could be regarded as passage 1 or p1) were then dissociated and suspended in growth media as per protocol (described in section 7.4.1). They were then seeded onto the 4 separate matrigel coated inserts at the following densities: 391,000; 270,000; 212,000; 70,000cell/cm² respectively. From here on, these will be noted in kcell/cm² or simply as 391k etc. These cells were allowed to attach and grow for 4 weeks. Media were changed 3 times a week.

7.4.5.2 Results

7.4.5.2.1 Macroscopic examination and light microscopy

Brightfield light micrographs (Figure 7.7A–D) revealed a progressively higher prevalence of pigmented cells as well as denser pigmentation from lower density to higher density seeded dsHESC-RPE as shown by macroscopic close-up images of the culture wells (Figure 7.7A–D insets). The cells in the highest density appear the most regular (Figure 7.7D). Pigmented cell counts were greater in the higher density seeding group, as was the cellular regularity index which is calculated by comparing to a perfect hexagonal array (Table 7-4).

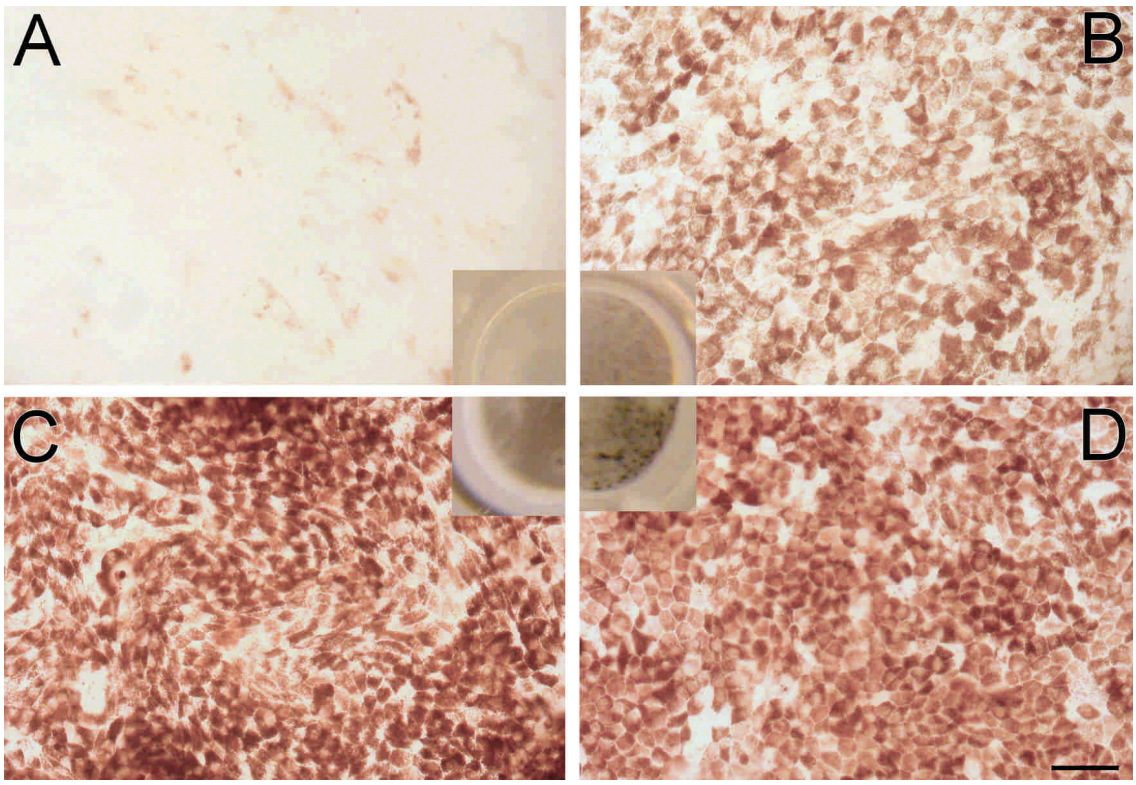

Figure 7.7 Brightfield 40X light micrographs of dsHESC-RPE at (A) 70k (B) 212k (C) 270k (D) 391 kcell/cm². Bar = 50µm. Insets: macroscopic image of culture insert represents overall pigmentation. In all there appears to be a progressive increase in pigmentation both at microscopic as well as macroscopic level with increasing cell seeding density.

Seeding Density (cell/cm²)	Pigmentation As seen with naked eye	Microscopic Examination	
		Pigmented cell count†	Delaunay Triangulation Regularity Index (Perfect Hexagon = zero)
70k	Nil	16	Cells too sparse to calculate
212k	Light	>400	0.023
270k	Dark (good)	>400	0.024
391k	Darkest (best)	>500	0.0175

Table 7-4 Optimal RPE characteristics such as darker pigmentation, regular polygonal morphology occurred at the higher seeding densities i.e >250 kcell/cm². It is worth noting that our laboratory has previously reported a regularity index of 0.0195 for non-dissociated HES-RPE. †per 40x microscopic field. No. of frames counted per group = 3.

7.4.5.2.2 Transepithelial Resistance

TER measured at 10 days and 4 weeks shows two trends: TER increases with seeding density as well as the duration in culture (Figure 7.8).

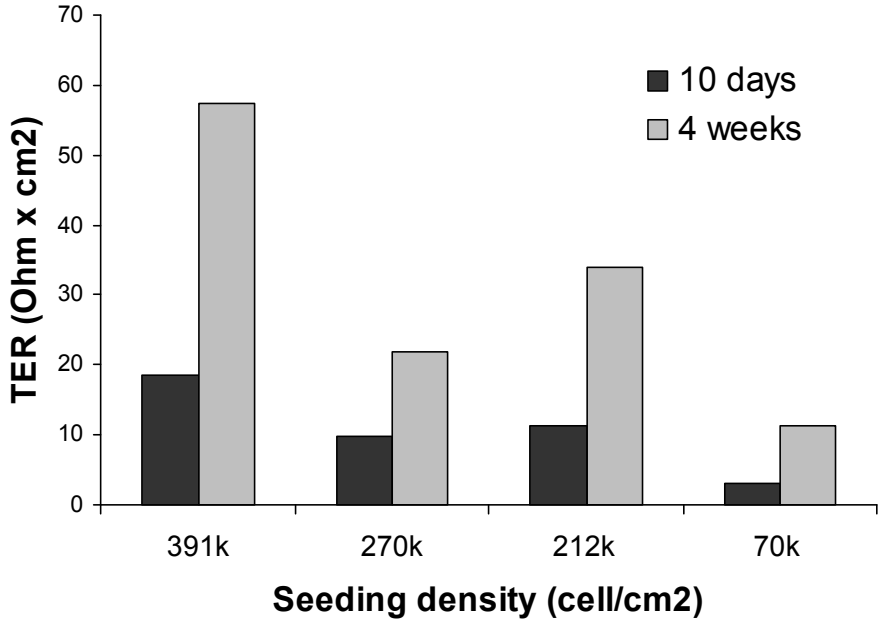

Figure 7.8 TER of p1 HES-RPE cells seeded at different densities on Transwell filters. No statistical inferences are made due to the small sample size, however two trends can be observed: TER increases with 1) seeding density as well as 2) duration in culture.

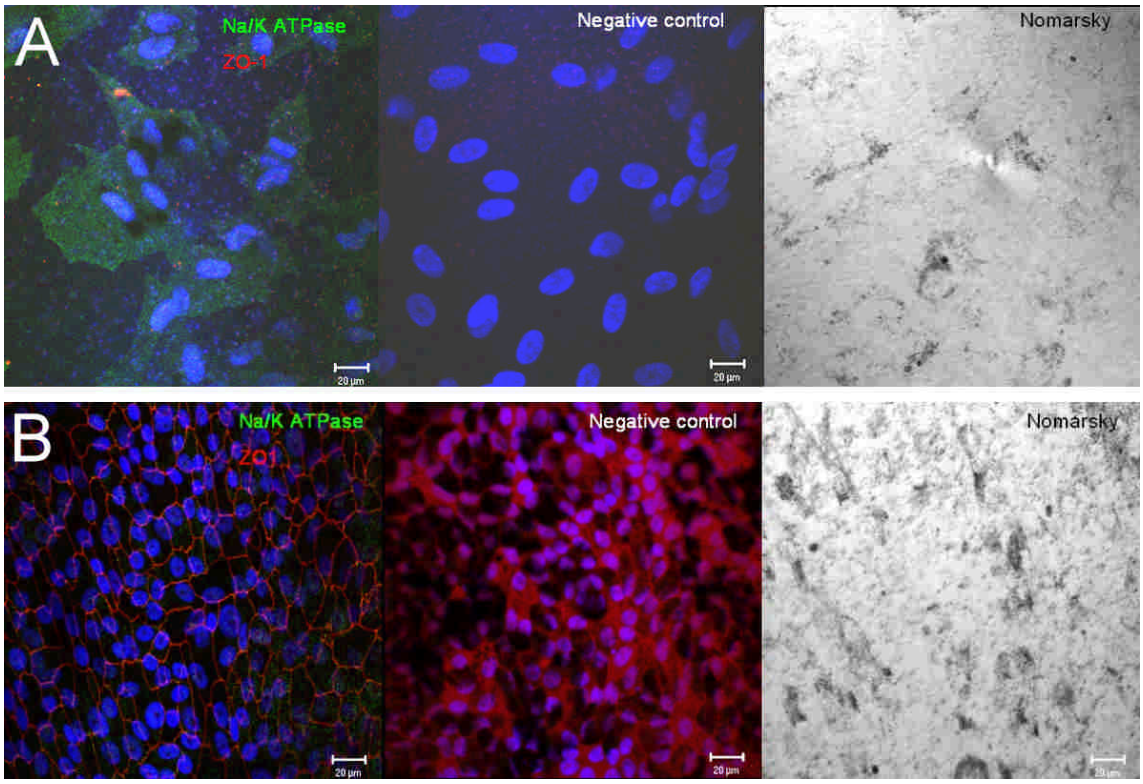

Figure 7.9. ICC of dsHESC-RPE at 4 weeks. Seeding densities are (A) 70,000 cell/cm² (B) 212,000 cell/cm². Pigmented cells are very sparse in the low seeding density group but visibly increase in the higher seeding density condition. Na,K-ATPase is cytoplasmic in the lowest seeding density group. See next figure for further comments on (B). Bar = 20µm.

7.4.5.2.3 Immunocytochemistry

The most apparent finding in the lowest seeding density group is the lack of pigmentation, both in terms of prevalence of pigmented cells as well as the apparent density of pigment per cell as seen with Nomarski optics. However an even more remarkable finding in this group is the lack of confluence of HESC in the 70k group despite the 4 week growth period. This is in contrast to the previous experiment and suggests seeding densities around 70k will not reliably achieve confluence. This is apparent from Na,K-ATPase staining which is pan-cytoplasmic in this phase of cell growth (Figure 7.9A). There is a progressive improvement in the profile of ICC markers as density is increased above 200k cell/cm². ZO-1 starts to appear at 212k (Figure 7.9B) and becomes clearly polygonal at 270k (Figure 7.10A), and becomes almost hexagonal at 391k (Figure 7.10C). Na,K-ATPase becomes more polarised in the highest density state (middle panels Figure 7.10B and D). Nomarski optics confirm light microscopy pigmentation levels (compare Figure 7.9A,B versus Figure 7.10C and D).

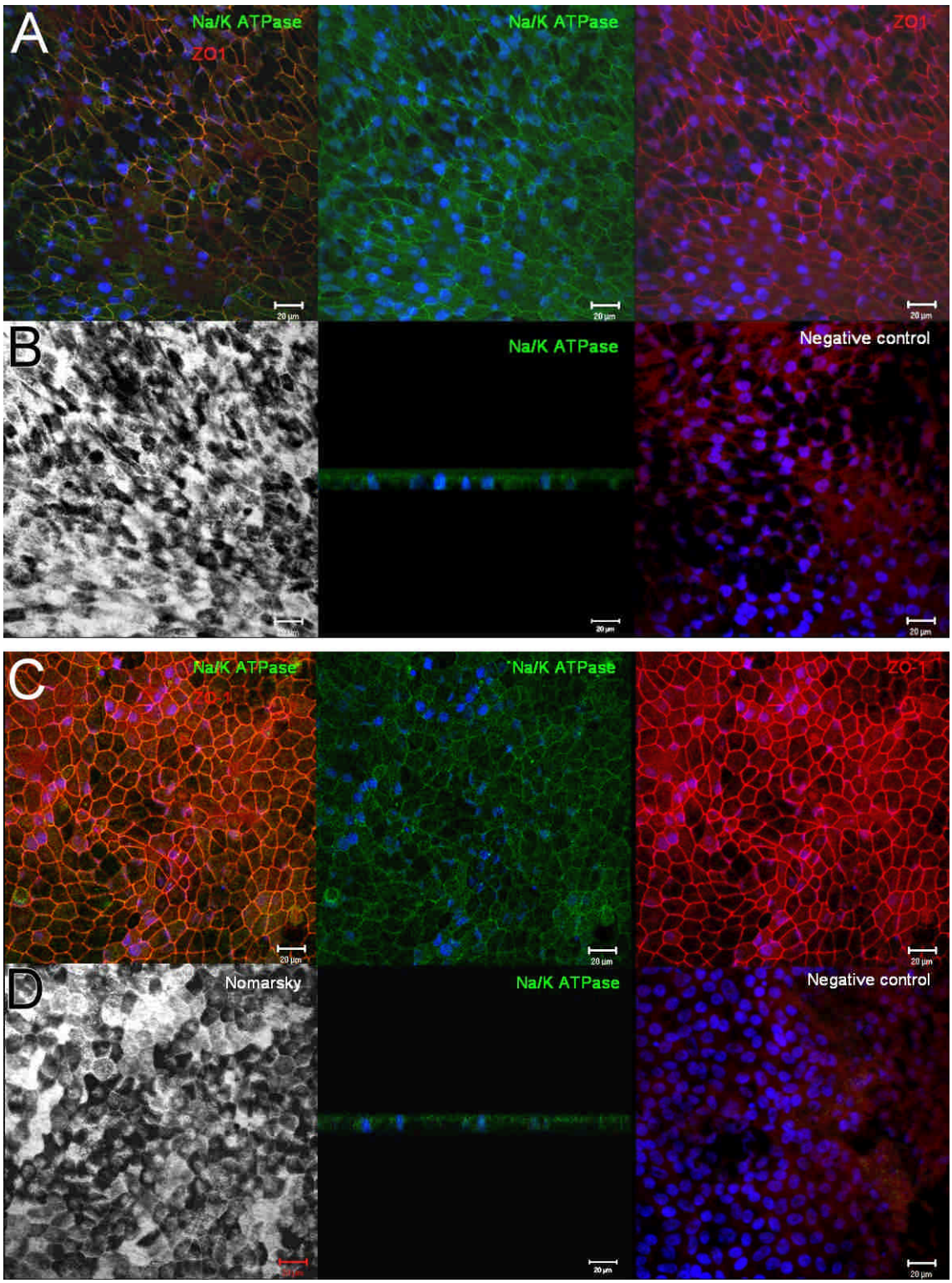

Figure 7.10. ICC of dsHESC-RPE at 4 weeks. Seeding densities are (A, B) 270,000 cell/cm2. (C, D) 391,000 cell/cm2. There is a progressive improvement in the profile of ICC markers as density is increased above 200k cell/cm². ZO-1 starts to appear at 212k (Figure 7.9B) and becomes clearly polygonal at 270k (A), and becomes almost hexagonal at 391k (C). Na,K-ATPase becomes more polarised in the highest density state (middle panels of B and D). Nomarski optics confirm light microscopy pigmentation levels (left panels of B, D). Bar = 20µm

7.4.5.3 Conclusion

The above data shows that HESC derived RPE maintain good RPE characteristics when seeded at cell densities greater than 200,000 cell/cm². These characteristics are:

- Regular morphology which is best seen with the highest density seeding. The 391,000 cell/cm² density group recorded a cellular regularity of 0.0175.
- ZO1, an important junctional marker, is expressed most in the highest seeding density
- Dark pigmentation, both macroscopic and microscopic, is more evident and increases in proportion to seeding density
- Good polarization is shown by apical distribution of Na,K-ATPase.
- TER readouts are consistent with theoretical expectation where TER is greatest at the highest density and lowest at the lowest density.

These results indicate that p1 dsHESC-RPE are a promisingly good source of differentiated RPE provided they are seeded at a density of at least 200,000 and most preferably within the range of 270,000 – 400,000 cell/cm² as seen in this experiment.

7.4.6 Growth factor release by seeded HESC-derived RPE cells, and assessment of barrier function

7.4.6.1 Introduction

It has been reported that polarised fhRPE, which is an exceptional in vitro model of RPE differentiation, produce 34 times more PEDF, and 6 times more VEGF than their non-polarised counterparts (Sonoda et al. 2010). Furthermore it has been reported by the same group that HESC-derived RPE are able to produce more than twice the amount of PEDF compared with fhRPE are capable of (Zhu et al. 2011;Kannan, Sreekumar, & Hinton 2011). These data indicate a strong positive correlation between differentiation and growth factor production and secretion, a relationship which exists in ARPE-19 (Ahmado et al. 2011). Thus, I sought to investigate PEDF and VEGF secretion by our Shef-1 dsHES-RPE (from here onwards also referred to as HESC-RPE as only dissociated cells are investigated), while assessing their barrier function. Comparisons are made with our standard RPE line ARPE-19 grown in optimal (DH+P) and standard (DFH) medium.

7.4.6.2 Methods:

HES-RPE cells were seeded onto identical concentrations of either matrigel- or pathclear-BME equivalent-coated 6.5mm Transwell polyester filters following dissociation, and maintained for up to 4 months. At around 10 weeks post-seeding, all cells were fed with growth medium devoid of all serum or serum-derived products and this medium was allowed to condition for 7 days. At the end of the seventh day media from apical and basal compartments from all cultures was collected into separate containers and stored at -80ºC or processed immediately on ice. ARPE-19 cells maintained in DFH and DH+P were used as controls. TER measurements continued and were taken at 8 weeks and 15 weeks post-seeding to assess barrier function while ARPE-19 maintained in DFH were used as TER controls.

7.4.6.3 Results

7.4.6.3.1 Transepithelial Resistance

TER rose gradually from week 8 to 15 (Figure 7.11). ARPE-19 cells grown in standard medium are also illustrated for comparison. Due to the large discrepancy in means, data was logarithmically transformed to satisfy parametric analysis assumptions of homogeneity of covariance matrices (which was severely violated without transformation). TER was significantly different according to time ($F(1,12) = 12.93$, $p < 0.01$, $\eta_p^2 = 0.519$) and cell type ($F(1,12) = 1913.89$, $p < 0.001$, $\eta_p^2 = 0.994$). There was also significant interaction ($F(1,12) = 26.47$, $p < 0.001$, $\eta_p^2 = 0.688$) indicating the TER difference between HESC and DFH maintained ARPE-19 was significantly affected by time. The non-logarithmically transformed data is illustrated in Figure 7.11.

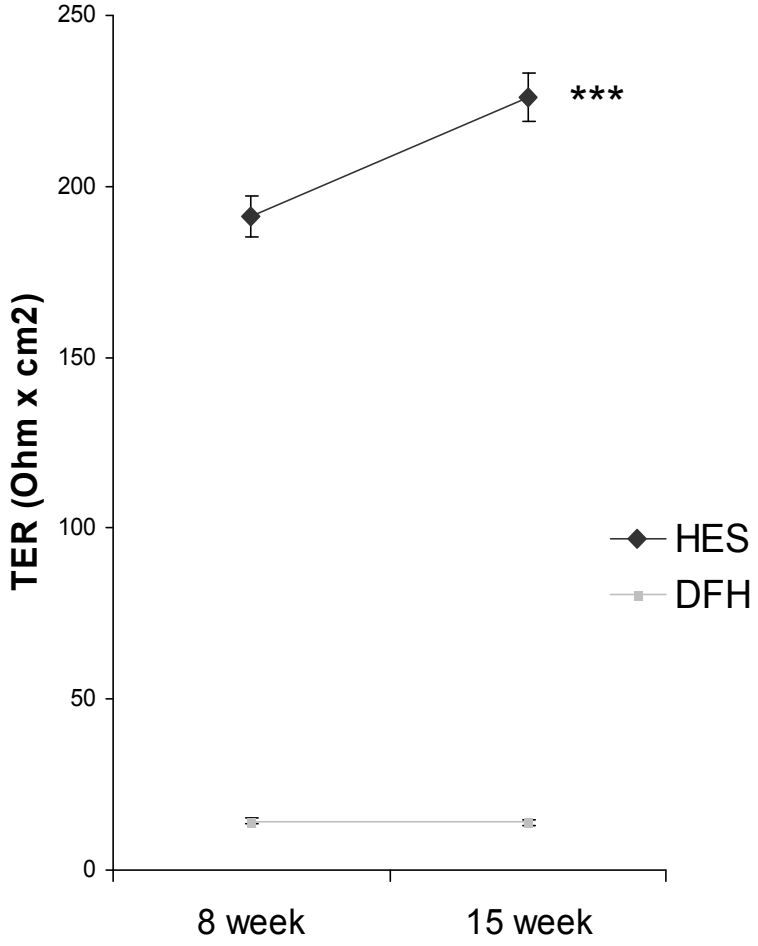

Figure 7.11 TER of dsHESC-RPE on pathclear BME-coated Transwell polyester filters (HES) is far superior to that of ARPE-19 cells grown in DMEM/F12 High glucose (DFH) at both 8 and 15 weeks ($p < 0.001$). TER was also significantly different in relation to time ($p < 0.01$). Non-logarithmically transformed data is shown (all data = means ± SEM; n = 6), whereas transformation was necessary to apply statistics and satisfy parametric analysis assumptions of homogeneity of covariance matrices. *** $p < 0.001$.

7.4.6.3.2 VEGF and PEDF secretion from Shef-1 HESC-RPE is consistent with a differentiated RPE phenotype

At 10 weeks post seeding, there was a significant difference between the groups in terms of apical ($F(2,8) = 62.364$, $p < 0.001$, $\eta_p^2 = 0.940$), basal ($F(2,8) = 29.755$, $p < 0.001$, $\eta_p^2 = 0.881$) and total ($F(2,8) = 77.274$, $p < 0.001$, $\eta_p^2 = 0.951$) VEGF secretion. ARPE-19 cells grown in DHP produced more apical, basal, and total VEGF than both HES-RPE and DFH groups (Figure 7.12A-B). Within groups, there was no statistically significant difference between apical and basal VEGF except for HES-RPE which secreted more VEGF basally than apically ($p < 0.05$). HES-RPE was also vastly

superior in secretion of apical PEDF ($F(2,8) = 17.998$, $p = 0.001$, $\eta_p^2 = 0.818$) and thus had significantly the highest PEDF/VEGF ratio ($F(2,8) = 34.124$, $p < 0.001$, $\eta_p^2 = 0.895$). HESC cells maintained a PEDF/VEGF ratio of 11.88 within the apical compartment (Figure 7.12D). PEDF was non-detectable from the basal compartments of any group therefore PEDF/VEGF ratios were non-applicable for basal compartments.

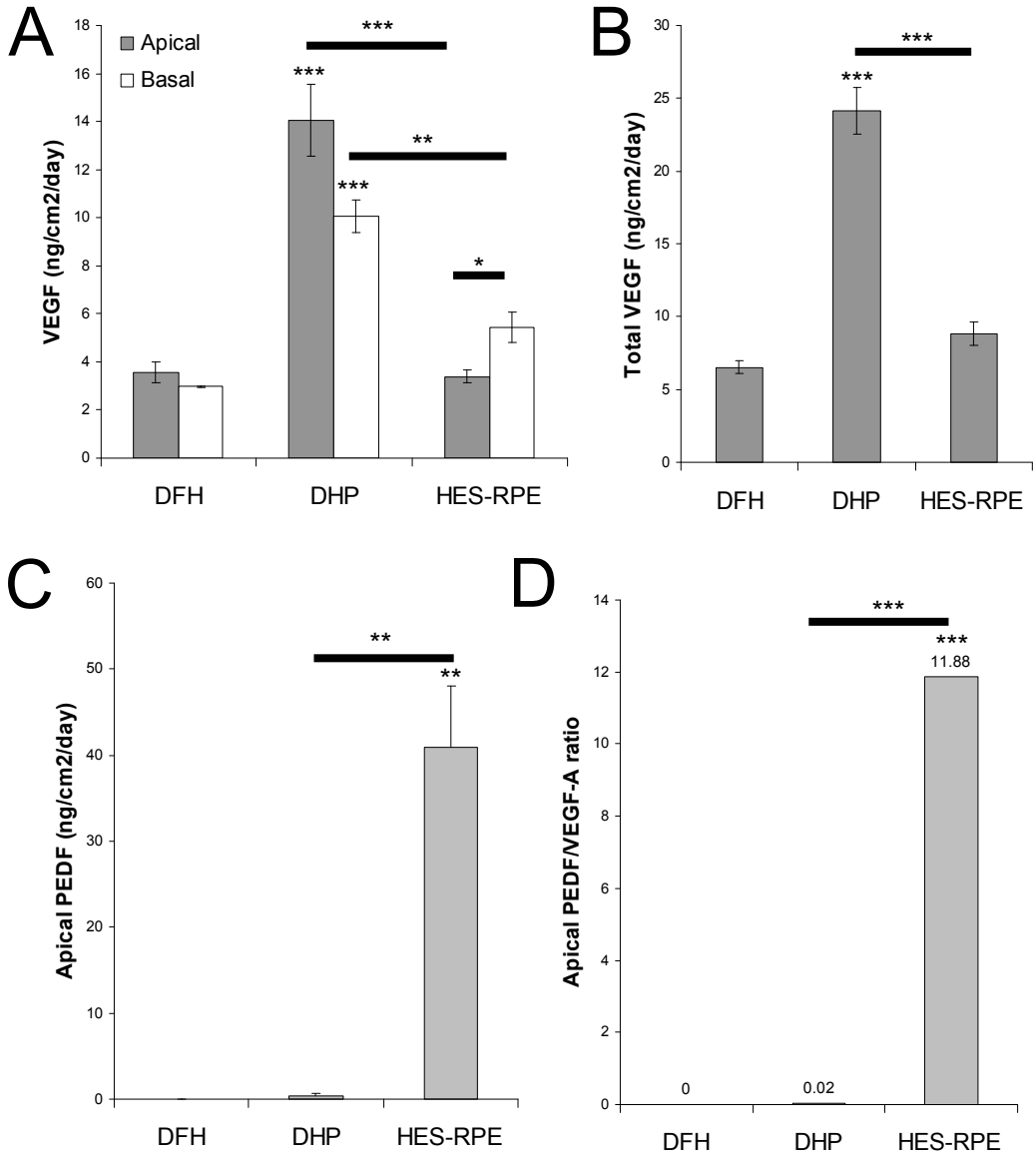

Figure 7.12 (A) Polarised and (B) Total VEGF secretion in ARPE-19 (DFH, DHP) versus HESC-RPE on Transwell PE filters at 10 weeks. (C) Apical PEDF comparing the same groups. (D) Apical PEDF/VEGF ratios. ARPE-19 cells grown in DHP (optimal medium) produced more apical, basal, and total VEGF than both HES-RPE and ARPE-19 in standard medium (DFH; A,B). Within groups, there was no statistically significant difference between apical and basal VEGF except HES-RPE which secreted more VEGF basally than apically ($p < 0.05$). HES-RPE was also vastly superior in secretion of apical PEDF ($p = 0.001$) and thus had significantly the highest PEDF/VEGF ratio ($p < 0.001$). HESC cells maintained a PEDF/VEGF ratio of 11.88 within the apical compartment (D). Basally secreted PEDF was not detectable in any condition therefore corresponding basal PEDF/VEGF ratios were not calculated. DFH = DMEM/F12 High glucose; DHP = DMEM High glucose + pyruvate. All data = mean ± SEM. Unless specified, asterisks indicate the following significance levels compared with DFH: *P < 0.05, **P <0.01, ***P <0.001 (n = 3).

7.4.6.3.3 Discussion

ARPE-19 secreted more VEGF than HESC. However both PEDF secretion and TER of HES-RPE vastly exceeded that of ARPE-19 grown in standard medium (DMEM/F12 with high glucose). HESC also secreted more VEGF basally than apically while secreting significant amounts of PEDF apically. These are promising indicators of HESC-RPE differentiation. Our HESC-RPE are capable of maintaining an apical PEDF/VEGF ratio of around 12 (Figure 7.12D). Although our HESC-RPE ratio is exceeded by other groups' fhRPE cultures (Maminishkis et al. 2006), it is still superior to ARPE-19 and is certainly consistent with in vivo vitreous samples obtained from human controls which harbour PEDF/VEGF ratios ranging from 5 to 50 (Dieudonne et al. 2007). The results are in favour of Shef-1 HESC-RPE as a very RPE-like cell line.

8

The Effect of a Highly Permeable Polyester Filter Substrate on the Characteristics of HESC-RPE

8 The Effect of a Highly Permeable Polyester Filter Substrate on the Characteristics of HESC-RPE

8.1 Introduction

The standard PE filter (Transwell®, 0.4μm pore size) is thoroughly characterised in this thesis and in many studies that I have mentioned as well as in other studies reviewed elsewhere (da Cruz et al. 2007;Binder et al. 2007). I have also shown that ARPE-19 is capable of RPE-like differentiation and pigmentation, while HESC-RPE possesses a superior phenotype and achieve excellent TER levels on this filter. Nevertheless, the hydraulic conductance of this filter is limited by its porosity. During the course of a wide search for an optimal substrate for the London Project, I and my colleagues were introduced to a highly permeable version of the polyester filter which retains an identical pore size of 0.4μm while harbouring a 25-fold higher pore density. This filter was obtained from Sterlitech Corp. (Kent, WA, USA) and will be designated as High Porosity Polyester Filter (HPPEF).

8.2 Results

8.2.1 Calculating the hydraulic conductance and resistance of high-porosity polyester filter and its comparison to Bruch's Membrane

Using the Hagen-Poiseuille (or Poiseuille's) law we can calculate a simplified version of hydraulic conductance/resistance through a given filter membrane since it is composed of a parallel group of individual pipes. This law requires full laminar flow of a Newtonian non-compressable fluid (such as water) along a pipe, but does not account for any frictional forces (negligible during laminar flow), and assumes pipe length considerably longer than diameter (with a risk of overestimating flow in short pipes). Since fluid flow at sub-cellular level is expected to be entirely laminar when flowing through the pores we can use this equation with only the pipe length/width ratio to worry about as the main substantial violation. The reason why laminar flow is guaranteed is due to its negligible velocity and thus minimal Reynold's index (calculation not shown). Therefore I proceeded to apply Poiseuille's law bearing in

mind the pipe length and width of polyester pores, in order to better understand the hydraulic properties of this filter.

By applying Poiseuille's law it indeed predicts the hydraulic conductance (C_A) of polyester filter at approximately 90% of manufacturer quoted conductance (calculation not shown):

Material	**Pore density (pores/cm²)**	**Theoretical C_A (m/sec/Pa)**	**Manufacturer C_A (m/sec/Pa)**
Transwell	4×10^{6}	2.82×10^{-9}	n/a
HPPEF	1×10^{8}	7.05×10^{-8}	8.02×10^{-8}

Table 8-1 Theoretical (Poiseuillean) versus measured hydraulic conductance CA (SI units) of polyester filter as per manufacturer website (checked November 2013). Sterlitech confirmed that testing is conducted at 25ºC (personal communication with Kristina Shahbazian, Applications Engineer, Sterlitech Corp.) thus calculations were performed at the same temperature.

It follows since pore density of Sterlitech filters are 25 times that of Transwell, the hydraulic conductance will also be 25 fold. Furthermore, from Table 8-1 we can see that the theoretical Poiseuillean conductance quite closely approximates the true conductance in HPPEF's case. Since adult BrM has a hydraulic conductivity ranging between $0.25 – 2.5 \times 10^{-9}$ m/Pa/sec at ambient temperature (Moore, Hussain, & Marshall 1995) it follows that Transwell exceeds native adult BrM's best conductivity by at least 1.1 – 1.4 fold, whereas Sterlitech exceeds BrM's by at least 32 fold. Since resistance is the reciprocal of these values, the resistance to water flow offered by Transwell filter would be considerable while that of HPPEF is negligible with respect to BrM characteristics. These calculations are in favour of using HPPEF for transplantation due to its minimal resistance to water flow.

8.2.2 SEM of plain filters

Plain sterilised polyester membranes were processed for SEM. The images are consistent with a greater porosity of the Sterlitech membrane versus the Transwell (Figure 8.1).

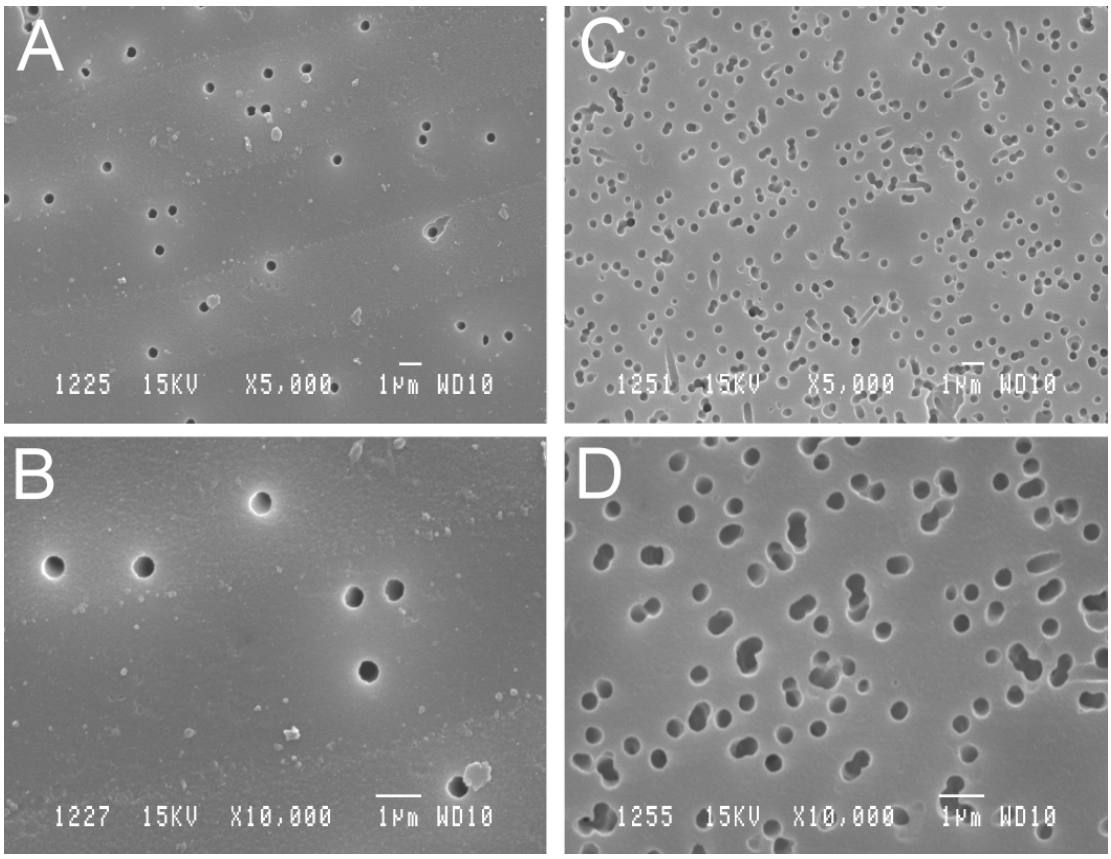

Figure 8.1 SEM images of uncoated filters. (A) X5,000 and (B) X10,000 magnification SEM images of Transwell® polyester filter which has a pore density of 4 x 10^6 , compared to (C,D) Sterlitech® filter which has a much higher density of 1 x 10^8 pores/cm². This represents a 25-fold increase in pore density which would theoretically increase water conductance by the same magnitude.

8.2.3 Assessment of uncoated HPPEF as a suitable substrate for cell growth, using the control Human RPE cell line ARPE-19

Before embarking on characterisation of this filter with HESC-RPE, it was imperative to ensure our standard RPE line was compatible with this filter. A quick ICC assay was conducted whereby ARPE-19 cells were seeded at a modest 50,000 cell/cm² onto uncoated HPPEF to check for compatibility with proliferation, as ARPE-19 are not affected by low seeding density providing other conditions are acceptable. Cultures were maintained for 10 days and ICC was performed checking for ZO-1. Full coverage of the HPPEF was achieved and junctional maturation was observed by successful staining for ZO-1 (not shown).

8.2.4 Investigating various coatings for HPPEF as a substrate for HESC-RPE Colony attachment

I have already investigated the effects of various coatings on the attachment and spreading of HESC-RPE colonies on TCPS and polyester surfaces and so far only laminin and matrigel coatings were successful (see section 7.3.1 above). As we intended to use our HPPEF for future transplantation studies we sought to compare the effect of a new set of coatings on attachment of HESC-RPE colonies to HPPEF membranes immobilised within TCPS dishes. This is because HESC-RPE colony attachment is a good indicator of dsHESC-RPE attachment. Samples were tested in duplicate (n = 2) as follows: Uncoated HPPEF, standard concentration poly L-Lysine, standard concentration mouse Collagen IV, standard concentration mouse Laminin, GFR-MG 1:30. In a separate experiment, YIGSR and IKVAV peptides (see methods 2.11) were used to coat a set of HPPEF membranes mounted in inserts with Kwik-sil™ silicone sealant (see methods 2.1). This method was used for peptides to enable coating a smaller area at an appropriately high concentration of peptide.

8.2.4.1 Results

HESC-RPE colonies started to expand on matrigel or laminin-1 coated HPPEF by 1 week. There was no evidence of spreading or attachment of colonies on any of the other substrates (Table 8-2). It is worth noting that the above laminin, collagen IV and matrigel are all products derived from the Murine EHS sarcoma basement membrane (ECM). Nevertheless, only the laminin product of the EHS sarcoma BM can function as an alternative to MG. Brightfield micrographs were not possible due to the opaque nature of the HPPEF membrane.

	Uncoated	**YIGSR Peptide**	**IKVAV Peptide**	**Poly L-Lysine**	**Collagen IV***	**Laminin***	**GFR-MG**
Attachment	0	0	0	0	0	Yes	Yes
Spreading	--	--	--	--	--	++	+++

Table 8-2: Comparing the effect of various coatings on attachment and spreading of primary (p0) HESC-RPE colonies on HPPEF membranes (Sterlitech) at 1 week. Spreading was subjectively graded according the following scale: 0 = no spreading; + =minimal spreading; ++ = apparent spreading; +++ = rapid spreading. * Please note that i) standard coating protocol for laminin is (1-2µg/cm²) ii) protocol for collagen IV is (1 - 10µg/cm²; 5µg/cm² used here).

8.2.5 Immunochemistry and SEM of Sterlitech filters seeded with dissociated HESC

HESC-RPE pigmented sheets were harvested from matrigel-coated dishes (p1), dissociated and seeded onto Sterlitech membranes at a density of approximately 350,000 cell/cm². Cultures were maintained and terminated at 8 weeks. Some inserts were fixed and stained for ICC, others were processed for SEM (Figure 8.2). Macroscopic examination reveals good coverage of the HPPEF membrane as seen in Figure 8.2A. Bright-field microscopy was not possible due to the opacity of the membrane. However due to the non-interference with reflected light, good ICC images were possible (Figure 8.2B – D). Cells were double ICC stained for CRALBP and Ki67 to assess differentiation and mitotic state. These show widespread positive staining for CRALBP (green) and the lack of Ki67 (red) indicating an overall substantial degree of maturation and likely terminal differentiation.

SEM shows a healthy, regularly arranged near-hexagonal polygonal array of RPE-like cells in a monolayer. These cells have abundant elongated microvilli (Figure 8.2E and inset) a marker for maturation.

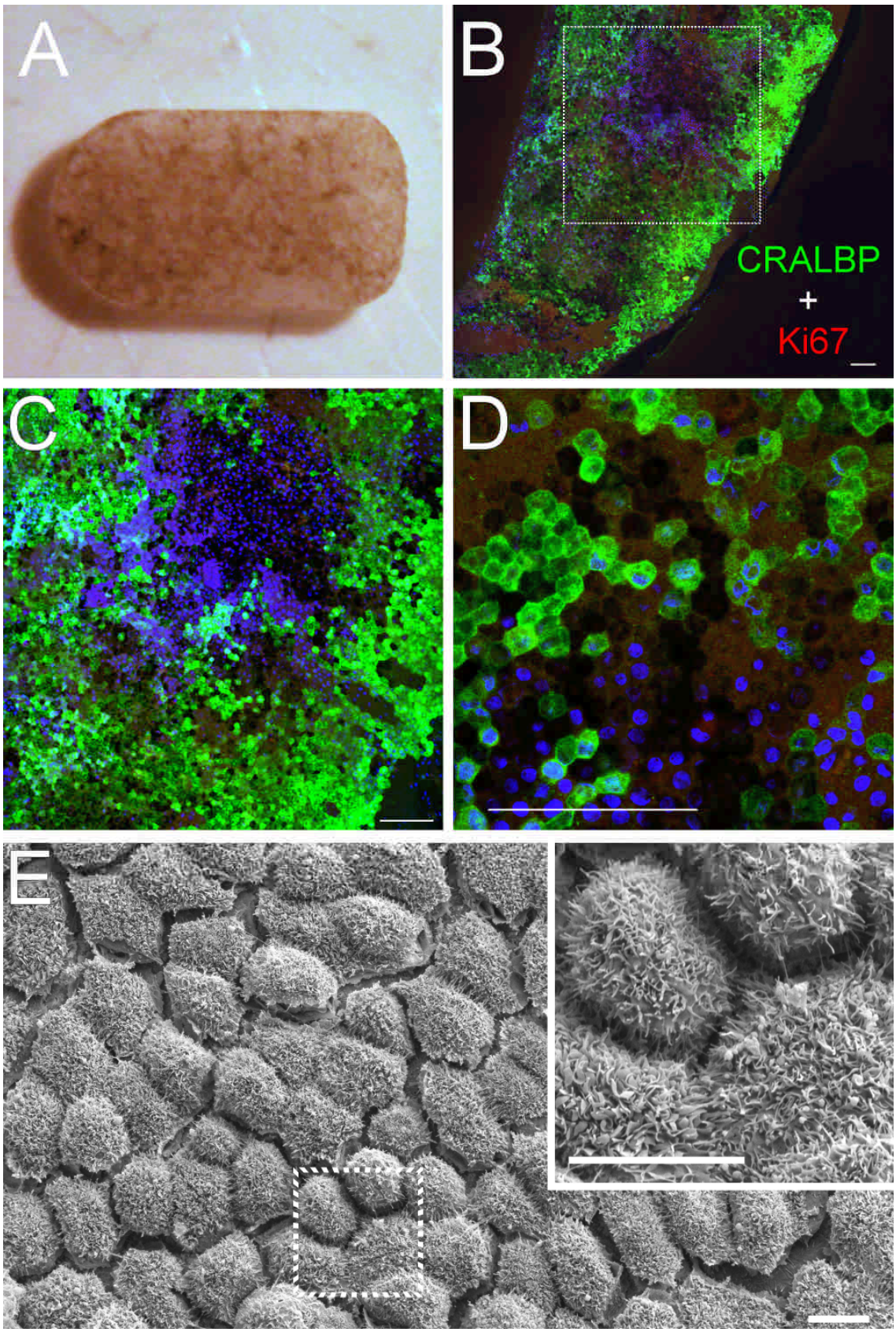

Figure 8.2 Assessment of HESC-RPE seeded on GFR-MG equivalent (GFR-Pathclear BME) coated HPPEF at 8 weeks. (A) Macroscopic image of a trephined 3 x 6mm HESC-RPE/HPPEF composite destined for transplantation in a pig. (B) Tile-scan composed of 10x tiles (C) 10x and (D) 40x frames. (E) SEM and inset: a healthy polygonal layer of RPE-like cells with abundant elongated microvilli. Scale bars = 100µm (B - D); 10µm (C).

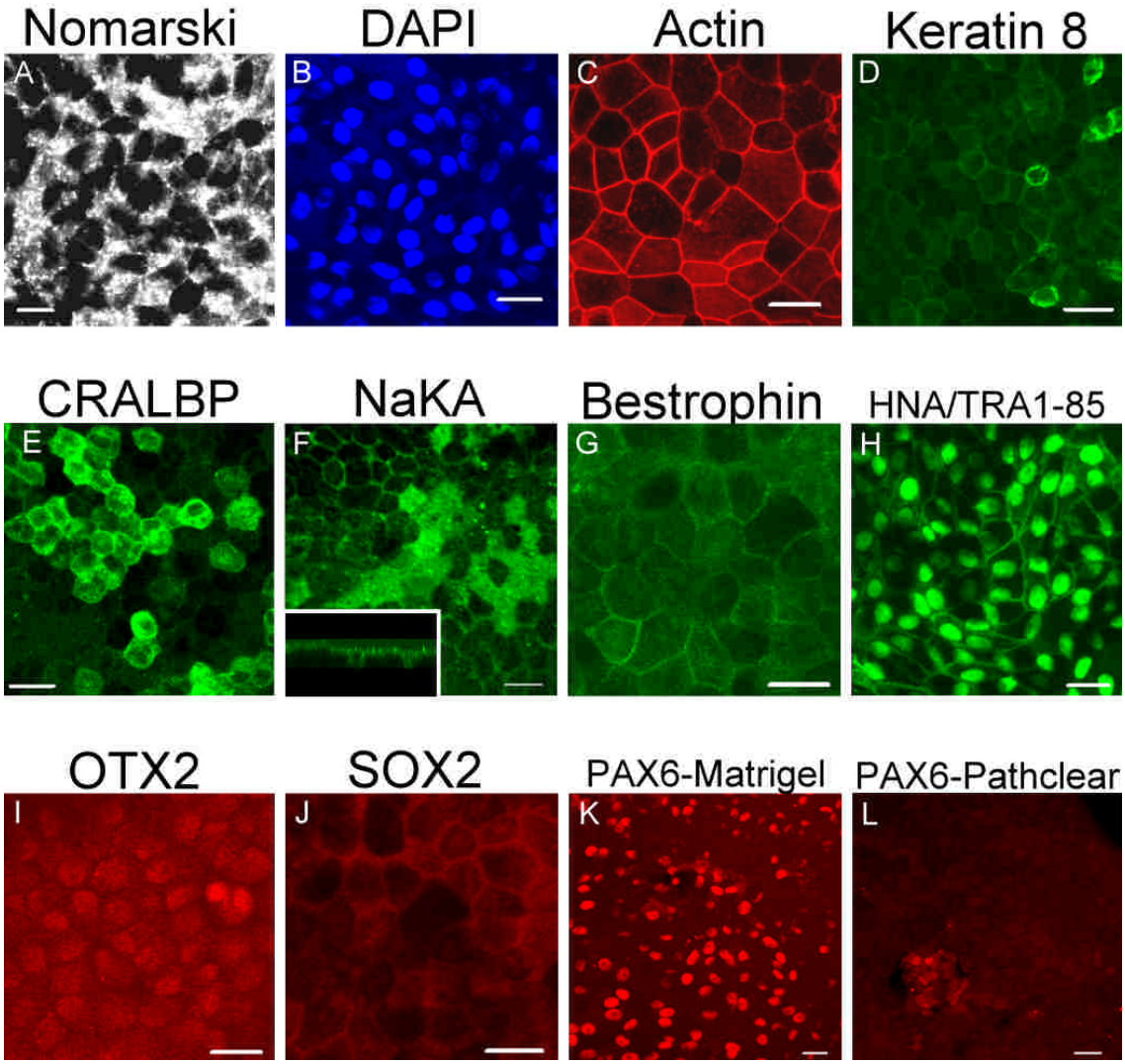

Figure 8.3 ICC markers of HESC seeded onto GFR-Pathclear-coated (or GFR-MG-coated) HPPEF at 8 weeks. ICC of both groups is identical (except Pax6) and images are representative of both groups unless indicated. Pax6 is largely negative in the pathclear group (except for occasional groups of cells) indicating a better degree of differentiation in this group, whereas matrigel seeded samples retain Pax6 positivity throughout the culture. Sox2 is negative in all groups indicating a departure from stem cell status, and a step towards terminal differentiation. Occasional groups of BIII-tubulin positive cells are seen within the cultures (not shown). Nestin was negative throughout the cultures (not shown). Bars = 20µm.

Immunochemistry was performed on both GFR-MG- as well as Pathclear-BME coated HPPEF. Results of ICC were almost identical on both coating types bar one of the ICC markers. Only Pax6 was different in that it became largely absent (occasional islands of Pax6 positive cells persisted) in the Pathclear-BME coated HPPEF (Figure 8.3L) whereas it was clearly positive throughout in the Matrigel group (Figure 8.3K). The rest of the ICC markers were identical among both murine-derived coatings and Figure 8.3 is representative of these. All of the remaining markers including CRALBP, Na,K-

ATPase, Bestrophin, and OTX2 are as expected of HESC derived-RPE. Nomarski optics show a large proportion of pigmented cells (Figure 8.3A). DAPI and other nuclear stains confirm the monolayered nature of these cells as there appears to be minimal if any overlap among the nuclei (Figure 8.3A,H,I,K). Actin staining appears circumferential which is consistent with native RPE, Keratin 8 is largely negative but periodically, positive cells are apparent within the culture. CRALBP staining displays a mosaic pattern i.e intensely positive in a subset of cells with the remainder of cells staining moderately and some weakly positive, which is consistent with native cells. Na,K-ATPase staining was positive and predominantly polarised to the apical membranes, while Bestrophin and TRA1-85 staining were weakly positive in the basolateral membranes in this series. Nuclei were OTX2 and HNA positive. Sox2 is negative indicating a considerable shift from pluripotence of cells towards a differentiated tissue phenotype.

8.2.6 Discussion:

Poor hydraulic conductance has been implicated in AMD due to the observation of pigment epithelial detachments (PED's) in AMD patients (Bird and Marshall 1986). Fluid accumulates underneath the RPE as BrM is overloaded with excess fluid originating from the neural retina, or from new vascular complexes which are a hallmark of exudative AMD. The selection of a polyester membrane with high water conductivity is an ideal choice since an additional barrier limiting clearance of fluid is undesirable, and its chemistry is identical to the well-characterised albeit less porous Transwell filter. Fortunately HPPEF satisfies requirements of porosity while possessing an equally superior profile to regular polyester filter, in terms of physical characteristics that enable superior differentiation and RPE morphology evident on ICC and SEM. The largely absent PAX6 staining in GFR-Pathclear-coated HPPEF was a welcome finding which confirms our HESC-RPE are capable of differentiation to a level that is closely consistent with native RPE ICC profile.

9

In Vivo Assessment of Suitability of Polyester for Subretinal Placement

9 In Vivo Assessment of Suitability of Polyester for Subretinal Placement

9.1 Acknowledgement

I am grateful for the assistance of Lyndon da Cruz and Fred K Chen with surgical implantation of rats and pigs, Carlos Gias and Peter Lundh von Leithner with in vivo imaging, and Jean Lawrence for her assistance with ICC in pig tissue.

9.2 Introduction

To further the translation of RPE-substrate composites it was deemed necessary to investigate the feasibility of transplantation of the base polymer (substrate alone) and to gauge the associated practical difficulties, and to observe mechanical, as well as any immunological complications, although the latter is expected to be minimal due to the already established use of this material in humans. For example, polyester (Dacron®) has been extensively used as a surgical implant for artificial vascular grafting (Roll et al. 2008). If successful we would then proceed to surgical transplantation of the cell-substrate composite and observe its behaviour in vivo.

9.3 In Vivo Methods

9.3.1 Small animal model

Due to their pigmented profile and manageable eye size pigmented 3-4 week old RCS dystrophic rats (rdy−/p+) were chosen as hosts for transplantation of experimental polymer (n = 6). Rats were provided with food and water ad libitum and maintained in a 12 h light:dark cycle. All animal procedures were performed within UK Home Office regulations in accordance with the Animals (Scientific procedures) Act 1986.

If needed, immunosuppression of rats was achieved by cyclosporine A (Sandoz, Camberley) at dose of 210 mg/l in drinking water. Immunosuppressant was commenced 48 h prior to the surgical transplantation procedure. Animals were then maintained on this immunosuppression protocol for the entire period during experiments.

9.3.2 Large animal model

Large White/Landrace crossbred pigs (Sus scrofa domestica) were purchased from a specialised local supplier and reared until they reached an age of around 2-4 months corresponding to a body weight of 25-45kg. They were typically delivered 7-14 days before surgery for an acclimatisation period. They were maintained in concrete pens, with appropriate bedding and fed twice daily with maintenance pig chow. Pens were cleaned out daily during which pigs were allowed daily physical exercise. Ambient temperature was maintained between 18-24ºC. Environmental enrichment was given by the responsible technicians who regularly interacted with the animals and provided appropriate verbal feedback. Drinking water was provided ad libitum from an automatic system. Pens were maintained in a 12 hour light:dark cycle within a specialised research facility at the Northwick Park Institute for Medical Research (NPIMR). Oral immunosuppression was achieved using a daily dose of 1mg/kg Prednisolone delivered with food once daily commencing 1 week prior to the surgical procedure and continued for 2 weeks afterwards. Starting from day 15 following the procedure, the dose of prednisolone was reduced by 10mg daily until zero. This oral immunosuppression regime was augmented with a intra-operative 40mg dose of peri-ocular triamcinolone acetonide (see surgical procedure for pigs).

9.3.3 Patch preparation

A stainless steel punch (trephine) was manufactured by our local workshop (UCL Institute of Ophthalmology) specifically for our rat experiments. The trephine was designed to punch a 1 x 3mm double D-ended rectanglar shape to minimise resistance to movement through tissues.

For pig experiments a stainless steel trephine that punches a 3 x 6mm single D-ended rectangular shape was manufactured by Maddison Product Design (Fittleworth, West Sussex), alongside a novel surgical stainless steel patch injector that utilises a surgical grade coiled wire to displace the cell-substrate composite out of the instrument tip.

9.3.4 Surgical procedure: Rats

General anesthetic cocktail was mixed on the day of surgery comprising 37.5% ketamine (Ketaset; Fort Dodge Animal Health, Fort Dodge, IA, USA), 25%

medetomidine (Dormitor; Pfizer, Havant), and 37.5% sterile water. This solution was administered at a dose of 2µl per gram weight as an intra-peritoneal injection. Both pupils were dilated with phenylephrine hydrochloride 2.5% and tropicamide 1% (Chauvin Pharmaceuticals, Kingston-Upon-Thames). Carbomer gel 0.2% (Viscotears; Alcon Laboratories, Hemel Hempstead) was applied to the eye surface as an optical interface for the 10mm glass cover-slips that enabled viewing of the fundus. Following a conjunctival peritomy, an approximately 1.5mm radial scleral incision was cut commencing from the limbus extending towards the equator. This incision was performed usually in the superior temporal quadrant of the left eye, or occasionally in the superior nasal quadrant of the right eye. The incision was gradually deepened until the choroid and, eventually, retina became visible, at which point an injection of a viscoelastic, comprising 10mg/ml sodium hyaluronate in a neutral pH sodium chloride phosphate buffer (Healon®; Abbott Laboratories, Maidenhead), was administered through the choroidal opening, while visualising the fundus, to create a subretinal bleb. The trephined polyester patch was pushed through the incision into the subretinal bleb at 90º to the incision, until it rested entirely within the subretinal space. Further viscoelastic was injected to manoeuvre the implant into a stable position. Following recovery, these rodents were maintained for upto 2 years. Termination was performed by transcardiac perfusion-fixation using 4% paraformaldehyde solution in 0.1 M Phosphate Buffer. Eyes were enucleated and post-fixed in 4% PFA overnight at 4 °C, incubated in 30% sucrose for at least 24 hours and embedded in Cellpath Embedding Matrix, OCT (Fisher Scientific) for future cryo-sectioning.

9.3.5 Surgical procedure: Pigs

Under an isofluorane/propofol general anaesthesia, pigs underwent a 3-port pars plana vitrectomy procedure on their left eye. Following vitrectomy, a subretinal bleb was created using a 40-gauge needle. One 3 x 6 mm Cell-substrate patch was trephined per animal. These were obtained from 6.5mm inserts which harboured our HPPEF/HESC-RPE composite as described in chapter 8. A retinotomy allowed the cell-substrate patch to be delivered beneath the retina using the novel patch injector. Endo-laser was applied to the retinotomy edges to prevent retinal detachment. Following air-fluid exchange, silicone oil was used to fill the eye to further secure the retina. After closure of all wounds, 40mg of triamcinolone acetonide was administered as a sub-tenon injection. Post-operatively the pigs were given eye drops consisting of cholramphenicol 0.5% four

times daily for 2 weeks. Oral prednisolone continued for at least 2 weeks as per immunosuppression protocol. Animals were maintained for upto 10 weeks. Termination was achieved by a 50ml injection of thiopentone given while under isofluorane anaesthesia. Eyes were subsequently enucleated and filled with 4% PFA and immersed into 4% PFA overnight at 4 °C. Subsequently eyes were incubated in 30% sucrose for at least 24 hours and embedded in Cellpath Embedding Matrix, OCT (Fisher Scientific) for cryo-sectioning.

9.3.6 Cell culture and patch preparation

HESC-RPE were grown on HPPEF as detailed in chapter 8. Briefly, HES-RPE/polyester culture inserts were typically maintained in culture for 4-6 weeks prior to implantation. Cultres were transported on the day of surgery in a warm insulated polystyrene box and transferred to the incubator at the surgical facility at NPIMR. At the time of surgery and during commencement of the vitrectomy phase of surgery two suitable (well pigmented) culture inserts were selected and were removed from their tray, in preparation for trephination, for each pig that was being procedured. These cell-substrate composite membranes were harvested by removal from the insert ring. This removal was done by manually excising the cellular membrane using a sharp micro-blade. The membrane was deposited into plain basal growth medium in preparation for trephination. Using the dedicated trephine a 3 x 6 mm patch was prepared and returned to the basal growth medium until further notice by the lead surgeon.

9.3.7 Imaging

Imaging in rats was performed under general anaesthetic and pupil dilation as above using either a Topcon 3DOCT-1000 or a confocal scanning laser ophthalmoscope (Spectralis HRA2; Heidelberg Engineering, Heidelberg, Germany). The focal plane was adjusted according to the area of interest, in some cases this was the transplant which often appeared much closer than the either the plane of the retina or RPE. An objective with either 30º or 55º field of view was selected. Images were captured either in OCT, infra-red (IR) or auto-fluorescence (AF) modes. A series of 100 consequetive 8-bit 1536 x 1536 pixel frames were captured and averaged and the result was the raw digital image.

9.4 Results of implantation of polyester membranes in rats

Surgical implantation of the polyester membrane into the subretinal space was feasible although it required additional time compared to simple subretinal injection in the experience of our laboratory. All animals (n = 6) were successfully procedured including one which succumbed shortly following the surgical procedure. Four animals were imaged with the Topcon 3DOCT-1000 at approximately 2 months and all demonstrated subretinal placement of the polyester membrane as evidenced by OCT scan and colour fundus images at 2 months (see representative images; Figure 9.1A and B). Two of these animals were imaged at 1 year. Representative images of one of the animals is shown in Figure 9.1C – E. This demonstrates lack of host reaction to the polymer since there is no opaque fibrosis or scarring associated with the membrane as evident from the infra-red image (Figure 9.1C). In addition autofluorescence demonstrates a lack of macrophage activity, in particular Figure 9.1D is focused on the RPE-choroid comples while Figure 9.1E is focused on the polyester membrane itself which shows very little hyperfluorescent activity. Sections from one of the animals were processed for H&E and show subretinal placement of the membrane with a lack of immune cell recruitment at 1 year (Figure 9.1F, G).

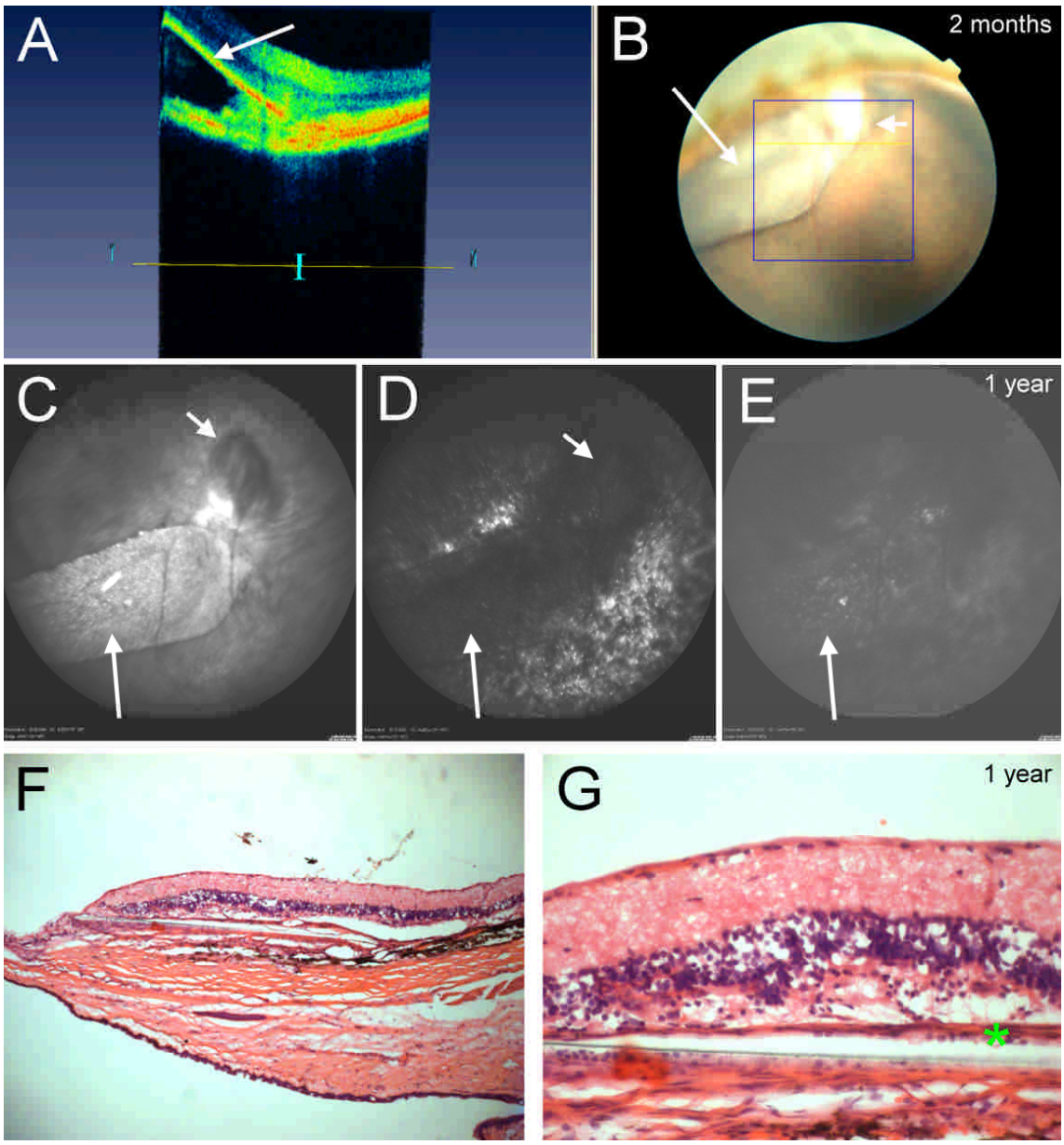

Figure 9.1 A-B)Topcon 3DOCT-1000 confirms subretinal placement of membrane (long arrows). C-E) Infrared (C), and autofluorescence (D,E) images of the subretinal membrane at 1 year confirm lack of encapsulation, fibrosis or scarring. In addition the autoflurescence images do not show an aggravated macrophage response. Note the sclera wound site (short arrows). F,G) H&E staining of cryosection confirms lack of an aggravated immune response to the membrane.

9.5 Results of transplantation of cell-substrate composites in pigs

Transplanted pigs were terminated at given intervals upto 10 weeks. Representative pig eye sections are shown in Figure 9.2 and Figure 9.3. The first figure demonstrates that the host immune system was not overcome by the steroid based immunosuppression

protocol consisting of oral prednisolone and peri-ocular triamcinolone acetonide. HESC-RPE/polyester composite survival is minimal at 10 weeks when post-fixation macroscopic images of fundus obtained at dissection are compared with pre-implantation pigmentation levels (Figure 9.2B and C) since their pigmentation levels do not correlate. This is strong indication of loss of donor HESC-RPE cells due to clearance by host immune system. ICC of cryosections of the transplanted composite shows non-pigmented TRA1-85 positive cells distributed in host retinal tissue above the polyester membrane. This indicates survival of a few human cells that migrated into host retinal tissue which may have given the cells increased immune privilege (Figure 9.2D and E).

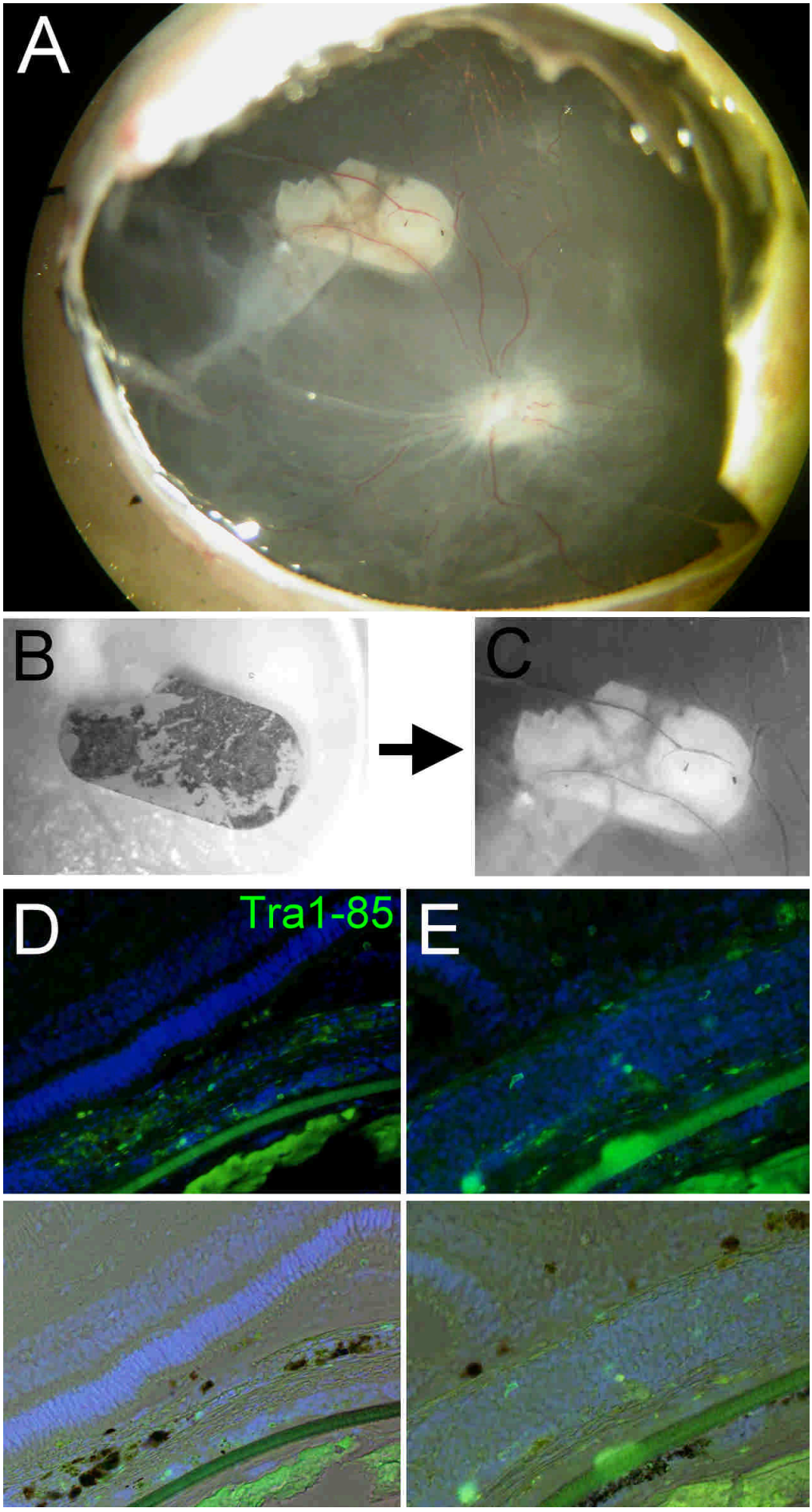
A
B
C
D
Tra1-85
E

Figure 9.2Analysis of HESC-RPE/polyester composite survival in the pig at 10 weeks. A) Post-fixation macroscopic image of fundus obtained at dissection. Note the fragility of the membrane that led to a characteristic tear which enables accurate orientation and comparison of pre- versus post-implantation pigmentation levels (B and C). B) Pre-implantation macroscopic image obtained while composite is suspended in growth medium at the time of surgery just before mounting in the injector device. C) Magnified grayscale view of composite at 10 weeks post-implantation obtained from (A) does not correlate with pigmentation seen in the pre-implantation photo (B) indicating loss of donor HESC-RPE cells due to clearance by host immune system. D, E) ICC of cryosections of the transplanted composite shows non-pigmented TRA1-85 positive cells distributed in host retinal tissue above the polyester membrane. This indicates survival of a few human cells that migrated into host retinal tissue which may have given the cells increased immune privelege.

In Figure 9.3 the animal was sacrificed 5 days following the surgical procedure to assess whether the cells survive the implantation procedure. We can see strong expression of the human marker Tra1-85 adjacent to the polyester membrane. Taken together these data indicate the host immune system was too hostile to allow prolonged survival of human tissue in the subretinal space of pigs immunosuppressed with steroids.

9.6 Conclusion from in vivo studies

Polyester is a well tolerated artificial non-degradable substance with supreme strength enabling usage of membranes with a thickness of 10μm or less. It's use in humans is well documented and therefore it was no surprise that it was tolerated well even in a restricted space such as the sub-retina.

HESC-RPE were aggressively cleared by their pig hosts as evidenced by the lack of human cells on cryo-sections and the non-correlation of pre- and post- implantation pigment patterns. The persistence of the HESC-RPE up to 5 days following the procedure indicates the cells are tolerant to this surgical manoeuvre. Thus vitrectomy is a promising route for delivery of HESC-RPE/polyester composites in a similar sized human eyes for clinical trials.

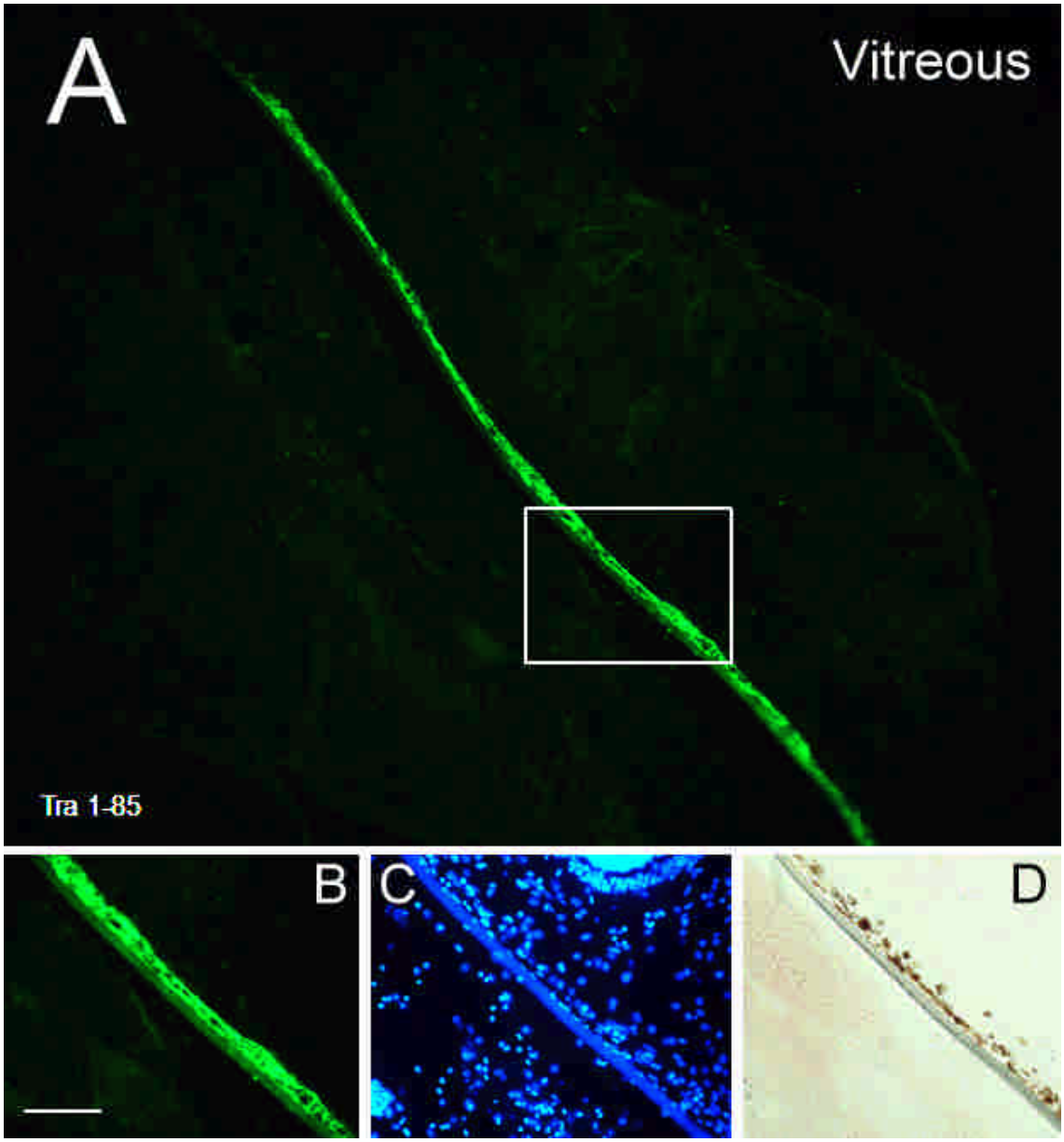

Figure 9.3 Survival of HESC-RPE on the polyester substrate 5 days following implantation when suspended within the vitreous in the pig. This shows an evenly distributed monolayer of RPE cells which stain brightly for Tra1-85 indicating their human origin. This data provides proof that donor cells survive the implantation procedure.

10

Discussion

10 Discussion:

In the recent years regenerative medicine in the eye has amassed significant attention from neuroscientists and the non-ophthalmic pharmaceutical industry alike. Apart from the increased prevalence of age-related eye disease due to rising life-expectancy, this surge of interest has been fuelled by the unique characteristics of the eye which are permissive to objective in vivo readouts in humans, as well as their numerous functional end points. For example, direct observation of results of transplanted cells in a patient is possible using a multitude of imaging modalities. Laser-scanning ophthalmoscopy, computerised tomography, as well as direct visualisation of the transplants are a few examples and this is a highly attractive virtue of working in the eye. Moreover, measuring functional parameters in the eye following transplantation is subject to numerous methods both subjective and objective, and this provides further confirmation of functional success or otherwise.

In order to embark on this noble journey, our project sought to develop an optimal cell-substrate composite with the aim of treating AMD. This meant elucidating an optimal substrate as well as a cellular layer of RPE, since AMD is a not only a disease of the RPE layer, but also a disease of their in vivo substrate known as Bruch's Membrane.

BrM becomes calcified (Spraul et al. 1999;Booij et al. 2010), cross-linked (Ramrattan et al. 1994) and accumulates hydrophobic debris with increasing age (Sheraidah et al. 1993;Guymer, Luthert, & Bird 1999;Huang et al. 2007). The type and age of layer available for transplantation will significantly affect the success of re-attachment of cells: attachment to the basal lamina (especially of young donors), offers a survival rate, repopulation rate, and ability to reach confluence better than all the other layers of BrM (Tezel, Kaplan, & Del Priore 1999). Several studies have highlighted that aged macular BrM obtained from cadavers is not a suitable substrate for supporting attachment, growth or survival of seeded cells in vitro. Indeed some believe aged submacular BrM does not support transplanted RPE survival and differentiation altogether (Zarbin 2004). It appears aged macular BrM is so hostile to attachment and growth of cells that no matter how many times this issue has been re-visited, the results have been largely unchanged: aged submacular BrM is simply unsuitable for repopulation by transplanted cells, regardless of the source of cells and which layer of BrM is being resurfaced (Tezel & Del Priore 1997;Tezel, Del Priore, & Kaplan 2004;Del Priore, Tezel, & Kaplan

2006;Sugino et al. 2011a;Sugino et al. 2011b). Furthermore, previous studies have demonstrated that young BrM is more efficient than old BrM in supporting cell attachment (Tezel, Kaplan, & Del Priore 1999;Gullapalli et al. 2005). Therefore, in order to treat AMD, not only must we find a source of RPE, but also we must identify a replacement for this aged substrate. Hence in the beginning of the thesis I sought to characterise substrates which will act as a BrM replacement.

10.1 Considerations for Bruch's Membrane Replacement

Several issues must be considered when searching for an artificial BrM replacement. Firstly, permeability to water (or hydraulic conductivity) is of paramount importance. It has been shown that hydraulic conductance of BrM declines substantially with age (Starita et al. 1996). Since hydraulic conductance is an assumed surrogate measure of permeability of other molecules, this further highlights the crisis experienced by aged macular RPE. Ageing is the strongest risk factor for AMD. Interestingly, hydraulic conductance of BrM declines rapidly and exponentially with age, halving almost every decade and can end up as low as 10% of that of a young adult (Starita et al. 1996). This rapid decline in conductance is due to remodelling of its components up to the age of about 40, after which lipid accumulation is blamed for further decline (Starita, Hussain, & Marshall 1995;Starita et al. 1996). The hypothesis that poor hydraulic conductance can contribute to AMD is based upon the observation of pigment epithelial detachments (PEDs) in AMD patients (Bird & Marshall 1986). Whether the source of the excess fluid underneath the RPE is outgoing from the neural retina, or whether it is incoming from a neovascular or 'wet' AMD is irrelevant since in both cases BrM appears to be a barrier preventing clearance of this fluid. For this reason, any transplantation effort involving an artificial substrate must ensure that the substrate has adequate hydraulic conductance in order to prevent pooling of fluid at the RPE-substrate interface. (Starita, Hussain, & Marshall 1995;Starita et al. 1996;Starita et al. 1997). It was therefore no great surprise that polyester filter consistently permitted a superior RPE phenotype of all the polymers tested.

Secondly, another important aspect of an artificial BrM replacement is its thickness. It is easily deducible from the Hagen-Poiseuille law of fluid dynamics, that no matter how permeable an artificial support, its conductivity will be halved when thickness is doubled (assuming cylindrical pores traversing the substrate). Native BrM thickness is

normally around 2μm, but this increases by more than 100% due to age (Ramrattan et al. 1994). This parallels an age-related decline in chorio-capillaris density as well. In AMD, although there is significant reduction in choriocapillaris density, the thickness of both BrM and that of the choroid was found to be no different from normal aged maculae, indicating that age is the main determinant of BrM thickness, not disease (Ramrattan et al. 1994). A later study which looked at the elastin layer (elastic lamina) integrity seemed to confirm this same principle for geographic AMD which did not affect elastin thickness or abundance compared to normals. However elastin integrity was significantly lower in all other forms of AMD compared to age-matched normals, as was thickness in advanced and late AMD. Surprisingly even in normal adults, macular elastin was 3 to 6 times thinner and 2 to 5 times more permeable than peripheral elastin in all individuals, confirming the macula to be mechanically susceptible in all age groups (Chong et al. 2005). Although investigation of the elastin layer has not been the subject of this thesis, this data is useful in understanding a crucial and unique biological trade-off whereby reducing elastin thickness and strength was necessary to achieve improved permeability of the native macular substrate. This trade-off constitutes a universal paradigm that will affect all RPE transplantation efforts: both substrate thickness and physical strength will have to be sacrificed to some degree in exchange for improved water permeability and nutrient transport.

Thirdly, the type of substrate is important for cell survival and behaviour. Several studies point to the relevance of substrate quality in playing a role in cellular function. First and foremost, anchorage-dependent cells such as the RPE require a substrate for survival (see references in introduction 1.3). Without substrate, a particular type of apoptosis called anoikis ensues resulting in cell death. Cells can be rescued from anoikis by interacting with extra-cellular matrix (Jeong et al. 2001) or an alternative suitable substrate (Tezel & Del Priore 1997). Furthermore, extra-cellular matrix provides vital cues for differentiation, polarisation and correct orientation of epithelial cells (Mak et al. 2006;Moyano et al. 2010). Turowski et al, found that ARPE-19 phenotype and gene expression is modulated by lens capsule basement membrane (Turowski et al. 2004). Others have found growth factor secretion to be increased with polarisation in culture (Sonoda et al. 2010), while some have stated that the phenotype of their embryonic stem cells could be modulated by seeding onto various substrate (Gong et al. 2008). Thus substrate selection as an artificial replacement for BrM, will have a profound effect on overall health, as well as the functional profile of the overlying cells.

10.2 Artificial RPE scaffolds for transplantation:

Artificial polymers that have been investigated for support of RPE growth and differentiation include biodegradable and non-biodegradable artificial membranes. Examples of biodegradables are poly lactic acid or PLLA (Thomson et al. 1996), and poly-lactide-co-glycolic acid or PLGA (Giordano et al. 1997;Hadlock et al. 1999) which have been discussed in section 2.5. These biodegradable substances have a good biocompatibility profile and are approved by the FDA for medical use.

10.2.1 Poly(D,L-lactide)-co-glycolic acid (PLGA)

PLGA is one of the most successful biodegradable substances in use. I have tested the PLGA polymer for compatibility with our in vitro RPE cell line ARPE-19 and I have documented its characteristics in this scenario. Its success as a substrate per se is promising as my results confirm compatibility with ARPE-19 and RPE cells in general. The type of PLGA I tested is Resomer® 503H which is a 50:50 mixture of poly-D,L-lactide and glycolide. Although it supported growth and proliferation of ARPE-19 cells, promoted junctional formation, and seemed not to exert visible toxic effects to these cells there were several problems with the membrane itself. Its high baseline thickness and tendency to swell and further increase its thickness are hurdles that will need to be overcome if it is to be used as a substrate for transplanted RPE. Acidification of growth medium is another concern as small PLGA fragments were able to acidify comparatively huge volumes of fluid in my experiments, due to their auto-catalytic behaviour. Thus, there is considerable concern that the potential acidification could be greater in a much smaller confined volume such as the subretinal space. Acidification could be a potential source of problems and will need to be quantified in future studies wishing to utilise PLGA for transplantation assuming the thickness issue is successfully resolved.

I then proceeded to investigate some of the non-biodegradable materials since the issue of whether to use a biodegradable or non-biodegradable membrane became clearer after the PLGA experiment. That said, several recent in vitro (Treharne et al. 2012;Shadforth et al. 2012;Lu et al. 2012) as well as in vivo studies (Hu et al. 2012;Stanzel et al. 2012)

suggest there is a current trend towards using non-degradable substrates for RPE transplantation.

10.2.2 Polyurethanes versus polyester

Polyurethanes are an attractive option for biocompatible implant materials as their manufacturing process can be varied to produce a vast spectrum of physical properties. They are technically *block co-polymers* consisting of so-called hard and soft *segments* whose ratio and chemistry can be manipulated to produce either hard or soft elastic/rubbery products. Some polyurethanes are susceptible to oxidation but polycarbonate urethanes and silicone-containing polyurethanes have been found to have good chemical stability and biocompatibility making polyurethanes a viable option for prosthetic device development (Martin et al. 2000). A major drawback of polyurethanes is their hydrophobicity but this can be overcome by modifying their surface charge, or by changing the ratio of hard and soft segments. Air-plasma treated poly-ether urethanes like Tecoflex® and Pellethane® and non-treated Zytar® have been used successfully to support growth of RPE (ARPE-19) cells to confluence and as a monolayer (Williams et al. 2005). Using a well known resazurin-based fluorometric proliferation assay, I demonstrated the performance of our control polyester filter significantly exceeded that of any of our tested polyurethanes by far, including the most hydrophilic ones. The performance gap in my study resembles that of the non-treated polyurethanes in Williams et al study (Williams et al. 2005) suggesting that plasma air or gas treatment is an absolute necessity for even the hydrophilic polyurethanes. Given that polyurethanes have been widely successful in many applications, one must conclude that it is not necessarily the polyurethanes that had a poor performance, but that polyester filter is a truly superior substrate for ARPE-19 cells.

It is worth noting similar favourable results were achieved using substrates of diverse chemistries by the same group of authors from the Williams et al study. A comparable result with good phagocytosis function of the RPE was achieved with Polydimethylsiloxane (PDMS) when it was ammonia gas treated. However the performance gap between control membrane and PDMS was greater in Krishna et al study of PDMS (Krishna et al. 2007) than that of the polyurethane study by Williams et al (2005) indicating polyurethanes are superior to PDMS assuming both were optimally surface treated. Ammonia-gas treated expanded PTFE (ePTFE) has also been tried by

these authors with good success that is comparable to their superior results obtained with treated polyurethane (Krishna et al. 2011). I have not examined the characteristics of PDMS in my studies, however I have examined both carbon- and non-carbon coated ePTFE and no cellular adhesion to either these membranes was detected by SEM (not shown), which highlights the importance of surface treatment for ePTFE. One limitation of my polyurethane study has been the use of cyano-acrylate adhesive to mount the membranes on the Transwell® insert. All experimental inserts were visually tested for water-tightness prior to inclusion in the study as well as during media exchange. However, the presence of a small amount of cyano-acrylate compound adjacent to the ARPE-19 cells in the polyurethane group is a variable that was not possible to control but must be kept in mind. Fortunately, cyano-acrylate has been used to mount lens capsule onto Transwell® inserts previously, with no reported problems (Turowski et al. 2004) although further studies utilising polyurethane might need to check for toxicity when polyurethane and cyano-acrylate are combined.

Thus, I have observed PE filter to be one of the most successful artificial membranes for RPE cells. This plastic has been well-established as an RPE substrate and has been shown to support native tissue characteristics such as polarised ARPE-19 monolayers as early as 4 weeks in culture (Dunn et al. 1996) perhaps due to its exceptional performance as a filtration material. In summary, I have demonstrated in section 4 that polyester filter far exceeds the performance of several polyurethane types in supporting the growth of ARPE-19 cells, including hydrophilic and porous polyurethanes. I have also shown in section 5 that this material is superior to glass when adsorbed with active peptide sequence coatings and supports the best morphology and ICC profile of this cell line. Indeed polyester has satisfied many requirements for RPE transplantation. Data in this thesis as well as many previous reports have shown that polyester has satisfied the following requirements: 1. It supports rapid growth and spreading of ARPE-19 cells, as well as supporting HESC-RPE. 2. It supports good differentiation and expression of RPE markers in both cell types. 3. It has excellent strength and handling properties which is evidenced by the ease of cutting, removal from the insert and mounting for histology (not shown). 4. It is surgically easy to transplant (unpublished work on rats and pigs in our laboratory, December 2007 to date) while acting as a permanent barrier against choroidal neovascularisation (Lee et al. 2006). 5. It is compatible with the host visual and immune system. Unfortunately the last condition is yet to be fully tested for polyester in long-term follow-up studies, thus the ideal substrate fully meeting all the

above criteria is awaiting elucidation. Given the superior performance of polyester combined with the complexity of polymer production—which requires specialist laboratory equipment—and that our laboratory could not source other suitable polymer types, no further polymers were tested.

10.2.3 Future directions in substrate selection

After a review and comparison of aforementioned past studies including RPE substrate studies that have been reviewed elsewhere (Binder et al. 2007;da Cruz et al. 2007), I have come to the conclusion that natural substrates are excellent cell-substrate materials that are capable of inducing marked polarisation, correct orientation, and expression of native markers of RPE differentiation, however they are either difficult to manufacture or very delicate to handle. Moreover, human explants or cadaver derived materials involve human tissue collection which comprises ethical issues that require authorisation of regulatory bodies (i.e in the United Kingdom, Human Tissue Authority). On the other hand, artificial substrates are also capable of supporting cells in a similar fashion to natural substrates.

A comparison of the artificial substrates used in this thesis shows a variety of polymers with diverse chemistries are able to successfully support cell attachment, growth and differentiation, and this echoes a principle obtained in other laboratories such as Williams et al (2005). What this really implies is the core chemistry of an artificial substrate is not the main determining factor for cell behaviour. Most of these studies demonstrated that RPE cells grow to confluence and express several favourable characteristics as well as ICC markers on the chosen artificial surface. Thus, rather than core chemistry, it seems surface texture as well as electrostatic profile may well be what ultimately determines how cell-friendly a surface truly is. It is already known that cells use surface mechanical cues within the ECM for orientation (Ulbrich et al. 2011). More recently, studies in polymer science utilising nano-technology have revealed surface nano-dimensional texturing as a more important determinant of cell behaviours (such as migration) than surface chemistry (Hasirci and Pepe-Mooney 2012;Slepicka et al. 2012). In addition, it is already known that hydrophilic surfaces allow cell attachment since they incorporate functional polar groups which produce a wettable plane, whereas hydrophobic surfaces do not attract water or cells (Williams et al. 2005). It has been postulated that certain hydrophilic surfaces carry a weak positive charge that attracts the

weak negative charge harboured by cells and proteins (Kearns et al. 2012). Furthermore, the electrostatic profile i.e. distribution of electric charges within a surface would, at least in theory and according to Gauss's law in physics, produce a multitude of electric fields. Incidentally, it is now known that cells, in particular RPE cells, do respond to the presence of an electric field. RPE cells orient their long axis perpendicularly to electric field vectors (galvanotropism) and migrate (galvanotaxis) either towards the anode (Gamboa et al. 2010) or the cathode (Sulik et al. 1992). Similar phenomena have been well documented in corneal cells (Soong et al. 1990;Dua et al. 1993). Sadly, little has been done to study electric field distributions within polymer surfaces since such dynamic characteristics of polymers are difficult to measure and thus remain largely uncharacterised. This may well be an interesting direction for future nano-scale substrate studies.

10.3 Peptides as a coating for artificial scaffolds:

There is a wealth of evidence that RPE utilise specific integrins for binding individual ECM components. It has been demonstrated that RPE cells bind to laminin 1 via α6β1 and laminins 10/11 using both α3β1 and α6β1 as expected (Aisenbrey et al. 2006), laminin 5 via α6β4 (Aisenbrey et al. 2006;Fang et al. 2009), vitronectin via αvβ5, thrombospondin-1 via αvβ5 and α5β1 (Mousa, Lorelli, & Campochiaro 1999) as well as fibronectin via α5β1 (Li et al. 2009). In addition it has been demonstrated that RPE cells attach and align along collagen I fibrils via α2β1 (Ulbrich et al. 2011). It also is known that the RPE basement membrane of BrM contains a wealth of ECM proteins such as Collagen IV-V, laminin and Heparin Sulphate, while the inner collagenous layer of BrM has a slightly different group of proteins including Collagen I, III, V, fibronectin, Chondroitin Sulphate and Dermatan Sulphate (Das et al. 1990;Thomson et al. 1998;Booij et al. 2010).

Peptides are now being widely used as substitutes to their more complex protein counterparts in a variety of scientific applications (Carlisle et al. 2000;Armstrong et al. 2004;Senyah, Hildebrand, & Liefeith 2005;Recalde et al. 2011;Sreekumar et al. 2013). ECM molecules are large molecules and difficult to define due to their complex structure and their heterogeneity in assembly, folding, and polymerisation, which is further compounded by in vivo remodelling and destruction (proteolysis) together with the resultant undefined peptide products (Collier and Segura 2011). Ever since the work

of Pierschbacher and Ruoslahti in 1984 (Pierschbacher & Ruoslahti 1984), it has been realised that ECM proteins do not interact in their entirety with cells. Each ECM protein molecule possesses an active peptide portion that is used to interact with corresponding integrin receptors on the cell surface. This active segment is usually a short sequence of amino acids often less than 20 amino acids long, but can be as short as tetramer peptides (Mann and West 2002;Harbers and Healy 2005). The advantages of using a short peptide rather than a protein is its purity, and ease of characterisation because such sequences are synthesised chemically, and thus can guaranteed free from pathogens and immunologically active foreign tissue or animal by-product (Bellis 2011). It is possible to coat artificial surfaces with such peptide fragments using either a covalent method or a simple adsorption method. The latter employs simple non-specific electrostatic attractions between the peptide and the ionised component within the surface of the artificial substrate. Although adsorption limits peptide orientation to the surface profile, neither method has been shown to guarantee perfect orientation and conformation of the peptide (Massia, Rao, & Hubbell 1993;Sigurdson et al. 2002). Furthermore, adsorption is easier, cost-effective to implement, and has been reported to work effectively when compared to the covalent method (Massia, Rao, & Hubbell 1993). Thus the ease of the adsorption process and its reported success justifies its use against the more sophisticated covalent bonding methods as these may fail despite added expense and effort. Peptide-grafted surfaces mimic ECM-coated substrate by presenting the cells with the sequence of the active peptide portion of a protein subunit usually associated with a whole ECM protein molecule. In the same way different ECM proteins provide a specific charged surface profile to the basal side of a cell monolayer, active peptide region sequences can be utilised to provide cells with a certain signal profile mimicking that protein from which they were derived i.e a natural substrate. This approach may, at least in theory, be more favourable than relying on artificial surfaces which often have an electrostatic profile that is largely undefined and thus unpredictable. Therefore I sought to test active minimal peptide sequences belonging to ECM components in order to elucidate a friendly surface mimicking some of the above BrM components.

10.3.1 The impact of individual peptides and polyester

I have demonstrated that ARPE-19 cells respond favourably, in one respect or the other, to the presence of short active peptides on the substrate surface. Peptide-adsorption has already been reported as a valid method for immobilising active short peptides and my

results demonstrate significant differences in behaviour between certain peptides. IKVAV excelled as an adhesion peptide, showed a similar attachment trend on glass, and maintained the highest trend in TER. However, IKVAV impeded both spreading on glass, and pigmentation of ARPE-19 cells. Surprisingly, a mixture of all the peptides (1:6 dilution of IKVAV) was equally detrimental to spreading, however pigmentation was rescued at 4 months. Thus 1:6 dilution of IKVAV is detrimental to spreading, but insufficient to inhibit pigmentation on glass. Furthermore, the morphology of cells cultured on this peptide mixture did not suffer and resembled mostly that of the RGD-based groups and not IKVAV. The other laminin-derived peptide YIGSR, was not significantly different to other peptides on any surface and this limited behaviour is not new (Sigurdson et al. 2002). These data suggest laminin-derived peptides provide some but not all functions of the original laminin molecule.

None of the RGD-based peptide groups excelled significantly in respect of cell attachment, but they did allow cell spreading, which is consistent with previous reports (Mahalingam, Gallagher, & Couchman 2007). RGD-based peptides produced superior cell morphology and ICC profiles in all experiments, such as better polarisation of the cells when grown both on glass and polyester. But one cannot ignore that ARPE-19 morphology was better while on adsorbed polyester than adsorbed glass for virtually all peptides.

Thus, none of the tested peptides was superior in every respect. It follows that the peptides used in this study could be providing the cells with a signal that may be too limited. It is conceivable that short peptides are able to provide the cells with only a selective instruction leading to a narrower series of events than those induced by a complete ECM molecule which comprises multiple active peptide sequences. Such limited events could consist of only one (or few) of the possible cellular behaviours e.g. spreading alone, or attachment with reduced spreading (as observed with the IKVAV peptide).

10.3.2 Considerations and future directions for peptide coatings

Although short peptide sequences produced a limited set of improvements in overlying cell culture profiles, it is inevitable that they produce a narrower set of events that fall short of mimicking the parent ECM molecule in its entirety. Parent ECM molecules are

vastly more complex and comprise multiple active peptide sequences which will conceivably bind multiple cell surface receptors simultaneously, while providing the correct orientation of peptides in 3-dimentional space.

An example of the complexity of ECM mimicry can be seen within the fibronectin molecule. It has already been reported that the active RGD sequences in fibronectin can enhance attachment and spreading of cells, whereas they cannot induce any of the focal adhesion-related signals such as cytoskeleton changes or stress fibre formation: These latter effects would, for example, depend on the syndecan-4- (or heparan-sulfate proteoglycan-) binding domain of fibronectin (or its peptide derivatives) in addition to the RGD sequence-containing sites (Mahalingam, Gallagher, & Couchman 2007). To further illustrate the complexity of fibronectin mimickry, its heparin binding domain comprises 4 main active peptide sequences that have been shown to interact with the cell syndecan-4 receptor: FN-C/HI (YEKPGSPPREVVPRPRPGV), FN-C/HII (KNNQKSEPLIGRKKT), FN-C/HIII (YRVRVTPKEKTGPMKE) and CS-1 (DELPQLVTLPHPNLHGPEILDVPST) (Iida et al. 1992). In turn, not all cell types will respond positively to each of these peptide sequences (even in conjunction with RGD), meaning that proper focal adhesion structure formation needs cell type-specific peptide sequences (Mooradian et al. 1992). It is intriguing to know that a major integrin for fibronectin, α5β1, is a receptor that requires co-receptor syndecan-4 to operate fully whereas α4β1 does not (Mostafavi-Pour et al. 2003). Therefore future studies might favour development of RGD sequences that are specific to α4β1 (rather than α5β1) in order to avoid the additional co-receptor requirement(s), thus allowing focal adhesion formation without resorting to complicated syndecan-4 ligands. In conclusion, further studies are required to simultaneously test multiple active peptide sequences mixed in optimal proportions while being customised for a specific cell type and its desired response(s). Table 10-1 summarises all the substrates characterised with ARPE-19 in this thesis.

Substrate	Type	Result
PLGA (Poly D,L-Lactide-co-Glycolide)	Biodegradable	Good support for RPE growth. Membrane is too thick and further swells in culture
Expanded Teflon (ePTFE)	Non-biodegradable	Too hydrophobic. Not wettable. Occasional solitary cells seen on SEM after cell culture (Not shown)
Carbon-coated ePTFE	Non-biodegradable	Too hydrophobic as for ePTFE (Not shown)
Solid, Porous, and Electrospun Polyurethane including hydrophilic types	Non-biodegradable	Supports growth and differentiation. But control membrane polyester filter (PE) was far superior
Peptide-adsorbed glass	Non-biodegradable	Supports growth and differentiation but to a lesser extent than peptide-adsorbed PE filter
Peptide-adsorbed PE filter	Non-biodegradable	Supports growth and differentiation with good morphology. Excellent morphology and marker expression for certain RGD-containing peptides
PE filter	Non-biodegradable	Supports growth and differentiation with good morphology and ICC profile
HPPEF*	Non-biodegradable	Supports growth and ZO-1 junctional ICC staining

Table 10-1 Summary of all the substrates characterised with ARPE-19 cells in this thesis and main findings. * = This polymer was further characterised using HESC-RPE (chapter 8).

10.4 The importance of media choice in RPE culture

The use of cell lines is highly efficient for examining properties of human RPE cells. Thus the ARPE-19 cell line has been widely studied. However, one of the major limitations of this line, and other established RPE lines has been its propensity to de-differentiate away from the classic RPE phenotype with repeated passage. Having chosen an optimal substrate, I sought to investigate whether it is possible to modulate the phenotype of ARPE-19 by varying the growth medium without resorting to specialised components such as retinal extracts.

One essential marker of RPE differentiation which has eluded many ARPE-19 studies is RPE65, the essential isomerohydrolase that converts retinyl esters to retinol (Moiseyev et al. 2005;Cai, Conley, & Naash 2009). Numerous studies have documented RPE65 mRNA in ARPE-19 but none could demonstrate RPE65 protein (Dunn et al. 1996;Janssen et al. 2000;Alizadeh et al. 2001;Boulanger and Redmond 2002;Kanuga et al. 2002;Krugluger et al. 2007;Vugler et al. 2008). Fortunately RPE65 was discernable on ICC and protein was present in our western blots of ARPE-19 cultures. Moreover, our RPE65 antibody has been validated on human eye sections in our laboratory (Vugler et al. 2008). RPE65 levels were highest in high glucose DMEM/pyruvate and were significantly reduced by removal of pyruvate or glucose, suggesting that both are contributory. MerTK is another marker of mature RPE cells and is regarded as *conditio sine qua non* for diurnal POS phagocytosis (D'Cruz et al. 2000;Gal et al. 2000;Vollrath et al. 2001;Carr et al. 2009a). Unfortunately, MerTK is absent when ARPE-19 cells are cultured in standard medium, although the phagocytosis-specific integrins αv and β5 are both detectable (Carr et al. 2009a). Since high glucose DMEM/pyruvate induced the highest expression of MerTK and since specific uptake of POS is dependant upon MerTK (D'Cruz et al. 2000;Gal et al. 2000;Vollrath et al. 2001;Carr et al. 2009a) I selected this optimal medium for the human POS phagocytosis assay. I have documented internalised human POS within the ARPE-19 cells maintained in this medium.

10.4.1 Pyruvate and DMEM contribute to improved differentiation characteristics of ARPE-19 irrespective of glucose

Pyruvate has been known as an energy source for nearly a century (Quastel 1925). Given sufficient oxygen within the cell, pyruvate is recruited—via enzymatic

decarboxylation to acetyl CoA—into the citric acid cycle (Krebs 1940), an important source of energy for the cell.

Pyruvate and lactate are readily converted one from the other by the *lactate dehydrogenase* enzyme (Stryer et al. 1995) which is subject to strict regulation. Thus the ratio of lactate to pyruvate (L/P) appears to be relatively stable within tissues. For example, blood L/P ratio ranges between 4:1 to 10:1. More recent studies have demonstrated the L/P ratio correlates closely with the cytosolic NADH/NAD^+ ratio—the ultimate measure of redox status within the cell (Luft 2001).

In this thesis, pyruvate per se enhanced several differentiation characteristics in ARPE-19. Dark pigmentation and strong CRALBP expression were hallmarks of cells grown with pyruvate in this thesis. Pyruvate also promoted significantly higher levels of MerTK by western blotting. The mechanism of the effect of pyruvate is still under investigation, and many studies have implicated pyruvate as a hydrogen peroxide scavenger, but none could demonstrate a molecular mechanism (Andrae, Singh, & Ziegler-Skylakakis 1985;Nath and Salahudeen 1993;Nath et al. 1994;Nath et al. 1995;Desagher, Glowinski, & Premont 1997;Giandomenico et al. 1997;Wang et al. 2007;Hegde & Varma 2008;Babich et al. 2009;Ahmado et al. 2010;Ahmado et al. 2011). Some studies have implicated pyruvate as a potent alkalising agent in the cytosol, which is able to reverse the certain inhibitory effects of high glucose on immune cell functions (Wu et al. 2003;Wu et al. 2005b). I have shown through the use of a well established pyruvate transport inhibitor, 4-CIN (Halestrap & Denton 1975;Halestrap 1975), that favourable effects of DMEM/pyruvate are markedly reduced by only modest (Bui, Kalloniatis, & Vingrys 2004) inhibition of pyruvate transport into and within the cell using 500μM 4-CIN. Since the metabolic pathways involving pyruvate and its subsequent derivatives are located within the cell, we can postulate that pyruvate must be allowed to exert intracellular presence in order for it to promote differentiation. In a strikingly similar tone to work in this thesis, induction of differentiation by pyruvate has been reported in myeloid cells but no mechanism was suggested (Liu, Geng, & Suo 2009). Pyruvate has also been reported to augment pigmentation in non-RPE cells such as cultured melanoma cells, which is strikingly similar to our results (Nakayasu et al. 1977;Saeki and Oikawa 1978). Surprisingly, authors of these studies attributed the benefits of pyruvate to shifts in pH. In their studies pyruvate and galactose were associated with increased tyrosinase in cultured

melanoma cells, whereas glucose was inversely associated with tyrosinase activity and this was believed to be related to a higher pH in the pyruvate/galactose group, while a lower pH existed in the glucose group due to lactate accumulation (Nakayasu et al. 1977;Saeki & Oikawa 1978). Fortunately for HESC-RPE, basic HESC medium contains pyruvate, so no modification was deemed necessary in the HESC studies which are discussed below.

10.4.2 Pigmentation in culture is an essential readout that follows other differentiated characteristics in cultured RPE

Pigmentation is a hallmark of native RPE but one of the most common limitations of cultured adult RPE cells has been lack of pigmentation. In vitro, virtually all cultured RPE cells undergo de-pigmentation with passage as melanin granules become diluted and pigment is not usually synthesised thereafter (Opas 1994). Some reports have suggested specialised substrates(Campochiaro & Hackett 1993;Tezel & Del Priore 1997;Tezel, Del Priore, & Kaplan 2004;Turowski et al. 2004;Stanzel et al. 2005), or specialised media can induce re-pigmentation, differentiation or both (Hu & Bok 2001;Luo et al. 2006), however no specific factors or ingredients were implicated. I have examined ARPE-19 pigmentation in DMEM/pyruvate on several substrates including some not shown in this thesis (Ahmado et al. 2008) but I observed no correlation between pigmentation and substrate, and this suggests that re-pigmentation of ARPE-19 is related to properties of culture medium. This is supported by the observation that DMEM/F12 never induced pigmentation.

It is known that melanin synthesis cannot occur in the absence of tyrosinase (Riley 1993), and that adult native-RPE have minimal tyrosinase and do not synthesise new melanin in vivo (bul-Hassan et al. 2000;Lopes et al. 2007;Biesemeier et al. 2010). On the other hand, my data demonstrates cultured RPE can express tyrosinase and synthesise pigment. Paradoxically, tyrosinase levels were highest in non-pigmented cultures of DMEM/F12, and significantly lower in the pigmented cultures maintained by DMEM. This suggests firstly that melanogenesis has been inhibited downstream of tyrosinase in DMEM/F12. Secondly, one or more melanogenesis by- or end-products maybe exerting feedback inhibition on tyrosinase in heavily pigmented cultures of DMEM/pyruvate. I acknowledge that Dunn et al (Dunn et al. 1996) reported pigmentation using DMEM/F12, but this was attributed to their use of low passage

ARPE-19, since the currently available high passages have consistently lacked pigment (Wang, Dillon, & Gaillard 2006;Song et al. 2008;Burke & Zareba 2009).

I have demonstrated that several aspects of ARPE-19 differentiation improved alongside pigmentation in DMEM/pyruvate. Firstly, lack of Keratin 8 correlated with pigmentation. This is consistent with previous studies including RPE from various sources including our HESC-RPE which demonstrated that although Keratin 8 is a marker for RPE cells (alongside 18) expression of Keratin 8 is lost in confluent RPE cultures (Hunt & Davis 1990;Riley 1993;Hunt 1994;McKay & Burke 1994;McKay et al. 1997;Schraermeyer & Heimann 1999;Lopes et al. 2007;Rozanowski et al. 2008;Vugler et al. 2008). Secondly, the expression of RPE ICC markers such as circumferential actin and the absence of stress fibres, expression of CRALBP as well as apical orientation of Na,K-ATPase are characteristics of native RPE (Opas 1989;McKay & Burke 1994) which was best seen in pigmented cultures. Thirdly, I have shown that DMEM-maintained cultures produced more VEGF (particularly basally secreted VEGF) while possessing higher TER. It is not clear whether VEGF adversely affects TER since previous studies show conflicting effects of VEGF on TER (Blaauwgeers et al. 1999;Ghassemifar, Lai, & Rakoczy 2006;Ablonczy and Crosson 2007;Miyamoto et al. 2008;Peng, Adelman, & Rizzolo 2010). My data suggests barrier function of ARPE-19 in DMEM was at the very least not affected by VEGF. Alternatively it may be that TER and VEGF are both independent products of differentiation that are expected to increase in tandem (Blaauwgeers et al. 1999). TER levels in ARPE-19 may also have been further sustained by the high glucose present in the experimental media, and this effect has been reported previously (Villarroel et al. 2009). Nevertheless, all ARPE-19 TER's were generally low, as is expected of this cell line (Luo et al. 2006). In contrast, I will discuss later how HESC-RPE maintain high levels of pigmentation while being vastly superior to ARPE-19 in terms of TER (section 10.5.3).

10.4.3 VEGF is an RPE differentiation marker that rises in tandem with other favourable characteristics of RPE

VEGF is a physiological product of RPE and an essential autocrine factor affecting RPE behaviour (Guerrin et al. 1995;Wu et al. 2005a;Krugluger et al. 2007). VEGF also provides maintenance for the choriocapillaris and retina (Saint-Geniez et al. 2008;Saint-Geniez et al. 2009), and is reported to rise in tandem with differentiation in primary

cultured RPE (Blaauwgeers et al. 1999;Ohno-Matsui et al. 2001;Sonoda et al. 2009;Sonoda et al. 2010). Although ARPE-19 cells secrete less VEGF than primary foetal RPE or HESC-RPE (Ablonczy et al. 2011;Kannan, Sreekumar, & Hinton 2011) it is quite reassuring that VEGF values for ARPE-19 under all media conditions in this series corresponded to concentrations between 1.9 and 12.1 ng/mL/24h which is closely comparable to levels in foetal as well as primary RPE (Blaauwgeers et al. 1999;Sonoda et al. 2010). A similar finding was also observed for VEGF secretion by our Shef1 HESC-RPE. It is interesting to note previous studies on primary cultured RPE indicate preferential basal VEGF secretion (Blaauwgeers et al. 1999;Maminishkis et al. 2006), while RPE cell lines exhibit apical secretion under standard conditions (Slomiany and Rosenzweig 2004;Kannan et al. 2006;Ahmado et al. 2009;Ahmado et al. 2011). However, ARPE-19 data presented in this thesis clearly demonstrates an increase in basal VEGF in DMEM compared to DMEM/F12. This improved basal secretion is a valuable element of differentiation in my study because it is one step closer to primary culture phenotype. High glucose can increase VEGF and this is reported widely (Sone et al. 1996a;Young et al. 2005;Heimsath, Jr. et al. 2006;Xiao et al. 2006). However reduction of glucose below 5.5mM is also reported to increase VEGF output by RPE (Sone et al. 1996a). This may explain the exaggerated VEGF levels in the low glucose DMEM since I have measured glucose consumption in 24mm inserts (not shown), and found that ARPE-19 cells consume approximately 1g/L over a 5 day starvation period. This would correspond to near-total glucose depletion in the low glucose group. It is of great interest that this was a more potent stimulus for VEGF than sustained high glucose. PEDF is an important neurotrophic growth factor which is regarded as a potent antagonist of VEGF and has been reported to be expressed by foetal and adult RPE (Tombran-Tink et al. 1995;Ohno-Matsui et al. 2001), but several studies documented its absence in ARPE-19 (Klimanskaya et al. 2004;Sharma et al. 2005;Tian et al. 2005). On the other hand, data in this thesis demonstrated that PEDF expression can be modulated by optimising growth medium. PEDF protein was also expressed in cells grown in high glucose DMEM/pyruvate, which corroborates Q-PCR findings.

10.4.4 The importance of glucose for ARPE-19

Other effects of glucose in our study are worthy of mention, since this has been a subject of debate in previous literature (Sone et al. 1996b;Heimsath, Jr. et al. 2006;Senanayake et al. 2006). When combined with pyruvate, high glucose was a

significant factor in determining increased expression of CRALBP, RPE65, tyrosinase and PEDF at both protein and mRNA level. High glucose also led to more MerTK message but the protein difference was not significant. Since each millimole of glucose is expected to yield 2mM of pyruvate via glycolysis, the lack of 1mM pyruvate, in energy terms, is equal to the loss of a mere 0.5mM of glucose. Therefore I do not believe the beneficial effects of pyruvate are a function of energy-substrate availability since the high glucose concentration in non-pyruvate medium would have compensated for the lack of pyruvate-derived energy. It is worth mentioning that high glucose in combination with pyruvate has previously been shown to improve neutrophil cell function (Wu et al. 2003).

10.4.5 The Concept of "Pigmentation Medium" for culture of RPE: should all future RPE culture use RPE-optimized medium?

Thus the question arises – why is DMEM/F12 preventing pigmentation and differentiation? Although DMEM/F12 cultures never developed pigmentation despite the presence of pyruvate, DMEM/F12 did express high levels of tyrosinase which indicates that the process of pigmentation was stalled by the presence/absence of one or more factors. The problem may be a presumed anti-melanogenic component of Ham's F12, or a pro-melanogenic component of DMEM that has become diluted below a requisite level (since DMEM/F12 is a 1:1 dilution of DMEM and F12). In addition to the ingredients unique to DMEM/F12, there are nearly 30 other ingredients occurring at different concentrations in basal preparations of these two media. Thus the list of media components to consider is too vast for this thesis (see Table 10-2). However, after an initial analysis, I found a noticeable difference in bicarbonate concentration: 44mM in DMEM compared with 29mM in DMEM/F12. I have come across two previous studies where 44mM bicarbonate is shown to increase pigmentation. In one study this level supported in vitro re-pigmentation of aged human RPE whereas 26mM did not (Kurtz and Edwards 1991). In the other study foetal RPE cultured on plastic underwent increased melanisation in the presence of higher bicarbonate (Miceli and Newsome 1996).

Pmel17 is enriched in pre-melanosomes and is an early marker for pigmentation. I now have unpublished data which indicates correction of bicarbonate levels to 44mM in DMEM/F12 dramatically increases Pmel17 expression among other markers, although

it does not remedy the lack of pigmentation (not shown). Therefore correction of bicarbonate, as well as inclusion of pyruvate, may well be a necessary step for any future RPE melanogenesis studies.

Amino Acids	MW	DMEM/F12 (mg/L)	DMEM (mg/L)
Glycine	75	18.75	30
L-Arginine hydrochloride	*211*	*147.5*	*84*
L-Cystine 2HCl	313	31.29	63
L-Glutamine	146	580*	580
L-Histidine hydrochloride-H2O	210	31.48	42
L-Isoleucine	131	54.47	105
L-Leucine	131	59.05	105
L-Lysine hydrochloride	183	91.25	146
L-Methionine	149	17.24	30
L-Phenylalanine	165	35.48	66
L-Serine	105	26.25	42
L-Threonine	119	53.45	95
L-Tryptophan	204	9.02	16
L-Tyrosine†	181	38.7	72
L-Valine	117	25.85	94
L-Cysteine hydrochloride-H2O	176	17.56	
L-Glutamic Acid	147	7.35	
L-Proline	115	17.25	
L-Alanine	89	4.45	
L-Asparagine-H2O	150	7.5	
L-Aspartic acid	133	6.65	
Vitamins			
Choline chloride	*140*	*8.98*	*4*
D-Calcium pantothenate	477	2.24	4
Folic Acid	441	2.65	4
Niacinamide	122	2.02	4
Pyridoxine hydrochloride	206	2	4
Riboflavin	376	0.219	0.4
Thiamine hydrochloride	337	2.17	4
i-Inositol	*180*	*12.6*	*7.2*
Biotin	244	0.0035	
Vitamin B12	1355	0.68	
Inorganic Salts			
Calcium Chloride (CaCl2) (anhyd.)	111	116.6	264
Ferric Nitrate (Fe(NO3)3"9H2O)	404	0.05	0.1
Magnesium Sulfate (MgSO4-7H2O)	246	100	200
Potassium Chloride (KCl)	75	311.8	400
Sodium Bicarbonate (NaHCO3)	84	2438	3700
Sodium Chloride (NaCl)	*58*	*6995.5*	*6400*
Sodium Phosphate monobasic (NaH2PO4-H2O)	138	62.5	141
Cupric sulfate (CuSO4-5H2O)	250	0.0013	
Ferric sulfate (FeSO4-7H2O)	278	0.417	
Magnesium Chloride (MgCl2-6H2O)	203	61	
Sodium Phosphate dibasic (Na2HPO4-7H2O)	268	134	
Zinc sulfate (ZnSO4-7H2O)	288	0.432	
Other Components			
D-Glucose (Dextrose)	180	4500*	4500‡ (1000)
Phenol Red	376.4	8.1	15
Sodium Pyruvate	110	55	110‡ (0)
Hypoxanthine Na	159	2.39	
Linoleic Acid	280	0.042	
Lipoic Acid	206	0.105	
Putrescine 2HCl	161	0.081	
Thymidine	242	0.365	

* Glutamine and glucose levels shown are the corrected values used in this thesis.
† This is the effective concentration of L-Tyrosine. In commercial DMEM/F12 L-Tyrosine is actually L-Tyrosine disodium salt dihydrate at 55.79mg/L (MW 261).
‡ Indicates components with alternative concentrations in brackets. Three versions of DMEM medium were used: High glucose i.e 4.5g/L no pyruvate (DH), high glucose with 1mM pyruvate (DH+P), and low glucose i.e 1g/L with pyruvate (DL+P). Alternative concentrations are included in brackets. Actual media purchased are DMEM/F12 -L-Glut #21331 (we corrected for glutamine and glucose), DMEM high glucose with pyruvate #41966, DMEM high glucose without pyruvate #41965 and DMEM low glucose with pyruvate #31885.
Italics indicate components that exist at higher concentrations in DMEM/F12 than in DMEM medium. All other common components exist at lower concentration in DMEM/F12.

Table 10-2 Comparison of DMEM/F12 and DMEM media used in this thesis.

10.5 HESC-RPE as a cell source for RPE transplantation

One of the limitations of in vitro tissue culture is that cultured cells have already undergone ageing in their host since normal diploid cells have a finite proliferation potential are limited in their doubling capacity (Hayflick and Moorhead 1961;Hayflick 1965). Whether primary culture or cell lines are used, studies are permanently tied to the age of the donor at the time of death, thus inheriting an array of irreversible changes brought about by ageing. Indeed some of the most successful and widely used lines ARPE-19 and D407 have originated from young donors under the age of 20 (Davis et al. 1995;Dunn et al. 1996). After a decade of work with in vitro RPE, Bruce A. Pfeffer extensively reviewed primate RPE culture methodology in 1991 (Pfeffer 1991) and indicated that RPE cultures from younger donors have characteristics that distinguish them from older ones: Young human donor RPE cultures resemble non-human primate RPE in that they firstly harbour homogenous growth i.e most cells are taking part in mitosis. Secondly, cells are more cohesive and have few if any cells migrating away from the main RPE sheet, and thirdly, cells are more epithelial-like, polygonal with bright phase borders and do not elaborate any processes. On the other hand, RPE cultures from older human donors were found by Pfeffer to have overall less mitosis, while a subset of cells remained highly mitotically active which lead to isolated foci of proliferation, and more cells appeared to migrate away from the main body of RPE and these migrating cells elaborated long processes. He also mentioned an arbitrary cut off of 15 years of age where a visible shift of human RPE behaviour occurs compared to older donors (Pfeffer 1991). Thus it is no surprise that primary foetal RPE has now been extensively characterised and methods for human foetal RPE primary cultures have been optimised with promising results (Maminishkis et al. 2006;Sonoda et al. 2009;Sonoda et al. 2010). Nevertheless, continually sourcing RPE from aborted foetuses will need experience and adherence to a fixed protocol (Sonoda et al. 2009) which ultimately carries a potential of variation between each cadaver. Thus embryonic stem cells have become a very promising option due to their unlimited doubling capability in their undifferentiated state (Vugler et al. 2007). The combined benefit of working with an unlimited source of ‘youthful’ cells, together with the experimental consistency achieved by working with identical or very similar batches of cells has become quite appealing, as is the case with embryonic stem cells.

10.5.1 Laminin or Matrigel?

One of the complexities associated with HESC-RPE culture has been their reliance on a compound basement membrane product, matrigel, for cell growth, differentiation and maturation. Therefore one of the first experiments I conducted was to find out whether only one of the major components of MG supported Shef-1 HESC-RPE. Although cultured RPE secrete both ECM proteins laminin and collagen IV (Turksen, Opas, & Kalnins 1989), it has been previously reported that RPE cells can have an adhesive preference for laminin among other ECM components (Zhou, Dziak, & Opas 1993;Campochiaro & Hackett 1993). Since laminin is the major component, comprising 60%, of total matrigel (Kleinman et al. 1986), I wondered whether HESC-RPE would be satisfied with this component alone. Indeed, HESC-RPE grown on laminin coated dishes behaved similarly to those grown on matrigel, except for some apparent lag in spreading which resulted in smaller colonies, and the appearance of detachment blebs. The development of blebs (domes) on laminin was presumed to be due to a more active pump mechanism in the laminin group, or a presumed weaker attachment to their matrix. Functional Na,K-ATPase has been associated with the development of blebs previously (McKay et al. 1997). This ion pump is a major transporter that normally resides in the basolateral membrane of most epithelial cells but is uniquely expressed apically in RPE cells. The basis for this inverted Na,K-ATPase localisation is quite complex and has been suggested to be related to an inversion of RPE cytoskeleton, along with RPE-specific adherens junction changes (Burke, Cao, & Irving 2000). But what is certain is that in situ RPE as well as optimally differentiated in vitro RPE harbour apically oriented Na,K-ATPase (Hu & Bok 2001;Ahmado et al. 2011). The apical positioning of Na,K-ATPase is an optimal adaptation of native RPE cells since they are required to actively pump fluid away from the subretinal space through the RPE cells and ultimately to the choroid, a process which in turn prevents fluid accumulation in the retina. However, it was reassuring to see that HESC-RPE express this marker apically in both laminin and matrigel groups. The observation that Na,K-ATPase expression appeared identical in ICC among laminin and matrigel groups strongly suggests that detachment blebs are not related to increased expression of this marker and that an alternative causation must be considered, such as cell-matrix interactions.

There are several considerations with respect to growth of HESC-RPE on laminin versus matrigel. Firstly, the apparent lag in the spreading speed of laminin-supported

HESC is not necessarily a disadvantage and may indicate rapid differentiation. This is supported by previous evidence that cell spreading and proliferation are inversely related to differentiation (Opas 1989). Secondly, differentiation of epithelial cells involves a shift from their cell-substrate adhesiveness to predominantly cell-cell adhesiveness (Opas 1985;Opas and Kalnins 1985) and that would be another explanation why the laminin coated dishes developed multiple detachment blebs while the matrigel group had none whatsoever. Thirdly, it is also worth noting that adhesive preference to laminin has been reported to disappear gradually with culture time in chick RPE cells (Zhou, Dziak, & Opas 1993) and this is in agreement with the occurrence of detachment blebs at 3 months in this study. At the very least, development of detachment blebs indicates that cells are engaged in unidirectional (vectorial) ion/fluid transport (Kennedy and Lever 1984) and also have developed good barriers against paracellular fluid leakage (Soler, Laughlin, & Mullin 1993) which is another welcome sign of differentiation shift towards the native phenotype. Despite these assumptions, the apparent lag in growth is not fully explained.

To summarise, murine-derived ECM such as matrigel, or laminin-1 are suitable for HESC-RPE differentiation and expansion. The appearance of numerous detachment blebs combined with a lag in growth of the HESC-RPE colony suggests laminin may increase the differentiation of HESC-RPE. Bleb formation in the laminin group was not a function of differential Na,K-ATPase expression but is possibly related to the balance between cell-cell versus cell-matrix interactions. Confirmation that the apparent lag in growth was not due to a detrimental effect of laminin requires further investigations. Therefore laminin was not selected as the main ECM coating for further studies.

10.5.2 Dissociation of HESC-RPE – a beneficial development

I have demonstrated HESC-RPE dissociation as a powerful tool for the investigation of cell properties. Initially various enzymatic methods for dissociating the HESC-RPE failed including regular trypsinisation, despite rinsing with PBS (without Ca^{++} and Mg^{++}). None of the enzymatic methods were successful except for 0.25% trypsin constituted in a non-enzymatic EDTA-containing dissociation buffer (Sigma-Aldrich). Subsequently our departmental protocol is now to use Trypsin-EDTA. These observations provide strong evidence that divalent ions play a pivotal role in HESC-RPE cell-cell and cell-matrix adhesion which is likely brought about by Mg^{++} or Ca^{++}-

dependent adhesion molecules such as integrins (integrin MIDAS) and the Ca^{++}-dependent cadherins.

Cadherins are present in RPE as well as other epithelial cells (McKay & Burke 1994). They perform diverse functions including cell-cell adhesion, recognition, signalling, morphogenesis and angiogenesis (Angst, Marcozzi, & Magee 2001) but were originally described for their adhesive functions. The word cadherin is an abbreviation arising from the full name Ca^{++}-dependent ADHERence proteIN. Thus it is known that Ca^{++} ions are important and mediate cell-cell adhesion through cadherin molecules (Alattia, Kurokawa, & Ikura 1999).

It is also worth noting that all beta integrins and half of all alpha integrins comprise I/A domains containing a MIDAS motif. This ion binding site is necessary for interaction with the ligand and activation of the integrin molecule (Lee et al. 1995;Hynes 2002). Integrin α5β1 in particular has been shown to lateralise to cell-cell contact sites in cultured RPE approximately 2 weeks after confluence is reached (Anderson et al. 1990). Apical integrins are also strongly reliant on Ca^{++} in vivo since Ca^{++} depletion loosens retinal adhesion in living animals (Kita, Negi, & Marmor 1992). Therefore it is imperative when performing dissociation of HES-RPE cells to deplete divalent cations such as Ca^{++} by using a chelating agent such as EDTA in order to dissociate cell-cell (cadherins, integrins) as well as cell-matrix (integrin) adhesion, and this is principle is now incorporated into the HESC-RPE dissociation protocol.

I demonstrated that seeding dsHESC-RPE at a low density is not suitable for transplantation due to the following reasons: Firstly, a significant number of cells developed neurite-like processes as well as a number of βIII-tubulin and NF200 positive cells across the cultures. Secondly, the cells lacked differentiated RPE characteristics. There was no pigmentation, no measurable TER, and cells were neither polygonal nor did they cover the surface area of the culture vessels at the least. Such neuronal characteristics in HESC-RPE are not recommended for further propagation. The development of such a neuronal phenotype is consistent with the experience of Klimanskaya and colleagues with low density passage (Klimanskaya et al. 2006).

I have also shown phenotypic improvements in HESC-RPE proportional to their seeding density. dsHESC-RPE maintained good RPE characteristics when seeded at

high densities greater than 200,000 cell/cm². Regular morphology was directly proportional to density of seeding as demonstrated by the regularity index. The 391,000 cell/cm² density group recorded a cellular regularity of 0.0175. This is similar to data published from our laboratory where non-dissociated optimal HESC-RPE demonstrates a regularity of 0.0195 (Vugler et al. 2008). Dark pigmentation both macroscopic and microscopic was more evident and was seen to increases in proportion to seeding density. One of the most notable ICC profiles of high density dsHESC-RPE was Na,K-ATPase which was invariably polarised to the apical membrane. This is a phenotypically significant characteristic since native RPE—unlike most epithelial cells—expresses this marker apically. dsHESC-RPE phenotype was further vindicated by TER which showed a trend in favour of higher cell densities.

10.5.3 Growth factor secretion and TER confirm HESC-RPE differentiation

Our HES-RPE are capable of maintaining a TER in excess of 200Ωcm² and an apical PEDF/VEGF ratio of around 12. Although this ratio is exceeded by recently generated fhRPE cultures which typically develop an apical ratio of >70 (Maminishkis et al. 2006), our HESC-RPE ratio is still vastly superior to that of ARPE-19 (0.02) and is certainly consistent with in vivo vitreous samples obtained from human controls which harbour PEDF/VEGF ratios ranging from 5 to 50 (Dieudonne et al. 2007). In addition our VEGF values resemble those observed in primary RPE (Blaauwgeers et al. 1999) and our PEDF values resemble those published in a study by Ablonczy et al (Ablonczy et al. 2011). On the other hand, fhRPE cultures may not always reflect the physiological adult PEDF/VEGF ratios. For example, some fhRPE are reported to generate PEDF/VEGF ratios in excess of 1000 (Sonoda et al. 2010). However, PEDF is also known as *early population doubling level c-DNA-1* (EPC-1) and thus can be likened to a low passage-marker according to in vitro (Kojima et al. 2006), as well as in vivo studies. Thus, it may not be desirable to have too high a PEDF/VEGF ratio as this ratio's decline in older persons may be a compensatory ageing mechanism to correct age-related decline in angiogenesis (Francis et al. 2004). In summary our HESC-RPE produce a physiological PEDF/VEGF ratio as well as acceptable concentrations of these factors.

10.5.4 High Porosity Polyester Filter (HPPEF) as a substrate for HESC-RPE

HPPEF is a physically identical filter to the Transwell polyester filter except it exceeds the latter's porosity by 25 fold. I was able to make comparisons between the hydraulic resistance of BrM, and the two mentioned PE filters using Poiseuille's law which approximated the true measured hydraulic resistance by nearly 90%. The reason this observation is very useful is two-fold:

1) First, it confirms that simple laminar flow is pre-dominant in this filter, whereas many real world situations require complex corrections due to turbulence without which discrepancies of up to two orders of magnitude can ensue (Sherman 1992). The mathematics needed to fully analyse fluid transport across membranes is too complex, and could well be the subject of another thesis (Foster, Fok, & Chou 2007). But the proximity of theoretical Poiseuillean conductance to the actual measured conductance illustrates that the requirements of Poiseuille's law were largely not violated. What this means is that our combination of pore size (0.4μm) and pore length (10μm) have largely satisfied the requirements for Poiseuillian water flow in our stated polyester filters, and may well be applied on other brands of filter with identical dimensions.

2) Secondly, by combining previously reported data on hydraulic conductivity of BrM with Poiseulle's law calculations, we can perform comparisons of hydraulic flow through commercial filters in comparison to BrM. Since adult BrM has a hydraulic conductivity ranging between 0.25 – 2.5 x 10^{-9} m/Pa/sec at ambient temperature (Moore, Hussain, & Marshall 1995) it follows that Transwell exceeds native adult BrM's best conductivity by at least 1.1 – 1.4 fold, whereas Sterlitech exceeds BrM's by at least 32 fold. On the other hand when considering subretinal transplantation of these filters, the filter should be considered as an additional barrier to conductivity. It follows from the above values that Transwell filter will offer an additional resistance against water flow by up to 70 – 90% BrM's resistance, while HPPEF only hinders water flow by 3.1% (at most) on top of BrM's innate resistance. Therefore the resistance to water flow offered by Transwell filter is considerable while that of HPPEF is negligible with respect to BrM characteristics. This is a significant finding which supported our selection of HPPEF for further studies.

I performed ICC and SEM on HES-RPE cells cultured on HPPEF which further confirmed the status of HPPEF as a superior filter for supporting differentiation. The ICC profile is identical to that observed on Transwell polyester filters (not shown) as

well as matrigel coated TCPS. Here, HESC-RPE expressed a host of favourable ICC markers. There was no SOX2 staining indicating a departure from pluripotence and a shift towards tissue differentiation. The absence of Ki67 is also a welcome sign, and virtually no Ki67 was visualised for HESC-RPE on HPPEF at 8 weeks suggesting post-confluent maturation of the culture. HESC-RPE was largely negative for Keratin8 barring the occasional group of cells. I have already discussed the absence of Keratin8 in ARPE-19 as well as our previous HESC study and this is a further sign of maturation (Vugler et al. 2008).

HESC-RPE were positive for OTX2 which (alongside MITF) is implicated in development of RPE and considered a master RPE transcription factor. There is evidence that both OTX2 and MITF are regulated by specific spatial and temporal Wnt/βcatenin signals (Fujimura et al. 2009). OTX2 also positively modulates expression of Bestrophin-1 alongside MITF. Forunately HESC-RPE developed some light basolateral staining for Bestrophin-1 indicating successful operation of OTX2 by transcriptional regulation of Bestrophin-1 which further suggests RPE phenotype.

Another strikingly evident marker that developed in HESC-RPE grown on HPPEF is CRALBP. Strong CRALBP expression is reassuring since CRALBP protein is abundant in RPE as well as Muller cells (Muller glia), while expression to a lesser extent is also reported in the ciliary epithelium (Saari and Crabb 2005;Salvador-Silva et al. 2005). Another reassuring aspect of CRALBP is it confirms optic vesicle lineage. Pax6 is a marker for cells derived from the optic vesicle/cup that ultimately differentiate to form the neuro-retina and RPE. Pax6 is considered one of the key transcription regulators required for RPE specification, together with OTX1/2 and MITF. However, RPE cells eventually cease to express Pax6 in vivo (Martinez-Morales, Rodrigo, & Bovolenta 2004) while ganglion and amacrine cells in the retina continue to express it (Ashery-Padan and Gruss 2001). Pax6 has been implicated in the developmental regulation of CRALBP expression in the CNS and eye. Pax6 is necessary for cells that ultimately require CRALBP expression even if Pax6 is eventually switched off. Thus, Pax6 knock-outs do not express CRALBP protein or RNA whatsoever (Boppana et al. 2012). The only other cells to express CRALBP are the pineal gland and oligodendrocytes of the brain (Martin-Alonso et al. 1993;Crabb et al. 1998). An intriguing finding in my study was the absence of Pax6 when pathclear-BME (pathogen tested, sterile version of matrigel was used). This has been confirmed on Transwell as well as HPPEF and is a

truly significant finding since it virtually completes RPE specification in our HESC-RPE. Our Shef-1 HESC-RPE have always been Pax6 positive until transplanted into the subretinal space of the RCS rat where they lose Pax6. However the additional finding of absence of Pax6 on pathclear-BME surfaces was a surprise as it is the our first evidence of Pax6 downregulation in vitro. This downregulation of Pax6 is unexplained and will need further characterisation of pathclear-BME. Although the manufacturer, Trevigen, states their product is identical to standard matrigel, barring purification and sterilisation, it may be these latter processes that are responsible. Since sterilisation of a protein product might have included filtration, one can postulate that the purification process used by Trevigen. may possibly have removed impurities which in turn permitted better polymerisation and improved interaction of HESC-RPE with the matrix. It is reported that loss of interaction with ECM can upregulate Pax6 in RPE (Nabeshima et al. 2013) which supports my speculation.

The final table below Table 10-3 outlines the main differences between regular polyester filter and HPPEF, the higher porosity filter from Sterlitech.

	Standard Polyester Filter (Transwell)	**High Porosity Polyester Filter (Sterlitech)**
Pore density (pores/cm²)	4×10^6	1×10^8
Water (Hydraulic) conductance	2.82×10^{-9} (calculated)	8.02×10^{-8} (measured)
Support for HES-RPE differentiation	Excellent	Excellent
Handling	Easy	Easy but tears due to mechanical stress are possible. Care is advised.
Cell visibility (transmitted light)	Fair. Non-pigmented cells can be difficult to visualise.	Poor. Pigmented cell silhouettes are just visible.
ICC visibility (reflected light)	Excellent	Excellent
Additional resistance to water flow (% of BrM's)	70 – 90%	Up to 3%

Table 10-3 A comparison of main characteristics of standard polyester filter versus HPPEF.

10.6 Conclusion and considerations for the future of RPE transplantation

PE filter has by far proven to be one of the most successful artificial membranes. This polymer is well established in this thesis as an RPE substrate and has been shown to support native tissue characteristics in previous studies perhaps due to its exceptional performance as a filtration material while maintaining cell adhesion. Performance of the PE filter exceeded the polyurethanes tested in this thesis and promoted good morphology when a peptide coating was used. Thus PE filter was selected for further media characterisation since ARPE-19, a widely available source of RPE, de-differentiates in standard culture medium. However I have shown that ARPE-19's phenotypic sensitivity is a tool that has enabled selection of more favourable growth media types. Pyruvate, in combination with DMEM, restored pigmentation and the expression of mature RPE cell markers such as RPE65, MerTK and CRALBP in ARPE-19 cells, and I have also demonstrated that ARPE-19 cells are capable of human POS phagocytosis while maintained in this medium, making it an excellent medium to study human RPE cell line function.

Correct phenotyping of embryonic stem cell-derived tissues is essential due to the multi-potent nature of these cells. This is particularly important when investigating new culture surfaces. Since HESC-RPE normally retain Pax6, which is also a hallmark of iris and ciliary pigment epithelium, and since phenotypic similarities and close embryologic relationships exist between RPE and pigmented ciliary epithelium this further emphasises the importance of careful examination of embryonic tissue derived-cells (Martin-Alonso et al. 1993;Ortego et al. 1996). I have shown that HESC-RPE possess several RPE characteristics when grown on polyester filter. As a follow up to our study in 2008, I have now documented that it is possible to downregulate Pax6 in vitro which identifies our Shef-1 HESC-RPE as truly RPE-like. Indeed it is anticipated that HESC will provide a very good source of differentiated RPE for the purpose of cellular therapy, provided they are seeded at high density. The reasons for the downregulation of Pax6 under pathogen-tested, purified versions of matrigel warrants further study.

Worldwide, clinical trials have begun in patients, focusing on cell suspensions, cell sheets or simply trophic factor release by the transplanted product. Masayo Takahashi and colleagues at the RIKEN Centre for Developmental Biology (Kobe, Japan) are testing the feasibility of IPS cell-based therapy for AMD. They were recently granted the go ahead by Japan's regulatory authorities to re-program skin cells into RPE cells for use as a cellular therapy in patients (Reardon and Cyranoski 2014). They recently transplanted a 1.3 x 3mm sheet of IPS cell-derived RPE into a Japanese lady in her 70's suffering with AMD (Nature; News 12th September 2014). Steven D. Schwartz and his team at the Jules Stein Eye Institute (Los Angeles, CA, USA) are part of a multi-centre Phase I/II trial conducted by Advanced Cell Technology (ACT; Marlborough, MA, USA) investigating the usefulness of subretinal injection of HESC-derived RPE suspensions utilising MA09-hRPE in both Stargardt's as well as AMD patients. They have reported the promising results of 18 patients comprisiong 9 for each condition whereby all patients bar one experienced an improvement or stabilisation in their vision compared to baseline (Schwartz et al. 2012;Schwartz et al. 2015). Non-regenerative trophic cell-based trials are also being conducted with the aim of treating AMD by release of trophic factors from the donor cells. Allen C. Ho and colleagues are involved in a phase I/II trial utilising human umbilical tissue derived cells to be injected into the subretinal space via a novel sclerotomy and choroidal fistula-based approach with the

subsequent passing of a microcatheter subretinally until it reaches its target at the patient's macula (Retina Today; October 2011; p59-61). I am delighted to say that our Shef1 HESC-derived RPE + polyester composite has now been approved for a phase I/II clinical trial at Moorfields Eye Hospital, funded by Pfizer Pharmaceuticals. This is a unique opportunity to assess the feasibility of cell-substrate composites in the human eye since we are the only clinical trial involving this type of composite at the time of writing this thesis. Our first patients will be recruited by early-mid 2015. I wish them all the best.

11

Bibliography

11 Bibliography

1. Abe, T., Yoshida, M., Tomita, H., Kano, T., Sato, M., Wada, Y., Fuse, N., Yamada, T., & Tamai, M. 2000. Auto iris pigment epithelial cell transplantation in patients with age-related macular degeneration: short-term results. *Tohoku Journal of Experimental Medicine*, 191, (1) 7-20 available from: PM:10896035

2. Abe, T., Yoshida, M., Yoshioka, Y., Wakusawa, R., Tokita-Ishikawa, Y., Seto, H., Tamai, M., & Nishida, K. 2007. Iris pigment epithelial cell transplantation for degenerative retinal diseases. *Progress in Retinal and Eye Research*, 26, (3) 302-321 available from: PM:17324604

3. Ablonczy, Z. & Crosson, C.E. 2007. VEGF modulation of retinal pigment epithelium resistance. *Experimental Eye Research*, 85, (6) 762-771 available from: PM:17915218

4. Ablonczy, Z., Dahrouj, M., Tang, P.H., Liu, Y., Sambamurti, K., Marmorstein, A.D., & Crosson, C.E. 2011. Human retinal pigment epithelium cells as functional models for the RPE in vivo. *Investigative Ophthalmology & Visual Science*, 52, (12) 8614-8620 available from: PM:21960553

5. Abramoff, M. D., Magelhaes, P. J., & Ram, S. J. Image Processing with ImageJ. Biophotonics International 11[7], 36-42. 2004.

6. Adamis, A.P., Shima, D.T., Yeo, K.T., Yeo, T.K., Brown, L.F., Berse, B., D'Amore, P.A., & Folkman, J. 1993. Synthesis and secretion of vascular permeability factor/vascular endothelial growth factor by human retinal pigment epithelial cells. *Biochemical and Biophysical Research Communications*, 193, (2) 631-638 available from: PM:8512562

7. Ahir, A., Guo, L., Hussain, A.A., & Marshall, J. 2002. Expression of metalloproteinases from human retinal pigment epithelial cells and their effects on the hydraulic conductivity of Bruch's membrane. *Investigative Ophthalmology & Visual Science*, 43, (2) 458-465 available from: PM:11818391

8. Ahmado, A., Carr, A.J., Vugler, A.A., Semo, M., Gias, C., Lawrence, J.M., Chen, L.L., Chen, F.K., Turowski, P., da, C.L., & Coffey, P.J. 2011. Induction of differentiation by pyruvate and DMEM in the human retinal pigment epithelium cell line ARPE-19. *Investigative Ophthalmology & Visual Science*, 52, (10) 7148-7159 available from: PM:21743014

9. Ahmado, A., Carr, A.-J.F., Vugler, A.A., Lawrence, J.M., da Cruz, L., & Coffey, P.J. 2009. Growth Media Related Cell Polarity and Apical/Basal VEGF Secretion in the Human Retinal Pigment Epithelium Cell Line ARPE-19. *Investigative Ophthalmology and Visual Science*, 50, (5) 3405 available from: http://abstracts.iovs.org/cgi/content/abstract/50/5/3405

10. Ahmado, A., Carr, A.-J.F., Vugler, A.A., Semo, M., Lawrence, J.M., da Cruz, L., & Coffey, P.J. 2010. Pyruvate Enhances the Differentiation Profile of the Human Retinal Pigment Epithelium Cell Line ARPE-19. *Investigative Ophthalmology and Visual Science*, 51, (5) 464 available from: http://abstracts.iovs.org/cgi/content/abstract/51/5/464

11. Ahmado, A., Vugler, A.A., Lawrence, J., & Coffey, P. 2008. Growth Media Related Pigmentation of the Cultured Human Retinal Pigment Epithelium Cell Line ARPE19. *Investigative Ophthalmology and Visual Science*, 49, (5) 489 available from: http://abstracts.iovs.org/cgi/content/abstract/49/5/489

12. Aisenbrey, S., Zhang, M., Bacher, D., Yee, J., Brunken, W.J., & Hunter, D.D. 2006. Retinal pigment epithelial cells synthesize laminins, including laminin 5, and adhere to them through alpha3- and alpha6-containing integrins. *Investigative Ophthalmology & Visual Science*, 47, (12) 5537-5544 available from: PM:17122146

13. Alattia, J.R., Kurokawa, H., & Ikura, M. 1999. Structural view of cadherin-mediated cell-cell adhesion. *Cellular and Molecular Life Science*, 55, (3) 359-367 available from: PM:10336300

14. Alfano, D., Iaccarino, I., & Stoppelli, M.P. 2006. Urokinase signaling through its receptor protects against anoikis by increasing BCL-xL expression levels.

Journal of Biological Chemistry, 281, (26) 17758-17767 available from: PM:16632475

15. Alge, C.S., Suppmann, S., Priglinger, S.G., Neubauer, A.S., May, C.A., Hauck, S., Welge-Lussen, U., Ueffing, M., & Kampik, A. 2003. Comparative proteome analysis of native differentiated and cultured dedifferentiated human RPE cells. *Investigative Ophthalmology & Visual Science*, 44, (8) 3629-3641 available from: PM:12882817

16. Algvere, P.V., Berglin, L., Gouras, P., Sheng, Y., & Kopp, E.D. 1997. Transplantation of RPE in age-related macular degeneration: observations in disciform lesions and dry RPE atrophy. *Graefes Archive for Clinical and Experimental Ophthalmology*, 235, (3) 149-158 available from: PM:9085110

17. Alizadeh, M., Wada, M., Gelfman, C.M., Handa, J.T., & Hjelmeland, L.M. 2001. Downregulation of differentiation specific gene expression by oxidative stress in ARPE-19 cells. *Investigative Ophthalmology & Visual Science*, 42, (11) 2706-2713 available from: PM:11581219

18. Amit, M., Carpenter, M.K., Inokuma, M.S., Chiu, C.P., Harris, C.P., Waknitz, M.A., Itskovitz-Eldor, J., & Thomson, J.A. 2000. Clonally derived human embryonic stem cell lines maintain pluripotency and proliferative potential for prolonged periods of culture. *Developmental Biology*, 227, (2) 271-278 available from: PM:11071754

19. Anderson, D.H., Guerin, C.J., Matsumoto, B., & Pfeffer, B.A. 1990. Identification and localization of a beta-1 receptor from the integrin family in mammalian retinal pigment epithelial cells. *Investigative Ophthalmology & Visual Science*, 31, (1) 81-93 available from: PM:2137116

20. Anderson, D.H., Johnson, L.V., & Hageman, G.S. 1995. Vitronectin receptor expression and distribution at the photoreceptor-retinal pigment epithelial interface. *The Journal of Comparative Neurology*, 360, (1) 1-16 available from: PM:7499556

21. Anderson, D.H., Radeke, M.J., Gallo, N.B., Chapin, E.A., Johnson, P.T., Curletti, C.R., Hancox, L.S., Hu, J., Ebright, J.N., Malek, G., Hauser, M.A., Rickman, C.B., Bok, D., Hageman, G.S., & Johnson, L.V. 2010. The pivotal role of the complement system in aging and age-related macular degeneration: hypothesis re-visited. *Progress in Retinal and Eye Research*, 29, (2) 95-112 available from: PM:19961953

22. Andrae, U., Singh, J., & Ziegler-Skylakakis, K. 1985. Pyruvate and related alpha-ketoacids protect mammalian cells in culture against hydrogen peroxide-induced cytotoxicity. *Toxicology Letters*, 28, (2-3) 93-98 available from: PM:4071565

23. Andrews, P.W., Benvenisty, N., Knowles, B.B., McKay, R.D., Oh, S.K., Pera, M.F., Rossant, J., & Stacey, G.N. 2010. Human ES cell lines--introduction. *In Vitro Cellular and Developmental Biology - Animal*, 46, (3-4) 167-168 available from: PM:20213278

24. Andrews, P.W., Benvenisty, N., McKay, R., Pera, M.F., Rossant, J., Semb, H., & Stacey, G.N. 2005. The International Stem Cell Initiative: toward benchmarks for human embryonic stem cell research. *Nature Biotechnology*, 23, (7) 795-797 available from: PM:16003358

25. Angst, B.D., Marcozzi, C., & Magee, A.I. 2001. The cadherin superfamily: diversity in form and function. *Journal of Cell Science*, 114, (Pt 4) 629-641 available from: PM:11171368

26. Armstrong, J., Salacinski, H.J., Mu, Q.S., Seifalian, A.M., Peel, L., Freeman, N., Holt, C.M., & Lu, J.R. 2004. Interfacial adsorption of fibrinogen and its inhibition by RGD peptide: a combined physical study. *Journal of Physics-Condensed Matter*, 16, (26) S2483-S2491 available from: ISI:000223086300024

27. Arya, D.S., Bansal, P., Ojha, S.K., Nandave, M., Mohanty, I., & Gupta, S.K. 2006. Pyruvate provides cardioprotection in the experimental model of myocardial ischemic reperfusion injury. *Life Sciences*, 79, (1) 38-44 available from: PM:16457854

28. Ashery-Padan, R. & Gruss, P. 2001. Pax6 lights-up the way for eye development. *Current Opinion in Cell Biology*, 13, (6) 706-714 available from: PM:11698186

29. Aumailley, M. & Smyth, N. 1998. The role of laminins in basement membrane function. *Journal of Anatomy*, 193 (Pt 1), 1-21 available from: PM:9758133

30. Ayache, S., Panelli, M.C., Byrne, K.M., Slezak, S., Leitman, S.F., Marincola, F.M., & Stroncek, D.F. 2006. Comparison of proteomic profiles of serum, plasma, and modified media supplements used for cell culture and expansion. *J.Transl.Med.*, 4, 40 available from: PM:17020621

31. Babich, H., Liebling, E.J., Burger, R.F., Zuckerbraun, H.L., & Schuck, A.G. 2009. Choice of DMEM, formulated with or without pyruvate, plays an important role in assessing the in vitro cytotoxicity of oxidants and prooxidant nutraceuticals. *In Vitro Cellular and Developmental Biology - Animal*, 45, (5-6) 226-233 available from: PM:19184251

32. Ban, Y. & Rizzolo, L.J. 1997. A culture model of development reveals multiple properties of RPE tight junctions. *Molecular Vision*, 3, 18 available from: PM:9479009

33. Belkin, A.M. & Stepp, M.A. 2000. Integrins as receptors for laminins. *Microscopy Research and Technique*, 51, (3) 280-301 available from: PM:11054877

34. Bellis, S.L. 2011. Advantages of RGD peptides for directing cell association with biomaterials. *Biomaterials*, 32, (18) 4205-4210 available from: PM:21515168

35. Bhutto, I.A., McLeod, D.S., Hasegawa, T., Kim, S.Y., Merges, C., Tong, P., & Lutty, G.A. 2006. Pigment epithelium-derived factor (PEDF) and vascular endothelial growth factor (VEGF) in aged human choroid and eyes with age-related macular degeneration. *Experimental Eye Research*, 82, (1) 99-110 available from: PM:16019000

36. Bhutto, I.A., Uno, K., Merges, C., Zhang, L., McLeod, D.S., & Lutty, G.A. 2008. Reduction of endogenous angiogenesis inhibitors in Bruch's membrane of the submacular region in eyes with age-related macular degeneration. *Archives of Ophthalmology*, 126, (5) 670-678 available from: PM:18474778

37. Biesemeier, A., Kreppel, F., Kochanek, S., & Schraermeyer, U. 2010. The classical pathway of melanogenesis is not essential for melanin synthesis in the adult retinal pigment epithelium. *Cell and Tissue Research*, 339, (3) 551-560 available from: PM:20140456

38. Binder, S. 2011. Scaffolds for retinal pigment epithelium (RPE) replacement therapy. *British Journal of Ophthalmology*, 95, (4) 441-442 available from: PM:21415062

39. Binder, S., Stanzel, B.V., Krebs, I., & Glittenberg, C. 2007. Transplantation of the RPE in AMD. *Progress in Retinal and Eye Research*, 26, (5) 516-554 available from: PM:17532250

40. Bird, A.C. & Marshall, J. 1986. Retinal pigment epithelial detachments in the elderly. *Transactions of the Ophthalmological Societies of the United Kingdom*, 105 (Pt 6), 674-682 available from: PM:3310342

41. Blaauwgeers, H.G., Holtkamp, G.M., Rutten, H., Witmer, A.N., Koolwijk, P., Partanen, T.A., Alitalo, K., Kroon, M.E., Kijlstra, A., van, H., V, & Schlingemann, R.O. 1999. Polarized vascular endothelial growth factor secretion by human retinal pigment epithelium and localization of vascular endothelial growth factor receptors on the inner choriocapillaris. Evidence for a trophic paracrine relation. *American Journal of Pathology*, 155, (2) 421-428 available from: PM:10433935

42. Bonilha, V.L. 2008. Age and disease-related structural changes in the retinal pigment epithelium. *Clin.Ophthalmol.*, 2, (2) 413-424 available from: PM:19668732

43. Booij, J.C., Baas, D.C., Beisekeeva, J., Gorgels, T.G., & Bergen, A.A. 2010. The dynamic nature of Bruch's membrane. *Progress in Retinal and Eye Research*, 29, (1) 1-18 available from: PM:19747980

44. Boppana, S., Scheglov, A., Geffers, R., & Tarabykin, V. 2012. Cellular retinaldehyde-binding protein (CRALBP) is a direct downstream target of transcription factor Pax6. *Biochimica et Biophysica Acta: Protein Structure and Molecular Enzymology*, 1820, (2) 151-156 available from: PM:21996446

45. Bosch, E., Horwitz, J., & Bok, D. 1993. Phagocytosis of outer segments by retinal pigment epithelium: phagosome-lysosome interaction. *Journal of Histochemistry and Cytochemistry*, 41, (2) 253-263 available from: PM:8419462

46. Boulanger, A. & Redmond, T.M. 2002. Expression and promoter activation of the Rpe65 gene in retinal pigment epithelium cell lines. *Current Eye Research*, 24, (5) 368-375 available from: PM:12434305

47. Boulton, M., Roanowska, M., & Wess, T. 2004. Ageing of the retinal pigment epithelium: implications for transplantation. *Graefes Archive for Clinical and Experimental Ophthalmology*, 242, (1) 76-84 available from: PM:14663593

48. Bridges, C.D., Alvarez, R.A., Fong, S.L., Gonzalez-Fernandez, F., Lam, D.M., & Liou, G.I. 1984. Visual cycle in the mammalian eye. Retinoid-binding proteins and the distribution of 11-cis retinoids. *Vision Research*, 24, (11) 1581-1594 available from: PM:6543481

49. Brown, K.T. & Crawford, J.M. 1967a. Intracellular recording of rapid light-evoked responses from pigment epithelium cells of the frog eye. *Vision Research*, 7, (3) 149-163 available from: PM:5613290

50. Brown, K.T. & Crawford, J.M. 1967b. Melanin and the rapid light-evoked responses from pigment epithelium cells of the frog eye. *Vision Research*, 7, (3) 165-178 available from: PM:5613291

51. Bui, B.V., Kalloniatis, M., & Vingrys, A.J. 2004. Retinal function loss after monocarboxylate transport inhibition. *Investigative Ophthalmology & Visual Science*, 45, (2) 584-593 available from: PM:14744902

52. bul-Hassan, K., Walmsley, R., Tombran-Tink, J., & Boulton, M. 2000. Regulation of tyrosinase expression and activity in cultured human retinal pigment epithelial cells. *Pigment Cell Research*, 13, (6) 436-441 available from: PM:11153695

53. Burke, J.M., Cao, F., & Irving, P.E. 2000. High levels of E-/P-cadherin: correlation with decreased apical polarity of Na/K ATPase in bovine RPE cells in situ. *Investigative Ophthalmology & Visual Science*, 41, (7) 1945-1952 available from: PM:10845621

54. Burke, J.M. & Zareba, M. 2009. Sublethal photic stress and the motility of RPE phagosomes and melanosomes. *Investigative Ophthalmology & Visual Science*, 50, (4) 1940-1947 available from: PM:19074812

55. Busk, M., Pytela, R., & Sheppard, D. 1992. Characterization of the integrin alpha v beta 6 as a fibronectin-binding protein. *Journal of Biological Chemistry*, 267, (9) 5790-5796 available from: PM:1532572

56. Cai, Q., Shi, G., Bei, J., & Wang, S. 2003. Enzymatic degradation behavior and mechanism of poly(lactide-co-glycolide) foams by trypsin. *Biomaterials*, 24, (4) 629-638 available from: PM:12437957

57. Cai, X., Conley, S.M., & Naash, M.I. 2009. RPE65: role in the visual cycle, human retinal disease, and gene therapy. *Ophthalmic Genetics*, 30, (2) 57-62 available from: PM:19373675

58. Campochiaro, P.A. & Hackett, S.F. 1993. Corneal endothelial cell matrix promotes expression of differentiated features of retinal pigmented epithelial cells: implication of laminin and basic fibroblast growth factor as active components. *Experimental Eye Research*, 57, (5) 539-547 available from: PM:8282040

59. Campochiaro, P.A., Sugg, R., Grotendorst, G., & Hjelmeland, L.M. 1989. Retinal pigment epithelial cells produce PDGF-like proteins and secrete them into their media. *Experimental Eye Research*, 49, (2) 217-227 available from: PM:2767169

60. Carlisle, E.S., Mariappan, M.R., Nelson, K.D., Thomes, B.E., Timmons, R.B., Constantinescu, A., Eberhart, R.C., & Bankey, P.E. 2000. Enhancing hepatocyte adhesion by pulsed plasma deposition and polyethylene glycol coupling. *Tissue Eng*, 6, (1) 45-52 available from: PM:10941200

61. Carr, A.J., Vugler, A., Lawrence, J., Chen, L.L., Ahmado, A., Chen, F.K., Semo, M., Gias, C., da, C.L., Moore, H.D., Walsh, J., & Coffey, P.J. 2009a. Molecular characterization and functional analysis of phagocytosis by human embryonic stem cell-derived RPE cells using a novel human retinal assay. *Molecular Vision*, 15, 283-295 available from: PM:19204785

62. Carr, A.J., Vugler, A.A., Hikita, S.T., Lawrence, J.M., Gias, C., Chen, L.L., Buchholz, D.E., Ahmado, A., Semo, M., Smart, M.J., Hasan, S., da, C.L., Johnson, L.V., Clegg, D.O., & Coffey, P.J. 2009b. Protective effects of human iPS-derived retinal pigment epithelium cell transplantation in the retinal dystrophic rat. *PLoS.One.*, 4, (12) e8152 available from: PM:19997644

63. Chao, M.P., Majeti, R., & Weissman, I.L. 2012. Programmed cell removal: a new obstacle in the road to developing cancer. *Nature Reviews: Cancer*, 12, (1) 58-67 available from: PM:22158022

64. Chong, N.H., Keonin, J., Luthert, P.J., Frennesson, C.I., Weingeist, D.M., Wolf, R.L., Mullins, R.F., & Hageman, G.S. 2005. Decreased thickness and integrity of the macular elastic layer of Bruch's membrane correspond to the distribution of lesions associated with age-related macular degeneration. *American Journal of Pathology*, 166, (1) 241-251 available from: PM:15632016

65. Collier, J.H. & Segura, T. 2011. Evolving the use of peptides as components of biomaterials. *Biomaterials*, 32, (18) 4198-4204 available from: PM:21515167

66. Colognato, H. & Yurchenco, P.D. 2000. Form and function: the laminin family of heterotrimers. *Developmental Dynamics*, 218, (2) 213-234 available from: PM:10842354

67. Crabb, J.W., Nie, Z., Chen, Y., Hulmes, J.D., West, K.A., Kapron, J.T., Ruuska, S.E., Noy, N., & Saari, J.C. 1998. Cellular retinaldehyde-binding protein ligand interactions. Gln-210 and Lys-221 are in the retinoid binding pocket. *Journal of Biological Chemistry*, 273, (33) 20712-20720 available from: PM:9694813

68. Crafoord, S., Algvere, P.V., Kopp, E.D., & Seregard, S. 2000. Cyclosporine treatment of RPE allografts in the rabbit subretinal space. *Acta Ophthalmologica Scandinavica*, 78, (2) 122-129 available from: PM:10794242

69. Crafoord, S., Algvere, P.V., Seregard, S., & Kopp, E.D. 1999. Long-term outcome of RPE allografts to the subretinal space of rabbits. *Acta Ophthalmologica Scandinavica*, 77, (3) 247-254 available from: PM:10406140

70. Cunha-Vaz, J.G. 1976. The blood-retinal barriers. *Documenta Ophthalmologica*, 41, (2) 287-327 available from: PM:1009819

71. D'Cruz, P.M., Yasumura, D., Weir, J., Matthes, M.T., Abderrahim, H., LaVail, M.M., & Vollrath, D. 2000. Mutation of the receptor tyrosine kinase gene Mertk in the retinal dystrophic RCS rat. *Human Molecular Genetics*, 9, (4) 645-651 available from: PM:10699188

72. da Cruz, L., Chen, F.K., Ahmado, A., Greenwood, J., & Coffey, P. 2007. RPE transplantation and its role in retinal disease. *Progress in Retinal and Eye Research*, 26, (6) 598-635 available from: PM:17920328

73. Daniele, L.L., Sauer, B., Gallagher, S.M., Pugh, E.N., Jr., & Philp, N.J. 2008. Altered visual function in monocarboxylate transporter 3 (Slc16a8) knockout mice. *American Journal of Physiology - Cell Physiology*, 295, (2) C451-C457 available from: PM:18524945

74. Das, A., Frank, R.N., Zhang, N.L., & Turczyn, T.J. 1990. Ultrastructural localization of extracellular matrix components in human retinal vessels and

Bruch's membrane. *Archives of Ophthalmology*, 108, (3) 421-429 available from: PM:2310346

75. Das, U.N. 2006a. Is pyruvate an endogenous anti-inflammatory molecule? *Nutrition*, 22, (9) 965-972 available from: PM:16814517

76. Das, U.N. 2006b. Pyruvate is an endogenous anti-inflammatory and anti-oxidant molecule. *Med.Sci.Monit.*, 12, (5) RA79-RA84 available from: PM:16641887

77. Davis, A.A., Bernstein, P.S., Bok, D., Turner, J., Nachtigal, M., & Hunt, R.C. 1995. A human retinal pigment epithelial cell line that retains epithelial characteristics after prolonged culture. *Investigative Ophthalmology & Visual Science*, 36, (5) 955-964 available from: PM:7706045

78. de Rham, C. & Villard, J. 2014. Potential and limitation of HLA-based banking of human pluripotent stem cells for cell therapy. *J.Immunol.Res.*, 2014, 518135 available from: PM:25126584

79. Del Priore, L.V., Tezel, T.H., & Kaplan, H.J. 2004. Survival of allogeneic porcine retinal pigment epithelial sheets after subretinal transplantation. *Investigative Ophthalmology & Visual Science*, 45, (3) 985-992 available from: PM:14985321

80. Del Priore, L.V., Tezel, T.H., & Kaplan, H.J. 2006. Maculoplasty for age-related macular degeneration: reengineering Bruch's membrane and the human macula. *Progress in Retinal and Eye Research*, 25, (6) 539-562 available from: PM:17071125

81. Desagher, S., Glowinski, J., & Premont, J. 1997. Pyruvate protects neurons against hydrogen peroxide-induced toxicity. *Journal of Neuroscience*, 17, (23) 9060-9067 available from: PM:9364052

82. Dieudonne, S.C., La Heij, E.C., Diederen, R.M., Kessels, A.G., Liem, A.T., Kijlstra, A., & Hendrikse, F. 2007. Balance of vascular endothelial growth factor and pigment epithelial growth factor prior to development of proliferative

vitreoretinopathy. *Ophthalmic Research*, 39, (3) 148-154 available from: PM:17534114

83. Draper, J.S., Pigott, C., Thomson, J.A., & Andrews, P.W. 2002. Surface antigens of human embryonic stem cells: changes upon differentiation in culture. *Journal of Anatomy*, 200, (Pt 3) 249-258 available from: PM:12033729

84. Dryden, I., Taylor, C., & Faghihi, M. 1999. Size Analysis of Nearly Regular Delaunay Triangulations. *Methodology and Computing in Applied Probability*, 1, (1) 97-117 available from: http://dx.doi.org/10.1023/A%3A1010064208174

85. Dua, H.S., Watson, N.J., Mathur, R.M., & Forrester, J.V. 1993. Corneal epithelial cell migration in humans: 'hurricane and blizzard keratopathy'. *Eye (Lond)*, 7 (Pt 1), 53-58 available from: PM:8325424

86. Dunn, K.C., otaki-Keen, A.E., Putkey, F.R., & Hjelmeland, L.M. 1996. ARPE-19, a human retinal pigment epithelial cell line with differentiated properties. *Experimental Eye Research*, 62, (2) 155-169 available from: PM:8698076

87. Elices, M.J., Urry, L.A., & Hemler, M.E. 1991. Receptor functions for the integrin VLA-3: fibronectin, collagen, and laminin binding are differentially influenced by Arg-Gly-Asp peptide and by divalent cations. *Journal of Cell Biology*, 112, (1) 169-181 available from: PM:1986004

88. Engelhardt, M., Tosha, C., Lopes, V.S., Chen, B., Nguyen, L., Nusinowitz, S., & Williams, D.S. 2012. Functional and morphological analysis of the subretinal injection of retinal pigment epithelium cells. *Visual Neuroscience*, 29, (2) 83-93 available from: PM:22391151

89. Eurell, T.E., Brown, D.R., Gerding, P.A., & Hamor, R.E. 2003. Alginate as a new biomaterial for the growth of porcine retinal pigment epithelium. *Vet.Ophthalmol.*, 6, (3) 237-243 available from: PM:12950655

90. Falk, T., Congrove, N.R., Zhang, S., McCourt, A.D., Sherman, S.J., & McKay, B.S. 2012. PEDF and VEGF-A output from human retinal pigment epithelial

cells grown on novel microcarriers. *Journal of Biomedicine and Biotechnology*, 2012, 278932 available from: PM:22547925

91. Fang, I.M., Yang, C.H., Yang, C.M., & Chen, M.S. 2009. Overexpression of integrin alpha6 and beta4 enhances adhesion and proliferation of human retinal pigment epithelial cells on layers of porcine Bruch's membrane. *Experimental Eye Research*, 88, (1) 12-21 available from: PM:18955047

92. Feeney-Burns, L. & Eldred, G.E. 1983. The fate of the phagosome: conversion to 'age pigment' and impact in human retinal pigment epithelium. *Transactions of the Ophthalmological Societies of the United Kingdom*, 103 (Pt 4), 416-421 available from: PM:6589859

93. Finnemann, S.C., Bonilha, V.L., Marmorstein, A.D., & Rodriguez-Boulan, E. 1997. Phagocytosis of rod outer segments by retinal pigment epithelial cells requires alpha(v)beta5 integrin for binding but not for internalization. *Proceedings of the National Academy of Sciences of the USA*, 94, (24) 12932-12937 available from: PM:9371778

94. Finnemann, S.C. & Rodriguez-Boulan, E. 1999. Macrophage and retinal pigment epithelium phagocytosis: apoptotic cells and photoreceptors compete for alphavbeta3 and alphavbeta5 integrins, and protein kinase C regulates alphavbeta5 binding and cytoskeletal linkage. *Journal of Experimental Medicine*, 190, (6) 861-874 available from: PM:10499924

95. Foster, W.J., Fok, P., & Chou, T. 2007. Nutrient Diffusion Through Subretinal Implants. *ARVO Meeting Abstracts*, 48, (5) 653 available from: http://abstracts.iovs.org/cgi/content/abstract/48/5/653

96. Francis, M.K., Appel, S., Meyer, C., Balin, S.J., Balin, A.K., & Cristofalo, V.J. 2004. Loss of EPC-1/PEDF expression during skin aging in vivo. *J.Invest Dermatol.*, 122, (5) 1096-1105 available from: PM:15140209

97. Frenzel, J., Richter, J., & Eschrich, K. 2005. Pyruvate protects glucose-deprived Muller cells from nitric oxide-induced oxidative stress by radical scavenging. *Glia*, 52, (4) 276-288 available from: PM:16001426

98. Frosch, K.H., Drengk, A., Krause, P., Viereck, V., Miosge, N., Werner, C., Schild, D., Sturmer, E.K., & Sturmer, K.M. 2006. Stem cell-coated titanium implants for the partial joint resurfacing of the knee. *Biomaterials*, 27, (12) 2542-2549 available from: PM:16368134

99. Fujimura, N., Taketo, M.M., Mori, M., Korinek, V., & Kozmik, Z. 2009. Spatial and temporal regulation of Wnt/beta-catenin signaling is essential for development of the retinal pigment epithelium. *Developmental Biology*, 334, (1) 31-45 available from: PM:19596317

100. Gal, A., Li, Y., Thompson, D.A., Weir, J., Orth, U., Jacobson, S.G., pfelstedt-Sylla, E., & Vollrath, D. 2000. Mutations in MERTK, the human orthologue of the RCS rat retinal dystrophy gene, cause retinitis pigmentosa. *Nature Genetics*, 26, (3) 270-271 available from: PM:11062461

101. Gamboa, O.L., Pu, J., Townend, J., Forrester, J.V., Zhao, M., McCaig, C., & Lois, N. 2010. Electrical estimulation of retinal pigment epithelial cells. *Experimental Eye Research*, 91, (2) 195-204 available from: PM:20457155

102. Ghassemifar, R., Lai, C.M., & Rakoczy, P.E. 2006. VEGF differentially regulates transcription and translation of ZO-1alpha+ and ZO-1alpha- and mediates trans-epithelial resistance in cultured endothelial and epithelial cells. *Cell and Tissue Research*, 323, (1) 117-125 available from: PM:16163490

103. Giandomenico, A.R., Cerniglia, G.E., Biaglow, J.E., Stevens, C.W., & Koch, C.J. 1997. The importance of sodium pyruvate in assessing damage produced by hydrogen peroxide. *Free Radical Biology and Medicine*, 23, (3) 426-434 available from: PM:9214579

104. Giordano, G.G., Thomson, R.C., Ishaug, S.L., Mikos, A.G., Cumber, S., Garcia, C.A., & Lahiri-Munir, D. 1997. Retinal pigment epithelium cells cultured on synthetic biodegradable polymers. *Journal of Biomedial Materials Research*, 34, (1) 87-93 available from: PM:8978657

105. Gong, J., Sagiv, O., Cai, H., Tsang, S.H., & Del Priore, L.V. 2008. Effects of extracellular matrix and neighboring cells on induction of human embryonic

stem cells into retinal or retinal pigment epithelial progenitors. *Experimental Eye Research*, 86, (6) 957-965 available from: PM:18472095

106. Gonzalez-Mariscal, L., Chavez de, R.B., & Cereijido, M. 1984. Effect of temperature on the occluding junctions of monolayers of epithelioid cells (MDCK). *Journal of Membrane Biology*, 79, (2) 175-184 available from: PM:6748055

107. Gouras, P., Flood, M.T., & Kjeldbye, H. 1984. Transplantation of cultured human retinal cells to monkey retina. *Anais da Academia Brasileira de Ciencias*, 56, (4) 431-443 available from: PM:6534229

108. Gouras, P., Lopez, R., Kjeldbye, H., Sullivan, B., & Brittis, M. 1989. Transplantation of retinal epithelium prevents photoreceptor degeneration in the RCS rat. *Progress in Clinical and Biological Research*, 314, 659-671 available from: PM:2608683

109. Grant, D.S., Tashiro, K., Segui-Real, B., Yamada, Y., Martin, G.R., & Kleinman, H.K. 1989. Two different laminin domains mediate the differentiation of human endothelial cells into capillary-like structures in vitro. *Cell*, 58, (5) 933-943 available from: PM:2528412

110. Graw, J. 2010. Eye development. *Current Topics in Developmental Biology*, 90, 343-386 available from: PM:20691855

111. Guerrin, M., Moukadiri, H., Chollet, P., Moro, F., Dutt, K., Malecaze, F., & Plouet, J. 1995. Vasculotropin/vascular endothelial growth factor is an autocrine growth factor for human retinal pigment epithelial cells cultured in vitro. *Journal of Cell Physiology*, 164, (2) 385-394 available from: PM:7622584

112. Gullapalli, V.K., Sugino, I.K., Van, P.Y., Shah, S., & Zarbin, M.A. 2004. Retinal pigment epithelium resurfacing of aged submacular human Bruch's membrane. *Transactions of the American Ophthalmological Society*, 102, 123-137 available from: PM:15747751

113. Gullapalli, V.K., Sugino, I.K., Van, P.Y., Shah, S., & Zarbin, M.A. 2005. Impaired RPE survival on aged submacular human Bruch's membrane. *Experimental Eye Research*, 80, (2) 235-248 available from: PM:15670802

114. Gullapalli, V.K., Sugino, I.K., & Zarbin, M.A. 2008. Culture-induced increase in alpha integrin subunit expression in retinal pigment epithelium is important for improved resurfacing of aged human Bruch's membrane. *Experimental Eye Research*, 86, (2) 189-200 available from: PM:18062966

115. Guymer, R., Luthert, P., & Bird, A. 1999. Changes in Bruch's membrane and related structures with age. *Progress in Retinal and Eye Research*, 18, (1) 59-90 available from: PM:9920499

116. Hadlock, T., Singh, S., Vacanti, J.P., & McLaughlin, B.J. 1999. Ocular cell monolayers cultured on biodegradable substrates. *Tissue Eng*, 5, (3) 187-196 available from: PM:10434067

117. Hageman, G.S., Luthert, P.J., Victor Chong, N.H., Johnson, L.V., Anderson, D.H., & Mullins, R.F. 2001. An integrated hypothesis that considers drusen as biomarkers of immune-mediated processes at the RPE-Bruch's membrane interface in aging and age-related macular degeneration. *Progress in Retinal and Eye Research*, 20, (6) 705-732 available from: PM:11587915

118. Halestrap, A.P. 1975. The mitochondrial pyruvate carrier. Kinetics and specificity for substrates and inhibitors. *Biochemical Journal*, 148, (1) 85-96 available from: PM:1156402

119. Halestrap, A.P. & Denton, R.M. 1975. The specificity and metabolic implications of the inhibition of pyruvate transport in isolated mitochondria and intact tissue preparations by alpha-Cyano-4-hydroxycinnamate and related compounds. *Biochemical Journal*, 148, (1) 97-106 available from: PM:1171687

120. Hammarberg, H., Piehl, F., Cullheim, S., Fjell, J., Hokfelt, T., & Fried, K. 1996. GDNF mRNA in Schwann cells and DRG satellite cells after chronic sciatic nerve injury. *Neuroreport*, 7, (4) 857-860 available from: PM:8724660

121. Hao, W. & Fong, H.K. 1999. The endogenous chromophore of retinal G protein-coupled receptor opsin from the pigment epithelium. *Journal of Biological Chemistry*, 274, (10) 6085-6090 available from: PM:10037690

122. Harbers, G.M. & Healy, K.E. 2005. The effect of ligand type and density on osteoblast adhesion, proliferation, and matrix mineralization. *"Journal of Biomedical Materials Research, Part A"*, 75, (4) 855-869 available from: PM:16121356

123. Haruta, M., Sasai, Y., Kawasaki, H., Amemiya, K., Ooto, S., Kitada, M., Suemori, H., Nakatsuji, N., Ide, C., Honda, Y., & Takahashi, M. 2004. In vitro and in vivo characterization of pigment epithelial cells differentiated from primate embryonic stem cells. *Investigative Ophthalmology & Visual Science*, 45, (3) 1020-1025 available from: PM:14985325

124. Hasirci, V. & Pepe-Mooney, B.J. 2012. Understanding the cell behavior on nano-/micro-patterned surfaces. *Nanomedicine.(Lond)*, 7, (9) 1375-1389 available from: PM:22812706

125. Hayashi, Y., Emoto, T., Futaki, S., & Sekiguchi, K. 2004. Establishment and characterization of a parietal endoderm-like cell line derived from Engelbreth-Holm-Swarm tumor (EHSPEL), a possible resource for an engineered basement membrane matrix. *Matrix Biology*, 23, (1) 47-62 available from: PM:15172037

126. Hayflick, L. 1965. THE LIMITED IN VITRO LIFETIME OF HUMAN DIPLOID CELL STRAINS. *Experimental Cell Research*, 37, 614-636 available from: PM:14315085

127. Hayflick, L. & Moorhead, P.S. 1961. The serial cultivation of human diploid cell strains. *Experimental Cell Research*, 25, 585-621 available from: PM:13905658

128. Hegde, K.R. & Varma, S.D. 2008. Prevention of oxidative stress to the retina by pyruvate. A preliminary report. *Ophthalmologica*, 222, (3) 194-198 available from: PM:18497529

129. Heimsath, E.G., Jr., Unda, R., Vidro, E., Muniz, A., Villazana-Espinoza, E.T., & Tsin, A. 2006. ARPE-19 cell growth and cell functions in euglycemic culture media. *Current Eye Research*, 31, (12) 1073-1080 available from: PM:17169846

130. Hoffmann, S., He, S., Jin, M., Ehren, M., Wiedemann, P., Ryan, S.J., & Hinton, D.R. 2005. A selective cyclic integrin antagonist blocks the integrin receptors alphavbeta3 and alphavbeta5 and inhibits retinal pigment epithelium cell attachment, migration and invasion. *BMC.Ophthalmol.*, 5, 16 available from: PM:15987521

131. Hollborn, M., Tenckhoff, S., Seifert, M., Kohler, S., Wiedemann, P., Bringmann, A., & Kohen, L. 2006. Human retinal epithelium produces and responds to placenta growth factor. *Graefes Archive for Clinical and Experimental Ophthalmology*, 244, (6) 732-741 available from: PM:16341703

132. Hosokawa, H., Ninomiya, H., Kitamura, Y., Fujiwara, K., & Masaki, T. 2002. Vascular endothelial cells that express dystroglycan are involved in angiogenesis. *Journal of Cell Science*, 115, (Pt 7) 1487-1496 available from: PM:11896196

133. Hu, D.N., Simon, J.D., & Sarna, T. 2008. Role of ocular melanin in ophthalmic physiology and pathology. *Photochemistry and Photobiology*, 84, (3) 639-644 available from: PM:18346089

134. Hu, J. & Bok, D. 2001. A cell culture medium that supports the differentiation of human retinal pigment epithelium into functionally polarized monolayers. *Molecular Vision*, 7, 14-19 available from: PM:11182021

135. Hu, Y., Liu, L., Lu, B., Zhu, D., Ribeiro, R., Diniz, B., Thomas, P.B., Ahuja, A.K., Hinton, D.R., Tai, Y.C., Hikita, S.T., Johnson, L.V., Clegg, D.O., Thomas, B.B., & Humayun, M.S. 2012. A novel approach for subretinal implantation of ultrathin substrates containing stem cell-derived retinal pigment epithelium monolayer. *Ophthalmic Research*, 48, (4) 186-191 available from: PM:22868580

136. Huang, J.D., Presley, J.B., Chimento, M.F., Curcio, C.A., & Johnson, M. 2007. Age-related changes in human macular Bruch's membrane as seen by quick-freeze/deep-etch. *Experimental Eye Research*, 85, (2) 202-218 available from: PM:17586493

137. HUCKABEE, W.E. 1956. Control of concentration gradients of pyruvate and lactate across cell membranes in blood. *J.Appl.Physiol*, 9, (2) 163-170 available from: PM:13376422

138. HUCKABEE, W.E. 1958a. Relationships of pyruvate and lactate during anaerobic metabolism. I. Effects of infusion of pyruvate or glucose and of hyperventilation. *J.Clin.Invest*, 37, (2) 244-254 available from: PM:13513755

139. HUCKABEE, W.E. 1958b. Relationships of pyruvate and lactate during anaerobic metabolism. II. Exercise and formation of O-debt. *J.Clin.Invest*, 37, (2) 255-263 available from: PM:13513756

140. HUCKABEE, W.E. 1958c. Relationships of pyruvate and lactate during anaerobic metabolism. III. Effect of breathing low-oxygen gases. *J.Clin.Invest*, 37, (2) 264-271 available from: PM:13513757

141. Hunt, R.C. 1994. Intermediate Filaments and Other Cytoskeletal Structures in Retinal-Pigment Epithelial-Cells. *Progress in Retinal and Eye Research*, 13, (1) 125-145 available from: ISI:A1994NK58100006

142. Hunt, R.C. & Davis, A.A. 1990. Altered expression of keratin and vimentin in human retinal pigment epithelial cells in vivo and in vitro. *Journal of Cell Physiology*, 145, (2) 187-199 available from: PM:1700982

143. Hynes, R.O. 2002. Integrins: bidirectional, allosteric signaling machines. *Cell*, 110, (6) 673-687 available from: PM:12297042

144. Iida, J., Skubitz, A.P., Furcht, L.T., Wayner, E.A., & McCarthy, J.B. 1992. Coordinate role for cell surface chondroitin sulfate proteoglycan and alpha 4 beta 1 integrin in mediating melanoma cell adhesion to fibronectin. *Journal of Cell Biology*, 118, (2) 431-444 available from: PM:1629241

145. Imoto, Y., Ohguro, N., Yoshida, A., Tsujikawa, M., Inoue, Y., & Tano, Y. 2003. Effects of RGD peptides on cells derived from the human eye. *Japanese Journal of Ophthalmology*, 47, (5) 444-453 available from: PM:12967858

146. Ishigooka, H., otaki-Keen, A.E., & Hjelmeland, L.M. 1992. Subcellular localization of bFGF in human retinal pigment epithelium in vitro. *Experimental Eye Research*, 55, (2) 203-214 available from: PM:1426056

147. Janssen, J.J., Kuhlmann, E.D., van Vugt, A.H., Winkens, H.J., Janssen, B.P., Deutman, A.F., & Driessen, C.A. 2000. Retinoic acid delays transcription of human retinal pigment neuroepithelium marker genes in ARPE-19 cells. *Neuroreport*, 11, (7) 1571-1579 available from: PM:10841379

148. Jeffery, G. 1998. The retinal pigment epithelium as a developmental regulator of the neural retina. *Eye (Lond)*, 12 (Pt 3b), 499-503 available from: PM:9775209

149. Jeong, J., Han, I., Lim, Y., Kim, J., Park, I., Woods, A., Couchman, J.R., & Oh, E.S. 2001. Rat embryo fibroblasts require both the cell-binding and the heparin-binding domains of fibronectin for survival. *Biochemical Journal*, 356, (Pt 2) 531-537 available from: PM:11368782

150. Jin, Y.J., Park, I., Hong, I.K., Byun, H.J., Choi, J., Kim, Y.M., & Lee, H. 2011. Fibronectin and vitronectin induce AP-1-mediated matrix metalloproteinase-9 expression through integrin alpha(5)beta(1)/alpha(v)beta(3)-dependent Akt, ERK and JNK signaling pathways in human umbilical vein endothelial cells. *Cell Signal.*, 23, (1) 125-134 available from: PM:20816750

151. Jun, H.W. & West, J. 2004. Development of a YIGSR-peptide-modified polyurethaneurea to enhance endothelialization. *J.Biomater.Sci.Polym.Ed*, 15, (1) 73-94 available from: PM:15027844

152. Jun, H.W. & West, J.L. 2005. Modification of polyurethaneurea with PEG and YIGSR peptide to enhance endothelialization without platelet adhesion. *"Journal of Biomedical Materials Research, Part B: Applied Biomaterials"*, 72, (1) 131-139 available from: PM:15389489

153. Kaibara, M., Iwata, H., Wada, H., Kawamoto, Y., Iwaki, M., & Suzuki, Y. 1996. Promotion and control of selective adhesion and proliferation of endothelial cells on polymer surface by carbon deposition. *Journal of Biomedial Materials Research*, 31, (3) 429-435 available from: PM:8806070

154. Kannan, R., Sreekumar, P.G., & Hinton, D.R. 2011. VEGF and PEDF secretion in ARPE-19 and fhRPE cells. *Investigative Ophthalmology & Visual Science*, 52, (12) 9047 available from: PM:22104197

155. Kannan, R., Zhang, N., Sreekumar, P.G., Spee, C.K., Rodriguez, A., Barron, E., & Hinton, D.R. 2006. Stimulation of apical and basolateral VEGF-A and VEGF-C secretion by oxidative stress in polarized retinal pigment epithelial cells. *Mol.Vis.*, 12, 1649-1659 available from: PM:17200665

156. Kannan, R.Y., Salacinski, H.J., Butler, P.E., Hamilton, G., & Seifalian, A.M. 2005. Current status of prosthetic bypass grafts: a review. *"Journal of Biomedical Materials Research, Part B: Applied Biomaterials"*, 74, (1) 570-581 available from: PM:15889440

157. Kannan, R.Y., Sales, K.M., Salacinski, H.J., Butler, P.E., & Seifalian, A.M. 2004. Endothelialisation of poly (carbonate-siloxane-urea) urethane. *Medical Journal of Malaysia*, 59 Suppl B, 107-108 available from: PM:15468841

158. Kanuga, N., Winton, H.L., Beauchene, L., Koman, A., Zerbib, A., Halford, S., Couraud, P.O., Keegan, D., Coffey, P., Lund, R.D., Adamson, P., & Greenwood, J. 2002. Characterization of genetically modified human retinal pigment epithelial cells developed for in vitro and transplantation studies. *Investigative Ophthalmology & Visual Science*, 43, (2) 546-555 available from: PM:11818403

159. Kawasaki, H., Suemori, H., Mizuseki, K., Watanabe, K., Urano, F., Ichinose, H., Haruta, M., Takahashi, M., Yoshikawa, K., Nishikawa, S., Nakatsuji, N., & Sasai, Y. 2002. Generation of dopaminergic neurons and pigmented epithelia from primate ES cells by stromal cell-derived inducing activity. *Proceedings of the National Academy of Sciences of the USA*, 99, (3) 1580-1585 available from: PM:11818560

160. Kearns, V., Mistry, A., Mason, S., Krishna, Y., Sheridan, C., Short, R., & Williams, R.L. 2012. Plasma polymer coatings to aid retinal pigment epithelial growth for transplantation in the treatment of age related macular degeneration. *Journal of Materials Science: Materials in Medicine*, 23, (8) 2013-2021 available from: PM:22618272

161. Keegan, D.J., Kenna, P., Humphries, M.M., Humphries, P., Flitcroft, D.I., Coffey, P.J., Lund, R.D., & Lawrence, J.M. 2003. Transplantation of syngeneic Schwann cells to the retina of the rhodopsin knockout (rho(-/-)) mouse. *Investigative Ophthalmology & Visual Science*, 44, (8) 3526-3532 available from: PM:12882803

162. Kennedy, B.G. & Lever, J.E. 1984. Regulation of Na+,K+-ATPase activity in MDCK kidney epithelial cell cultures: role of growth state, cyclic AMP, and chemical inducers of dome formation and differentiation. *Journal of Cell Physiology*, 121, (1) 51-63 available from: PM:6090479

163. Kita, M., Negi, A., & Marmor, M.F. 1992. Lowering the calcium concentration in the subretinal space in vivo loosens retinal adhesion. *Investigative Ophthalmology & Visual Science*, 33, (1) 23-29 available from: PM:1730543

164. Kivela, T. & Uusitalo, M. 1998. Structure, development and function of cytoskeletal elements in non-neuronal cells of the human eye. *Progress in Retinal and Eye Research*, 17, (3) 385-428 available from: PM:9695798

165. Klaver, C.C., Wolfs, R.C., Vingerling, J.R., Hofman, A., & de Jong, P.T. 1998. Age-specific prevalence and causes of blindness and visual impairment in an older population: the Rotterdam Study. *Archives of Ophthalmology*, 116, (5) 653-658 available from: PM:9596502

166. Kleinman, H.K., McGarvey, M.L., Hassell, J.R., Star, V.L., Cannon, F.B., Laurie, G.W., & Martin, G.R. 1986. Basement membrane complexes with biological activity. *Biochemistry*, 25, (2) 312-318 available from: PM:2937447

167. Klimanskaya, I., Chung, Y., Becker, S., Lu, S.J., & Lanza, R. 2006. Human embryonic stem cell lines derived from single blastomeres. *Nature*, 444, (7118) 481-485 available from: PM:16929302

168. Klimanskaya, I., Hipp, J., Rezai, K.A., West, M., Atala, A., & Lanza, R. 2004. Derivation and comparative assessment of retinal pigment epithelium from human embryonic stem cells using transcriptomics. *Cloning and Stem Cells*, 6, (3) 217-245 available from: PM:15671670

169. Kojima, T., Nakahama, K., Yamamoto, K., Uematsu, H., & Morita, I. 2006. Age- and cell cycle-dependent changes in EPC-1/PEDF promoter activity in human diploid fibroblast-like (HDF) cells. *Mol.Cell Biochem.*, 293, (1-2) 63-69 available from: PM:16896539

170. Krebs, H.A. 1940. The citric acid cycle and the Szent-Gyorgyi cycle in pigeon breast muscle. *Biochemical Journal*, 34, (5) 775-779 available from: PM:16747218

171. Krijgsman, B., Seifalian, A.M., Salacinski, H.J., Tai, N.R., Punshon, G., Fuller, B.J., & Hamilton, G. 2002. An assessment of covalent grafting of RGD peptides to the surface of a compliant poly(carbonate-urea)urethane vascular conduit versus conventional biological coatings: its role in enhancing cellular retention. *Tissue Eng*, 8, (4) 673-680 available from: PM:12202006

172. Krishna, Y., Sheridan, C., Kent, D., Kearns, V., Grierson, I., & Williams, R. 2011. Expanded polytetrafluoroethylene as a substrate for retinal pigment epithelial cell growth and transplantation in age-related macular degeneration. *British Journal of Ophthalmology*, 95, (4) 569-573 available from: PM:21317216

173. Krishna, Y., Sheridan, C.M., Kent, D.L., Grierson, I., & Williams, R.L. 2007. Polydimethylsiloxane as a substrate for retinal pigment epithelial cell growth. *"Journal of Biomedical Materials Research, Part A"*, 80, (3) 669-678 available from: PM:17058209

174. Krugluger, W., Seidel, S., Steindl, K., & Binder, S. 2007. Epidermal growth factor inhibits glycogen synthase kinase-3 (GSK-3) and beta-catenin transcription in cultured ARPE-19 cells. *Graefes Archive for Clinical and Experimental Ophthalmology*, 245, (10) 1543-1548 available from: PM:17690899

175. Kurtz, M.J. & Edwards, R.B. 1991. Influence of bicarbonate and insulin on pigment synthesis by cultured adult human retinal pigment epithelial cells. *Experimental Eye Research*, 53, (5) 681-684 available from: PM:1743267

176. Kurtz, S.M., MacDonald, D., Ianuzzi, A., van, O.A., Isaza, J., Ross, E.R., & Regan, J. 2009. The natural history of polyethylene oxidation in total disc replacement. *Spine (Phila Pa 1976.)*, 34, (22) 2369-2377 available from: PM:19789469

177. Lavik, E., Teng, Y.D., Snyder, E., & Langer, R. 2002. Seeding neural stem cells on scaffolds of PGA, PLA, and their copolymers. *Methods in Molecular Biology*, 198, 89-97 available from: PM:11951644

178. Lavik, E.B., Hrkach, J.S., Lotan, N., Nazarov, R., & Langer, R. 2001. A simple synthetic route to the formation of a block copolymer of poly(lactic-co-glycolic acid) and polylysine for the fabrication of functionalized, degradable structures for biomedical applications. *Journal of Biomedial Materials Research*, 58, (3) 291-294 available from: PM:11319743

179. Lawrence, J.M., Keegan, D.J., Muir, E.M., Coffey, P.J., Rogers, J.H., Wilby, M.J., Fawcett, J.W., & Lund, R.D. 2004. Transplantation of Schwann cell line clones secreting GDNF or BDNF into the retinas of dystrophic Royal College of Surgeons rats. *Investigative Ophthalmology & Visual Science*, 45, (1) 267-274 available from: PM:14691183

180. Lawrence, J.M., Sauve, Y., Keegan, D.J., Coffey, P.J., Hetherington, L., Girman, S., Whiteley, S.J., Kwan, A.S., Pheby, T., & Lund, R.D. 2000. Schwann cell grafting into the retina of the dystrophic RCS rat limits functional deterioration. Royal College of Surgeons. *Investigative Ophthalmology & Visual Science*, 41, (2) 518-528 available from: PM:10670484

181. Lee, C.J., Fishman, H.A., & Bent, S.F. 2007. Spatial cues for the enhancement of retinal pigment epithelial cell function in potential transplants. *Biomaterials*, 28, (13) 2192-2201 available from: PM:17267030

182. Lee, C.J., Vroom, J.A., Fishman, H.A., & Bent, S.F. 2006. Determination of human lens capsule permeability and its feasibility as a replacement for Bruch's membrane. *Biomaterials*, 27, (8) 1670-1678 available from: PM:16199085

183. Lee, J.O., Bankston, L.A., Arnaout, M.A., & Liddington, R.C. 1995. Two conformations of the integrin A-domain (I-domain): a pathway for activation? *Structure.*, 3, (12) 1333-1340 available from: PM:8747460

184. Li, R., Maminishkis, A., Zahn, G., Vossmeyer, D., & Miller, S.S. 2009. Integrin alpha5beta1 mediates attachment, migration, and proliferation in human retinal pigment epithelium: relevance for proliferative retinal disease. *Investigative Ophthalmology & Visual Science*, 50, (12) 5988-5996 available from: PM:19608542

185. Li, X., Tang, K., Xie, B., Li, S., & Rozanski, G.J. 2008. Regulation of Kv4 channel expression in failing rat heart by the thioredoxin system. *Am.J.Physiol Heart Circ.Physiol*, 295, (1) H416-H424 available from: PM:18515646

186. Liao, Y.F., Gotwals, P.J., Koteliansky, V.E., Sheppard, D., & Van De, W.L. 2002. The EIIIA segment of fibronectin is a ligand for integrins alpha 9beta 1 and alpha 4beta 1 providing a novel mechanism for regulating cell adhesion by alternative splicing. *Journal of Biological Chemistry*, 277, (17) 14467-14474 available from: PM:11839764

187. Linsenmeier, R.A. & Steinberg, R.H. 1983. A light-evoked interaction of apical and basal membranes of retinal pigment epithelium: c-wave and light peak. *Journal of Neurophysiology*, 50, (1) 136-147 available from: PM:6875643

188. Liu, Y., Geng, L., & Suo, Z. 2009. Differentiation effect of pyruvate and uridine on cultured U937-rho degrees cells. *Ultrastructural Pathology*, 33, (4) 160-164 available from: PM:19728232

189. Long, K.O., Fisher, S.K., Fariss, R.N., & Anderson, D.H. 1986. Disc shedding and autophagy in the cone-dominant ground squirrel retina. *Experimental Eye Research*, 43, (2) 193-205 available from: PM:3758219

190. Lopes, V.S., Wasmeier, C., Seabra, M.C., & Futter, C.E. 2007. Melanosome maturation defect in Rab38-deficient retinal pigment epithelium results in instability of immature melanosomes during transient melanogenesis. *Molecular Biology of the Cell*, 18, (10) 3914-3927 available from: PM:17671165

191. Lu, B., Zhu, D., Hinton, D., Humayun, M.S., & Tai, Y.C. 2012. Mesh-supported submicron parylene-C membranes for culturing retinal pigment epithelial cells. *Biomed.Microdevices.*, 14, (4) 659-667 available from: PM:22391881

192. Lu, J.M., Wang, X., Marin-Muller, C., Wang, H., Lin, P.H., Yao, Q., & Chen, C. 2009. Current advances in research and clinical applications of PLGA-based nanotechnology. *Expert.Rev.Mol.Diagn.*, 9, (4) 325-341 available from: PM:19435455

193. Lu, L., Garcia, C.A., & Mikos, A.G. 1999. In vitro degradation of thin poly(DL-lactic-co-glycolic acid) films. *Journal of Biomedial Materials Research*, 46, (2) 236-244 available from: PM:10380002

194. Lu, L., Peter, S.J., Lyman, M.D., Lai, H.L., Leite, S.M., Tamada, J.A., Uyama, S., Vacanti, J.P., Langer, R., & Mikos, A.G. 2000. In vitro and in vivo degradation of porous poly(DL-lactic-co-glycolic acid) foams. *Biomaterials*, 21, (18) 1837-1845 available from: PM:10919687

195. Luft, F.C. 2001. Lactic acidosis update for critical care clinicians. *Journal of the American Society of Nephrology*, 12 Suppl 17, S15-S19 available from: PM:11251027

196. Lund, R.D., Wang, S., Klimanskaya, I., Holmes, T., Ramos-Kelsey, R., Lu, B., Girman, S., Bischoff, N., Sauve, Y., & Lanza, R. 2006. Human embryonic stem cell-derived cells rescue visual function in dystrophic RCS rats. *Cloning and Stem Cells*, 8, (3) 189-199 available from: PM:17009895

197. Luo, Y., Zhuo, Y., Fukuhara, M., & Rizzolo, L.J. 2006. Effects of culture conditions on heterogeneity and the apical junctional complex of the ARPE-19 cell line. *Investigative Ophthalmology & Visual Science*, 47, (8) 3644-3655 available from: PM:16877439

198. Mahalingam, Y., Gallagher, J.T., & Couchman, J.R. 2007. Cellular adhesion responses to the heparin-binding (HepII) domain of fibronectin require heparan sulfate with specific properties. *Journal of Biological Chemistry*, 282, (5) 3221-3230 available from: PM:17130131

199. Mak, G.Z., Kavanaugh, G.M., Buschmann, M.M., Stickley, S.M., Koch, M., Goss, K.H., Waechter, H., Zuk, A., & Matlin, K.S. 2006. Regulated synthesis and functions of laminin 5 in polarized madin-darby canine kidney epithelial cells. *Molecular Biology of the Cell*, 17, (8) 3664-3677 available from: PM:16775009

200. Maminishkis, A., Chen, S., Jalickee, S., Banzon, T., Shi, G., Wang, F.E., Ehalt, T., Hammer, J.A., & Miller, S.S. 2006. Confluent monolayers of cultured human fetal retinal pigment epithelium exhibit morphology and physiology of native tissue. *Investigative Ophthalmology & Visual Science*, 47, (8) 3612-3624 available from: PM:16877436

201. Mann, B.K. & West, J.L. 2002. Cell adhesion peptides alter smooth muscle cell adhesion, proliferation, migration, and matrix protein synthesis on modified surfaces and in polymer scaffolds. *Journal of Biomedial Materials Research*, 60, (1) 86-93 available from: PM:11835163

202. Marmorstein, A.D., Finnemann, S.C., Bonilha, V.L., & Rodriguez-Boulan, E. 1998. Morphogenesis of the retinal pigment epithelium: toward understanding retinal degenerative diseases. *Annals of the New York Academy of Sciences*, 857, 1-12 available from: PM:9917828

203. Marshall, G.E., Konstas, A.G., Reid, G.G., Edwards, J.G., & Lee, W.R. 1994. Collagens in the aged human macula. *Graefes Archive for Clinical and Experimental Ophthalmology*, 232, (3) 133-140 available from: PM:8188061

204. Martin, D.J., Warren, L.A., Gunatillake, P.A., McCarthy, S.J., Meijs, G.F., & Schindhelm, K. 2000. Polydimethylsiloxane/polyether-mixed macrodiol-based polyurethane elastomers: biostability. *Biomaterials*, 21, (10) 1021-1029 available from: PM:10768754

205. Martin-Alonso, J.M., Ghosh, S., Hernando, N., Crabb, J.W., & Coca-Prados, M. 1993. Differential expression of the cellular retinaldehyde-binding protein in bovine ciliary epithelium. *Experimental Eye Research*, 56, (6) 659-669 available from: PM:8595808

206. Martinez-Morales, J.R., Rodrigo, I., & Bovolenta, P. 2004. Eye development: a view from the retina pigmented epithelium. *Bioessays*, 26, (7) 766-777 available from: PM:15221858

207. Massia, S.P. & Hubbell, J.A. 1991. Human endothelial cell interactions with surface-coupled adhesion peptides on a nonadhesive glass substrate and two polymeric biomaterials. *Journal of Biomedial Materials Research*, 25, (2) 223-242 available from: PM:1829082

208. Massia, S.P., Rao, S.S., & Hubbell, J.A. 1993. Covalently immobilized laminin peptide Tyr-Ile-Gly-Ser-Arg (YIGSR) supports cell spreading and co-localization of the 67-kilodalton laminin receptor with alpha-actinin and vinculin. *Journal of Biological Chemistry*, 268, (11) 8053-8059 available from: PM:8463322

209. McKay, B.S. & Burke, J.M. 1994. Separation of phenotypically distinct subpopulations of cultured human retinal pigment epithelial cells. *Experimental Cell Research*, 213, (1) 85-92 available from: PM:7517370

210. McKay, B.S., Irving, P.E., Skumatz, C.M., & Burke, J.M. 1997. Cell-cell adhesion molecules and the development of an epithelial phenotype in cultured human retinal pigment epithelial cells. *Experimental Eye Research*, 65, (5) 661-671 available from: PM:9367646

211. McKechnie, N.M., Boulton, M., Robey, H.L., Savage, F.J., & Grierson, I. 1988. The cytoskeletal elements of human retinal pigment epithelium: in vitro and in vivo. *Journal of Cell Science*, 91 (Pt 2), 303-312 available from: PM:2477385

212. McLaughlin, B.J., Fan, W., Zheng, J.J., Cai, H., Del Priore, L.V., Bora, N.S., & Kaplan, H.J. 2003. Novel role for a complement regulatory protein (CD46) in retinal pigment epithelial adhesion. *Investigative Ophthalmology & Visual Science*, 44, (8) 3669-3674 available from: PM:12882822

213. Meir, A.R., Freeman, B.J., Fraser, R.D., & Fowler, S.M. 2013. Ten-year survival and clinical outcome of the AcroFlex lumbar disc replacement for the treatment of symptomatic disc degeneration. *Spine J.*, 13, (1) 13-21 available from: PM:23384880

214. Meyer, C., Notari, L., & Becerra, S.P. 2002. Mapping the type I collagen-binding site on pigment epithelium-derived factor. Implications for its antiangiogenic activity. *Journal of Biological Chemistry*, 277, (47) 45400-45407 available from: PM:12237317

215. Meyer, M., Matsuoka, I., Wetmore, C., Olson, L., & Thoenen, H. 1992. Enhanced synthesis of brain-derived neurotrophic factor in the lesioned peripheral nerve: different mechanisms are responsible for the regulation of BDNF and NGF mRNA. *Journal of Cell Biology*, 119, (1) 45-54 available from: PM:1527172

216. Miceli, M.V. & Newsome, D.A. 1996. Effects of extracellular matrix and Bruch's membrane on retinal outer segment phagocytosis by cultured human retinal pigment epithelium. *Current Eye Research*, 15, (1) 17-26 available from: PM:8631200

217. Miller, S.S., Steinberg, R.H., & Oakley, B. 1978. The electrogenic sodium pump of the frog retinal pigment epithelium. *Journal of Membrane Biology*, 44, (3-4) 259-279 available from: PM:313450

218. Miyamoto, N., de, K.Y., Normand, N., Courtois, Y., Jeanny, J.C., Benezra, D., & Behar-Cohen, F. 2008. PlGF-1 and VEGFR-1 pathway regulation of the

external epithelial hemato-ocular barrier. A model for retinal edema. *Ophthalmic Research*, 40, (3-4) 203-207 available from: PM:18421240

219. Miyamoto, T.A., Ueno, T., Iguro, Y., Yotsumoto, G., Fukumoto, Y., Nakamura, K., & Sakata, R. 2009. Taurine-mediated cardioprotection is greater when administered upon reperfusion than prior to ischemia. *Advances in Experimental Medicine and Biology*, 643, 27-36 available from: PM:19239133

220. Moiseyev, G., Chen, Y., Takahashi, Y., Wu, B.X., & Ma, J.X. 2005. RPE65 is the isomerohydrolase in the retinoid visual cycle. *Proc.Natl.Acad.Sci.U.S.A*, 102, (35) 12413-12418 available from: PM:16116091

221. Mongan, P.D., Capacchione, J., Fontana, J.L., West, S., & Bunger, R. 2001. Pyruvate improves cerebral metabolism during hemorrhagic shock. *Am.J.Physiol Heart Circ.Physiol*, 281, (2) H854-H864 available from: PM:11454591

222. Mongan, P.D., Fontana, J.L., Chen, R., & Bunger, R. 1999. Intravenous pyruvate prolongs survival during hemorrhagic shock in swine. *Am.J.Physiol*, 277, (6 Pt 2) H2253-H2263 available from: PM:10600844

223. Mooradian, D.L., McCarthy, J.B., Cameron, J.D., Skubitz, A.P., & Furcht, L.T. 1992. Rabbit corneal epithelial cells adhere to two distinct heparin-binding synthetic peptides derived from fibronectin. *Investigative Ophthalmology & Visual Science*, 33, (11) 3034-3040 available from: PM:1399408

224. Moore, D.J., Hussain, A.A., & Marshall, J. 1995. Age-related variation in the hydraulic conductivity of Bruch's membrane. *Investigative Ophthalmology & Visual Science*, 36, (7) 1290-1297 available from: PM:7775106

225. Moshiri, A., Close, J., & Reh, T.A. 2004. Retinal stem cells and regeneration. *International Journal of Developmental Biology*, 48, (8-9) 1003-1014 available from: PM:15558491

226. Mostafavi-Pour, Z., Askari, J.A., Parkinson, S.J., Parker, P.J., Ng, T.T., & Humphries, M.J. 2003. Integrin-specific signaling pathways controlling focal

adhesion formation and cell migration. *Journal of Cell Biology*, 161, (1) 155-167 available from: PM:12695503

227. Mousa, S.A., Lorelli, W., & Campochiaro, P.A. 1999. Role of hypoxia and extracellular matrix-integrin binding in the modulation of angiogenic growth factors secretion by retinal pigmented epithelial cells. *J.Cell Biochem.*, 74, (1) 135-143 available from: PM:10381270

228. Moyano, J.V., Greciano, P.G., Buschmann, M.M., Koch, M., & Matlin, K.S. 2010. Autocrine transforming growth factor-{beta}1 activation mediated by integrin {alpha}V{beta}3 regulates transcriptional expression of laminin-332 in Madin-Darby canine kidney epithelial cells. *Molecular Biology of the Cell*, 21, (21) 3654-3668 available from: PM:20844080

229. Nabeshima, A., Nishibayashi, C., Ueda, Y., Ogino, H., & Araki, M. 2013. Loss of cell-extracellular matrix interaction triggers retinal regeneration accompanied by Rax and Pax6 activation. *Genesis.*, 51, (6) 410-419 available from: PM:23362049

230. Nakayasu, M., Saeki, H., Tohda, H., & Oikawa, A. 1977. Effects of sugars on melanogenesis in cultured melanoma cells. *Journal of Cell Physiology*, 92, (1) 49-55 available from: PM:19484

231. Nandrot, E.F., Anand, M., Sircar, M., & Finnemann, S.C. 2006. Novel role for alphavbeta5-integrin in retinal adhesion and its diurnal peak. *American Journal of Physiology - Cell Physiology*, 290, (4) C1256-C1262 available from: PM:16338970

232. Nath, K.A., Enright, H., Nutter, L., Fischereder, M., Zou, J.N., & Hebbel, R.P. 1994. Effect of pyruvate on oxidant injury to isolated and cellular DNA. *Kidney International*, 45, (1) 166-176 available from: PM:8127006

233. Nath, K.A., Ngo, E.O., Hebbel, R.P., Croatt, A.J., Zhou, B., & Nutter, L.M. 1995. alpha-Ketoacids scavenge H2O2 in vitro and in vivo and reduce menadione-induced DNA injury and cytotoxicity. *Am.J.Physiol*, 268, (1 Pt 1) C227-C236 available from: PM:7840152

234. Nath, K.A. & Salahudeen, A.K. 1993. Autoxidation of cysteine generates hydrogen peroxide: cytotoxicity and attenuation by pyruvate. *Am.J.Physiol*, 264, (2 Pt 2) F306-F314 available from: PM:8447440

235. Neff, J.A., Caldwell, K.D., & Tresco, P.A. 1998. A novel method for surface modification to promote cell attachment to hydrophobic substrates. *Journal of Biomedial Materials Research*, 40, (4) 511-519 available from: PM:9599026

236. Neuberger, T.J. & De Vries, G.H. 1993. Distribution of fibroblast growth factor in cultured dorsal root ganglion neurons and Schwann cells. II. Redistribution after neural injury. *Journal of Neurocytology*, 22, (6) 449-460 available from: PM:7688414

237. Ocrant, I., Fay, C.T., & Parmelee, J.T. 1991. Expression of insulin and insulin-like growth factor receptors and binding proteins by retinal pigment epithelium. *Experimental Eye Research*, 52, (5) 581-589 available from: PM:1712313

238. Ohno-Matsui, K., Ichinose, S., Nakahama, K., Yoshida, T., Kojima, A., Mochizuki, M., & Morita, I. 2005. The effects of amniotic membrane on retinal pigment epithelial cell differentiation. *Molecular Vision*, 11, 1-10 available from: PM:15660020

239. Ohno-Matsui, K., Mori, K., Ichinose, S., Sato, T., Wang, J., Shimada, N., Kojima, A., Mochizuki, M., & Morita, I. 2006. In vitro and in vivo characterization of iris pigment epithelial cells cultured on amniotic membranes. *Molecular Vision*, 12, 1022-1032 available from: PM:16971894

240. Ohno-Matsui, K., Morita, I., Tombran-Tink, J., Mrazek, D., Onodera, M., Uetama, T., Hayano, M., Murota, S.I., & Mochizuki, M. 2001. Novel mechanism for age-related macular degeneration: an equilibrium shift between the angiogenesis factors VEGF and PEDF. *Journal of Cell Physiology*, 189, (3) 323-333 available from: PM:11748590

241. Okami, T., Yamamoto, A., Omori, K., Takada, T., Uyama, M., & Tashiro, Y. 1990. Immunocytochemical localization of Na+,K(+)-ATPase in rat retinal

pigment epithelial cells. *Journal of Histochemistry and Cytochemistry*, 38, (9) 1267-1275 available from: PM:2167328

242. Opas, M. 1985. The focal adhesions of chick retinal pigmented epithelial cells. *Canadian Journal of Biochemistry and Cell Biology*, 63, (6) 553-563 available from: PM:3930052

243. Opas, M. 1989. Expression of the differentiated phenotype by epithelial cells in vitro is regulated by both biochemistry and mechanics of the substratum. *Developmental Biology*, 131, (2) 281-293 available from: PM:2492240

244. Opas, M. 1994. Substratum mechanics and cell differentiation. *International Review of Cytology*, 150, 119-137 available from: PM:8169077

245. Opas, M. & Dziak, E. 1988. Effects of substrata and method of tissue dissociation on adhesion, cytoskeleton, and growth of chick retinal pigmented epithelium in vitro. *In Vitro Cell Dev.Biol.*, 24, (9) 885-892 available from: PM:3139624

246. Opas, M. & Kalnins, V.I. 1985. Spatial distribution of cortical proteins in cells of epithelial sheets. *Cell and Tissue Research*, 239, (2) 451-454 available from: PM:3919953

247. Ortego, J., Escribano, J., Becerra, S.P., & Coca-Prados, M. 1996. Gene expression of the neurotrophic pigment epithelium-derived factor in the human ciliary epithelium. Synthesis and secretion into the aqueous humor. *Investigative Ophthalmology & Visual Science*, 37, (13) 2759-2767 available from: PM:8977492

248. Pan, C.K., Heilweil, G., Lanza, R., & Schwartz, S.D. 2013. Embryonic stem cells as a treatment for macular degeneration. *Expert.Opin.Biol.Ther.*, 13, (8) 1125-1133 available from: PM:23705996

249. Paquin, J., Aouffen, M., De, G.E., Nadeau, R., Langlois, D., & Mateescu, M.A. 2005. Neuroprotective and cardioprotective actions of an association of

pyruvate, vitamin E and fatty acids. *Arzneimittel-Forschung*, 55, (7) 359-369 available from: PM:16080274

250. Pauleikhoff, D., Wojteki, S., Muller, D., Bornfeld, N., & Heiligenhaus, A. 2000. [Adhesive properties of basal membranes of Bruch's membrane. Immunohistochemical studies of age-dependent changes in adhesive molecules and lipid deposits]. *Ophthalmologe*, 97, (4) 243-250 available from: PM:10827458

251. Peirson, S.N., Butler, J.N., & Foster, R.G. 2003. Experimental validation of novel and conventional approaches to quantitative real-time PCR data analysis. *Nucleic Acids Research*, 31, (14) e73 available from: PM:12853650

252. Peng, S., Adelman, R.A., & Rizzolo, L.J. 2010. Minimal effects of VEGF and anti-VEGF drugs on the permeability or selectivity of RPE tight junctions. *Investigative Ophthalmology & Visual Science*, 51, (6) 3216-3225 available from: PM:20042644

253. Peters, T., Traboulsi, D., Tibbles, L.A., & Mydlarski, P.R. 2014. Sirolimus: a therapeutic advance for dermatologic disease. *Skin Therapy.Lett.*, 19, (4) 1-4 available from: PM:25188522

254. Pfeffer, B.A. 1991. Chapter 10 Improved methodology for cell culture of human and monkey retinal pigment epithelium. *Progress in Retinal Research*, 10, 251-291 available from: http://www.sciencedirect.com/science/article/B757Y-4859KKV-10/2/1047196c86cde7aaf2a347dda8435e91

255. Pierschbacher, M.D. & Ruoslahti, E. 1984. Cell attachment activity of fibronectin can be duplicated by small synthetic fragments of the molecule. *Nature*, 309, (5963) 30-33 available from: PM:6325925

256. Plow, E.F., Haas, T.A., Zhang, L., Loftus, J., & Smith, J.W. 2000. Ligand binding to integrins. *Journal of Biological Chemistry*, 275, (29) 21785-21788 available from: PM:10801897

257. Porjazoska, A., Goracinova, K., Mladenovska, K., Glavas, M., Simonovska, M., Janjevic, E.I., & Cvetkovska, M. 2004. Poly(lactide-co-glycolide) microparticles as systems for controlled release of proteins -- preparation and characterization. *Acta Pharm.*, 54, (3) 215-229 available from: PM:15610618

258. Proulx, S., Guerin, S.L., & Salesse, C. 2003. Effect of quiescence on integrin alpha5beta1 expression in human retinal pigment epithelium. *Molecular Vision*, 9, 473-481 available from: PM:14551535

259. Quastel, J.H. 1925. On a Possible Role of Pyruvic Acid in Bacterial Growth. *Biochemical Journal*, 19, (4) 641-644 available from: PM:16743554

260. Rajasekaran, S.A., Hu, J., Gopal, J., Gallemore, R., Ryazantsev, S., Bok, D., & Rajasekaran, A.K. 2003. Na,K-ATPase inhibition alters tight junction structure and permeability in human retinal pigment epithelial cells. *American Journal of Physiology - Cell Physiology*, 284, (6) C1497-C1507 available from: PM:12570983

261. Ramrattan, R.S., van der Schaft, T.L., Mooy, C.M., de Bruijn, W.C., Mulder, P.G., & de Jong, P.T. 1994. Morphometric analysis of Bruch's membrane, the choriocapillaris, and the choroid in aging. *Investigative Ophthalmology & Visual Science*, 35, (6) 2857-2864 available from: PM:8188481

262. Reardon, S. & Cyranoski, D. 2014. Japan stem-cell trial stirs envy. *Nature*, 513, (7518) 287-288 available from: PM:25230622

263. Recalde, S., Zarranz-Ventura, J., Fernandez-Robredo, P., Garcia-Gomez, P.J., Salinas-Alaman, A., Borras-Cuesta, F., Dotor, J., & Garcia-Layana, A. 2011. Transforming growth factor-beta inhibition decreases diode laser-induced choroidal neovascularization development in rats: P17 and P144 peptides. *Investigative Ophthalmology & Visual Science*, 52, (10) 7090-7097 available from: PM:21810978

264. Refojo, M.F. 1971. Polymers in ophthalmic surgery. *Journal of Biomedial Materials Research*, 5, (1) 113-119 available from: PM:5554094

265. Refojo, M.F., Dohlman, C.H., Ahmad, B., Carroll, J.M., & Allen, J.C. 1968. Evaluation of adhesives for corneal surgery. *Archives of Ophthalmology*, 80, (5) 645-656 available from: PM:4879226

266. Riley, P.A. 1993. Mechanistic aspects of the control of tyrosinase activity. *Pigment Cell Research*, 6, (4 Pt 1) 182-185 available from: PM:8248014

267. Rizzolo, L.J. 1990. The distribution of Na+,K(+)-ATPase in the retinal pigmented epithelium from chicken embryo is polarized in vivo but not in primary cell culture. *Experimental Eye Research*, 51, (4) 435-446 available from: PM:2170160

268. Rizzolo, L.J. 1991. Basement membrane stimulates the polarized distribution of integrins but not the Na,K-ATPase in the retinal pigment epithelium. *Cell Regulation*, 2, (11) 939-949 available from: PM:1667092

269. Robey, H.L., Hiscott, P.S., & Grierson, I. 1992. Cytokeratins and retinal epithelial cell behaviour. *Journal of Cell Science*, 102 (Pt 2), 329-340 available from: PM:1383245

270. Roll, S., Muller-Nordhorn, J., Keil, T., Scholz, H., Eidt, D., Greiner, W., & Willich, S.N. 2008. Dacron vs. PTFE as bypass materials in peripheral vascular surgery--systematic review and meta-analysis. *BMC.Surg.*, 8, 22 available from: PM:19099583

271. Rozanowski, B., Burke, J.M., Boulton, M.E., Sarna, T., & Rozanowska, M. 2008. Human RPE melanosomes protect from photosensitized and iron-mediated oxidation but become pro-oxidant in the presence of iron upon photodegradation. *Investigative Ophthalmology & Visual Science*, 49, (7) 2838-2847 available from: PM:18326697

272. Saari, J.C. & Crabb, J.W. 2005. Focus on molecules: cellular retinaldehyde-binding protein (CRALBP). *Experimental Eye Research*, 81, (3) 245-246 available from: PM:16085009

273. Saari, J.C., Nawrot, M., Kennedy, B.N., Garwin, G.G., Hurley, J.B., Huang, J., Possin, D.E., & Crabb, J.W. 2001. Visual cycle impairment in cellular retinaldehyde binding protein (CRALBP) knockout mice results in delayed dark adaptation. *Neuron*, 29, (3) 739-748 available from: PM:11301032

274. Saeki, H. & Oikawa, A. 1978. Effects of pH and type of sugar in the medium on tyrosinase activity in cultured melanoma cells. *Journal of Cell Physiology*, 94, (2) 139-145 available from: PM:23384

275. Saint-Geniez, M., Kurihara, T., Sekiyama, E., Maldonado, A.E., & D'Amore, P.A. 2009. An essential role for RPE-derived soluble VEGF in the maintenance of the choriocapillaris. *Proceedings of the National Academy of Sciences of the USA*, 106, (44) 18751-18756 available from: PM:19841260

276. Saint-Geniez, M., Maharaj, A.S., Walshe, T.E., Tucker, B.A., Sekiyama, E., Kurihara, T., Darland, D.C., Young, M.J., & D'Amore, P.A. 2008. Endogenous VEGF is required for visual function: evidence for a survival role on muller cells and photoreceptors. *PLoS.One.*, 3, (11) e3554 available from: PM:18978936

277. Salvador-Silva, M., Ghosh, S., Bertazolli-Filho, R., Boatright, J.H., Nickerson, J.M., Garwin, G.G., Saari, J.C., & Coca-Prados, M. 2005. Retinoid processing proteins in the ocular ciliary epithelium. *Molecular Vision*, 11, 356-365 available from: PM:15928609

278. Santiago, L.Y., Nowak, R.W., Rubin, J.P., & Marra, K.G. 2006. Peptide-surface modification of poly(caprolactone) with laminin-derived sequences for adipose-derived stem cell applications. *Biomaterials*, 27, (15) 2962-2969 available from: ISI:000236434000007

279. Schiller, H.B., Hermann, M.R., Polleux, J., Vignaud, T., Zanivan, S., Friedel, C.C., Sun, Z., Raducanu, A., Gottschalk, K.E., Thery, M., Mann, M., & Fassler, R. 2013. beta1- and alphav-class integrins cooperate to regulate myosin II during rigidity sensing of fibronectin-based microenvironments. *Nature Cell Biology*, 15, (6) 625-636 available from: PM:23708002

280. Schnapp, L.M., Hatch, N., Ramos, D.M., Klimanskaya, I.V., Sheppard, D., & Pytela, R. 1995. The human integrin alpha 8 beta 1 functions as a receptor for tenascin, fibronectin, and vitronectin. *Journal of Biological Chemistry*, 270, (39) 23196-23202 available from: PM:7559467

281. Schraermeyer, U. & Heimann, K. 1999. Current understanding on the role of retinal pigment epithelium and its pigmentation. *Pigment Cell Research*, 12, (4) 219-236 available from: PM:10454290

282. Schwartz, S.D., Hubschman, J.P., Heilwell, G., Franco-Cardenas, V., Pan, C.K., Ostrick, R.M., Mickunas, E., Gay, R., Klimanskaya, I., & Lanza, R. 2012. Embryonic stem cell trials for macular degeneration: a preliminary report. *The Lancet*, 379, (9817) 713-720 available from: PM:22281388

283. Schwartz, S.D., Regillo, C.D., Lam, B.L., Eliott, D., Rosenfeld, P.J., Gregori, N.Z., Hubschman, J.P., Davis, J.L., Heilwell, G., Spirn, M., Maguire, J., Gay, R., Bateman, J., Ostrick, R.M., Morris, D., Vincent, M., Anglade, E., Del Priore, L.V., & Lanza, R. 2015. Human embryonic stem cell-derived retinal pigment epithelium in patients with age-related macular degeneration and Stargardt's macular dystrophy: follow-up of two open-label phase 1/2 studies. *The Lancet*, 385, (9967) 509-516 available from: PM:25458728

284. Sedlak, T.W. & Snyder, S.H. 2006. Messenger molecules and cell death: therapeutic implications. *JAMA*, 295, (1) 81-89 available from: PM:16391220

285. Senanayake, P., Calabro, A., Hu, J.G., Bonilha, V.L., Darr, A., Bok, D., & Hollyfield, J.G. 2006. Glucose utilization by the retinal pigment epithelium: evidence for rapid uptake and storage in glycogen, followed by glycogen utilization. *Experimental Eye Research*, 83, (2) 235-246 available from: PM:16690055

286. Sendtner, M., Schmalbruch, H., Stockli, K.A., Carroll, P., Kreutzberg, G.W., & Thoenen, H. 1992. Ciliary neurotrophic factor prevents degeneration of motor neurons in mouse mutant progressive motor neuronopathy. *Nature*, 358, (6386) 502-504 available from: PM:1641039

287. Senyah, N., Hildebrand, G., & Liefeith, K. 2005. Comparison between RGD-peptide-modified titanium and borosilicate surfaces. *Analytical and Bioanalytical Chemistry*, 383, (5) 758-762 available from: PM:16151591

288. Shadforth, A.M., George, K.A., Kwan, A.S., Chirila, T.V., & Harkin, D.G. 2012. The cultivation of human retinal pigment epithelial cells on Bombyx mori silk fibroin. *Biomaterials*, 33, (16) 4110-4117 available from: PM:22406408

289. Sharma, P. & Mongan, P.D. 2010. Hypertonic sodium pyruvate solution is more effective than Ringer's ethyl pyruvate in the treatment of hemorrhagic shock. *Shock*, 33, (5) 532-540 available from: PM:19953008

290. Sharma, R.K., Orr, W.E., Schmitt, A.D., & Johnson, D.A. 2005. A functional profile of gene expression in ARPE-19 cells. *BMC.Ophthalmol.*, 5, 25 available from: PM:16262907

291. Sheline, C.T., Behrens, M.M., & Choi, D.W. 2000. Zinc-induced cortical neuronal death: contribution of energy failure attributable to loss of NAD(+) and inhibition of glycolysis. *Journal of Neuroscience*, 20, (9) 3139-3146 available from: PM:10777777

292. Sheraidah, G., Steinmetz, R., Maguire, J., Pauleikhoff, D., Marshall, J., & Bird, A.C. 1993. Correlation between lipids extracted from Bruch's membrane and age. *Ophthalmology*, 100, (1) 47-51 available from: PM:8433826

293. Sherman, M. 1992. A Power-Law Formulation of Laminar-Flow in Short Pipes. *Journal of Fluids Engineering-Transactions of the Asme*, 114, (4) 601-605 available from: ISI:A1992KF65300017

294. Shima, D.T., Adamis, A.P., Ferrara, N., Yeo, K.T., Yeo, T.K., Allende, R., Folkman, J., & D'Amore, P.A. 1995. Hypoxic induction of endothelial cell growth factors in retinal cells: identification and characterization of vascular endothelial growth factor (VEGF) as the mitogen. *Molecular Medicine*, 1, (2) 182-193 available from: PM:8529097

295. Sigurdson, L., Carney, D.E., Hou, Y., Hall, L., III, Hard, R., Hicks, W., Jr., Bright, F.V., & Gardella, J.A., Jr. 2002. A comparative study of primary and immortalized cell adhesion characteristics to modified polymer surfaces: toward the goal of effective re-epithelialization. *Journal of Biomedial Materials Research*, 59, (2) 357-365 available from: PM:11745573

296. Slepicka, P., Kasalkova, N.S., Bacakova, L., Kolska, Z., & Svorcik, V. 2012. Enhancement of Polymer Cytocompatibility by Nanostructuring of Polymer Surface. *Journal of Nanomaterials* available from: ISI:000307661300001

297. Slomiany, M.G. & Rosenzweig, S.A. 2004. IGF-1-induced VEGF and IGFBP-3 secretion correlates with increased HIF-1 alpha expression and activity in retinal pigment epithelial cell line D407. *Investigative Ophthalmology & Visual Science*, 45, (8) 2838-2847 available from: PM:15277511

298. Soler, A.P., Laughlin, K.V., & Mullin, J.M. 1993. Effects of epidermal growth factor versus phorbol ester on kidney epithelial (LLC-PK1) tight junction permeability and cell division. *Experimental Cell Research*, 207, (2) 398-406 available from: PM:7688317

299. Sone, H., Kawakami, Y., Okuda, Y., Kondo, S., Hanatani, M., Suzuki, H., & Yamashita, K. 1996a. Vascular endothelial growth factor is induced by long-term high glucose concentration and up-regulated by acute glucose deprivation in cultured bovine retinal pigmented epithelial cells. *Biochemical and Biophysical Research Communications*, 221, (1) 193-198 available from: PM:8660335

300. Sone, H., Okuda, Y., Kawakami, Y., Kondo, S., Hanatani, M., Matsuo, K., Suzuki, H., & Yamashita, K. 1996b. Progesterone induces vascular endothelial growth factor on retinal pigment epithelial cells in culture. *Life Sciences*, 59, (1) 21-25 available from: PM:8684267

301. Song, Q., Risco, R., Latina, M., Berthiaume, F., Nahmias, Y., & Yarmush, M.L. 2008. Selective targeting of pigmented retinal pigment epithelial (RPE) cells by a single pulsed laser irradiation: an in vitro study. *Optics Express*, 16, (14) 10518-10528 available from: PM:18607465

302. Sonoda, S., Spee, C., Barron, E., Ryan, S.J., Kannan, R., & Hinton, D.R. 2009. A protocol for the culture and differentiation of highly polarized human retinal pigment epithelial cells. *Nature Protocols*, 4, (5) 662-673 available from: PM:19373231

303. Sonoda, S., Sreekumar, P.G., Kase, S., Spee, C., Ryan, S.J., Kannan, R., & Hinton, D.R. 2010. Attainment of polarity promotes growth factor secretion by retinal pigment epithelial cells: relevance to age-related macular degeneration. *Aging (Albany.NY)*, 2, (1) 28-42 available from: PM:20228934

304. Soong, H.K., Parkinson, W.C., Bafna, S., Sulik, G.L., & Huang, S.C. 1990. Movements of cultured corneal epithelial cells and stromal fibroblasts in electric fields. *Investigative Ophthalmology & Visual Science*, 31, (11) 2278-2282 available from: PM:2242993

305. Spraul, C.W., Lang, G.E., Grossniklaus, H.E., & Lang, G.K. 1999. Histologic and morphometric analysis of the choroid, Bruch's membrane, and retinal pigment epithelium in postmortem eyes with age-related macular degeneration and histologic examination of surgically excised choroidal neovascular membranes. *Survey of Ophthalmology*, 44 Suppl 1, S10-S32 available from: PM:10548114

306. Sreekumar, P.G., Chothe, P., Sharma, K.K., Baid, R., Kompella, U., Spee, C., Kannan, N., Manh, C., Ryan, S.J., Ganapathy, V., Kannan, R., & Hinton, D.R. 2013. Antiapoptotic Properties of alpha-Crystallin-Derived Peptide Chaperones and Characterization of Their Uptake Transporters in Human RPE Cells. *Investigative Ophthalmology & Visual Science*, 54, (4) 2787-2798 available from: PM:23532520

307. Stanzel, B.V., Espana, E.M., Grueterich, M., Kawakita, T., Parel, J.M., Tseng, S.C., & Binder, S. 2005. Amniotic membrane maintains the phenotype of rabbit retinal pigment epithelial cells in culture. *Experimental Eye Research*, 80, (1) 103-112 available from: PM:15652531

308. Stanzel, B.V., Liu, Z., Brinken, R., Braun, N., Holz, F.G., & Eter, N. 2012. Subretinal delivery of ultrathin rigid-elastic cell carriers using a metallic shooter

instrument and biodegradable hydrogel encapsulation. *Investigative Ophthalmology & Visual Science*, 53, (1) 490-500 available from: PM:22167099

309. Starita, C., Hussain, A.A., & Marshall, J. 1995. Decreasing hydraulic conductivity of Bruch's membrane: relevance to photoreceptor survival and lipofuscinoses. *American Journal of Medical Genetics*, 57, (2) 235-237 available from: PM:7668336

310. Starita, C., Hussain, A.A., Pagliarini, S., & Marshall, J. 1996. Hydrodynamics of ageing Bruch's membrane: implications for macular disease. *Experimental Eye Research*, 62, (5) 565-572 available from: PM:8759524

311. Starita, C., Hussain, A.A., Patmore, A., & Marshall, J. 1997. Localization of the site of major resistance to fluid transport in Bruch's membrane. *Investigative Ophthalmology & Visual Science*, 38, (3) 762-767 available from: PM:9071230

312. STEIN, W.D. 1955. Ultra-violet absorption investigation of melanins. *Nature*, 175, (4454) 472 available from: PM:14356206

313. Steinberg, R.H. 1974. Phagocytosis by pigment epithelium of human retinal cones. *Nature*, 252, (5481) 305-307 available from: PM:4431450

314. Steinberg, R.H., Linsenmeier, R.A., & Griff, E.R. 1983. Three light-evoked responses of the retinal pigment epithelium. *Vision Research*, 23, (11) 1315-1323 available from: PM:6606894

315. Steindl-Kuscher, K., Krugluger, W., Boulton, M.E., Haas, P., Schrattbauer, K., Feichtinger, H., Adlassnig, W., & Binder, S. 2009. Activation of the beta-catenin signaling pathway and its impact on RPE cell cycle. *Investigative Ophthalmology & Visual Science*, 50, (9) 4471-4476 available from: PM:19369241

316. Stevens, P.W. & Kelso, D.M. 1995. Estimation of the protein-binding capacity of microplate wells using sequential ELISAs. *Journal of Immunological Methods*, 178, (1) 59-70 available from: PM:7829866

317. Strick, D.J. & Vollrath, D. 2010. Focus on molecules: MERTK. *Experimental Eye Research*, 91, (6) 786-787 available from: PM:20488176

318. Strom, S., Holm, F., Bergstrom, R., Stromberg, A.M., & Hovatta, O. 2010. Derivation of 30 human embryonic stem cell lines--improving the quality. *In Vitro Cellular and Developmental Biology - Animal*, 46, (3-4) 337-344 available from: PM:20198446

319. Stryer, L., Tasker, R., Rhodes, C., & Stanford University. 1995. *Biochemistry*, 4th ed. ed. New York : W.H. Freeman.

320. Sugino, I.K., Gullapalli, V.K., Sun, Q., Wang, J., Nunes, C.F., Cheewatrakoolpong, N., Johnson, A.C., Degner, B.C., Hua, J., Liu, T., Chen, W., Li, H., & Zarbin, M.A. 2011a. Cell-deposited matrix improves retinal pigment epithelium survival on aged submacular human Bruch's membrane. *Investigative Ophthalmology & Visual Science*, 52, (3) 1345-1358 available from: PM:21398292

321. Sugino, I.K., Sun, Q., Wang, J., Nunes, C.F., Cheewatrakoolpong, N., Rapista, A., Johnson, A.C., Malcuit, C., Klimanskaya, I., Lanza, R., & Zarbin, M.A. 2011b. Comparison of FRPE and human embryonic stem cell-derived RPE behavior on aged human Bruch's membrane. *Investigative Ophthalmology & Visual Science*, 52, (8) 4979-4997 available from: PM:21460262

322. Sulik, G.L., Soong, H.K., Chang, P.C., Parkinson, W.C., Elner, S.G., & Elner, V.M. 1992. Effects of steady electric fields on human retinal pigment epithelial cell orientation and migration in culture. *Acta Ophthalmol.(Copenh)*, 70, (1) 115-122 available from: PM:1557964

323. Tanihara, H., Yoshida, M., Matsumoto, M., & Yoshimura, N. 1993. Identification of transforming growth factor-beta expressed in cultured human retinal pigment epithelial cells. *Investigative Ophthalmology & Visual Science*, 34, (2) 413-419 available from: PM:8440596

324. Tashiro, K., Sephel, G.C., Weeks, B., Sasaki, M., Martin, G.R., Kleinman, H.K., & Yamada, Y. 1989. A synthetic peptide containing the IKVAV sequence from

the A chain of laminin mediates cell attachment, migration, and neurite outgrowth. *Journal of Biological Chemistry*, 264, (27) 16174-16182 available from: PM:2777785

325. Taylor, M.D., Grand, T.J., Cohen, J.E., Hsu, V., Liao, G.P., Zentko, S., Berry, M.F., Gardner, T.J., & Woo, Y.J. 2005. Ethyl pyruvate enhances ATP levels, reduces oxidative stress and preserves cardiac function in a rat model of off-pump coronary bypass. *Heart Lung Circ.*, 14, (1) 25-31 available from: PM:16352248

326. Tezel, T.H. & Del Priore, L.V. 1997. Reattachment to a substrate prevents apoptosis of human retinal pigment epithelium. *Graefes Archive for Clinical and Experimental Ophthalmology*, 235, (1) 41-47 available from: PM:9034841

327. Tezel, T.H., Del Priore, L.V., & Kaplan, H.J. 2004. Reengineering of aged Bruch's membrane to enhance retinal pigment epithelium repopulation. *Investigative Ophthalmology & Visual Science*, 45, (9) 3337-3348 available from: PM:15326159

328. Tezel, T.H., Kaplan, H.J., & Del Priore, L.V. 1999. Fate of human retinal pigment epithelial cells seeded onto layers of human Bruch's membrane. *Investigative Ophthalmology & Visual Science*, 40, (2) 467-476 available from: PM:9950607

329. Thomson, H.A., Treharne, A.J., Walker, P., Grossel, M.C., & Lotery, A.J. 2011. Optimisation of polymer scaffolds for retinal pigment epithelium (RPE) cell transplantation. *British Journal of Ophthalmology*, 95, (4) 563-568 available from: PM:19965827

330. Thomson, J.A., Itskovitz-Eldor, J., Shapiro, S.S., Waknitz, M.A., Swiergiel, J.J., Marshall, V.S., & Jones, J.M. 1998. Embryonic stem cell lines derived from human blastocysts. *Science*, 282, (5391) 1145-1147 available from: PM:9804556

331. Thomson, R.C., Giordano, G.G., Collier, J.H., Ishaug, S.L., Mikos, A.G., Lahiri-Munir, D., & Garcia, C.A. 1996. Manufacture and characterization of

poly(alpha-hydroxy ester) thin films as temporary substrates for retinal pigment epithelium cells. *Biomaterials*, 17, (3) 321-327 available from: PM:8745329

332. Thumann, G., Bartz-Schmidt, K.U., Heimann, K., & Schraermeyer, U. 1998. Phagocytosis of rod outer segments by human iris pigment epithelial cells in vitro. *Graefes Archive for Clinical and Experimental Ophthalmology*, 236, (10) 753-757 available from: PM:9801890

333. Thumann, G., Hueber, A., Dinslage, S., Schaefer, F., Yasukawa, T., Kirchhof, B., Yafai, Y., Eichler, W., Bringmann, A., & Wiedemann, P. 2006. Characteristics of iris and retinal pigment epithelial cells cultured on collagen type I membranes. *Current Eye Research*, 31, (3) 241-249 available from: PM:16531281

334. Thumann, G., Viethen, A., Gaebler, A., Walter, P., Kaempf, S., Johnen, S., & Salz, A.K. 2009. The in vitro and in vivo behaviour of retinal pigment epithelial cells cultured on ultrathin collagen membranes. *Biomaterials*, 30, (3) 287-294 available from: PM:18929407

335. Tian, J., Ishibashi, K., Honda, S., Boylan, S.A., Hjelmeland, L.M., & Handa, J.T. 2005. The expression of native and cultured human retinal pigment epithelial cells grown in different culture conditions. *British Journal of Ophthalmology*, 89, (11) 1510-1517 available from: PM:16234463

336. Tombran-Tink, J., Aparicio, S., Xu, X., Tink, A.R., Lara, N., Sawant, S., Barnstable, C.J., & Zhang, S.S. 2005. PEDF and the serpins: phylogeny, sequence conservation, and functional domains. *Journal of Structural Biology*, 151, (2) 130-150 available from: PM:16040252

337. Tombran-Tink, J., Shivaram, S.M., Chader, G.J., Johnson, L.V., & Bok, D. 1995. Expression, secretion, and age-related downregulation of pigment epithelium-derived factor, a serpin with neurotrophic activity. *J.Neurosci.*, 15, (7 Pt 1) 4992-5003 available from: PM:7623128

338. Tomita, M., Lavik, E., Klassen, H., Zahir, T., Langer, R., & Young, M.J. 2005. Biodegradable polymer composite grafts promote the survival and

differentiation of retinal progenitor cells. *Stem Cells*, 23, (10) 1579-1588 available from: PM:16293582

339. Treharne, A.J., Thomson, H.A., Grossel, M.C., & Lotery, A.J. 2012. Developing methacrylate-based copolymers as an artificial Bruch's membrane substitute. *"Journal of Biomedical Materials Research, Part A"*, 100, (9) 2358-2364 available from: PM:22528296

340. Turksen, K., Opas, M., & Kalnins, V.I. 1989. Cytoskeleton, adhesion, and extracellular matrix of fetal human retinal pigmented epithelial cells in culture. *Ophthalmic Research*, 21, (1) 56-66 available from: PM:2710498

341. Turowski, P., Adamson, P., Sathia, J., Zhang, J.J., Moss, S.E., Aylward, G.W., Hayes, M.J., Kanuga, N., & Greenwood, J. 2004. Basement membrane-dependent modification of phenotype and gene expression in human retinal pigment epithelial ARPE-19 cells. *Investigative Ophthalmology & Visual Science*, 45, (8) 2786-2794 available from: PM:15277505

342. Uetama, T., Ohno-Matsui, K., Nakahama, K., Morita, I., & Mochizuki, M. 2003. Phenotypic change regulates monocyte chemoattractant protein-1 (MCP-1) gene expression in human retinal pigment epithelial cells. *Journal of Cell Physiology*, 197, (1) 77-85 available from: PM:12942543

343. Ulbrich, S., Friedrichs, J., Valtink, M., Murovski, S., Franz, C.M., Muller, D.J., Funk, R.H., & Engelmann, K. 2011. Retinal pigment epithelium cell alignment on nanostructured collagen matrices. *Cells Tissues.Organs*, 194, (6) 443-456 available from: PM:21411961

344. Usher, F., Allen, J., Jr., Crosthwait, R., & Cogan, J. 1962. Polypropylene monofilament. A new, biologically inert suture for closing contaminated wounds. *JAMA*, 179, 780-782 available from: PM:13923961

345. van der Flier, A. & Sonnenberg, A. 2001. Function and interactions of integrins. *Cell and Tissue Research*, 305, (3) 285-298 available from: PM:11572082

346. Varma, S.D., Hegde, K.R., & Kovtun, S. 2006. Oxidative damage to lens in culture: reversibility by pyruvate and ethyl pyruvate. *Ophthalmologica*, 220, (1) 52-57 available from: PM:16374049

347. Villarroel, M., Garcia-Ramirez, M., Corraliza, L., Hernandez, C., & Simo, R. 2009. Effects of high glucose concentration on the barrier function and the expression of tight junction proteins in human retinal pigment epithelial cells. *Experimental Eye Research*, 89, (6) 913-920 available from: PM:19660451

348. Vollrath, D., Feng, W., Duncan, J.L., Yasumura, D., D'Cruz, P.M., Chappelow, A., Matthes, M.T., Kay, M.A., & LaVail, M.M. 2001. Correction of the retinal dystrophy phenotype of the RCS rat by viral gene transfer of Mertk. *Proceedings of the National Academy of Sciences of the USA*, 98, (22) 12584-12589 available from: PM:11592982

349. Vopalensky, P. & Kozmik, Z. 2009. Eye evolution: common use and independent recruitment of genetic components. *Philos.Trans.R.Soc.Lond B Biol.Sci.*, 364, (1531) 2819-2832 available from: PM:19720647

350. Vugler, A., Carr, A.J., Lawrence, J., Chen, L.L., Burrell, K., Wright, A., Lundh, P., Semo, M., Ahmado, A., Gias, C., da, C.L., Moore, H., Andrews, P., Walsh, J., & Coffey, P. 2008. Elucidating the phenomenon of HESC-derived RPE: anatomy of cell genesis, expansion and retinal transplantation. *Experimental Neurology*, 214, (2) 347-361 available from: PM:18926821

351. Vugler, A., Lawrence, J., Walsh, J., Carr, A., Gias, C., Semo, M., Ahmado, A., da, C.L., Andrews, P., & Coffey, P. 2007. Embryonic stem cells and retinal repair. *Mechanisms of Development*, 124, (11-12) 807-829 available from: PM:17881192

352. Waldbillig, R.J., Pfeffer, B.A., Schoen, T.J., Adler, A.A., Shen-Orr, Z., Scavo, L., LeRoith, D., & Chader, G.J. 1991. Evidence for an insulin-like growth factor autocrine-paracrine system in the retinal photoreceptor-pigment epithelial cell complex. *Journal of Neurochemistry*, 57, (5) 1522-1533 available from: PM:1717648

353. Wang, X., Perez, E., Liu, R., Yan, L.J., Mallet, R.T., & Yang, S.H. 2007. Pyruvate protects mitochondria from oxidative stress in human neuroblastoma SK-N-SH cells. *Brain Research*, 1132, (1) 1-9 available from: PM:17174285

354. Wang, Z., Dillon, J., & Gaillard, E.R. 2006. Antioxidant properties of melanin in retinal pigment epithelial cells. *Photochemistry and Photobiology*, 82, (2) 474-479 available from: PM:16613501

355. Williams, R.L., Krishna, Y., Dixon, S., Haridas, A., Grierson, I., & Sheridan, C. 2005. Polyurethanes as potential substrates for sub-retinal retinal pigment epithelial cell transplantation. *Journal of Materials Science: Materials in Medicine*, 16, (12) 1087-1092 available from: PM:16362205

356. Wood, J.P., Chidlow, G., Graham, M., & Osborne, N.N. 2004. Energy substrate requirements of rat retinal pigmented epithelial cells in culture: relative importance of glucose, amino acids, and monocarboxylates. *Investigative Ophthalmology & Visual Science*, 45, (4) 1272-1280 available from: PM:15037596

357. Wood, J.P., Chidlow, G., Graham, M., & Osborne, N.N. 2005. Energy substrate requirements for survival of rat retinal cells in culture: the importance of glucose and monocarboxylates. *Journal of Neurochemistry*, 93, (3) 686-697 available from: PM:15836627

358. Wood, J.P. & Osborne, N.N. 2003. Zinc and energy requirements in induction of oxidative stress to retinal pigmented epithelial cells. *Neurochemical Research*, 28, (10) 1525-1533 available from: PM:14570397

359. Wu, J.H., Wang, F., Xu, P., & Huang, Q. 2005a. [In vitro transdifferentiation of adult human retinal pigment epithelium cells to neuro-like cells induced by blocking VEGF expression.]. *Zhonghua Yan.Ke.Za Zhi.*, 41, (2) 114-118 available from: PM:15840334

360. Wu, Y.T., Wu, Z.L., Jiang, X.F., Li, S., & Zhou, F.Q. 2003. Pyruvate preserves neutrophilic superoxide production in acidic, high glucose-enriched peritoneal

dialysis solutions. *Artificial Organs*, 27, (3) 276-281 available from: PM:12662215

361. Wu, Y.T., Wu, Z.L., Jiang, X.F., Li, S., & Zhou, F.Q. 2005b. Pyruvate improves neutrophilic nitric oxide generation in peritoneal dialysis solutions. *Artificial Organs*, 29, (12) 976-980 available from: PM:16305654

362. Xiao, Q., Zeng, S., Ling, S., & Lv, M. 2006. Up-regulation of HIF-1alpha and VEGF expression by elevated glucose concentration and hypoxia in cultured human retinal pigment epithelial cells. *J.Huazhong.Univ Sci.Technolog.Med.Sci.*, 26, (4) 463-465 available from: PM:17120749

363. Yang, X.B., Roach, H.I., Clarke, N.M., Howdle, S.M., Quirk, R., Shakesheff, K.M., & Oreffo, R.O. 2001. Human osteoprogenitor growth and differentiation on synthetic biodegradable structures after surface modification. *Bone*, 29, (6) 523-531 available from: PM:11728922

364. Yeung, C.K., Chiang, S.W., Chan, K.P., Lam, D.S., & Pang, C.P. 2004. The transfer of ocular cells using collagen. *Cell Transplantation*, 13, (5) 585-594 available from: PM:15565870

365. Yoo, M.H., Lee, J.Y., Lee, S.E., Koh, J.Y., & Yoon, Y.H. 2004. Protection by pyruvate of rat retinal cells against zinc toxicity in vitro, and pressure-induced ischemia in vivo. *Investigative Ophthalmology & Visual Science*, 45, (5) 1523-1530 available from: PM:15111611

366. Yoshioka, T., Kawazoe, N., Tateishi, T., & Chen, G. 2008. In vitro evaluation of biodegradation of poly(lactic-co-glycolic acid) sponges. *Biomaterials*, 29, (24-25) 3438-3443 available from: PM:18514306

367. Yoshioka, T., Kawazoe, N., Tateishi, T., & Chen, G.P. 2011. Effects of Structural Change Induced by Physical Aging on the Biodegradation Behavior of PLGA Films at Physiological Temperature. *Macromolecular Materials and Engineering*, 296, (11) 1028-1034 available from: ISI:000297552200005

368. Young, R.W. & Bok, D. 1969. Participation of the retinal pigment epithelium in the rod outer segment renewal process. *Journal of Cell Biology*, 42, (2) 392-403 available from: PM:5792328

369. Young, T.A., Wang, H., Munk, S., Hammoudi, D.S., Young, D.S., Mandelcorn, M.S., & Whiteside, C.I. 2005. Vascular endothelial growth factor expression and secretion by retinal pigment epithelial cells in high glucose and hypoxia is protein kinase C-dependent. *Experimental Eye Research*, 80, (5) 651-662 available from: PM:15862172

370. Yu, W., Datta, A., Leroy, P., O'Brien, L.E., Mak, G., Jou, T.S., Matlin, K.S., Mostov, K.E., & Zegers, M.M. 2005. Beta1-integrin orients epithelial polarity via Rac1 and laminin. *Molecular Biology of the Cell*, 16, (2) 433-445 available from: PM:15574881

371. Zamiri, P., Masli, S., Kitaichi, N., Taylor, A.W., & Streilein, J.W. 2005. Thrombospondin plays a vital role in the immune privilege of the eye. *Investigative Ophthalmology & Visual Science*, 46, (3) 908-919 available from: PM:15728547

372. Zarbin, M.A. 2003. Analysis of retinal pigment epithelium integrin expression and adhesion to aged submacular human Bruch's membrane. *Transactions of the American Ophthalmological Society*, 101, 499-520 available from: PM:14971591

373. Zarbin, M.A. 2004. Current concepts in the pathogenesis of age-related macular degeneration. *Archives of Ophthalmology*, 122, (4) 598-614 available from: PM:15078679

374. Zeng, J., Liu, J., Yang, G.Y., Kelly, M.J., James, T.L., & Litt, L. 2007a. Exogenous ethyl pyruvate versus pyruvate during metabolic recovery after oxidative stress in neonatal rat cerebrocortical slices. *Anesthesiology*, 107, (4) 630-640 available from: PM:17893460

375. Zeng, J., Yang, G.Y., Ying, W., Kelly, M., Hirai, K., James, T.L., Swanson, R.A., & Litt, L. 2007b. Pyruvate improves recovery after PARP-1-associated

energy failure induced by oxidative stress in neonatal rat cerebrocortical slices. *J.Cereb.Blood Flow Metab*, 27, (2) 304-315 available from: PM:16736046

376. Zhou, F.Q. 2005. Pyruvate in the correction of intracellular acidosis: a metabolic basis as a novel superior buffer. *American Journal of Nephrology*, 25, (1) 55-63 available from: PM:15731550

377. Zhou, Y., Dziak, E., & Opas, M. 1993. Adhesiveness and proliferation of epithelial cells are differentially modulated by activation and inhibition of protein kinase C in a substratum-dependent manner. *Journal of Cell Physiology*, 155, (1) 14-26 available from: PM:8468359

378. Zhu, D., Deng, X., Spee, C., Sonoda, S., Hsieh, C.L., Barron, E., Pera, M., & Hinton, D.R. 2011. Polarized secretion of PEDF from human embryonic stem cell-derived RPE promotes retinal progenitor cell survival. *Investigative Ophthalmology & Visual Science*, 52, (3) 1573-1585 available from: PM:21087957

379. Zimmermann, W.H. & Eschenhagen, T. 2003. Cardiac tissue engineering for replacement therapy. *Heart Fail.Rev.*, 8, (3) 259-269 available from: PM:12878835

380. Zinkl, G.M., Zuk, A., van der, B.P., van, M.G., & Matlin, K.S. 1996. An antiglycolipid antibody inhibits Madin-Darby canine kidney cell adhesion to laminin and interferes with basolateral polarization and tight junction formation. *Journal of Cell Biology*, 133, (3) 695-708 available from: PM:8636242

381. Ziolkowski, W., Wierzba, T.H., Kaczor, J.J., Olek, R.A., Wozniak, M., Kmiec, Z., Mysliwski, A., & Antosiewicz, J. 2008. Intravenous sodium pyruvate protects against cerulein-induced acute pancreatitis. *Pancreas*, 37, (2) 238-239 available from: PM:18665097